SOLUBILISATION AND CHARACTERISATION OF G-PROTEIN-COUPLED RECEPTORS USING STYRENE MALEIC ACID POLYMER

JACK CHARLTON

A thesis submitted to the University of Birmingham

for the degree of Doctor of Philosophy

School of Biosciences

College of Life and Environmental Science

University of Birmingham

Birmingham

B15 2TT

September 2015

UNIVERSITY OF BIRMINGHAM

University of Birmingham Research Archive

e-theses repository

Abstract

Detergent-free solubilisation using a polymer of styrene maleic acid (SMA) has proven useful in the study of membrane proteins. SMA was employed to solubilise G-protein-coupled receptors (GPCRs) from mammalian cells, into SMA lipid particles (SMALPs). Optimal SMALP-solubilisation conditions were determined to be 2 % (w/v) SMA, at 37 °C for 1 h retaining wild-type (WT)-like pharmacological profiles and conferring improved stability on GPCRs over detergent micelles.

Endoplasmic reticulum (ER)-retention motifs –KDEL and –KHILFRRRRRGFRQ were found not to be applicable to all proteins. Study of SMALP-solubilisation of intracellular membranes was prevented by the inability to retain the adenosine 2a receptor ($A_{2a}R$) in the ER. A cysteine-nul $A_{2a}R$ construct was produced containing two reporter groups and behaved as WT-$A_{2a}R$. This construct is ready for use in fluorescence studies to further understanding of $A_{2a}R$ and the use of SMALPs in biophysical techniques.

A range of GPCRs, from different GPCR subfamilies, were SMALP-solubilised with retention of ligand binding capability. Methods were successfully developed to reduce non-specific binding arising from ionic interactions of ligand and SMA. Finally, in a world first, the SMA analogue styrene maleimide, was shown to solubilise GPCRs with retention of ligand binding capability.

I would like to dedicate this thesis to my wife Magda

Your love and support from start to finish made this all possible

Acknowledgements

TABLE OF CONTENTS

Abbreviations

Throughout this thesis, abbreviations are used as recommended by the Journal of Biological Chemistry. In addition, the following abbreviations have been used:

A_1R	adenosine 1 receptor
$A_{2a}R$	adenosine 2a receptor
$A_{2b}R$	adenosine 2b receptor
A_3R	adenosine 3 receptor
Amy_{1-3}	amylin receptor 1-3
AVP	[arginine^8]vasopressin
BSA	bovine serum albumin
bp	base pairs
cAMP	cyclic 3'-5'-adenosine monophosphate
CD	circular dichroism
cDNA	complementary DNA
CHS	cholesteryl hemisuccinate
CTR	calcitonin receptor
CXCR1	chemokine receptor type 1
DAG	diacylglycerol
DDM	n-dodecyl β-D-maltoside
ECL	extracellular loop
E.coli	*Escherichia coli*
EDTA	ethylenediaminetetraacetic acid
EGTA	ethyleneglycoltetraacetic acid
ELISA	enzyme-linked immunosorbent assay
ER	endoplasmic reticulum
FRET	Förster resonance energy tranfer
G-protein	guanine nucleotide binding protein
GDP	guanosine diphosphate
GPCR	G-protein-coupled receptor
GTP	guanosine triphosphate

HA	haemagluttinin
HRP	horseraddish peroxidase
IAEDANS	5-({2-[(iodoacetyl)amino]ethyl}amino)naphthalene-1-sulfonic acid
ICL	intracellular loop
InsP$_3$	inositol 1,4,5-trisphosphate
M1R	muscarinic acetylcholine receptor 1
MT-cells	mock transfected cells
M$_W$	molecular weight
Nanodiscs	apolipoprotein stabilised nanodiscs
NECA	n-ethylcarboxamidoadenosine
NDI	nephrogenic diabetes insipidus
NMR	nuclear magnetic resonance
NMS	n-methyl scopolamine
OT	oxytocin
OTR	oxytocin receptor
PAGE	polyacrylamide gel electrophoresis
PBS	phosphate buffered saline
PEI	polyethylenimine
RAMP	receptor activity modifying protein
sCT	salmon calcitonin
SDS	sodium dodecyl sulphate
SMA	styrene maleic acid
SMALP	styrene maleic acid lipid particle
SMI	styrene maleimide
SMILP	styrene maleimide lipid particle
TM	transmembrane

TMD	transmembrane domain
$V_{1a}R$	vasopressin 1a receptor
$V_{1b}R$	vasopressin 1b receptor
V_2R	vasopressin 2 receptor
WT	wild-type
XAC	xanthine amine congener
α_{2c}-AR	α_{2c} adrenergic receptor
β_2-AR	β_2 adrenergic receptor

CHAPTER 1: INTRODUCTION

1.1 G-protein-coupled receptors

Coded for by approximately 4 % of the entire human genome there are over 800 distinct types of G-protein-coupled receptors (GPCRs), making them the largest family of membrane proteins (Fredriksson et al., 2003). GPCRs have become an important target for the pharmaceutical industry due to their abundance and role in a wide range of biological processes. Currently around 40 % of all clinically available drugs target GPCRs (Rask-Andersen et al., 2011).

1.2 G-proteins

GPCRs are primarily identified through their ability to signal through heterotrimeric guanine nucleotide binding proteins (G-proteins). G-proteins consist of three subunits: $G\alpha$, $G\beta$ and $G\gamma$. $G\alpha$ is the largest of the subunits and contains the guanine nucleotide binding site with intrinsic GTPase activity. In the inactive state, $G\alpha$ is GDP-bound. The $G\beta$ and $G\gamma$ subunits are tightly linked to each other and non-covalently bound to the $G\alpha$ subunit in the inactive state. Active GPCRs induce GDP exchange for GTP in the $G\alpha$ subunit. The mechanisms by which this occurs have been elucidated from crystallographic data, including a $G\alpha$ subunit ($G\alpha_s$) coupled to the β_2 adrenergic receptor in an active confromation (Oldham and Hamm, 2008, Rasmussen et al., 2011b, Chung et al., 2011). GTP binding at the $G\alpha$ subunit results in dissociation of the functional subunits $G\alpha$ and $G\beta\gamma$ to mediate their effects through effector molecules. G-protein signalling continues until GTP is hydrolysed by the intrinsic GTPase activity of the $G\alpha$ subunit, driving reassociation of GDP-bound $G\alpha$ with $G\beta\gamma$.

There are 16 known Gα subtypes which are classified into 4 main families: $G\alpha_s$, $G\alpha_i$, $G\alpha_{q/11}$ and $G\alpha_{12}$ (Simon et al., 1991). $G\alpha_s$ and $G\alpha_i$ stimulate and inhibit, respectively, adenylyl cyclase. Adenylyl cyclase produces cyclic-adenosine 3'-5'-monophosphate (cAMP) to regulate cAMP-dependent protein kinases and some guanine nucleotide exchange factors. $G\alpha_q$ stimulates phospholipase C to produce: inositol 1,4,5-trisphosphate ($InsP_3$), stimulating calcium release from the endoplasmic reticulum (ER) and diacylglycerol (DAG) for activation of protein kinase C. $G\alpha_{12}$ subunits produce their effect through Rho family GTPases involved in cytoskeletal rearrangements. The activation and intracellular effects of G-proteins are summarised in figure 1.1 (Ritter and Hall, 2009).

1.3 GPCR classification

Across the superfamily, GPCRs share a characteristic 7 transmembrane (7TM) helical bundle connected by alternating intracellular and extracellular loops (ICL and ECL respectively). They also possess an extracellular amino (N-) terminus and intracellular carboxyl (C-) terminus (shown in figure 1.2). Despite the conservation of overall structure, there is little sequence homology across the GPCR superfamily. However, groups of GPCRs do share some sequence homology and characteristic motifs. This has allowed for GPCRs to be subcategorised by the family A-F system (Kolakowski, 1994). Human GPCRs can be further subcategorised by the GRAFS system into: glutamate, rhodopsin-like, adhesion, frizzled/smoothened and secretin-like (Fredriksson et al., 2003).

Families A-C are the three major GPCR subfamilies. Ligand binding at family A and B GPCRs involves an orthosteric ligand binding site at the TM core. However, as demonstrated in figure 1.3, family C GPCRs possess a long N-terminal sequence (~ 580 residues), structured to form a "Venus flytrap" orthosteric binding site for the endogenous
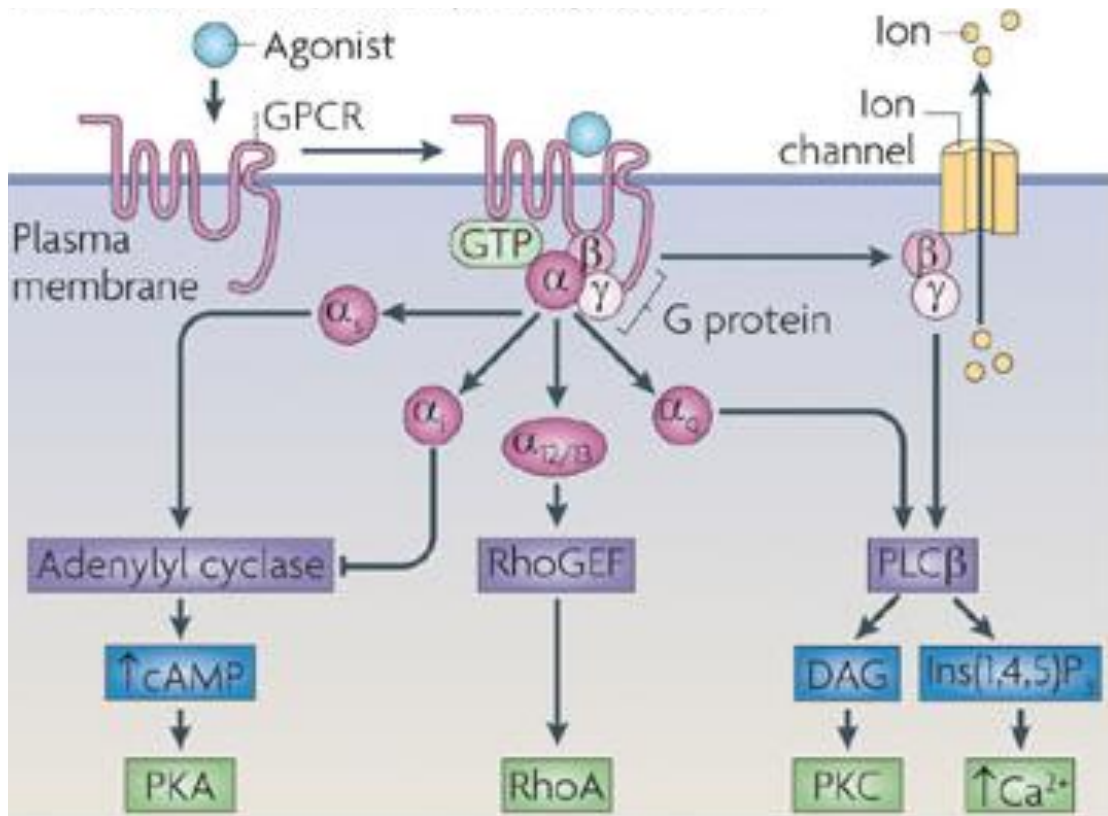
Figure 1.1. G-protein signalling pathways. GPCR activation of G-proteins resulting in functional Gα and Gβγ subunits that produce signals through effector molecules. $G\alpha_s$ and $G\alpha_i$ stimulate and inhibit adenylyl cyclase respectively, responsible for cAMP production. $G\alpha_q$ stimulates phospholipase C to produce $InsP_3$ and DAG. $G\alpha_{12/13}$ modulate Rho GTPases. The second messenger molecules are involved in protein activation, calcium homeostasis and cytoskeletal arrangement. Image taken from Ritter and Hall, 2009.
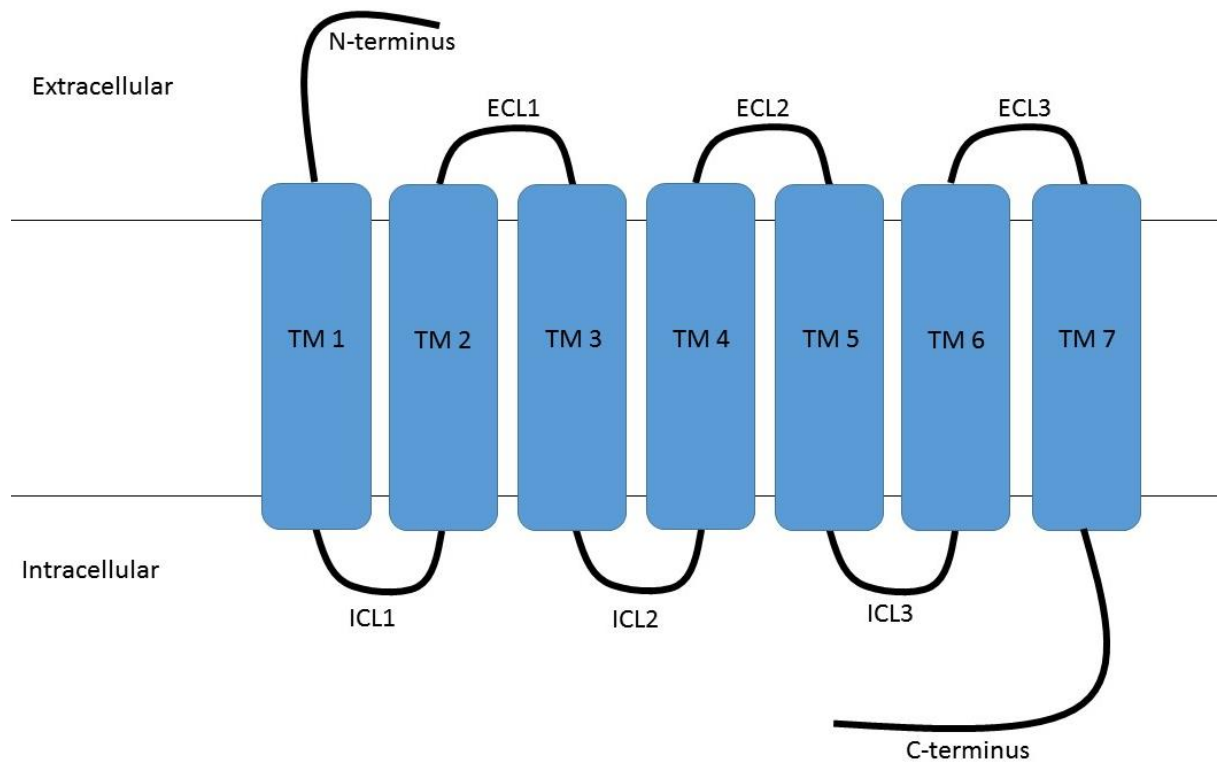
Figure 1.2. Schematic representation of the general structure of a GPCR. The 7 transmembrane helices, characteristic of GPCRs, are shown in blue, numbered 1-7 and connected by alternating intracellular loops (ICL1-3) and extracellular loops (ECL1-3). The GPCR is embedded in the membrane with the extracellular N-terminus connected to TM1 and intracellular C-terminus connected to TM7.

ligand (Pin et al., 2003). Family C includes the metabotropic glutamate receptors (mGluR) 1-5. The structure of the TM domain of mGluR1 has recently been solved through x-ray crystallography (Wu et al., 2014) and was shown to possess similar architecture to family A and B GPCRs. This common architecture, exemplified in figure 1.4, has each helix tilted differently in relation to the membrane bilayer and several kinked helices (Krebs et al., 2003). Also, despite the ECLs being regions of low sequence homology within and between subfamilies, there is a highly conserved Cys-Cys disulphide bridge tethering ECL2 to the top of TM3 (Wheatley et al., 2012, Wu et al., 2014). The conserved architecture is likely to be important to the fundamental mechanisms of signal transduction, resulting in GPCR signalling through G-proteins. However, with so little sequence homology across the GPCR superfamily, the residues and motifs employed to maintain this structure differ between subfamilies.

1.3.1 Family A GPCRs

Family A is comprised of > 700 GPCRs, making it by far the largest of the GPCR subfamilies. As a result of the number of distinct GPCRs, there is a wide range of ligands that interact with, and produce their effect through family A. Although the size and type of ligand can vary, from small biogenic amines to peptides (Strader et al., 1994), the ligand will bind the orthosteric binding site in the TM core of the GPCR. For small molecule ligands the orthosteric binding pocket is deep in the TM core. As a result small molecule ligands do not form interactions with ECLs (Tota and Strader, 1990). Peptide ligands however, are larger than small molecule ligands such as biogenic amines. As a result they form interactions with the TM core and the extracellular domains to promote their effect.
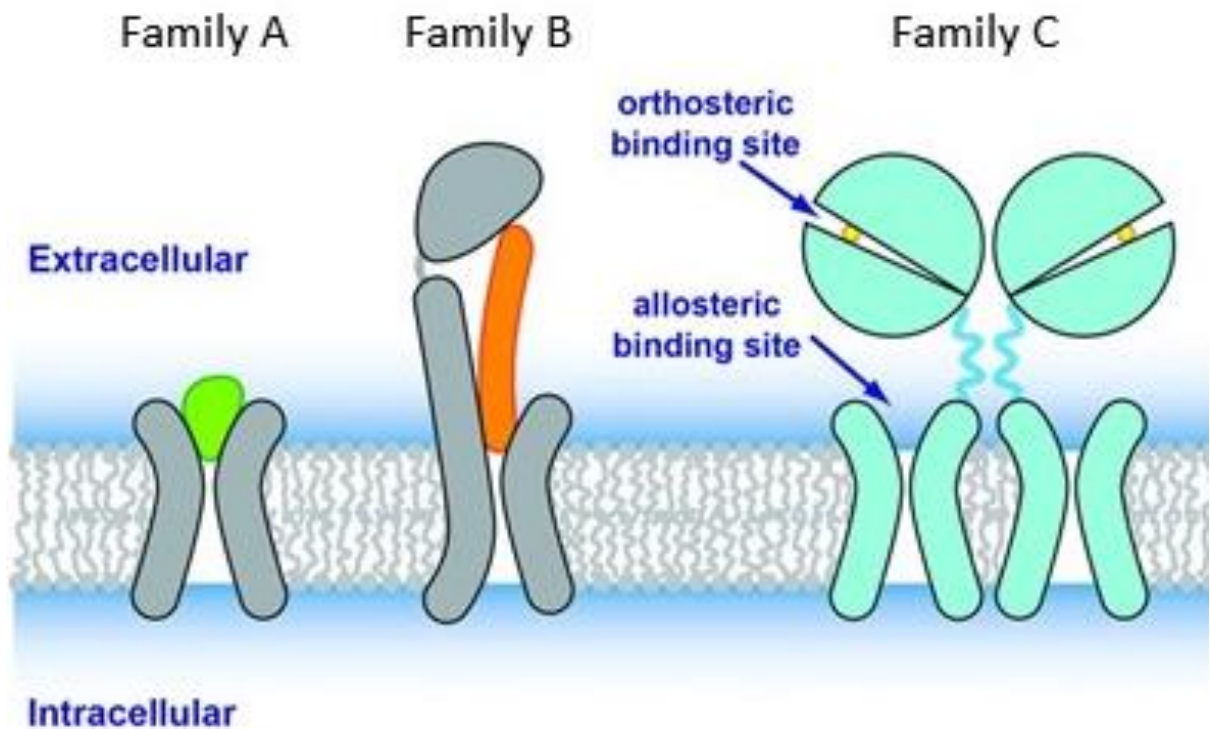
Figure 1.3. The difference in N-terminal domains and orthosteric binding sites from family A-C. Family A GPCRs typically contain the shortest N-terminus of families A-C and the orthosteric binding pocket for ligands is in the TM core with some contacts at the ECLs. Family B, with a larger N-terminus than family A, has more ligand contacts in the N-terminus but the orthosteric binding site is at the TM bundle. Family C possess the largest N-terminus of the 3 families which is the orthosteric binding site for ligands, with only small molecule ligands binding the allosteric site in the TM bundle. Adapted from Wu et al., 2014.
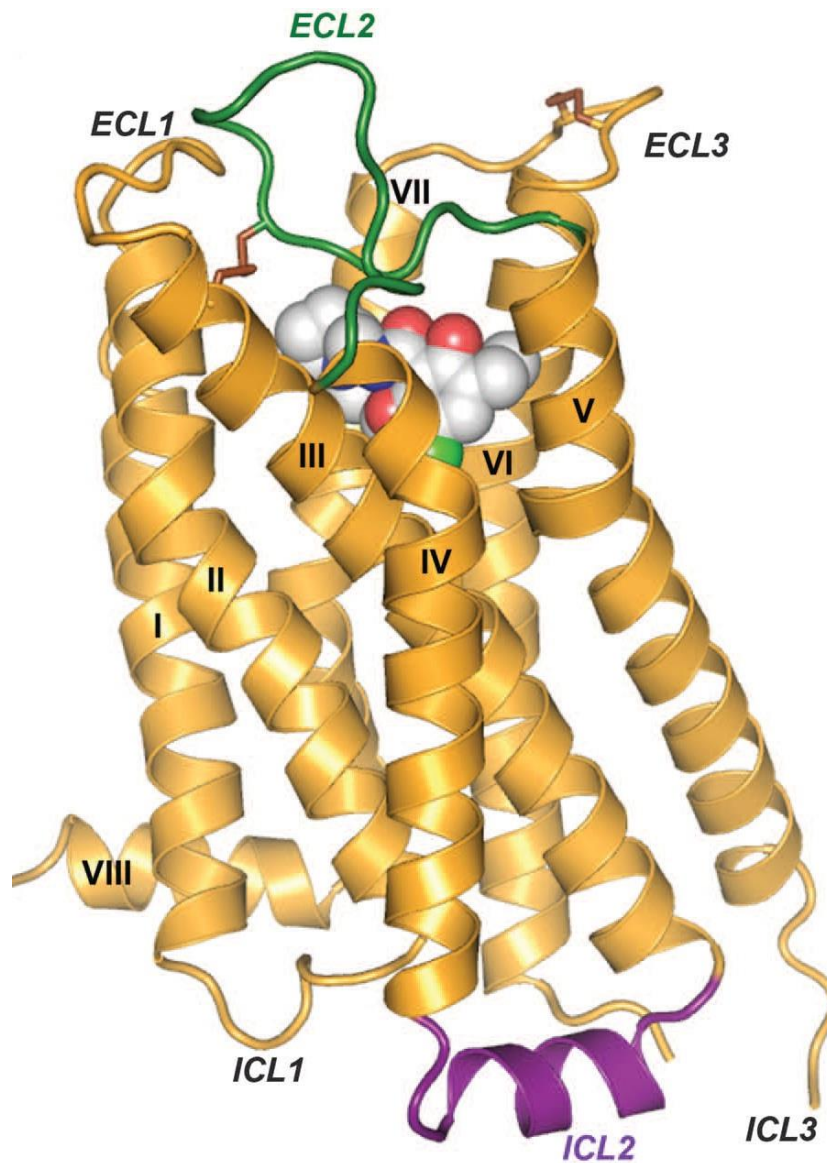
Figure 1.4. Crystal structure of the dopamine D3 receptor. Transmembrane helices, yellow, labelled with roman numerals, are connected by annotated ICLs and ECLs. At the centre is the dopamine receptor antagonist eticlopride bound to the orthosteric binding pocket of this family A GPCR. Image taken from (Chien et al., 2010).

The conformational changes induced by ligand binding to family A GPCRs are controlled through a series of highly conserved residues and motifs that typify family A GPCRs (Mirzadegan et al., 2003). Highlighted in figure 1.5 are highly conserved motifs (in blue) and the most highly conserved individual residues of each TM helix (in red). Identification of the latter has allowed a common numbering system for residues across family A GPCRs. This allows the comparison of similarly positioned residues between family A GPCRs (Ballesteros and Weinstein, 1995). In the Ballesteros-Weinstein numbering system, the most highly conserved residue in each TM-helix is a reference point denoted as X.50 (where X is the TM number). Residues following X.50 are denoted as an increase from 50 and preceding residues as a decrease from 50. For example 3 residues before the most highly conserved residue of TM1 (1.50) would be referred to as 1.47.

The E/DRY motif is one of the most highly conserved motifs across family A. $R^{3.50}$, located at the bottom of TM3 interacts with an acidic residue in TM6($^{6.30}$) (Scheer et al., 1996, Palczewski et al., 2000). This is referred to as the "ionic lock" as it constrains GPCRs in an inactive conformation. Upon GPCR activation, the ionic lock is broken and $R^{3.50}$ forms interactions with $Y^{5.58}$ (Park et al., 2008), allowing movement of TM6 away from TM3. This movement is based around the CWxP motif and is the basis for GPCR signal transduction to G-proteins. $P^{6.50}$ in CWxP induces a pronounced kink in TM6, modulated by $W^{6.48}$, termed the "rotamer toggle switch". This allows the extracellular side of TM6 to move towards TM3 upon agonist binding. The result is the intracellular side of TM6 moves away from TM3, opening the G-protein binding pocket (Shi et al., 2002, Ruprecht et al., 2004, Schwartz et al., 2006). Stability of active conformations is thought to be based around the NPxxY motif in TM7. $N^{7.49}$ of NPxxY is believed to stabilise the active conformation
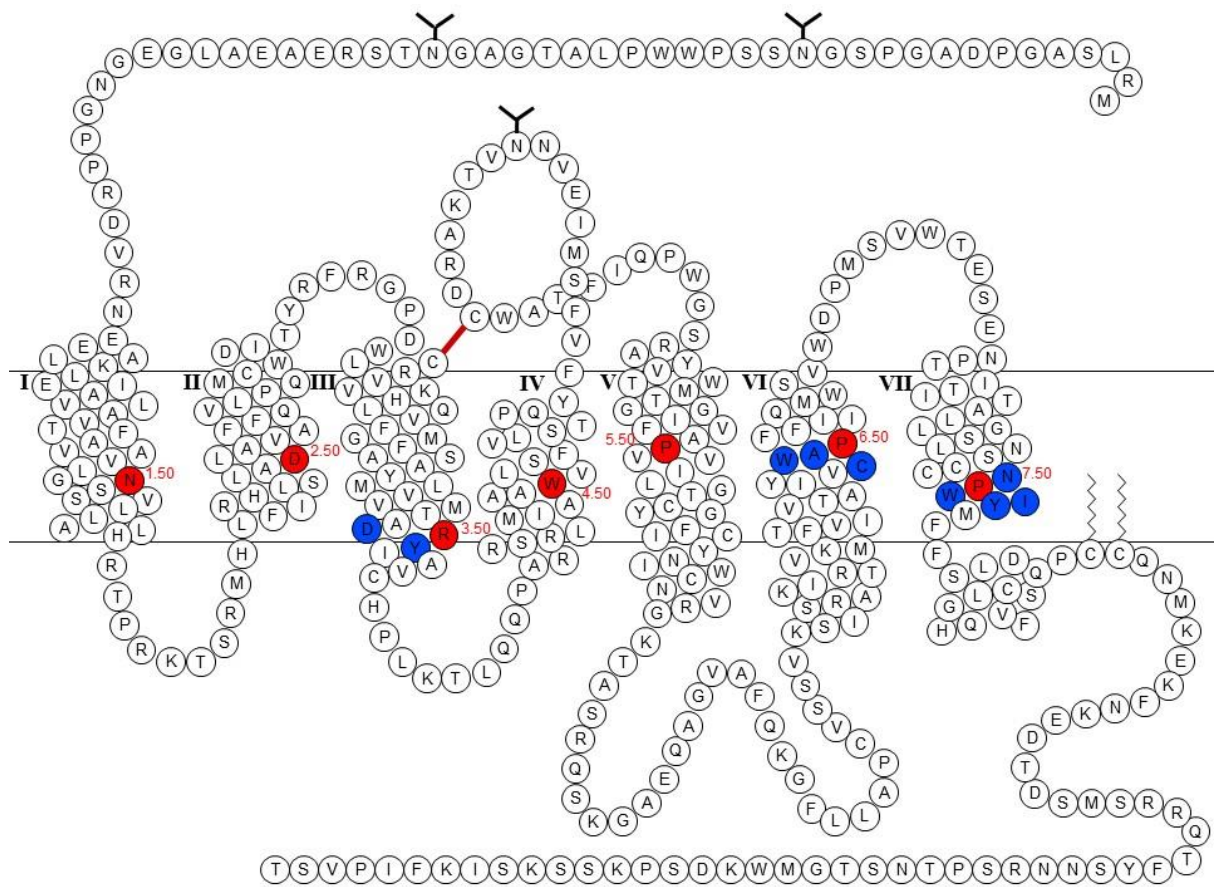
Figure 1.5. Schematic representation of a family A GPCR. Transmembrane helices are numbered with roman numerals (I-VII). The most highly conserved residues of each helix are displayed in red with their Ballosteros-Weinstein number displayed (Ballesteros and Weinstein, 1995). Highly conserved motifs are displayed in blue. Conserved Cys-Cys disulphide bridge is demonstrated by a thick red line. Zig-zag black lines indicate palmitoylation and black branches indicate sites of glycosylation.

through interactions with $N^{1.50}$ and $D^{2.50}$ (Govaerts et al., 2001, Urizar et al., 2005). Upon activation $Y^{7.53}$ causes $Y^{5.58}$ to move into the helical bundle, allowing its interaction with $R^{3.50}$ (Fritze et al., 2003, Standfuss et al., 2011).

1.3.2 Family B GPCRs

Family B GPCRs have a characteristic N-terminus of ~100-160 residues. This is a large N-terminus in relation to family A GPCRs, but not as large as family C GPCRs (~580 residues). The increased size of the family B N-terminus is required for identification of their large peptide ligands (~30-40 residues). Family B are receptors for 15 peptide hormones that are grouped into 5 subfamilies. Peptide ligands bind to family B GPCRs via a two-domain model (Hoare et al., 2004). Initially, the C-terminus of the peptide ligand binds the large N-terminus of the GPCR. This then orientates the N-terminus of the ligand to bind to the top of the TM domain (TMD). The extracellular surface of the TMD is held in a chalice-like conformation, as determined through two solved structures of family B GPCR TMDs (Hollenstein et al., 2013, Siu et al., 2013).

Family B GPCRs contain a largely different set of conserved residues and motifs. One residue, $Y^{7.53}$ of family A, has an equivalent tyrosine in TM7 of family B GPCRs that occupies a similar position. No crystal structures of an agonist bound active family B GPCR have been published so it is unknown whether it has a similar role in receptor activation. However, as family B GPCRs do not contain the E/DRY ionic lock motif, it is unlikely to perform an identical role in family B. There is an alternative ionic lock mechanism in some family B GPCRs, which stabilises an inactive state by tethering TM2 to TM3. Sequence homology has shown a conserved GWGxP motif in TM4 of family B GPCRs. The role for this GWGxP motif is believed to be structural, based around the kink formation of proline

residues in a helix. However, the exact role for this motif is unclear as the two crystal structures of inactive family B TMDs show this motif in different conformations.

Some family B GPCRs have the ability to interact with receptor activity modifying proteins (RAMPs) (McLatchie et al., 1998). RAMPs are a small family of 3 proteins (named RAMP1-3) which consist of an N-terminus (~90-103 residues), a single transmembrane spanning helix (~22 residues) and a short C-terminus (~9 residues). RAMPs form complexes with some family B GPCRs to produce an altered receptor pharmacology. The structured N-terminus of RAMPs is the main site of interaction with GPCRs and the main determinant of the pharmacology of the resulting complex (Fraser et al., 1999, Zumpe et al., 2000). Spontaneous hetero-dimerisation with RAMPs, ubiquitously expressed in all cell types studied (Sexton et al., 2001), has introduced extra complexity to the study of family B GPCRs.

1.4   Post-translational modifications

There are several post-translational modifications that are conferred to GPCRs. Their effect on structure and function seems to vary between GPCRs. Palmitoylation of cysteine residues in the C-terminus can lead to the formation and anchoring of an 8th helix to the membrane, as seen in some crystal structures (Palczewski et al., 2000). This has been shown to play a role in structure and function of some GPCRs (Hawtin et al., 2001). Ubiquitination is the application of ubiquitin to the intracellular domains of GPCRs. Ubiquitin is a determinant of GPCR fate upon endocytosis, presence of ubiquitin targets the GPCR to lysosomes for degradation (Ciechanover, 2010).

Most GPCRs undergo glycosylation of their extracellular domains before trafficking to the cell surface. Glycosylation involves the addition of an oligosaccharide to the Asn or Ser/Thr

of an NxS/T motif. There are two forms of glycosylation: in N-linked glycosylation, performed initially in the ER and refined in Golgi apparatus, the oligosaccharide is linked to the nitrogen of asparagine; O-linked glycosylation, performed in the Golgi apparatus, is rare in GPCRs but can occur as oligosaccharides are linked to hydroxyl groups of serine or threonine. Glycosylation can result in a variety of oligosaccharide chains being attached to the GPCR. Different oligosaccharide chains, created from different combinations of saccharides, can be applied. This results in unpredictable molecular weights of glycosylated proteins (Wheatley and Hawtin, 1999). The role of glycosylation varies depending on the GPCR. It has been demonstrated that glycosylation is largely important for correct protein folding and transport to the membrane (Zhang et al., 1995, Davidson et al., 1996). For some receptors glycosylation has been shown to be important in correct protein function, as demonstrated by ligand binding and G-protein interaction (Rands et al., 1990). Other receptors have no known functional implications of glycosylation (van Koppen and Nathanson, 1990, Piersen et al., 1994, Kimura et al., 1997).

1.5   Models for GPCR activation and signalling

The idea that GPCRs were inactive until agonist bound, at which point coupling and signalling through G-proteins was permitted, is insufficient to explain the complex nature of GPCR signalling. Models of GPCR activation have been proposed and extended as the complexity of GPCR signalling has been elucidated from experimental data. The original ternary complex model explained the ability of a GPCR to bind an agonist, leading to signalling via an intracellular intermediary (De Lean et al., 1980). This was found to be insufficient when constitutively active GPCRs were observed. The extended ternary complex incorporated constitutive activity to explain agonist independent signalling via G-

proteins. This investigation also elucidated the effect of G-protein pre-coupling to GPCRs, increasing agonist affinity of GPCRs (Samama et al., 1993). A progression on the extended ternary complex model was the cubic ternary complex model (Weiss et al., 1996). This explained the ability of receptors to form complexes with G-proteins, without signalling, in the presence of an inverse agonist.

The basis for each of the ternary complex models is that GPCRs signal only through G-proteins. However, it has also been shown that GPCRs signal through G-protein independent pathways. This has been well documented to involve β-arrestin. It has long been understood that β-arrestins prevent GPCR:G-protein coupling. According to previous models, this should decrease GPCR agonist affinity, instead the opposite was observed (Gurevich et al., 1997). β-arrestins act as protein scaffolds, by drawing together different components of signalling pathways within close proximity of each other, they facilitate GPCR signal transduction without G-proteins (DeWire et al., 2007). Since the discovery that GPCRs signal via different pathways than just G-proteins, agonists have been identified that can preferentially signal through specific pathways. The ability of "biased agonists" to signal through specific pathways is facilitated by the close proximity of the GPCR and the appropriate transducer as a result of β-arrestin acting as a protein scaffold (Strachan et al., 2014). Although precise mechanisms underlying biased agonism are not fully understood, there is great interest from pharmaceutical companies to design and create biased agonists. The ability to signal through one pathway, while antagonising others, thus reducing side-effects from low specificity, could lead to the discovery of much safer drugs (Whalen et al., 2011, Kenakin, 2012).

1.6 Inactivation of GPCR signalling

GPCR signal regulation is essential and can be effected through several mechanisms. Signalling via second messenger molecules: cAMP, InsP$_3$ and DAG is stopped by: cAMP phosphodiesterases (cleavage of cAMP into phosphate and adenosine), phosphatidylinositol phosphatases (cleavage of InsP$_3$ into inositol and phosphates) and diacylglycerol kinases (applies phosphates to diacyglycerol) respectively (Luttrell, 2008). Regulation of signalling can occur upstream of second messengers. The inherant GTPase activity of the Gα subunit can be increased, deactivating the G-protein and preventing its signalling through reassociation with Gβγ (Ross, 1995, Ross and Wilkie, 2000). Regulation of the GPCR upon agonist binding is presented in figure 1.6. Within seconds of agonist exposure the GPCR is desensitised, preventing GPCR:G-protein coupling. Initially, serine and threonine residues on the intracellular loops and C-terminus of the GPCR are phosphorylated by G-protein-coupled receptor kinases (GRKs). This has been shown to uncouple GPCR:G-protein interactions in some cases (Pitcher et al., 1992). GPCR:G-protein coupling is completely prevented when arrestin molecules interact with the phosphorylated residues of the GPCR and occupy the TM-core (Gurevich and Gurevich, 2004, Shukla et al., 2013, Shukla et al., 2014). Longer-term regulation of GPCR signalling involves sequestration. Arrestins contain a C-terminal motif that binds to clathrin and β$_2$-adaptin of the adaptin complex AP-2 (Goodman et al., 1996, Laporte et al., 1999). The GPCR then undergoes clathrin-coated pit mediated endocytosis. Upon endocytosis the GPCR faces one of two fates: dissociation from arrestin and subsequent recycling to the cell surface or lysosomal degradation as a GPCR:arrestin complex (Oakley et al., 1999).
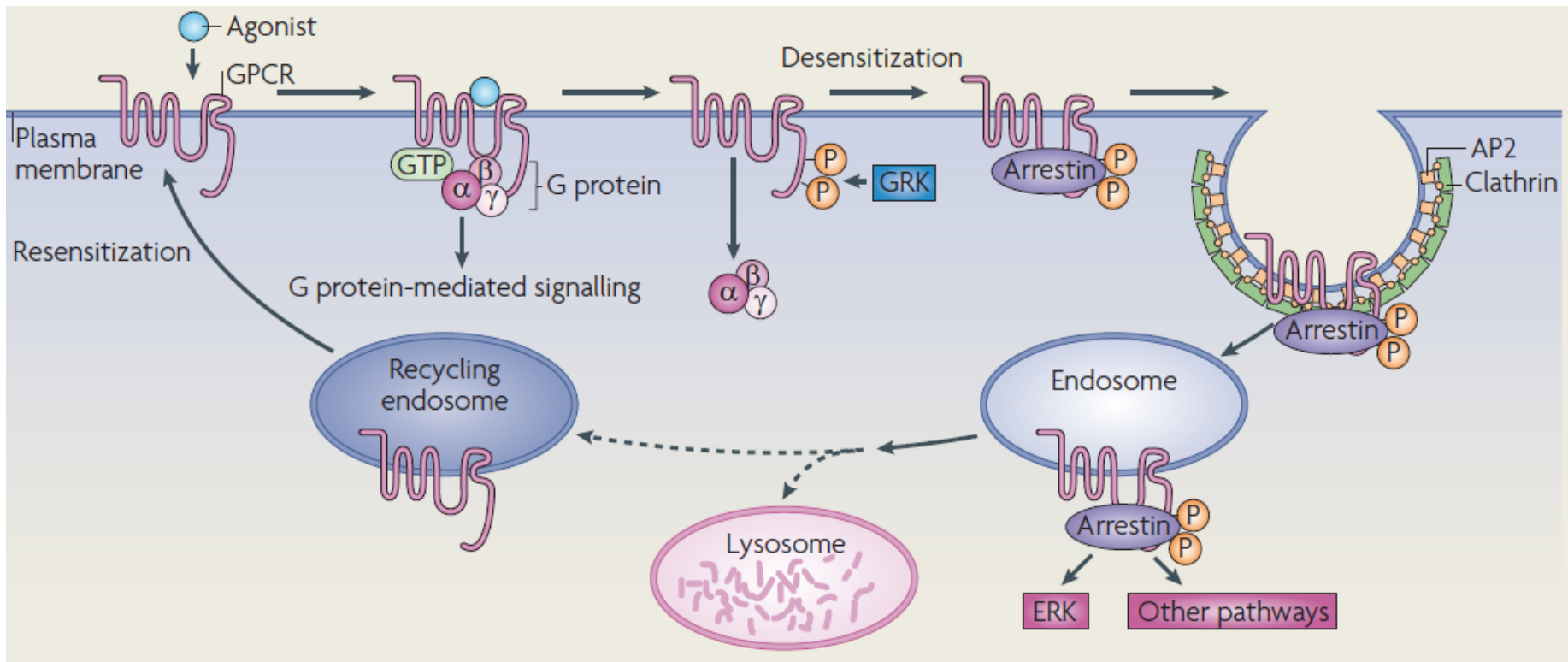
Figure 1.6. Mechanisms of GPCR inactivation. Agonist binding to GPCRs results in G-protein mediated intracellular signalling. Phosphorylation of GPCR intracellular domains by G-protein-coupled receptor kinases (GRK) is followed by arrestin recruitment, preventing GPCR:G-protein coupling leading to GPCR desensitisation. Arrestin targets the GPCR to clathrin-coated pits and is sequestered by endocytosis to be either lysosomally degraded or recycled back to the cell surface. Image taken from Ritter and Hall, 2009.

1.7 Adenosine

Adenosine is a small molecule with an approximate molecular weight (M_W) of 267 Da. A purine nucleoside, adenosine is often produced as a result of the breakdown of adenine nucleosides and adenosine phosphates. In the human body, in cells and tissue fluid, adenosine is present at 10-200 nM as a resting concentration, this rises to ~30 μM under biological stress (Fredholm, 2010). First identified as a signalling molecule in 1929 (Drury and Szent-Gyorgyi, 1929), adenosine is the endogenous ligand for a subsect of family A GPCRs known as adenosine receptors.

1.7.1 Adenosine receptors

The ability of adenosine receptors to bind adenosine and stimulate or inhibit cAMP production was first identified in 1979 (van Calker et al., 1979). Since then, sequence homology and the ability of adenosine receptor subtypes to produce different responses has lead to the identification of 4 distinct adenosine receptors (Londos et al., 1980, Bruns et al., 1986, Zhou et al., 1992). The major roles of adenosine receptor subtypes A1 (A_1R), A2a ($A_{2a}R$), A2b ($A_{2b}R$) and A3 (A_3R) are summarised in table 1.1. The overall role of adenosine receptors is for cytoprotection (Fredholm, 2007). $A_{2a}R$ is one of the most thoroughly studied GPCRs. The structure of $A_{2a}R$ has been solved 9 times in inactive (Dore et al., 2011) and active (Xu et al., 2011) conformations. Interest in adenosine receptors is high due to their cytoprotective nature. Development of better drugs at adenosine receptors is believed to aid treatment of: cardiac arrest (by targeting A_1R), neurodegenerative disorders Alzheimer's disease and Parkinson's disease and immunosuppression for graft versus host disease ($A_{2a}R$), nociception ($A_{2b}R$) and inflammation associated with immune response (A_3R).

There exists a library of well characterised ligands with defined specificities for each adenosine receptor. Among the vast library of adenosine receptor ligands there are adenosine analogues such

Adenosine receptor subtype	G-protein	Major physiological roles
A_1R	G_i	Bradychardia and antinociception
$A_{2a}R$	G_s	Vasodilation, inhibition of platelet aggregation and ischaemic damage limitation
$A_{2b}R$	G_s	Monocyte and macrophage inhibition and vascular smooth muscle relaxation
A_3R	G_i	Promotes mediator release from mast cells

Table 1.1. Physiological roles of adenosine receptor subtypes. Physiological roles affected by adenosine receptor subtypes and the G-protein they are mediated through.

as NECA, which have been developed as agonists (figure 1.7). Regadenoson is an agonist at $A_{2a}R$ that has FDA approval for use in medical studies of the heart. Xanthine analogues such as caffeine, approved for use in treatment of Parkinson's disease, and ZM241385 are adenosine receptor antagonists (figure 1.7). Other antagonists of adenosine receptors that have FDA approval for use in Parkinson's disease treatment are theophylline and istradefylline, both of which are caffeine analogues.

1.8 Neurohypophysial hormones

Oxytocin (OT) and [Arg^8]vasopressin (AVP) (figure 1.8) are the canonical neurohypophysial hormones. OT and AVP are structurally similar nonapeptides containing a Cys^1-Cys^6 disulphide bond. The two hormones differ in sequence in two positions: Ile^3 and Leu^8 of OT are Phe^3 and Arg^8 in AVP. Synthesised in the hypothalamus, they are released into the blood stream to travel to their receptors and effect their response.

1.8.1 Neurohypophysial hormone receptors

Upon OT binding, the oxytocin receptor (OTR) stimulates contraction of the uterus during labour and lactation from mammary glands (Soloff et al., 1979). OTR is a family A GPCR that signals through the G_q-coupled pathway. OTR binds OT with high affinity but also binds AVP with high affinity, however OT behaves as a full agonist, while AVP acts as a partial agonist, displaying reduced efficacy compared to OT (Wootten et al., 2011).

AVP acts as a full agonist at three receptor subtypes: vasopressin 1a, 1b and 2 receptors ($V_{1a}R$, $V_{1b}R$ and V_2R respectively) (Michell et al., 1979). Each of the three vasopressin receptor subtypes is a family A GPCR. $V_{1a}R$ is responsible for the majority of the effects of AVP. AVP binding to
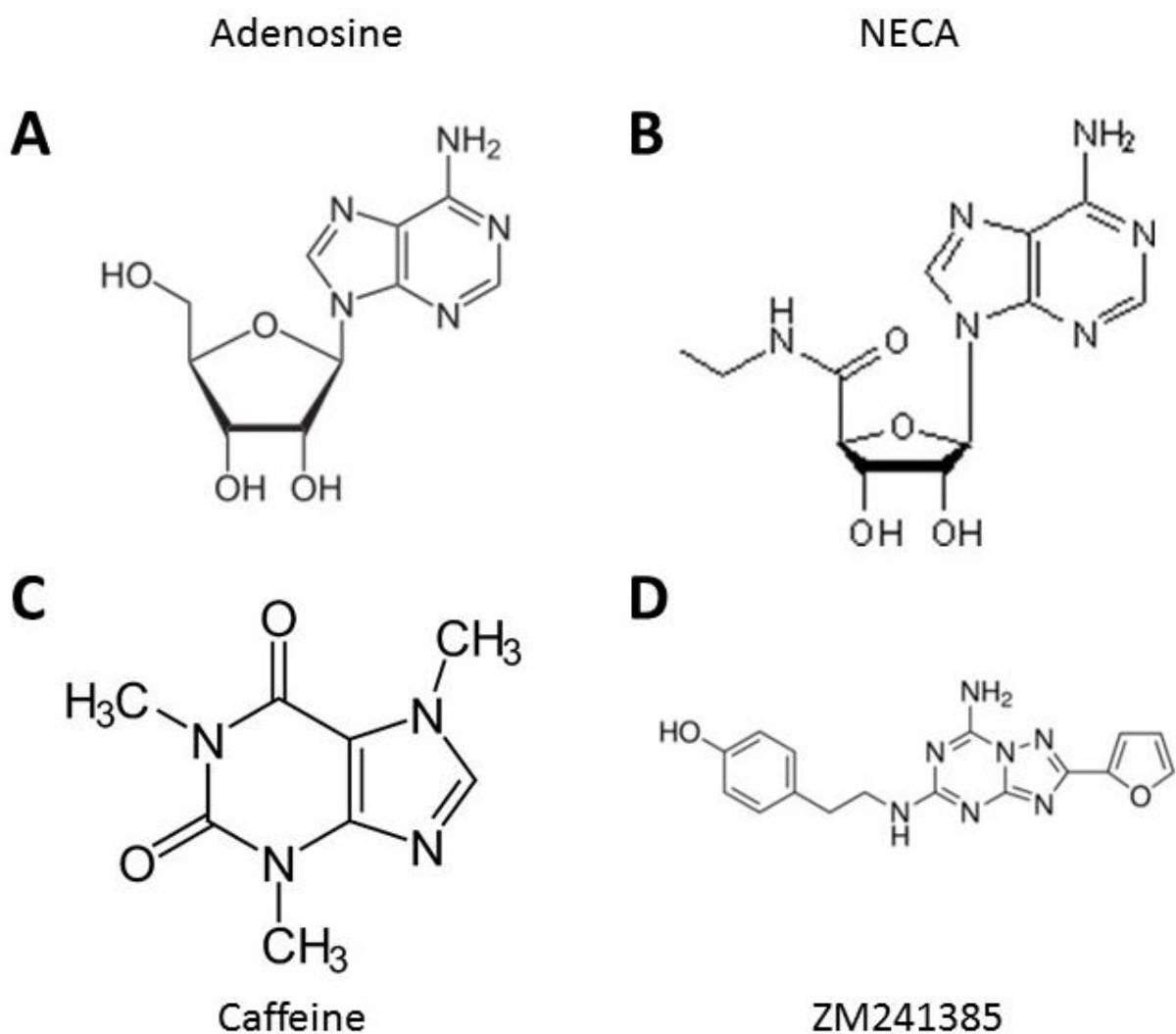
Figure 1.7. Ligands for the adenosine receptor family of GPCRs. (A) adenosine, the endogenous ligand for adenosine receptors, is constructed of the purine adenine and ribose. (B) NECA is a synthetic adenosine analogue that is an agonist at the adenosine receptors. (C) caffeine is one of the most commonly used drugs in the world and acts as an antagonist at adenosine receptors. (D) ZM241385 is a synthetic inverse agonist at adenosine receptors.

Oxytocin
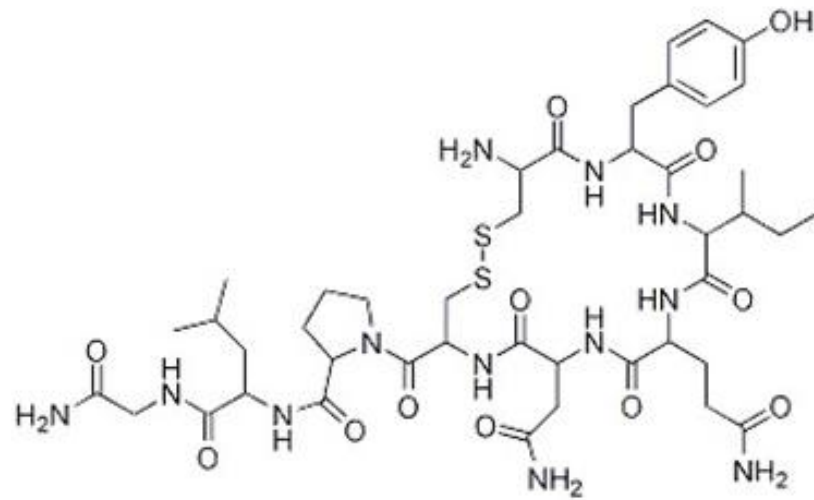
[Arg⁸]vasopressin

Cys-Tyr-Ile-Gln-Asn-Cys-Pro-Leu-Gly
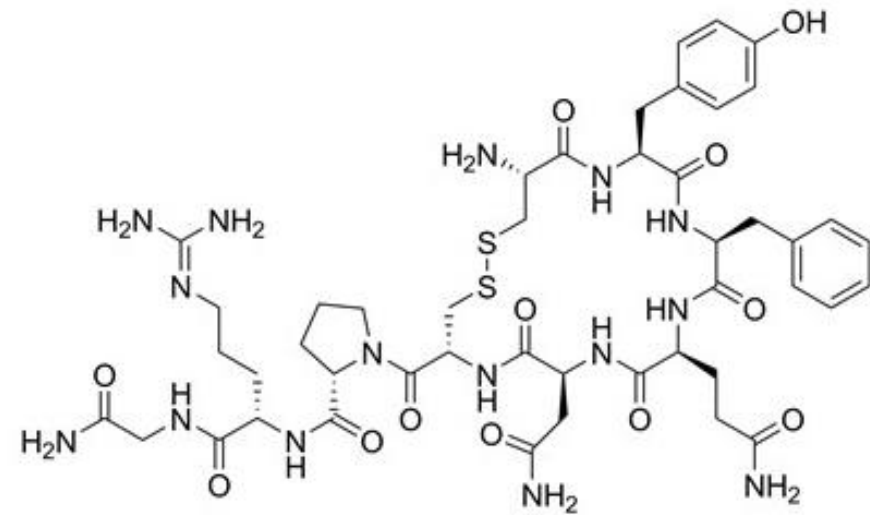
Cys-Tyr-Phe-Gln-Asn-Cys-Pro-Arg-Gly

Figure 1.8. Structure of oxytocin and AVP. Structure and peptide sequence of the nonapeptides oxytocin and AVP are displayed on the left and right respectively.

$V_{1a}R$ results in: contraction of smooth muscle (Penit et al., 1983); increased glycogenolysis (Howl et al., 1991); modulation of insulin secretion (Dunning et al., 1984) and platelet aggregation (Filep and Rosenkranz, 1987). $V_{1a}R$ signals via the G_q-coupled pathway, as does $V_{1b}R$ responsible for adrenocorticotropic hormone release (Gillies et al., 1982). V_2R is expressed predominantly in the kidneys where it plays a key role in antidiuresis (Jard et al., 1975), signalling via the G_s-coupled pathway.

1.9   Acetylcholine and muscarinic receptors

Acetylcholine is a small molecule that acts in signal transmission across synapses. Acetylcholine is a low affinity agonist at muscarinic receptors which are expressed throughout the central and peripheral nervous systems. Members of GPCR family A, the muscarinic acetylcholine receptors have 5 subtypes: muscarinic acetylcholine receptors 1-5 (M1-5R) (Peralta et al., 1987, Bonner et al., 1988). M2R and M4R both signal via the G_i-coupled pathway, whereas M1R, M3R and M5R signal through the G_q-coupled pathway. Muscarinic acetylcholine receptors have been implicated in several diseases, such as: Alzheimer's disease, schizophrenia and diabetes (Wess et al., 2007), making them popular targets for drug development. Structure-based drug design will have been aided by the solved crystal structures of: antagonist-bound M2R (Haga et al., 2012) and M3R (Thorsen et al., 2014) as well as agonist-bound M2R (Kruse et al., 2013).

1.10 Calcitonin and amylin

Calcitonin is a peptide of 32 residues involved in protection of the skeleton during periods of high calcium requirement (Wimalawansa, 1997). As a member of the calcitonin gene peptide superfamily, calcitonin is closely related to calcitonin gene-related peptide (involved in vasodilation) and amylin. Amylin is secreted from pancreatic cells and works to decrease the

requirement of insulin by slowing the influx of glucose into the bloodstream following a meal (Pittner et al., 1994).

The calcitonin receptor (CTR) is a family B GPCR that signals through the G_s-coupled pathway. The endogenously expressed calcitonin subtype in humans will only bind to CTR in the absence of RAMPs (Hay et al., 2005). CTR interaction with RAMPs creates high affinity amylin receptors named AMY_{1-3} based on the RAMP they associate with (Armour et al., 1999). This has made study of CTR difficult as all cell types express at least one form of RAMP (Sexton et al., 2001). However, the unique pharmacological profiles of each amylin receptor in comparison to each other and CTR can allow identification of specifc heterodimeric complexes. Expression of specific AMY receptors and CTR can be achieved through expression in carefully selected cell types (Christopoulos et al., 1999). This can allow study of this pharmaceutically relevant class of receptors that have already been identified as drug targets for bone disorders and diabetes (Henriksen et al., 2010, Younk et al., 2011).

1.11 Biophysical analysis of GPCRs

In drug development, understanding of the structure and dynamics of target proteins can provide insights into how to create more specific drugs, or identify new binding sites for new drugs. Biophysical analysis allows detailed information, at a molecular level, of the structure, function and dynamics of proteins. However, a prerequisite for many of these techniques is that the protein is soluble in aqueous solution. Solubilisation of hydrophobic membrane proteins is commonly achieved through use of surfactants, often referred to as detergents.

1.11.1 Detergents

Detergents are amphipathic molecules which possess hydrophobic and hydrophilic groups. In aqueous solution they are driven to form detergent micelles in which the polar head groups confer solubility on the micelle, while the hydrophobic hydrocarbon chains are shielded from

solution. When introduced to cell plasma membranes, detergents readily incorporate into the outer layer of lipid. Curvophilic detergents introduce a curvature to the membrane, unfavourable for the close- packing of curvophobic lipids (Stuart and Boekema, 2007).The smaller detergent molecules, such as Triton X-100 (Alonso et al., 1987), are able to rapidly change, "flip-flop", between the two layers of lipid (Kragh-Hansen et al., 1998). When the detergent has saturated both layers of the membrane, the membrane will fully solubilise into detergent micelles. The flip-flop of these smaller detergents allows solubilisation to occur quickly. Larger detergents, such as n-dodecyl β-D-maltoside (DDM), are unable to flip-flop between lipid layers. Instead these detergents continue to saturate only the outer layer of the membrane, resulting in a curvature that is unfavourable for lipid packing. When the detergent concentration in the membrane outer layer is high enough, the induced curvature causes perturbations in the lipid packing, allowing detergent access to the other layer (de Foresta et al., 1989). This ultimately allows sections of membrane to be solubilised in detergent micelles. Inablity to flip-flop means the larger detergents are slower at solubilising membranes. However, the reduced speed of solubilisation does appear to increase the stability of the solubilised proteins (de Foresta et al., 1989, Kragh-Hansen et al., 1998, Stuart and Boekema, 2007). Cholesterol is also routinely added during detergent solubilisation, in the form of cholesteryl hemisuccinate (CHS), to further increase the stability of the extracted protein (Toro et al., 2009, Attrill et al., 2009).

Detergent-solubilisation of membranes results in fragments of the membrane being incorporated into detergent micelles. This includes membrane proteins, which hydrophobically interact with the detergents, creating molecularly dispersed proteins that are soluble in aqueous solution and able to be studied in a wide range of biophysical techniques. For each protein to be solubilised, many detergents are investigated to identify which detergent will extract the protein while retaining protein structure and function. For GPCR solubilisation with detergents,

DDM is known to extract GPCRs with better retention of protein function than most other detergents. However, the solubilised membrane protein sample never retains 100 % functional activity. This is thought to be a result of the induced membrane perturbations caused by high detergent concentration in the outer lipid layer causing membrane protein structural defects (Pantaler et al., 2000).

Detergent micelles are constantly changing in order to minimise the volume of solvent contained in their centre. As a result, the presence of curvophobic lipid molecules are minimised in detergent micelles. This effectively strips membrane proteins of their lipid annulus (lipid which immediately surrounds the protein), which has been shown to contribute towards membrane protein stability and function (Sixl and Watts, 1983, Gibson and Brown, 1993, Lee, 2004). The detergent micelle that forms around the membrane protein is a poor mimic of the native lipid annulus. There is a subsequent change in lateral pressure exerted on the membrane protein, resulting in an altered protein conformation (Marsh, 2007). As a result of this, detergent-solubilised proteins are known to be unstable, often irreversibly aggregated and generally require use within hours of preparation. Detergents are therefore able to solubilise membrane proteins, but the detergent-solubilised protein may not be in a native conformation or behave as in its native lipid environment. Furthermore, irreversible aggregation of detergent-solubilised proteins can render the protein unviable for use in downstream analyses.

1.11.2 Alternatives to detergents

Despite the knowledge of membrane proteins detergents have provided, their inherent disadvantages have necessitated the search for alternative means of stabilising solubilised membrane proteins in aqueous solution. Among the most successful alternatives to be investigated are: apolipoprotein stabilised nanodiscs; fluorinated surfactants and amphipathic polymers. High density lipoprotein apoA-1-stabilised nanodiscs (herein referred to as

nanodiscs), pioneered by the Sligar group, are one of the most thoroughly investigated systems to date (Bayburt et al., 1998). There have been a range of different membrane proteins that have been studied using nanodiscs, including one of the canonical family A GPCRs β_2 adrenergic receptor (Leitz et al., 2006). Nanodiscs provide a defined lipid bilayer, surrounded by a belt of apolipoproteins, as shown in figure 1.9, with defined diameters between 10 and 20 nm (Nath et al., 2007). The defined nature of the nanodisc allows for specific lipid environments, displaying phase transitions similar to those observed in lipid bilayers (Shaw et al., 2004, Denisov et al., 2005). Although it is possible for more than one protein to exist in each individual nanodisc, aggregation of proteins between nanodiscs is prevented by the apolipoprotein belt. This allows for predominantly monodisperse membrane protein preparations with little variation between samples that have displayed increased thermostability to membrane proteins in detergent micelles (Banerjee et al., 2008).

Nanodisc assembly involves incubation of detergent-solubilised proteins with a desired lipid and the apolipoprotein. These reagents then assemble to form the apolipoprotein-belted, defined nanodiscs, in which the membrane protein is surrounded by a native-like lipid annulus (Leitz et al., 2006, Nath et al., 2007). The major problem with nanodiscs as a method of stabilising membrane proteins in aqueous solution is the initial requirement for detergent solubilisation. All structural defects created by detergent solubilisation of membrane proteins are introduced before stabilisation of the protein by nanodiscs. The lipid environment inside the nanodisc can only be "native-like". Although providing a better mimic than detergents for the native membrane environment, it lacks the diversity of lipids that constitutes the native lipid annulus. Finally, the apolipoprotein belt is constructed of α-helical proteins. This prevents the use of nanodiscs for the study of membrane proteins in several biophysical techniques, including nuclear magnetic resonance (NMR) and circular dichroism (CD).
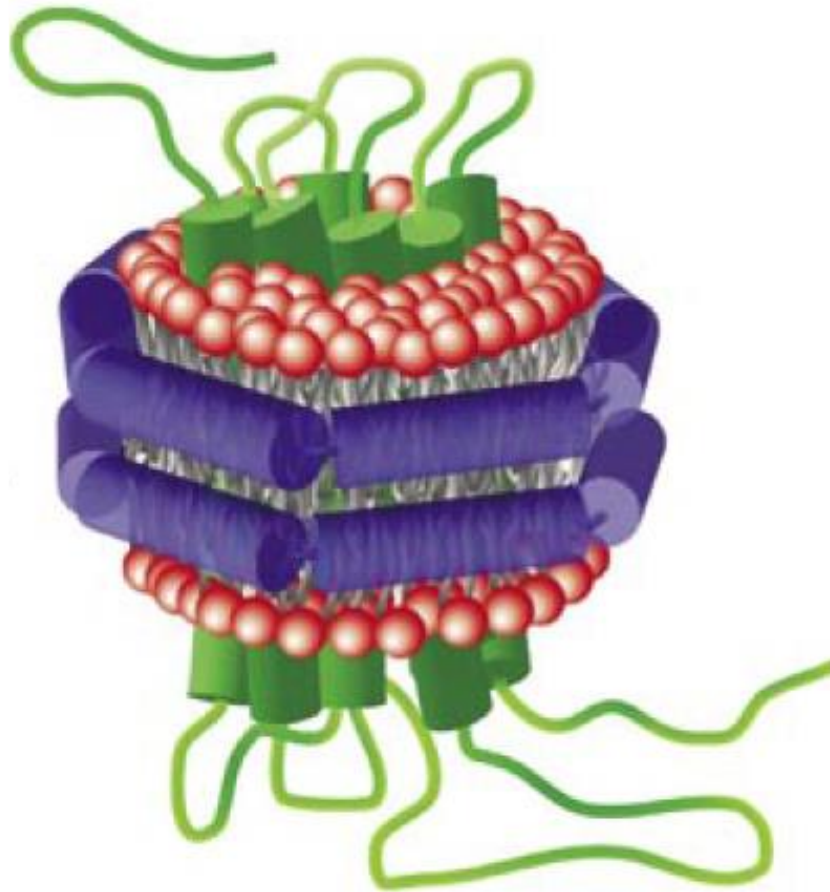
Figure 1.9. Representation of the β2 adrenergic receptor in an apolipoprotein stabilised nanodisc. The family A GPCR β2 adrenergic receptor, displayed in green, as it may look in a nanodisc. Native-like lipid bilayer, displayed in red, surrounds the GPCR and stabilised by the apolipoprotein belt (purple) surrounding the nanodisc. Image taken from Leitz et al., 2006.

Fluorinated and hemifluorinated surfactants are structurally similar to detergents, but contain fluorine in the alkyl chains. The presence of fluorine causes the alkyl chains to adopt a more rigid conformation than detergents. This has reportedly improved membrane protein stability in small, well-defined complexes and has not impeded membrane protein studies (Chabaud et al., 1998, Breyton et al., 2004). However, as with nanodiscs, fluorinated surfactants are unable to solubilise membrane proteins (Chabaud et al., 1998) and rely on an initial detergent-solubilisation step. Proteins are stabilised by fluorinated surfactants due to: less favourable partitioning of lipids and other hydrophobic membrane components; low affinity of fluorinated alkyl chains for the lipophilic transmembrane regions of proteins, allowing retention of protein:protein interactions (Popot, 2010). These properties prevent any part of the lipid annulus to be retained with the solubilised protein, affecting receptor function. They have also been shown to drive protein aggregation, limiting their use in biophysical analyses (Chabaud et al., 1998, Der Mardirossian et al., 1998).

Amphipols are short amphipathic polymers that can associate with the lipophilic TM region of membrane proteins (Popot, 2010). Use of detergents prior to membrane protein stabilisation is a major disadvantage for most of the systems that have been investigated for protein stabilisation, and this is the case for the majority of amphipols (Zoonens et al., 2007, Gohon et al., 2008). However, some amphipathic polymers have been shown to solubilise proteins directly from membranes, in the absence of detergents (Popot et al., 2003). The non-peptide nature of the amphipols has allowed biophysical analysis of proteins through Förster resonance energy transfer (FRET) (Zoonens et al., 2007) and NMR (Zoonens et al., 2005) which would not be possible with the protein-based nanodisc system. However, even when proteins can be solubilised directly from membranes, the association of amphipols with the TM regions of membrane proteins prevents the solubilisation of much of the annular lipid. Protein structure and function is therefore still altered upon solubilisation. Protein aggregation is still a problem

seen through use of amphipols (Popot, 2010), limiting their use in biophysical analyses. The alkyl chain of amphipols has also been shown to interact with the hydrophobic core of solubilised receptors, preventing their use in studies requiring ligand binding (Popot, 2010).

1.12 Styrene maleic acid

Styrene maleic acid (SMA) is an amphipathic polymer consisting of hydrophilic maleic acid and hydrophobic styrene repeating subunits (displayed in figure 1.10). SMA can exist as polymers of styrene:maleic acid subunits at different ratios, providing different characteristics to the resulting polymer. SMA has been used to confer improved heat and impact resistance to several plastics, as well as paint emulsifiers and production of glossed paper. Other than its applications in the plastics industry, SMA has also been used in the cosmeceutical industry, by Malvern cosmeceuticals, and has passed phase II clinical trials for use as a reversible male sterilising agent (Guha et al., 1997). SMA has also been used as a drug delivery system specifically targeting tumours (Greish et al., 2005, Parayath et al., 2015). In recent years SMA has been identified as a means of solubilising membrane proteins without the use of detergents (Knowles et al., 2009).

Most alternative methods of stabilising solubilised membrane proteins have required an initial detergent solubilisation step. This is detrimental to protein structure and function as a result of the detergent solubilisation of membranes, and removal of annular lipid from membrane proteins. The ideal method of protein solubilisation would not require the use of detergents at any stage, and solubilise proteins with their lipid annulus intact. SMA was found to spontaneously incorporate fragments of membranes, including membrane proteins, without the need for prior solubilisation (Knowles et al., 2009, Jamshad et al., 2011). SMA is a hydrophobically associating polymer (Tonge and Tighe, 2001) which partitions into the lipid bilayer of a membrane, driven by the hydrophobic styrene groups.
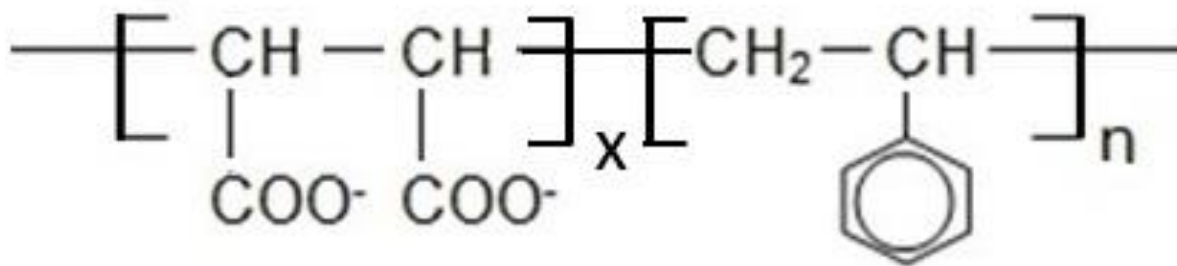
Figure 1.10. Structure of styrene maleic acid. SMA polymer is comprised of repeating subunits of maleic acid and styrene. The ratio of styrene:maleic acid can produce a more (increased styrene) or less (increased maleic acid) hydrophobic polymer.

Although the exact mechanism of membrane solubilisation with SMA has not been fully elucidated, it is believed that in the membrane SMA chains undergo spontaneous polymerisation to form longer chains. This spontaneous polymerisation in the membrane allows for SMA discs of different diameters. Once a disc has been formed there is a re-orientation of the styrene and maleic acid groups around the highly flexible, carbon-carbon single bond, backbone. This allows the lipophilic styrene groups to interact with lipids and membrane proteins (Postis et al., 2015), while the hydrophilic maleic acid groups orientate to the outside of the disc conferring a strong negative charge, and solubility in aqueous solution, to the discs (Scheidelaar et al., 2015). SMA lipid particles (SMALPs) are then freely dispersed in aqueous solution, displayed in figure 1.11. This has allowed analysis through a range of biophysical techniques including CD (Knowles et al., 2009) and electron paramagnetic resonance (Orwick-Rydmark et al., 2012) which would not be available in systems such as the nanodiscs.

Since the initial study, interest in the SMALP-solubilisation technique has grown. Although some studies have used the more hydrophobic 3:1 styrene:maleic acid (molar ratio) polymer (Orwick-Rydmark et al., 2012, Long et al., 2013, Bell et al., 2015); SMA in a 2:1 styrene:maleic acid molar ratio has been the more commonly studied form of SMA. It has been demonstrated that SMALPs have no preference for any lipid type investigated and that proteins can be SMALP-solubilised and reconstituted into lipid bilayers in a functional state (Dorr et al., 2014). SMALP containing only lipids have an average size of approximately 10-12 nm in diameter (Knowles et al., 2009, Scheidelaar et al., 2015). However, presence of one or more proteins within the SMALP has been shown to increase the diameter of the SMALP up to 24 ± 5 nm (Paulin et al., 2014). This allows for incorporation of large proteins and complexes which would not be possible in the restricted nanodisc system (Postis et al., 2015).
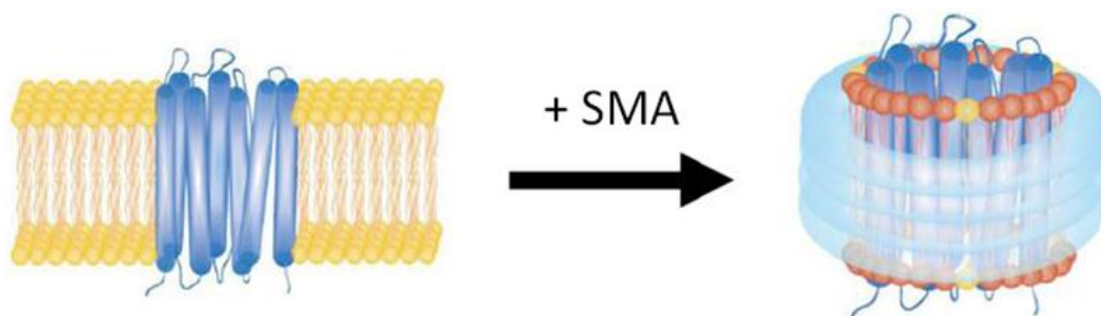
Figure 1.11. SMALP-solubilisation of a GPCR. A membrane bound GPCR (left, blue) is extracted directly from the membrane by SMA, without the use of detergents. The resulting SMALP-solubilised GPCR (right) is still surrounded by its lipid annulus and is soluble in aqueous solution with the SMA belt surrounding it (light blue). Image taken from Jamshad et al., 2011.

1.13 Aims of this study

This study aims to determine the utility of SMALPs in the solubilisation and subsequent study of the pharmaceutically relevant GPCR superfamily from mammalian cells.

The SMALP technique was first investigated for its ability to extract the pharmaceutically relevant GPCR $A_{2a}R$ from mammalian cells. SMALP-solubilised $A_{2a}R$ was further probed for retention of function through radioligand binding. The additional stability conferred to the $A_{2a}R$ through SMALP-solubilisation with its lipid annulus intact was investigated for a series of challenging conditions.

The ability of SMA to solubilise plasma membranes has been well documented. However, the ability of SMA to solubilise from intracellular membranes has not been thoroughly explored. To probe this in mammalian cells, $A_{2a}R$ constructs were engineered with ER-retention motifs to prevent plasma membrane expression and provide a tool to study the ability of SMA to solubilise intracellular membranes.

The ability of SMALPs to be used in spectroscopic studies has been documented. Based on previous studies on β_2 adrenergic receptor, an $A_{2a}R$ construct was developed. Introduction of suitable residues for derivatisation by fluorescent probes and removal of other derivitisable sites would allow fluorescence studies of $A_{2a}R$.

The need to identify different detergents for solubilisation of different proteins is a long and expensive process. The ability of SMA to be used in the solubilisation, and subsequent study of, a range of different GPCRs, from different GPCR subfamilies, was explored.

CHAPTER 2: MATERIALS AND METHODS

2.1 Materials

2.1.1 Antibodies

Polyclonal, rabbit, anti-G_s primary antibody (catalogue number: SC-823) was purchased from Santa Cruz Biotechnology (Texas, U.S.A). Monoclonal, mouse clone HA-7, anti-haemagglutanin (HA) (catalogue number: H9658) was purchased from Sigma (Dorset, UK). Horseraddish peroxidase-conjugated: anti-mouse (catalogue number: 70765) and anti-rabbit (catalogue number: 7074P2) secondary antibodies were purchased from New England Biolabs (NEB) (Hitchin, UK).

2.1.2 Cell tissue culture

Cell culture plasticware was purchased from Greiner Bio One (Gloucestershire, UK). Dulbecco's Modified Eagle's Medium (DMEM) was purchased from Scientific Laboratory Supplies (SLS) (Hessle, UK). Foetal Bovine Serum (FBS) was purchased from Sigma (Dorset, UK). Linear polyethylenimine (PEI) (catalogue number: 9002-98-6) was purchased from Polysciences Inc. (Eppelheim, Germany).

2.1.3 Molecular biology reagents

Custom oligonucleotides (synthesised to 0.2 μmole scale) and pcDNA3.1(+) mammalian expression vector were purchased from Invitrogen/Life technologies (Paisley, UK). Deoxyribonucleotides triphosphates (dNTPs) and Isolate II plasmid mini prep kit were purchased from Bioline (London, UK). Axyprep DNA gel extraction kit was purchased from Fisher scientific (Loughbourough, UK). *Pfu* DNA polymerase and Pureyield plasmid maxiprep kit were purchased from Promega (Southampton, UK). *Dpn*I, *Apa*I and *Xba*I restriction enzymes and T4 DNA ligase were purchased from NEB (Hitchin, UK).

2.1.4 Radioligand binding reagents

N-(2-aminoethyl)-2-[4-(2,3,6,7-tetrahydro-2,6-dioxo-1,3-dipropyl-1*H*-purin-8-yl)phenoxy]-acetamide, Xanthine Amine Congener (XAC); 4-(2-[7-amino-2-[2-furyl][1,2,4]triazolo[2,3-a][1,3,5]triazin-5-yl-amino]ethyl)phenol (ZM241385); 1-(6-amino-9H-purin-9-yl)-1-deoxy-N-ethyl-β-D-ribofuranuronamide, 5'(N-ethylcarboxamido)adenosine (NECA); 3,7-dihydro-1,3-dimethyl-1*H*-purine-2,6-dione (theophylline); (*RS*)-(8-Methyl-8-azabicyclo[3,2,1]oct-3-yl) 3-hydroxy-2-phenylpropanoate (atropine); Sephadex G-15, G-25, G-50 and G-75 were purchased from Sigma (Dorset, UK). [Arginine^8]vasopressin (AVP) and oxytocin (OT) were purchased from Bachem (Weil am Rhine, Germany). Adenosine deaminase was purchased from Roche (Burgess Hill, UK). Tritiated ZM241385 ([2-^{3}H]-4-(2-[7-amino-2-[2-furyl][1,2,4]triazolo[2,3-a][1,3,5]triazin-5-yl-amino]ethyl)phenol), specific activity (SA): 50 Ci/mmol, was purchased from American Radiolabelled Chemicals (Royston, UK). Tritiated AVP, [Phe-3,4,5-^{3}H]AVP, SA: 67.7-69 Ci/mmol; tritiated oxytocin, [Tyr2,6-^{3}H]oxytocin, SA: 49.9 Ci/mmol, and tritiated N-methyl scopolamine, [N-methyl-^{3}H] NMS, SA: 70-87 Ci/mmol, soluene®-350 and optiphase Hisafe™ 3 scintillant were purchased from PerkinElmer (Stevenage, UK).

2.1.5 Solubilisation reagents

Styrene maleic anhydride was purchased from Cray Valley (Pennsylvania, U.S.A). n-dodecyl β-D-maltoside (DDM) and cholesteryl hemisuccinate (CHS) were purchased from Sigma (Dorset, UK).

2.1.6 Substrates

Sigma-fast *o*-phenylenediamine dihydrochloride (OPD) was purchased from Sigma (Dorset, UK).

2.1.7 Western blotting reagents

Tetramethylethylenediamine (TEMED) and ammonium persulphate (APS) were purchased from Sigma (Dorset, UK). Hyperpage protein ladder was purchased from Bioline (London, UK). Nitrocellulose membrane was purchased from GE healthcare (Amersham, UK). 30% acrylamide 0.8% bisacrylamide and EZ-ECL chemiluminescence detection kit were purchased from Geneflow (Staffordshire, UK).

2.2 Methods

2.2.1 Site-directed mutagenesis

Mutagenic primers were designed to contain the desired mutation flanked by sequences complementary to the template DNA (pcDNA3.1(+) coding for $A_{2a}R$). Reaction mixtures were made to a final volume of 50 μl in 1 x *Pfu* buffer, containing: 100 ng of template DNA; 10 pmol of sense and antisense primers; dNTP mix (dATP, dCTP, dGTP, dTTP) at final molarity of 0.4 mM and 2-3 units of *Pfu* DNA polymerase.

Reaction conditions: Initial 95 °C for 1 min; denaturation at 95 °C for 30 sec; annealing at 55 °C for 1 min and elongation at 68 °C for 14 min. denaturation, annealing and elongation steps were repeated 11 times.

2.2.2 Polymerase-chain reaction (PCR)

Reaction mixtures were set up as above. Reaction conditions were: initial 95 °C for 1 min; denaturation at 95 °C for 1 min; annealing at 55 °C for 30 sec; elongation at 72 °C for 2.5 min; denaturation, annealing and elongation were repeated for 30 cycles before a final 72 °C elongation step for 5 min.

2.2.3 Restriction enzyme digest

Samples incubated at 37 °C for minimum of 1 h with 20 units of restriction enzyme in 1 x restriction enzyme buffer.

2.2.4 Gel electrophoresis

Samples from site-directed mutagenesis, PCR and restriction enzyme digests were examined by gel electrophoresis for identification of products. Samples were mixed with 10 x running buffer (0.25 % (w/v) bromophenol blue, 10 mM Tris, 1mM EDTA and 30 % (v/v) glycerol) 9:10. Samples were run on 1 % (w/v) agarose gels, containing 0.5 µg/ml ethidium bromide, in TAE buffer (40 mM Tris, 20 mM acetic acid and 1 mM EDTA) at approximately 80 mV for 1 h. Gels were observed using an ultraviolet light transilluminator.

2.2.5 Transformation

Chemically competent *E.coli* XL-10 gold cells were made as previously described (Sambrook, 1989). 30 µl of XL-10 gold cells were incubated with cDNA samples on ice for 20 min. Samples were heatshocked at 42 °C for 45 sec and incubated on ice for 2 min. Samples were recovered in lysogeny broth (LB-Lennox) (10 g/L peptone, 5 g/L NaCl and 5 g/L yeast extract) for 1 h at 37 °C. Cells were sedimented through centrifugation (9,500 x g, 5 min) and spread on LB agar plates containing 100 µg/ml ampicillin. Agar plates were incubated at 37 °C overnight. Individual colonies were picked to inoculate 15 ml LB-Lennox containing 100 µg/ml ampicillin and incubated, shaking, overnight at 37 °C.

2.2.6 Plasmid cDNA extraction and purification

Isolate II plasmid mini-prep kit was used as per manufacturers instructions to extract and purify approximately 5 µg of cDNA from *E.coli*. Mini-prep cDNA sequence was confirmed by automated fluorescence cDNA sequencing. cDNA production was scaled up using Pureyield plasmid maxiprep kit as per manufacturers instructions. This yielded approximately 0.5 mg of cDNA. Precise concentrations of cDNA solutions were calculated by use of a nanodrop 2000 U.V.-Vis spectrophotometer.

2.2.7 Automated fluorescence DNA sequencing

All DNA sequences were confirmed by automated fluorescence DNA sequencing (functional genomics, proteomics and metabolomics facility, University of Birmingham, UK).

2.2.8 Cell tissue culture

HEK 293T cells were cultured in Dulbecco's modified Eagle's medium supplemented with 10 % (v/v) foetal bovine serum (FBS) (hereon referred to as DMEM) and incubated at 37 °C, 5 % (v/v) CO_2. Cells were routinely passaged during log phase (~80 % confluence) every 3-4 days. Cell stocks in 90 % (v/v) FBS and 10 % (v/v) DMSO were stored in liquid nitrogen.

HEK 293T cells were seeded at a density of: ~5 x 10^5 in a 92 mm diameter dish for membrane harvesting and whole cell SMALP-solubilisation; ~1 x 10^5 per well of a 24-well plate for enzyme-linked immunosorbent assays (ELISAs); and ~2.5 x 10^4 per well of a 96-well plate for cAMP alphascreen assays. Cells were incubated at 37 °C, 5 % (v/v) CO_2 for 48 h (membrane harvesting) or 24 h (ELISAs and cAMP alphascreen assays) before transfection.

2.2.9 PEI transfection

5 % (w/v) glucose solution (sterile filtered) and 0.8 mg/ml (32 µM, based on average M_W of linear PEI polymer) PEI solution (sterile filtered) were added to DNA samples. These were allowed to complex for 30 min at room temperature (16 °C) before addition of fresh DMEM and applied to cells.

Transfection solutions for membrane harvesting and SMALP-solubilisation consisted of: 1 ml glucose solution; 48 µg PEI; and 5 µg of DNA per 92 mm dish. Transfection solutions for use in ELISAs: 30 µl glucose solution, 2 µg PEI; 0.5 µg DNA; and 500 µl DMEM per well. Transfection solutions for use in cAMP alphascreen assays: 7.5 µl glucose solution; 0.8 µg PEI; 0.125 µg DNA; and 125 µl DMEM per well.

2.2.10 Cell membrane harvesting

As previously reported (Wheatley et al., 1997). Briefly: 48 h after transfection, cells were washed with 5 ml ice cold PBS. Cells were scraped from dishes in harvesting buffer (20 mM HEPES, 1 mM EGTA, 10 mM magnesium acetate, pH 7.4) containing 250 mM sucrose and 0.1 mg/ml bacitracin. Cells were sedimented through centrifugation (4500 x g, 5 min). Cells were resuspended in harvesting buffer containing 0.1 mg/ml bacitracin and incubated on ice for 20 min. Membranes were sedimented through centrifugation (4500 x g, 5 min) and resuspended in harvesting buffer containing 250 mM sucrose. Membranes were stored at -20 °C.

2.2.11 SMA preparation

As previously described (Knowles et al., 2009). Briefly: 10 % (w/v) styrene maleic anhydride was dissolved in 1 M NaOH overnight before heating under reflux for 2 h. SMA/NaOH solution was dialysed against dialysis buffer (20 mM HEPES, 1 mM EGTA, 1 mM magnesium acetate, pH 7.4). SMA was stored at 4 °C.

2.2.12 SMALP-solubilisation of mammalian cells

Unless stated otherwise, SMALP-solubilisation was performed as follows: 48 h after transfection, cells were washed with ice cold PBS. Cells were scraped from dishes in SMALP buffer (20 mM HEPES, 1 mM EGTA, 10 mM magnesium acetate, 2 % (w/v) SMA, pH 7.4) containing 5 units/ml of benzonase and protease inhibitors. Samples were incubated at 37 °C for 1 h before centrifugation at 100,000 x g for 1 h. Supernatants were saved and insoluble material was resuspended in initial volume of harvesting buffer (20 mM HEPES, 1 mM EGTA, 10 mM magnesium acetate, pH 7.4). Samples were stored at -20 °C.

2.2.13 Detergent-solubilisation

Mammalian cell membranes were prepared as above. n-dodecyl β-D-maltoside (DDM) and cholesteryl hemisuccinate (CHS) were added to harvested membranes to a final concentration of 2.5 % (w/v) and 0.5 % (w/v) respectively. Samples were incubated rotating at 4 °C for 3 h with protease inhibitors. Samples centrifuged at 100,000 x g for 1 h and supernatants used immediately.

2.2.14 BCA protein concentration assay

Approximate protein concentrations were obtained using the Pierce BCA assay kit (life technologies, Paisley, UK), as per manufacturer's instructions. Briefly: Reagent A (containing bicinchoninic acid) was mixed with reagent B (cupric sulphate) 50:1. 1 ml was added to BSA standards and samples and incubated for 30 min at 37 °C. Absorbance readings were taken at 562 nm.

2.2.15 Alphascreen cAMP assay

Performed as per manufacturer's instructions (PerkinElmer, Stevenage, UK). Briefly: 48 h after transfection cells were incubated for 1 h, 37 °C, with stimulation buffer (Hank's balanced salt solution, 0.1 % (w/v) BSA, 5 mM HEPES, 50 μM rolipram and cilostamide, pH 7.4). Cells expressing $A_{2a}R$ constructs were stimulated for 20 min with 1×10^{-4} M NECA. Stimulation solutions were removed through aspiration before 100 % ethanol was added and allowed to evaporate. Cell lysis buffer (5 mM HEPES, 0.1 % (w/v) BSA, 0.3 % TWEEN20, pH 7.4) was added and incubated at room temperature, shaking, for 15 min. Samples were frozen at − 20 °C. Samples were thawed and transferred to opaque, white, ½ area 96 well plates and 0.5 units of acceptor beads added per well. After 30 min incubation at room temperature, 1.5 units of donor beads containing biotinylated cAMP were added. Samples were incubated overnight at room temperature and read using a Mithras LB 940 (Berthold, Bad Wildbad, Germany).

2.2.16 Competition radioligand binding assay for membrane-bound receptors

Reaction mixtures composed of: tritiated ligand; competing ligand at stated final concentrations; and harvested membrane-bound protein sample containing 25-50 μg protein, were made up to 500 μl using binding buffer (20 mM HEPES, 1 mM EGTA, 10 mM magnesium acetate, pH 7.4) containing: 0.1 % (w/v) BSA for peptide ligands; 0.1 units of adenosine deaminase for $A_{2a}R$ constructs. Non-specific binding was defined in the presence of a saturating concentration of competing ligand. Reaction mixtures were incubated at 30 °C until equilibrium was established (30-90 min). Centrifugation at 9,500 x g for 10 min separated bound from free ligand. Membranes were superficially washed and solubilised in 50 μl Soluene 350. 1 ml Hisafe3 liquid scintillation cocktail was added and samples counted using Tri-carb 2810 TR liquid scintillation analyser (PerkinElmer, Stevenage, UK) for 3 min.

2.2.17 Competition radioligand binding assay for soluble receptors

Reaction mixtures were prepared as above, containing 20-60 μg of soluble protein in a final volume of 100 μl. Non-specific binding was defined in the presence of a saturating concentration of competing ligand. Equilibrium was established at 30 °C (30-90 min). Separation of bound from free ligand was achieved by centrifugation (1000 x g, 4 min) of 50 μl reaction mixture through Sephadex packed spin columns. Void volumes were collected and 1 ml of Hisafe3 liquid scintillation cocktail was added to samples. Counting was performed on Tri-carb 2810 TR liquid scintillation analyser (PerkinElmer, Stevenage, UK) for 3 min.

2.2.18 Thermostability experiments

Protein samples were stored at set temperatures for 30 min. After 5 min on ice, specific binding was determined using the equation:

$$Specific\ binding = Total\ binding - Non-specific\ binding$$

Where: total binding was defined as DPM recorded in the absence of competing ligand; Non-specific binding was defined as DPM recorded in the presence of saturating concentrations of competing ligands.

2.2.19 Cell-surface ELISA

48 h after transfection: cells expressing $A_{2a}R$ constructs for internalisation investigations were stimulated with 1 x 10^{-4} M NECA for 1 h at 37 °C. Cells were fixed with 3.7 % (v/v) formaldehyde in PBS for 15 min at room temperature. Cells were washed 3 times with PBS and incubated in block solution (1 % (w/v) BSA in PBS), shaking, for 45 min at room temperature. Primary antibody was added to cells, at a dilution of 1:4000 in block solution, and incubated for 1 h, shaking, at room temperature. Cells were washed as before and incubated with block solution for 15 min. HRP-linked secondary antibody was added, at a dilution of 1:4000 in PBS, and incubated for 1 h (shaking at room temperature). Cells were washed 3 times in PBS and allowed to develop in the dark with 250 µl of OPD substrate (made as per manufacturer's instructions). 100 µl of sample was taken and added to 100 µl 1 M sulphuric acid to stop the reaction. Absorbance was read on an Anthos, zenyth 340 rt plate reader at 492 nm.

2.2.20 Whole cell expression ELISA

As above, including a 1 h incubation in 0.1 % (v/v) Triton X-100 in PBS after fixation with formaldehyde.

2.2.21 SDS-PAGE and Western blot

Samples were run by SDS-PAGE as previously described (Laemmli, 1970). Protein samples were incubated at room temperature for 30 min with loading buffer (50 mM Tris, 2 % (w/v) SDS, 10 % (v/v) glycerol, 0.004 % (w/v) (bromophenol blue) and 2 % (v/v) β-mercaptoethanol). Samples were loaded onto a 10 % (w/v) polyacrylamide gel with a 4 % (w/v)

polyacrylamide stacking gel. Protein markers were included for identification of protein size. 200 V was applied for approximately 45 min in denaturing running buffer (25 mM tris, 200 mM glycine, 0.1 % (w/v) SDS). Gels were washed in transfer buffer (25 mM tris, 200 mM glycine, 10 % (v/v) methanol) for 10 min, shaking at room temperature. Proteins were transferred to nitrocellulose at 100 V for 1 h in transfer buffer. Nitrocellulose was blocked in 5 % (w/v) milk in PBS for 1 h. Primary antibody was added to a final dilution of 1:5000 and incubated overnight, shaking, at 4 °C. Nitrocellulose was washed twice in wash buffer (PBS containing 0.2 % (v/v) TWEEN20) for 5 min, shaking at room temperature. HRP-linked secondary antibody was added (1:5000 dilution in 5 % (w/v) milk in PBS) and incubated at room temperature, shaking, for 45 min. Nitrocellulose was washed twice, as before, and proteins detected using EZ-ECL detection kit (as per manufacturer's instructions). Image was captured using a Uvitec alliance chemiluminescent detection system (Cambridge instruments, U.K).

2.2.22 Data analysis

All data analysis was performed using the Prism 4.0 (Graphpad, San Diego, U.S.A) computer program. All values given as the mean of 3 indiviual replicates ± S.E.M unless otherwise stated. Radioligand binding assays were plotted as a percentage of specific binding. Each plot was of at least 3 indiviudal replicates, each performed in triplicate. Nonlinear regression was used to fit one-site Langmuir binding isotherms to identify IC_{50} values. IC_{50} values were corrected for the presence of radioligand using the following equations:

$$[3H] Ligand\ concentration\ (nM)$$

$$= \frac{DPM}{Specific\ Activity\ (Cimmol^{-1}) + Sample\ Volume\ (\mu l) \times 2.22}$$

$$K_i(nM) = IC_{50} - [Free\ Radioligand](nM)$$

$$K_i \, (nM) = IC_{50} \times \frac{K_d \left[\,^3H \right] Ligand}{K_d \left[\,^3H \right] Ligand \times [Free \ Radioligand]}$$

$$Fractional \ occupancy = \frac{[Free \ Radioligand]}{K_d \left[\,^3H \right] Ligand \times [Free \ Radioligand]}$$

ELISA data were presented as histograms of percentage expression for at least 3 individual replicates, performed in at least triplicate. Internal standards for 100 % expression (wild-type (WT) receptor) and 0 % expression (mock transfected cells) were included in all investigations.

cAMP assays were plotted as a percentage of bound biotinylated-cAMP. Unstimulated WT-receptor values were taken as 100 % and forskolin stimulated cells 0 %. Each plot was of 3 individual replicates performed in duplicate. Nonlinear regression was used to fit one-site Langmuir binding isotherms for calculation of EC_{50} values and E_{max}.

CHAPTER 3: SMALP-SOLUBILISATION AND CHARACTERISATION OF $A_{2a}R$ FROM MAMMALIAN CELLS

3.1 Introduction

The study of membrane proteins has lagged behind studies of soluble proteins due to the inherent hydrophobicity of membrane proteins preventing their use in certain biophysical techniques. The use of detergents to solubilise membrane proteins has allowed some biophysical analysis. However, detergents strip away annular lipid (lipid that immediately surrounds the protein), and other membrane components, from the protein. The detergent micelle then provides only a poor mimic of the plasma membrane and exerts a different lateral pressure on proteins. This leads to conformational changes of proteins that can affect their behaviour. As a result, detergent-solubilised proteins are often conformationally unstable. Methods to stabilise detergent-solubilised proteins includes modifying proteins (a good summary has been previously reported (Maeda and Schertler, 2013)). Alternatively, insertion of detergent-solubilised proteins into apolipoprotein-stabilised nanodiscs, amphipathic polymers, or substitution of detergent for fluorinated surfactants, after detergent-solubilisation, can limit the proteins exposure to detergent. Stabilising membrane proteins by any of these mechanisms results in conformationally altered proteins that do not behave as in their natural envinronment. In order to keep the protein in its native conformation, extraction with its native lipid environment would be required.

Use of styrene maleic acid (SMA) polymer to solubilise membrane proteins into SMA lipid particles (SMALPs) appeared an attractive prospect as it allowed extraction of unmodified proteins, still with their lipid annulus intact. Solubilisation of membrane proteins, using the 2:1 (molar ratio of styrene:maleic acid) SMA polymer, has previously been demonstrated from

bacterial, yeast and insect cell expression systems (Jamshad et al., 2011, Swainsbury et al., 2014, Gulati et al., 2014). Although these systems provided a large quantity of protein, they lacked the pharmacological relevance of a mammalian expression system. For pharmaceutical studies and drug screens, a mammalian cell membrane composition would allow for the most physiologically relevant data.

Differences in membrane composition can lead to a change in receptor behaviour. Yeast membranes, for example, do not contain cholesterol, instead containing ergosterol (Finean et al., 1978). The importance of cholesterol, present in mammalian plasma membranes, has been demonstrated for the correct functioning of some GPCRs such as the oxytocin receptor, galanin receptor and β_2 adrenergic receptor (Gimpl et al., 1997, Pang et al., 1999, Zocher et al., 2012). The structure of β2 adrenergic receptor in complex with cholesterol has been solved, prompting the suggestion of a cholesterol binding motif (Hanson et al., 2008). Therefore proteins expressed and studied in yeast may lack a key component for their function. Lipid composition may also affect protein behaviour and, in some cases, such as the β_2 adrenergic receptor and rhodopsin, limit protein function (Sixl and Watts, 1983, Gibson and Brown, 1993, Lee, 2004, Hanson et al., 2012). This is especially important considering the lipid-stripping action of detergents. By using a mammalian expression system to overexpress specific proteins, SMALP-solubilisation may be employed to study proteins with their native lipid annulus intact.

The aims of this part of the study were to establish whether the SMA polymer was able to solubilise a GPCR from mammalian cells and to pharmacologically characterise the SMALP-GPCR. Using a glycosylation deficient $A_{2a}R$ (with N-terminal haemagglutinin (HA) epitope tag) as an exemplar GPCR, SMALP-solubilisation conditions were optimised.

3.2 Results

3.2.1 Optimisation of SMALP-extraction from HEK 293T cells

It was important to determine the optimal conditions for SMALP-solubilisation of $A_{2a}R$ from HEK 293T cells. This was determined for a range of conditions which can affect extraction. Each condition (SMA concentration, temperature and time) was tested sequentially and optimal extraction was taken and used as a standard condition in testing the next parameter. Samples were prepared as described in methods but with systematic variation to the condition being optimised. Briefly, HEK 293T cells expressing $A_{2a}R$ were incubated with SMA solution. Samples were centrifuged at 100,000 x g for 1 h before supernatants were collected and pellets resuspended to initial volume. Extraction efficiency was determined by Western blot analysis using anti-HA antibody to target the $A_{2a}R$.

3.2.1.1 SMA concentration

Samples were incubated for 1 h at 37 °C in the presence of SMA at concentrations of 1 % to 4 % (w/v). Samples were centrifuged for 1 h at 100,000 x g and supernatants collected before pellet was resuspended to initial volume. Supernatant and pellet fractions were separated by SDS-PAGE and transferred to nitrocellulose before probing with anti-HA antibody to reveal relative abundances of $A_{2a}R$ (expected M_W: ~45790 Da) in each sample, displayed in figure 3.1. In the absence of SMA, no extraction was observed. 1 % (w/v) SMA was able to extract a minor fraction of the total receptor, but the majority was left unsolubilised. SMA at concentrations of 2 %, 3 % and 4 % (w/v) extracted similar amounts of $A_{2a}R$ by visual inspection, solubilising the majority of $A_{2a}R$ from the cells. Optimal concentration of SMA was 2 % (w/v), providing maximum extraction using the minimum amount of polymer.
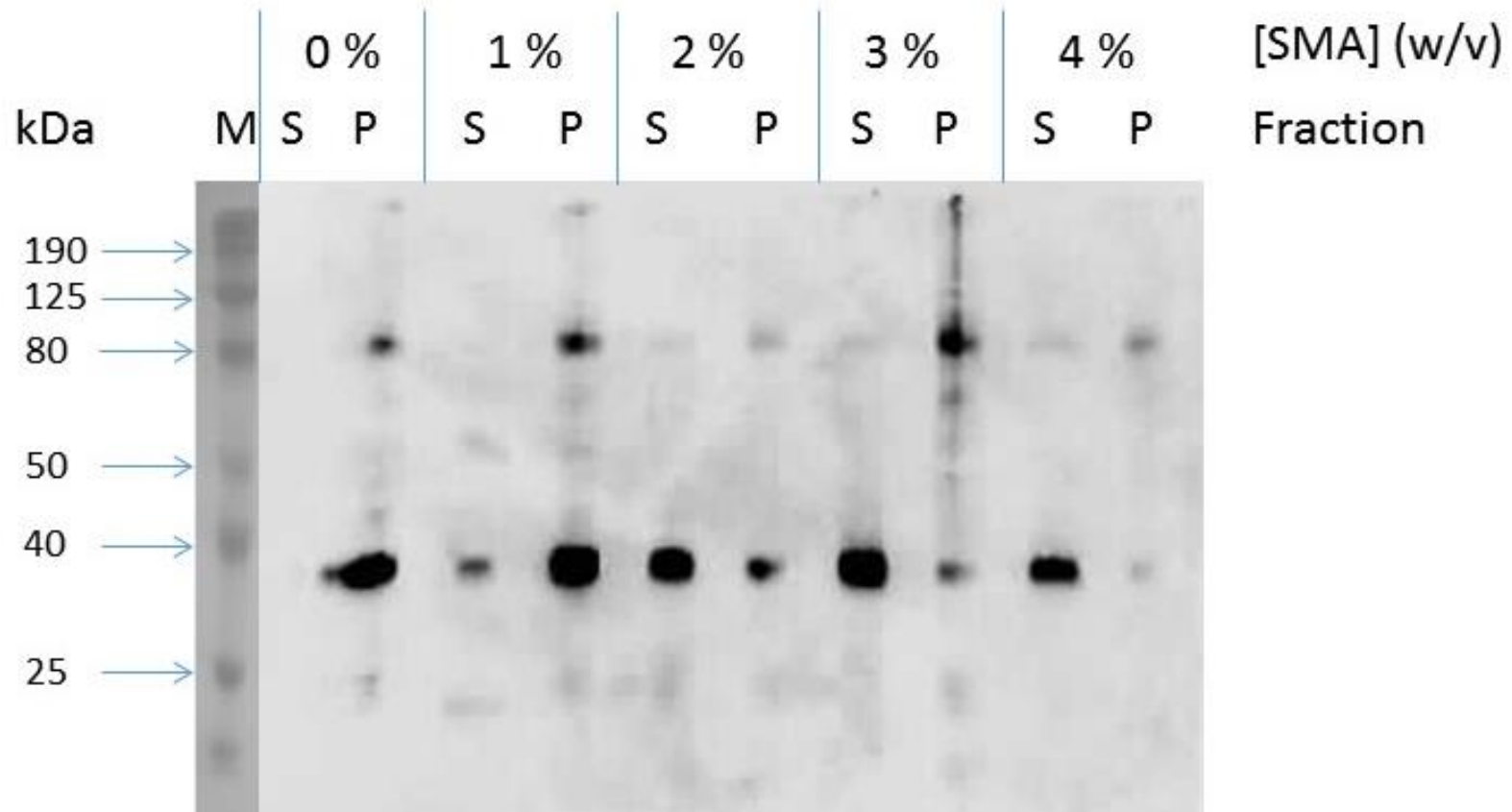
Figure 3.1. Western blot analysis of SMALP-solubilisation of $A_{2a}R$ using different concentrations of SMA. Molecular weight marker (M), soluble (S) and pellet (P) fractions of SMALP preparations, prepared with indicated concentrations of SMA, were probed with anti-HA antibody. Characteristic gel of three experiments.

3.2.1.2 Temperature of incubation

Optimal concentration of SMA, 2 % (w/v), was used to extract $A_{2a}R$ from mammalian cell membranes that were then incubated at a range of temperatures, as indicated in figure 3.2, for 1 h. Samples were then analysed by Western blot to identify the optimal incubation temperature. It was observed that at 4 °C SMALP-solubilisation of $A_{2a}R$ was not as efficient as at higher temperatures. Although samples incubated at ambient room temperature (14 °C), 25 °C and 30 °C all extracted the majority of receptor, the $A_{2a}R$ remaining in the pellet decreased with increasing temperature, with 37 °C the most efficient temperature employed. Therefore, 37 °C was considered optimal as it provided maximum extraction of $A_{2a}R$. Higher temperatures were deemed inappropriate. Although protein would be extracted, higher temperatures were thought to be detrimental to the preservation of ligand binding capabilities of $A_{2a}R$.

3.2.1.3 Time of incubation

Samples were prepared using 2 % (w/v) SMA and incubated at 37 °C for the lengths of time indicated in figure 3.3. Extraction efficiency was determined visually from Western blot analysis. It was observed that less than 1 h at 37 °C reduced the efficiency of extraction. Obviously at 0 h incubation, pre-centrifugation, only a minor fraction of the receptor was extracted to the supernatant. After 1 h the majority of the receptor was extracted to the supernatant. Time of incubation was investigated at 3 h, as shown in figure 3.4 where the amount of soluble $A_{2a}R$ after 3 h at 37 °C was similar to the amount seen without incubation at 37 °C (0 h). This was therefore less efficient than 1 h at 37 °C with 2 % (w/v) SMA (figure 3.4: incubation temperature 37 °C) which was shown to be the set of conditions that produced maximum extraction of $A_{2a}R$. From figure 3.4 it was also observed that a pre-centrifugation incubation time of 0 h provides predominantly monomeric $A_{2a}R$. The presence of apparent dimeric $A_{2a}R$ in SMALP samples was observed to increase when samples were incubated for
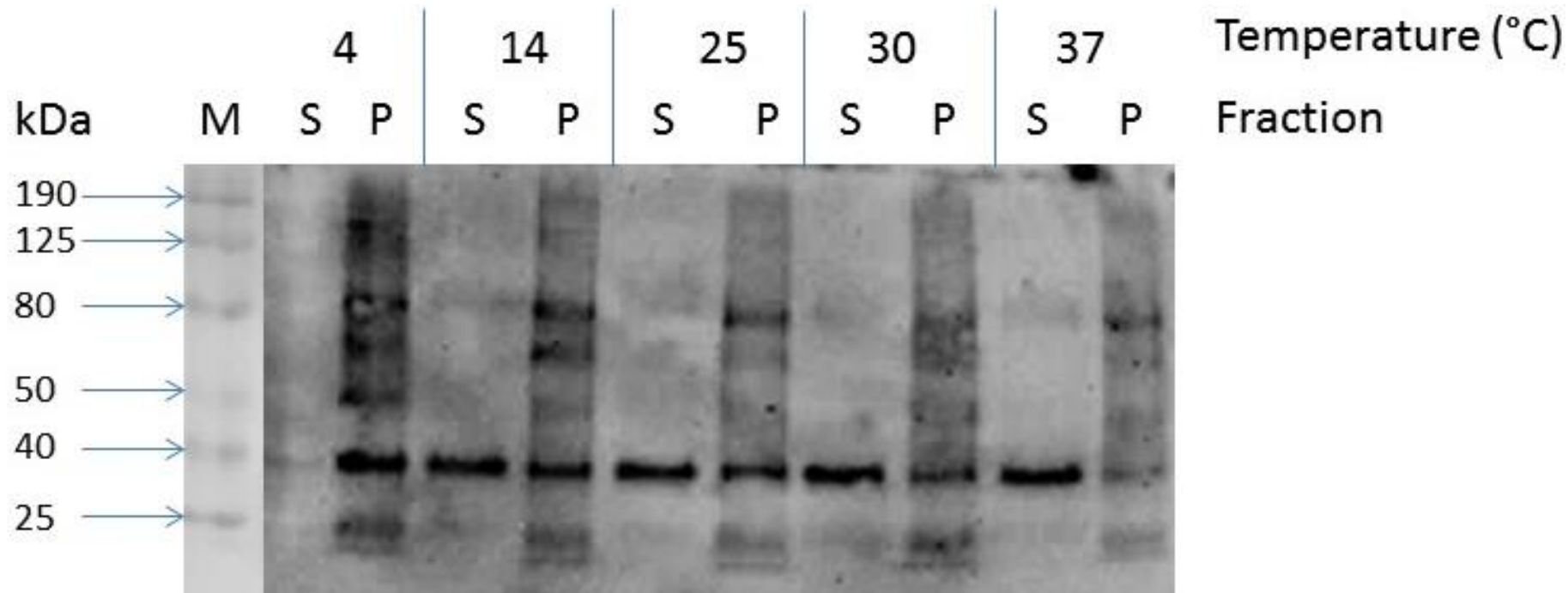
Figure 3.2. Western blot analysis of SMALP-solubilisation of A$_{2a}$R at different temperatures. Molecular weight marker (M), soluble (S) and pellet (P) fractions of SMALP-A$_{2a}$R were probed with anti-HA antibody. SMALP-A$_{2a}$R samples were prepared with 2 % (w/v) SMA and incubated at the indicated temperatures for 1 h. Characteristic gel of four experiment
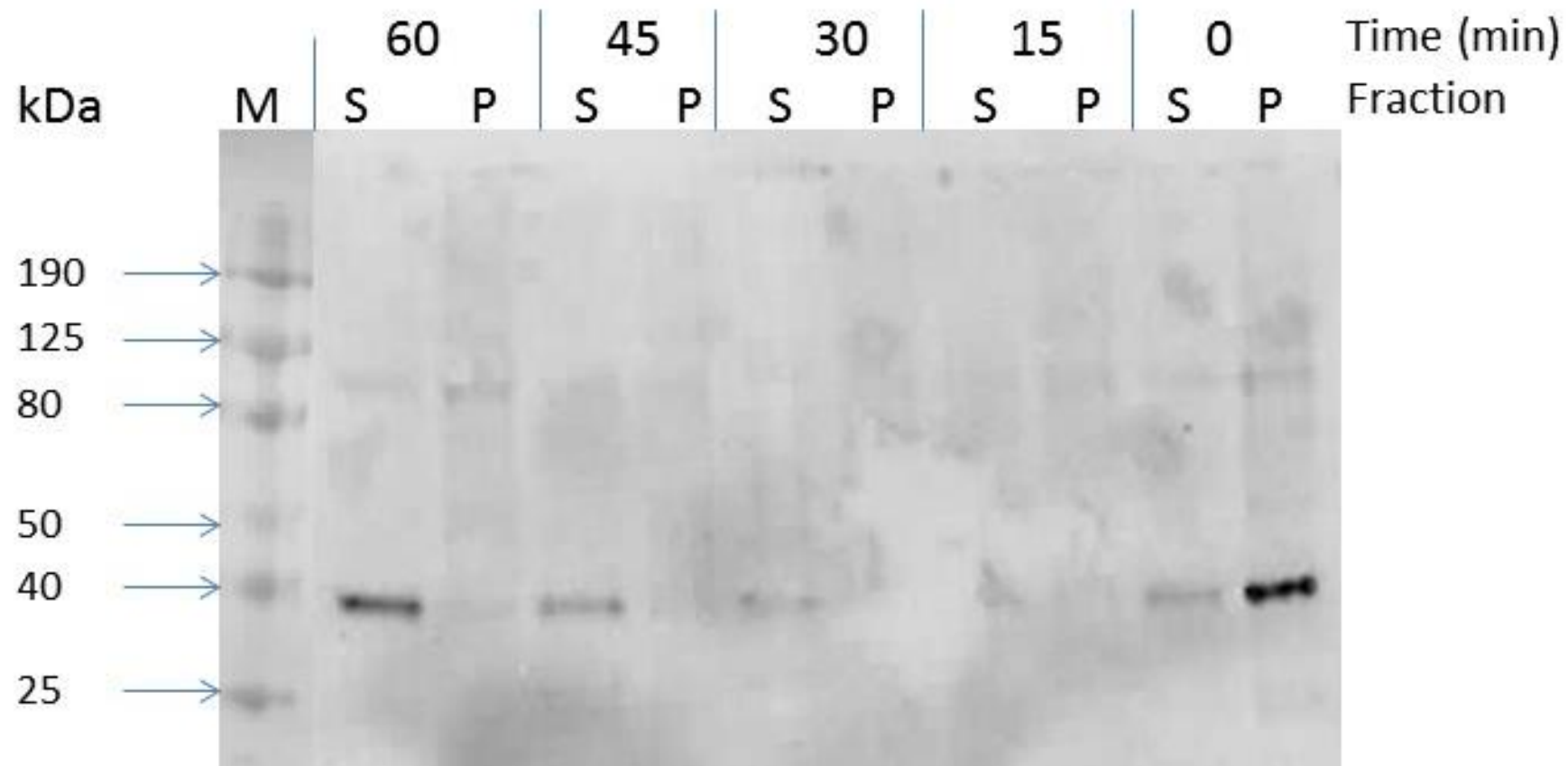
Figure 3.3. Western blot analysis of SMALP-solubilisation of A$_{2a}$R incubated for different lengths of time. Molecular weight marker (M), soluble (S) and pellet (P) fractions of SMALP-A$_{2a}$R prepared with 2 % (w/v) SMA and incubated at 37 °C for the indicated time. Samples were probed with anti-HA antibody. Characteristic gel of three experiments.
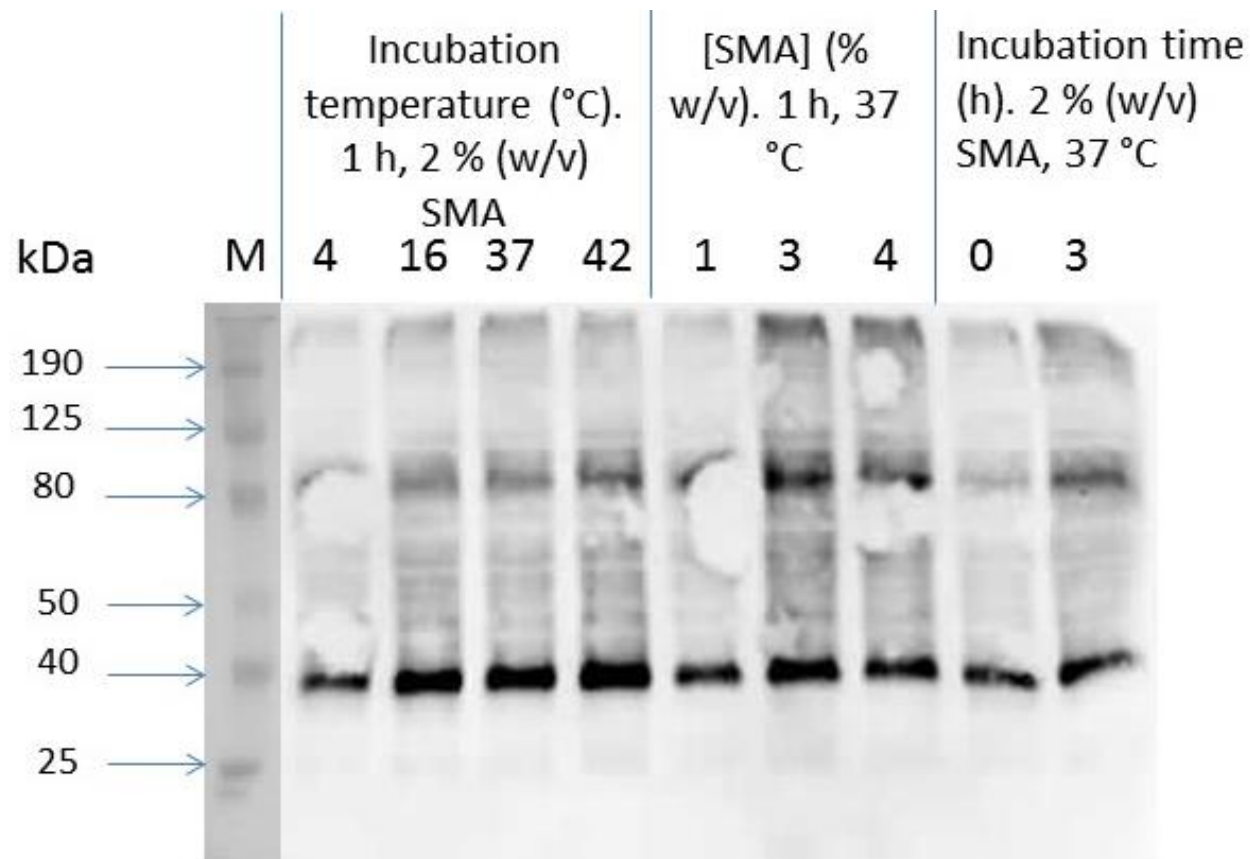
Figure 3.4. Western blot analysis of SMALP-solubilised A₂ₐR incubated under various conditions. Molecular weight markers (M). Soluble

fraction of SMALP-A₂ₐR incubated for 3 h with 2 % (w/v) SMA at 37 °C was compared to SMALP-A₂ₐR prepared with different incubation times,

temperatures and SMA concentrations. Samples were probed with anti-HA antibody. Characteristic gel of two experiment

longer times during solubilisation or in the presence of greater amounts of SMA. The optimised conditions of 1 h at 37 °C with 2 % (w/v) SMA were investigated for the amount of $A_{2a}R$ solubilised in comparison the amount that was originally expressed. As seen in figure 3.5, compared to the total amount of $A_{2a}R$ expressed, the vast majority, as determined visually, was solubilised using optimised SMALP conditions (1 h, 37 °C, 2 % (w/v) SMA). Figure 3.5 also demonstrated the specificity of the anti-HA antibody for the HA-tag present on $A_{2a}R$. HEK 293T cells were treated with PEI as though being transiently transfected (as in section 2.2.9), but no DNA was introduced. SMALP-solubilisation and subsequent Western blot analysis demonstrated no reactivity of the anti-HA antibody for these SMALP-mock transfected cell samples. All bands observed from other samples were therefore a clear indication of the HA-tagged receptor being present. As seen during optimisation, the amount remaining in the pellet fraction was minimal by comparison to the soluble fraction.

3.2.2 Pharmacological characterisation of SMALP-$A_{2a}R$

Having established optimal conditions for SMALP-solubilising $A_{2a}R$ based on extraction of the HA-tagged protein, it was important to determine the functional characteristics of SMALP-$A_{2a}R$. Radioligand binding assays were performed on SMALP-$A_{2a}R$ samples solubilised under optimised conditions. Using [^{3}H]ZM241385 as a tracer ligand, as described in section 2.2.17, and a range of well characterised $A_{2a}R$ ligands, agonists and antagonists, to probe the effect of SMALP-solubilisation on the $A_{2a}R$ ligand binding site. The pharmacological profile of SMALP-$A_{2a}R$ was compared to membrane preparations of $A_{2a}R$ (mem-$A_{2a}R$) to determine whether SMALP-solubilised $A_{2a}R$ retained wild type (WT)-like pharmacology.

SMALP-$A_{2a}R$ was able to bind the agonist NECA, as well as antagonists: ZM241385, XAC and theophylline with WT-like pK_i values (figure 3.6 and table 3.1). The total binding of the SMALP-$A_{2a}R$ was 2.0 ± 0.24 pmol/mg of protein (n=3) equivalent to a yield of 23.3 ± 2.7 %
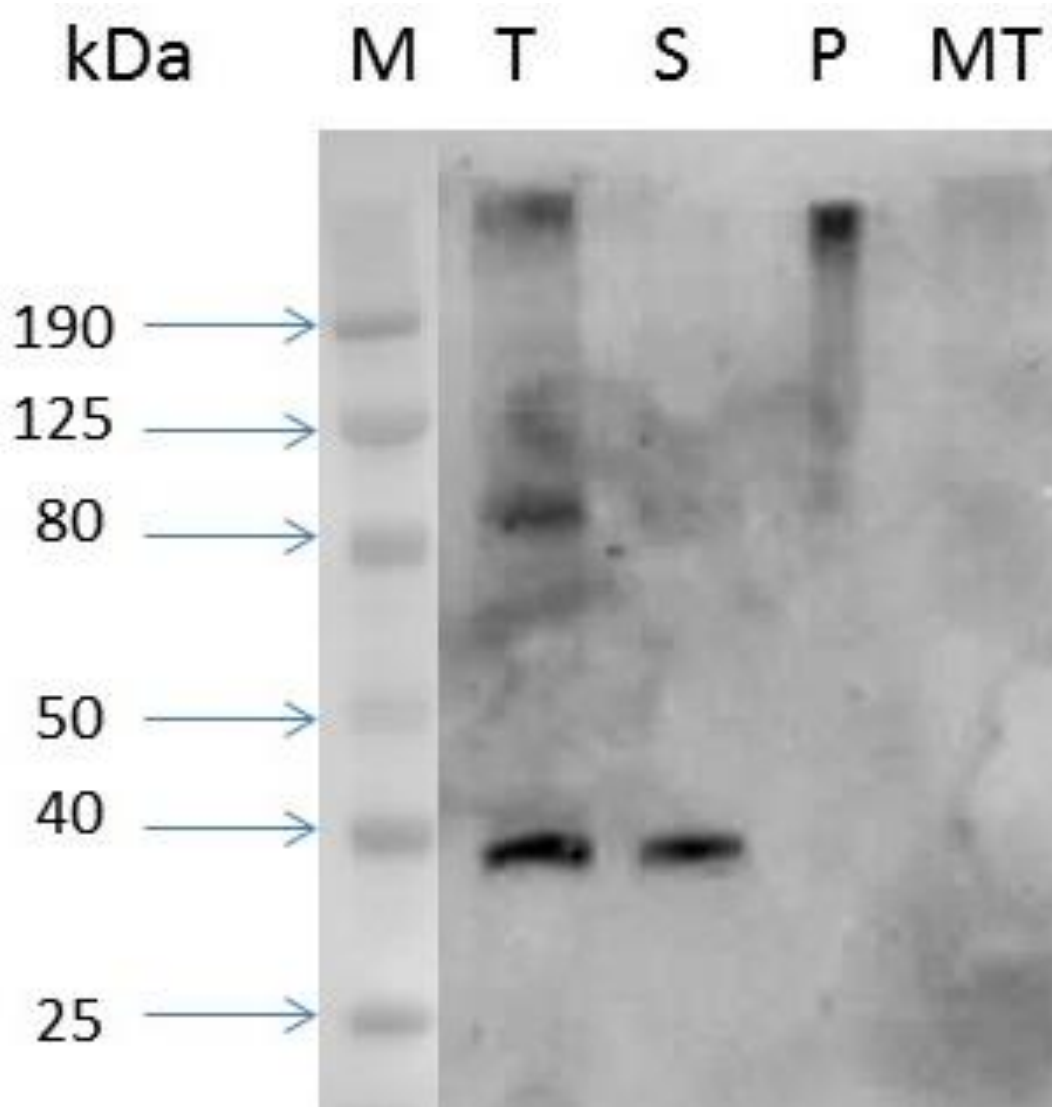
Figure 3.5. Western blot analysis of SMALP-A$_{2a}$R in comparison to the total A$_{2a}$R expressed. Molecular weight markers (M). Total A$_{2a}$R present in the sample before SMALP-solubilisation (T), SMALP-solubilised A$_{2a}$R using optimised conditions (1 h, 37 °C, 2 % (w/v) SMA) (S) and A$_{2a}$R remaining in the pellet fraction (P). SMALP-mock transfected HEK 293T cells (MT) run as a negative control. Samples were probed with anti-HA antibody. Characteristic gel of three experiments.
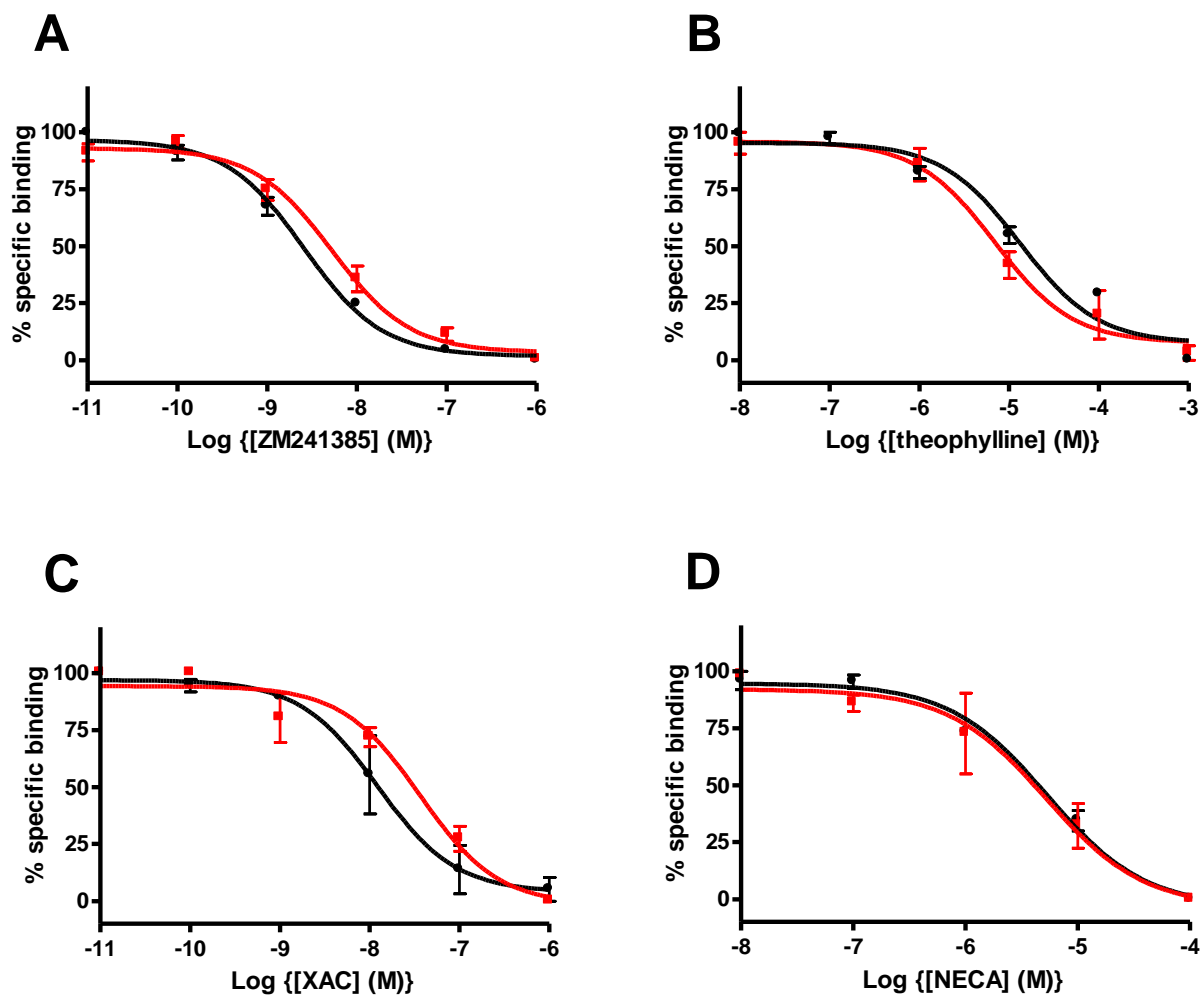
Figure 3.6. Competition radioligand binding of A_{2a}R in SMALPs and membrane preparations with a range of competing ligands. Mem-A$_{2a}$R (●) and SMALP-A$_{2a}$R (■) competition radioligand binding curves using [^{3}H]ZM241385 as a tracer in all assays. Panel A, ZM241385; panel B, theophylline; panel C, XAC and panel D, NECA were competing ligands. Data are mean ± s.e.m. of three experiments performed in triplicate.

Ligand	Mem-$A_{2a}R$	SMALP-$A_{2a}R$
ZM241385	8.87 ± 0.1	8.53 ± 0.0
Theophylline	4.87 ± 0.1	4.97 ± 0.3
XAC	7.17 ± 0.2	6.38 ± 0.2
NECA	5.29 ± 0.1	5.39 ± 0.4

Table 3.1. pK_i values of [³H]ZM241385 in the presence of competing ligands. Data are mean $\pm$ s.e.m. of three experiments performed in triplicate

compared to the original HEK 293T cell membrane preparation. This was similar to the recovery seen from detergent (DDM) solubilisation of $A_{2a}R$ (27.6 ± 11.4 %, n=3). The recovery with SMALP-$A_{2a}R$ was less variable than with DDM-$A_{2a}R$.

3.2.3 Thermostability of SMALP-$A_{2a}R$

It was hypothesised that SMALP encapsulation of receptors with retention of the lipid annulus would increase the stability of the receptor over that of detergent-solubilised receptors. To investigate this, SMALP-$A_{2a}R$ was investigated for its thermostability in comparison to mem-$A_{2a}R$ and DDM-$A_{2a}R$. Thermostability of $A_{2a}R$ in the environment of its membrane, SMALP and detergent micelle was determined by exposing the receptor sample to the temperatures stated in figure 3.7 for 30 min. After incubation the samples were cooled on ice and ligand binding assessed and compared to the 20 °C control values. From data presented in figure 3.7 and table 3.2, it was observed that SMALP-$A_{2a}R$ displayed an increased thermostability over DDM-$A_{2a}R$ of approximately 4 °C. No other sample was as stable as mem-$A_{2a}R$. SMALP-$A_{2a}R$ had >90 % binding activity remaining at physiological temperature. DDM-$A_{2a}R$ had lost over 50 % of its binding activity by 37 °C. Cholesterol has been linked to increased GPCR stability. The original HEK 293T cell would have contained cholesterol that would therefore be present in SMALPs. DDM would try to separate cholesterol from GPCRs when forming micelles and so additional cholesterol, in the form of cholesteryl hemisuccinate (CHS) is routinely added in detergent solubilisation to stabilise the protein. When CHS (0.5 % (w/v)) was introduced during SMALP-$A_{2a}R$ preparation, as it was in DDM-$A_{2a}R$ preparation, thermostability of SMALP-$A_{2a}R$ was increased a further 9 °C. This was 13 °C more stable than DDM-$A_{2a}R$.

3.2.3.1 SMALPs as a potential platform for drug discovery assays

GPCRs are already a major target for the development of drugs. In order to create more specific drugs, reducing side-effects, information on how compounds behave at GPCRs under

physiological conditions is required. Assays related to drug discovery, such as high-throughput assays, are therefore likely to be performed at physiological temperature (37 °C). Observing how different compounds behave at the same receptor can be affected by differences in receptor activity between preparations. The ability to create a large preparation that could be stored for later use without detriment to the proteins activity would be of great advantage. This is not possible with unstable detergent-solubilised receptors which require immediate use. To investigate the potential use of SMALPs as a platform for drug discovery assays, $A_{2a}R$ was prepared in membranes, SMALPs and DDM-micelles. Samples were then incubated at 37 °C or 4 °C and aliquots taken for specific binding determination at the time points indicated in figure 3.8. Specific binding at time points was then compared to the specific binding observed before incubation (0 h). As seen in figure 3.8 and table 3.3, at 37 °C SMALP-$A_{2a}R$ showed increased stability of 7-fold over DDM-$A_{2a}R$. This meant that after 1 h DDM-$A_{2a}R$ had less than 25 % of its binding activity remaining, whereas SMALP-$A_{2a}R$ still had over 80 %. However, neither method of solubilisation provided stability equal to mem-$A_{2a}R$ which retained almost 100 % ligand binding activity after 7 h. At 4 °C the profile of remaining binding activity for SMALP-$A_{2a}R$ was indistinguishable from mem-$A_{2a}R$ and after 10 days had ~80 % specific binding remaining. However, DDM-$A_{2a}R$ had 80 % specific binding remaining after 1 day and had only ~3 % ligand binding activity remaining after 3 days.
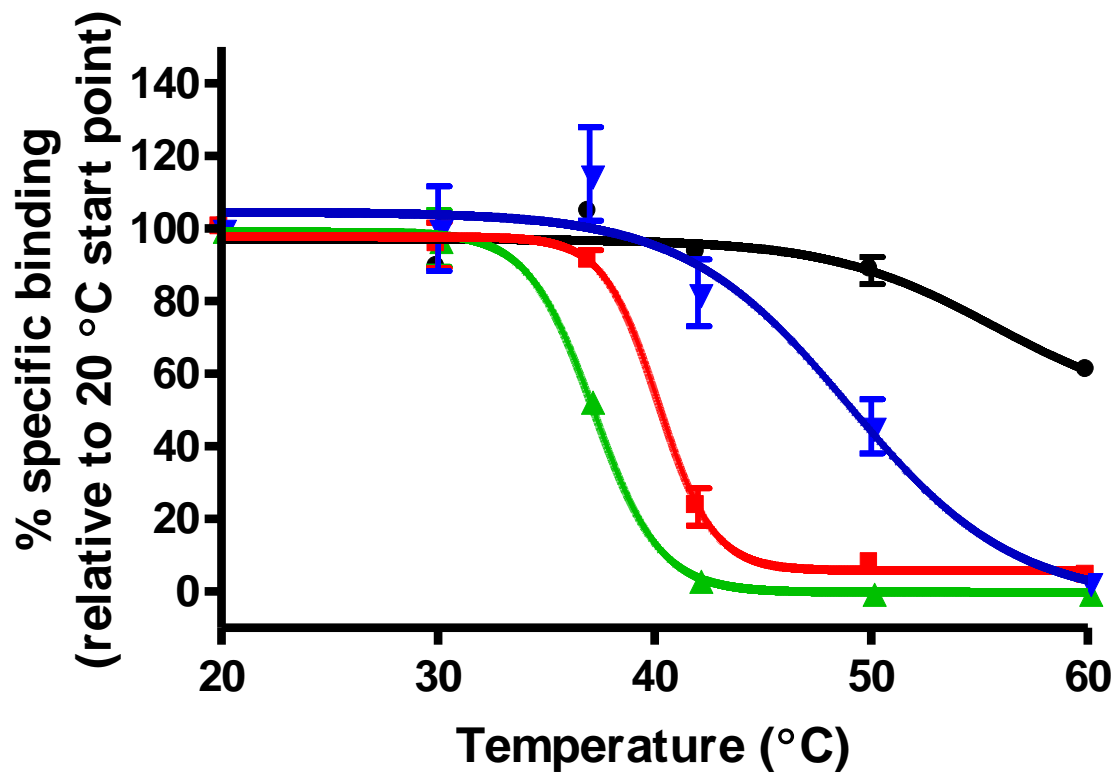
Figure 3.7. Radioligand binding activity of A$_{2a}$R prepared by different methods following incubation at different temperatures. Mem-A$_{2a}$R (●), SMALP-A$_{2a}$R (■), DDM-A$_{2a}$R (▲) and SMALP-A$_{2a}$R + 0.5 % (w/v) CHS (▼) specific binding activities were determined using self-competition radioligand binding of ZM241385. Data are expressed as relative to 20 °C data point (mean ± s.e.m. of three experiments performed in triplicate).

Sample	T_{50} (°C)
Mem-A_{2a}R	>60
DDM-A_{2a}R	36.2 ± 0.5
SMALP-A_{2a}R	40.2 ± 0.4
SMALP-A_{2a}R + CHS	49.0 ± 0.9

Table 3.2. Thermostability of A_{2a}R in different preparations. Thermostability expressed as T_{50} (°C), the temperature at which 50 % ligand binding activity was lost for A_{2a}R prepared in membranes (mem-A_{2a}R), DDM detergent micelles (DDM-A_{2a}R), SMALPs (SMALP-A_{2a}R), and SMALPs + 0.5 % (w/v) cholesteryl hemisuccinate (SMALP-A_{2a}R + CHS). Data given are mean ± s.e.m. of three experiments performed in triplicate.
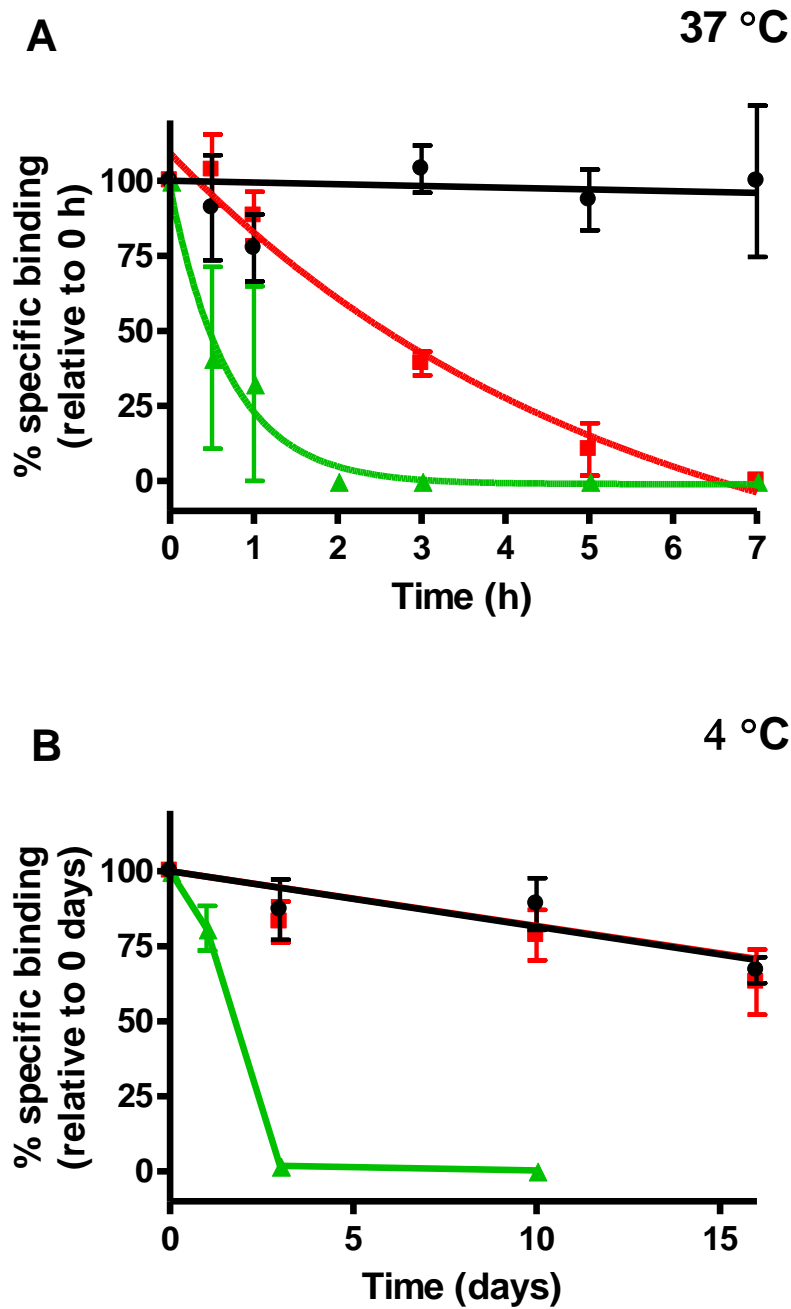
Figure 3.8. Specific binding activity remaining in various A$_{2a}$R samples over time when stored at different temperatures. Mem-A$_{2a}$R (●), SMALP-A$_{2a}$R (■) and DDM-A$_{2a}$R (▲) samples were stored at 37 °C (upper panel, A) 4 °C (lower panel, B). Aliquots were taken at the times indicated and specific binding was determined. Data are mean ± s.e.m. of three experiments performed in triplicate.

Sample	$t_{1/2}$ at 37 °C (min)	$t_{1/2}$ at 4 °C (days)
Mem-$A_{2a}R$	>420	>16
DDM-$A_{2a}R$	21 ± 7	1.8 ± 0.3
SMALP-$A_{2a}R$	148 ± 13	>16

Table 3.3. Thermostability of $A_{2a}R$ preparations. Thermostability expressed as $t_{1/2}$, the time required for $A_{2a}R$ samples to lose 50 % ligand binding activity, when incubated at 37 °C or 4 °C. $A_{2a}R$ samples prepared in membranes (mem-$A_{2a}R$), DDM detergent micelles (DDM-$A_{2a}R$) or SMALPs (SMALP-$A_{2a}R$) were stored at temperatures indicated. At set time points, aliquots were taken and specific binding determined and compared to specific binding before incubation. Data are mean ± s.e.m. of three experiments performed in triplicate.

SMALP-A$_{2a}$R was further studied for its ability to be stored by commonly used methods. If samples could be stored, it would allow preparation of large sample volumes for prolonged use. For this, the ability of SMALP-A$_{2a}$R to retain ligand binding activity following repeated freeze-thaw cycles at -20 °C was investigated as was retention of binding activity following lyophilisation and subsequent resuspension in buffer. It was found, as shown in figure 3.9, that SMALP-A$_{2a}$R presented resilience to common storage methods. Samples were stored at -20 °C until frozen (minimum 1 h) before thawing at room temperature (~16-18 °C for approximately 20 min). Aliquots were taken from the thawed SMALP-A$_{2a}$R sample and radioligand binding performed to assess retention of ligand binding capability. After 5 freeze-thaw cycles SMALP-A$_{2a}$R showed no decrease in binding capability. Furthermore, even after the extreme process of lyophilisation through freeze-drying and re-hydration in buffer, SMALP-A$_{2a}$R retained ~ 70 % of its initial binding activity.
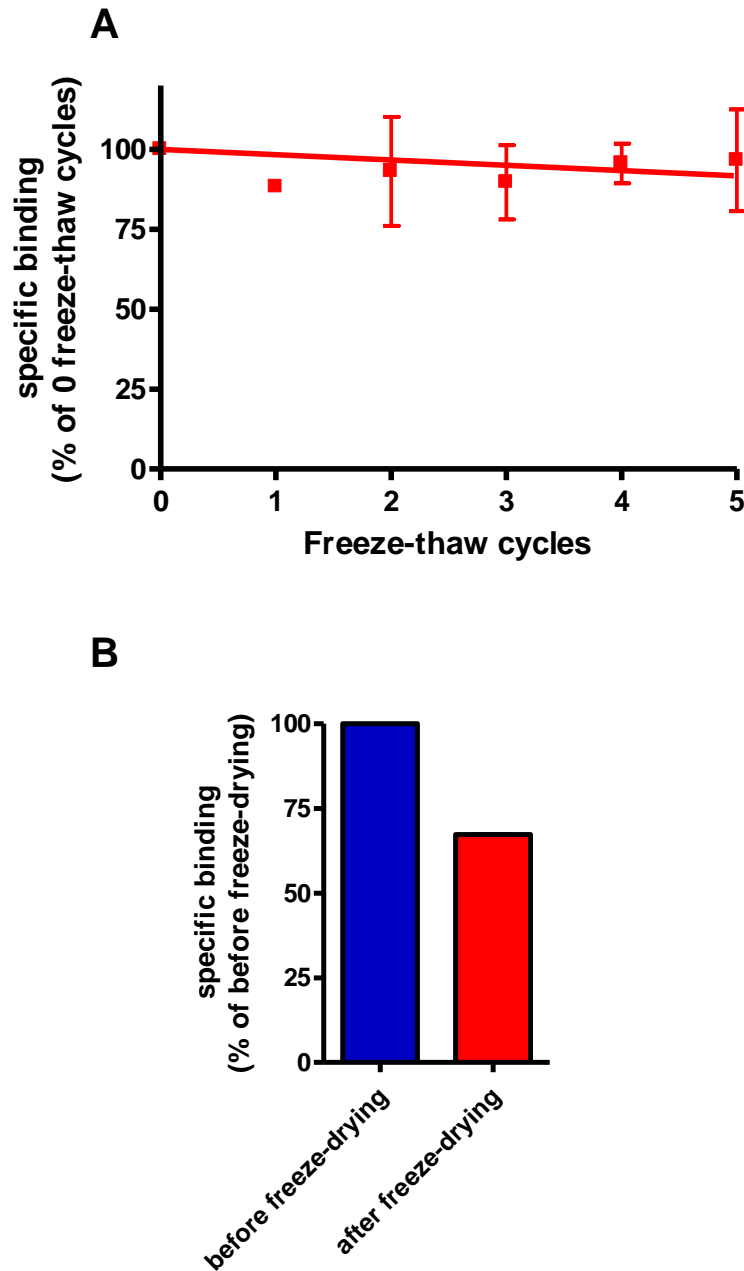
Figure 3.9. Retention of SMALP-A$_{2a}$R binding activity following storage by different methods. Specific binding was determined for: (A) SMALP-A$_{2a}$R that underwent repeated freeze-thaw cycles; (B) SMALP-A$_{2a}$R that underwent freeze-drying before resuspending to initial volume in buffer. Data are compared to specific binding from before storage (mean ± s.e.m. of three experiments performed in triplicate).

3.3 Discussion

The inherent disadvantages of using detergents for protein solubilisation, such as protein instability and irreversible aggregation, have led to the search for improved methods of stabilising membrane proteins when soluble in aqueous solution. Amphipols, fluorinated surfactants and apolipoprotein stabilised nanodiscs have all been investigated. Apart from the rare occurrence with certain amphipols, none of these systems can solubilise proteins directly, and require an initial detergent solubilisation of the protein. This introduces all the structural instability, known to be caused by detergent solubilisation, before the protein is stabilised in the chosen system. This is, at least in part, a result of the removal of the lipid annulus from around the protein. SMALP-solubilisation has been proven to extract protein directly from membranes, with their lipid annulus intact. SMALPs have been increasingly utilised in the study of membrane proteins since their first use in 2009 (Knowles et al., 2009). Since then, SMALP-solubilisation has been used for membrane proteins expressed in bacteria, yeast, insect and mammalian cells.

The ratio of styrene:maleic acid is known to affect extraction efficiency but has been varied in SMA use. This study is the very first GPCR solubilised without detergent from mammalian cells. Previous studies using 2:1 (molar ratio styrene:maleic acid) SMA to solubilise membrane proteins have largely focused on extraction from yeast and bacterial overexpression systems. Extraction of active membrane proteins, ABC transporters, from mammalian cells has only been published once (Gulati et al., 2014), and this was not of a pharmaceutically relevant GPCR. Other studies have looked at extraction of naturally expressed membrane proteins from yeast mitochondria (Long et al., 2013) and extraction from plant cells (Bell et al., 2015) using 3:1 (molar ratio styrene:maleic acid) SMA. However, after solubilisation the samples were only centrifuged at 20,000 x g for 10 min and therefore doubts are raised as to whether only solubilised protein was present in these studies. This study has looked at SMALP-solubilisation

of overexpressed protein at the plasma membrane of mammalian cells using 2:1 SMA. Before functional assays could be performed on SMALP-solubilised protein, optimisation of the extraction conditions was necessary.

3.3.1 Optimisation of SMALP-solubilisation from mammalian cells

Optimisation was performed sequentially: SMA concentration; temperature of incubation; length of incubation. 1 % (w/v) SMA was too little to effectively extract $A_{2a}R$ from the plasma membrane. 3 and 4 % (w/v) SMA were unable to extract more protein than 2 % (w/v) SMA. It was therefore chosen that 2 % (w/v) SMA would be used. This would limit the amount of free SMA (that which did not form nanodiscs) in the sample as free SMA may affect downstream analysis. 37 °C is physiological temperature for humans and therefore should have allowed extraction of protein while the membrane was in its physiological state. The fluidity of the lipid bilayer at 37 °C would also allow for easier insertion of polymer into the membrane. Lower temperatures than 37 °C were investigated in the interest of protein preservation. However, at lower temperatures, as seen at 4 °C, extraction was reduced. Low temperatures, such as 4 °C, are known to reduce the fluidity of the membrane through tighter packing of lipid molecules. It has been shown that tighter packing of lipids reduces the extraction capabilities of SMA (Scheidelaar et al., 2015). The low temperature therefore would make insertion of SMA into the lipid membrane more difficult and extraction less efficient. As the temperature was increased, the fluidity of the membrane would increase allowing greater extraction. Generally with detergent-solubilisation, samples are maintained at 4 °C throughout use to preserve biological function and processes performed in a cold room. This would be detrimental to SMALP preparation, so an alternative approach to temperature is required. A 1 h incubation (pre-centrifugation) provided optimal extraction of receptor. Less than 1 h incubation reduced the extraction efficiency. During the 1 h centrifugation at 4 °C the SMA was still able to extract a small amount of receptor. However this was much less than was seen with a 1 h incubation

at 37 °C before centrifugation. This correlated well with what was observed with the 4 °C incubation for 1 h during the temperature trials. Incubating for 3 h at 37 °C, as seen in the 37 °C stability investigations, was detrimental to protein function.

Despite $A_{2a}R$ having a predicted mass of approximately 45790 Da (~45.8 kDa), bands attributed to monomeric $A_{2a}R$ were observed at ~40 kDa. This was likely due to the hydrophobicity of the $A_{2a}R$ causing it to run ~5 kDa further than expected, a known phenomenon amongst hydrophobic proteins. The band present at 80-90 kDa was attributed to dimeric $A_{2a}R$. There is a possibility that this observed dimeric $A_{2a}R$ was merely an artefact of the SDS-PAGE, commonly seen with the very hydrophobic 7TM receptors. However, as there was an observed increase in levels of dimeric $A_{2a}R$ with increasing incubation times and SMA concentrations, SMALP-solubilisation appears to be able to preferentially solubilise GPCRs as monomers or monomer/dimer mixtures with varying ratios of monomer:dimer. Without a defined mechanism for the formation of SMALP discs, the reasons for increased presence of dimers is speculative. However, if SMA forms discs by individual chains of SMA inserting into membranes before forming a belt around a section of membrane, increased time and SMA concentrations would aid in the formation of larger discs and therefore the encapsulation of larger protein complexes. With careful selection of solubilisation conditions, SMALP-solubilisation may be a useful tool in the future study of GPCR dimers.

3.3.2 Pharmacological characterisation of SMALP-$A_{2a}R$

Radioligand binding assays showed that SMALP-solubilisation had not affected the pharmacology of the $A_{2a}R$. Antagonists (XAC and theophylline), that occupy the receptor but elicit no response, and the inverse agonist ZM241385, that stabilises the inactive state of $A_{2a}R$, were able to bind to SMALP-$A_{2a}R$ with no obvious deviation from the membrane-bound $A_{2a}R$. Agonists, such as NECA, interact with a receptor and cause conformational changes resulting in intracellular signalling. NECA displayed WT-like binding affinity at SMALP-$A_{2a}R$. This

provided a more stringent study of the pharmacology of SMALP-A_{2a}R as an agonist interacts with the receptor differently to antagonists as it induces an active conformation in the receptor. The native ligand of A_{2a}R, adenosine, could not be used to investigate radioligand binding of A_{2a}R. This is due to the necessary addition of adenosine deaminase to remove endogenous adenosine in the samples which would occupy the binding site and compete with other ligands (Jenner et al., 2009, Fredholm, 2010).

The recovery of ligand binding activity calculated for solubilised-A_{2a}R, compared to mem-A_{2a}R, showed that SMALPs extracted as much active receptor as DDM (23.3 ± 2.75 % in SMALPs compared to 27.6 ± 11.4 % for DDM, compared to membrane preparations). However, there was much less variability between SMALP samples than between DDM samples. Therefore any replicates performed will be able to more accurately calculate the amount of active receptor present in SMALPs over DDM.

3.3.3 Stability of A_{2a}R in SMALPs

Retention of important membrane components (e.g. cholesterol and annular lipid), in SMALPs increased thermostability of A_{2a}R over DDM-A_{2a}R. The 4 °C increase in thermostability was approximately the same as was observed in SMALP-A_{2a}R over DDM-A_{2a}R prepared from yeast membranes (Jamshad et al., 2015). This would suggest that the SMALP process itself infers an element of stability on the receptor, regardless of the initial membrane composition. The addition of cholesterol, in the form of CHS, to SMALP-A_{2a}R further increased its thermostability. By comparison, even the presence of CHS in all detergent samples, routinely used in detergent solubilisation (Toro et al., 2009, Attrill et al., 2009), still did not stabilise A_{2a}R to the same level as in SMALPs. The presence of natural cholesterol, possibly other stabilising components from the membrane and lateral pressure exerted by the retained bilayer structure in SMALPs were possibe reasons for the increased stability at 37 °C. SMALP-A_{2a}R retained the native membrane bilayer structure and so was able to stabilise the A_{2a}R at higher

temperatures and for longer. SMALPs were not as stable as native membrane, suggesting there was a stabilising factor lost during the SMALP process. However, in comparison to detergent-solubilised proteins, SMALPs would be a much better platform for drug screens at 37 °C.

Whether storing SMALPs at 4 °C or -20 °C, there would be no detriment to the sample in comparison to mem-A_{2a}R. This infers that the lipid bilayer extracted in the SMALP behaved similarly to native membrane, with membrane components acting as cryopreservatives resulting in SMALP-A_{2a}R behaving indistinguishably from mem-A_{2a}R at low temperatures. This allows for easier handling of samples, large sample preparation and storage without fear of protein degradation.

In summary, presented here is the very first report of a GPCR of any description being solubilised in the total absence of detergent from a mammalian cell with retention of pharmacological activity. SMALPs were shown to be a method of solubilising functional GPCRs from mammalian cells that inferred greater stability than detergent solubilisation. Samples could be prepared in advance of their use and stored in different ways without loss of binding activity. Finally, SMALPs provided a better platform for drug screens at physiological temperature compared to detergent micelles. This work resulted in a joint first author paper (Jamshad et al., 2015).

CHAPTER 4: SMALP-SOLUBILISATION OF

INTRACELLULAR MEMBRANES

4.1 Introduction

Retention of proteins in the endoplasmic reticulum (ER) is the leading cause of several diseases. Retinitis pigmentosa is the degeneration, and ultimately loss, of sight and can be caused as a result of ER-retention of rhodopsin (Dryja et al., 1990), a cononical family A GPCR. Hypogonadotrophic hypogonadism, a condition that can be caused by retention of gonadotrophin releasing hormone receptor (de Roux et al., 1997). Some melanocortin 4 receptor mutations lead to ER-retention and familial obesity (Nijenhuis et al., 2003). hypothyroidism (thyroid stimulating hormone receptor (Tonacchera et al., 2004)), familial glucocorticoid deficiency (melanocortin 2 receptor (Chung et al., 2008)) and Leydig cell hypoplasia leading to infertility (leutinizing hormone receptor (Dickinson et al., 2009)) are all diseases caused by mutations in GPCRs which result in ER-retention. ER-retention is not restricted to GPCRs, other proteins are known to be retained in the ER as a consequence of mutation. These can lead to serious disease states such as: lysosomal storage diseases e.g. Gaucher's disease (mutations in β-glucosidase (Beutler et al., 2004)); and has been well documented in many mutations of cystic fibrosis transmembrane conductance regulator in cystic fibrosis.

One of the most studied diseases caused by ER-retention of a protein is nephrogenic diabetes insipidus (NDI), a disease characterised by polyuria leading to severe dehydration and potentially death. There have been >130 mutations identified in the V_2 vasopressin receptor (V_2R), a family A GPCR, which cause approximately 90 % of all cases of NDI (Knoers, 1993, Birnbaumer, 2000). These mutations often lead to ER-retention due to misfolded V_2R. As a

result, circulating [arginine⁸]vasopressin (AVP) acts upon far fewer receptors, preventing effective reabsorption of water in the kidneys. Attempts to aid correct folding, and thus recover cell-surface expression, of V_2R through pharmacological chaperones has been attempted (Robben *et al.*, 2007) but with limited success. Were there more details known of the conformational changes induced through these disease-causing mutations, it may be possible to design and develop better chaperones and drugs to aid in recovery of cell surface expression. The SMALP method of solubilisation could potentially be used for this purpose.

SMALP studies to date have predominantly focused on extraction from cell plasma membranes. Two reports have investigated the ability of 3:1 (styrene:maleic acid molar ratio) SMA to extract proteins from the membranes of organelle preparations (Long *et al.*, 2013, Skaar *et al.*, 2015). However, doubts are raised over the samples used in these studies as post-SMALP-solubilisation samples were centrifuged at only 20,000 x g for 10 min. This may not have removed all insoluble material from the supernatant. These, and all other SMALP studies, have looked at SMALP-solubilisation from membrane preparations (Knowles et al., 2009, Orwick-Rydmark et al., 2012, Gulati et al., 2014, Prabudiansyah et al., 2015). However, here, SMALP-solubilisation was performed on whole cells. It was therefore not known whether the solubilised membrane fragments were of the plasma membrane only or of intracellular membranes as well.

It has been shown that SMA displays no preference in relation to lipid type when forming nanodiscs (Scheidelaar *et al.*, 2015). Lipids possessing negative charge have been SMALP-solubilised (Prabudiansyah et al., 2015) demonstrating a lack of ionic interference in nanodisc formation. In *E.coli,* SMA extracted proteins efficiently regardless of the lipid composition they were present in (Dorr *et al.*, 2014). It was therefore plausible that SMA would be able to extract proteins from intracellular membranes of whole, mammalian cells.

In this part of the study, use of SMA to extract protein from intracellular membranes of whole mammalian cells was investigated. This would provide a new method of studying diseases caused by intracellular retention of proteins. Study of the misfolded proteins, and their interactions with known pharmacological chaperones, could open new possibilities for drug design, discovery and mechanisms of action for pharmacological chaperones.

4.1.1 KDEL

The KDEL sequence (- lysine – aspartate – glutamate – leucine -) is a well-known ER retention motif that has proved efficient at retaining proteins in the ER. KDEL is a common sequence at the extreme c-terminal tail of 3 proteins known to be retained in the ER; binding immunoglobulin protein; heat shock protein 90 kDa beta member 1; protein disulphide-isomerase (Jackson *et al.*, 1990, Munro and Pelham, 1987). Each of these 3 soluble proteins are present in the ER and have roles in the correct folding of nascent polypeptides. Mutagenesis studies have concluded that the C-terminal KDEL sequence was essential for their retention in the ER, but they must be the final 4 residues to confer ER-retention. However, providing this was the case, not even a change in the tertiary structure could prevent their retention (Munro and Pelham, 1987).

Upon engineering the KDEL sequence to the extreme C-terminus of a transmembrane protein (CD8), ER retention was observed (Stornaiuolo *et al.*, 2003). This showed that the KDEL sequence did not just affect soluble proteins, but membrane-bound proteins as well. However, studies of the budding pattern of the KDEL-tagged CD8 showed its leaving from the ER. Presence of N-linked glycosylation was proof of processing through the ER, but lack of O-linked glycosylation suggested the protein had not reached the Golgi apparatus. It was proposed that KDEL-receptors act to identify nascent polypeptides that are still marked by ER-chaperones (Hamada *et al.*, 2004). KDEL-receptors are responsible for binding misfolded proteins and returning them to the ER. With knowledge that membrane proteins were retainable

in the ER (Jackson et al., 1990), $A_{2a}R$ was engineered with a KDEL, ER-retention motif at the C-terminus ($A_{2a}R$-KDEL) to allow investigation of the ability of SMA to solubilise intracellular membranes.

4.1.2 Glycosylation of $A_{2a}R$

The passage of nascent polypeptides through the ER results in correct folding of the protein and derivatisation by polysaccharides to appropriate N-linked glycosylation sites (N-X-S/T). After processing in the ER, proteins are transported to the Golgi for further (O-linked) glycosylation and processing of the N-linked glycosylation before transport to their ultimate destination. The vast majority of GPCRs have N-linked glycosylation sites on the N-terminus or ECLs. Often multiple glycosylation sites are utilised (Wheatley and Hawtin, 1999). There are very few O-linked glycosylation sites on GPCRs, V_2R is one of the few that does receive O-linked glycosylation (Sadeghi and Birnbaumer, 1999). The precise role of glycosylation is not clear for $A_{2a}R$ (Piersen et al., 1994). Since the $A_{2a}R$ construct used in these studies, as mentioned in section 3.1, was glycosylation deficient, re-introduction of the glycosylation site in $A_{2a}R$ was performed as this may play a role in GPCR trafficking. $A_{2a}R$ was developed with the N154Q mutation reversed, reintroducing the sole glycosylation site of $A_{2a}R$. This construct was characterised before introduction into the $A_{2a}R$-KDEL sequence to investigate $A_{2a}R$ ER-retention.

4.2 Results

4.2.1 A$_{2a}$R-KDEL

Primers, as shown in table 4.1, were designed to introduce the KDEL sequence, in-frame, on to the C-terminus of A$_{2a}$R in one reaction. A Quikchange-like, site-directed mutagenesis protocol was employed, as described in section 2.2.1. This reaction required the insertion of 12 base pairs (bp) rather than the more usual 1-3 bp changes required for a single point mutation. Consequently, the complementary sequence at the 5' and 3' ends were extended, from the usual 9-12 to 21, to ensure efficient primer annealing. Once the DNA sample had been prepared and correct DNA sequence confirmed by sequencing in both directions, the A$_{2a}$R-KDEL construct generated was characterised.

Given that KDEL is an established ER-retention sequence, it was anticipated that A$_{2a}$R-KDEL would exhibit reduced cell surface expression in comparison to A$_{2a}$R lacking the KDEL sequence. Cell-surface expression levels of A$_{2a}$R-KDEL were determined by ELISA, as described in section 2.2.19. A$_{2a}$R-KDEL was compared to A$_{2a}$R for cell-surface expression levels. As was evident from figure 4.1, the KDEL sequence on the C-terminus of A$_{2a}$R did not cause any decrease in cell surface expression as A$_{2a}$R-KDEL expression levels were WT-like. The ability of agonist challenge to drive receptor internalisation was also investigated for A$_{2a}$R-KDEL and compared to A$_{2a}$R. Stimulation with a saturating concentration of NECA (100 μM) was employed to study the ability of any A$_{2a}$R-KDEL expressed at the cell surface to internalise. A$_{2a}$R-KDEL responded to saturating amounts of NECA with the same level of internalisation as A$_{2a}$R (~20 %)

Receptor construct	Sense primer	Antisense primer
A₂ₐR-KDEL	5' – CAG-GAT-GGA-GCA-GGA-GTG-TCC-AAG-GAT-GAA-CTG-TAG-GCG-GCC-GCT-CGA-GTC-TAG - 3'	5' – CTA-GAC-TCG-AGC-GGC-CGC-CTA-CAG-TTC-ATC-CTT-GGA-CAC-TCC-TGC-TCC-ATC-CTG - 3'

Table 4.1. Oligonucleotide sequences designed to introduce the KDEL ER-retention motif to the C-terminus of A₂ₐR. Sequences shown in red denote the bases inserted. Sequence shown in black denotes bases complementary to template DNA.
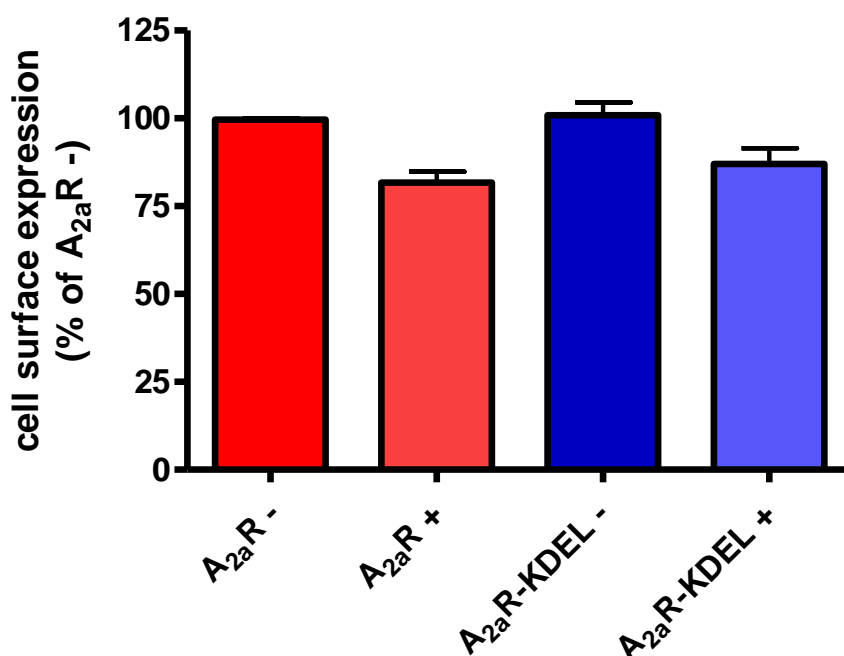
Figure 4.1. Cell surface expression of A₂ₐR-KDEL compared to A₂ₐR and response to agonist challenge. Cell-surface expression was determined by ELISA. Data presented normalised to untransfected cells (0 %) and unstimulated A₂ₐR (100 %). Internalisation following agonist stimulation was determined using NECA (100 μM) for 1 h. Data are mean ± s.e.m. of three experiments performed in triplicate.

4.2.2 Glycosylation of A$_{2a}$R-KDEL

Primers, shown in table 4.2, were designed to re-introduce the glycosylation site of A$_{2a}$R and A$_{2a}$R-KDEL at residue 154 by mutating Gln back to the native Asn. A one-step mutagenesis strategy was employed and the sequence of constructs confirmed by automated fluorescence sequencing in both directions, as described in section 2.2.7. Glycosylated A$_{2a}$R herein referred to as glyco-A$_{2a}$R and glycosylated A$_{2a}$R-KDEL herein referred to as glyco-A$_{2a}$R-KDEL

The effect of re-creating the N-glycosylation site on cell surface expression was investigated. It was determined by ELISA, figure 4.2, that there was no notable change in cell-surface expression levels, nor ability of agonist stimulation to internalise the receptor construct, upon re-introduction of the glycosylation site (glyco-A$_{2a}$R). Western blot analysis of A$_{2a}$R and glyco-A$_{2a}$R revealed a clear difference. Whereas the A$_{2a}$R (lacking glycosylation) migrated as a single band (~40 kDa), glyco-A$_{2a}$R generated a series of bands between 40 – 50 kDa coinciding with the appearance of not only non-glycosylated A$_{2a}$R but glycosylated intermediates (figure 4.3).

Having demonstrated the glycosylation site had resulted in glycosylated A$_{2a}$R without detriment to the cell surface expression levels or the ability to internalise upon agonist binding, glycosylation was investigated for the ability to induce ER-retention in A$_{2a}$R-KDEL. Glyco-A$_{2a}$R-KDEL was studied in comparison to A$_{2a}$R cell surface expression levels. As shown in figure 4.4, there was no notable change in cell-surface expression levels for the glyco-A$_{2a}$R-KDEL construct in comparison to A$_{2a}$R. Presence of the N-glycosylation also did not affect the levels of A$_{2a}$R internalisation upon agonist stimulation.

Receptor construct	Sense primer	Antisense primer
Glyco-A$_{2a}$R	5' –CA-AAG-GAG-GGC-AAG-AAC-CAC-TCC-CAG-GGC- 3'	5' –GCC-CTG-GGA-GTG-GTT-CTT-GCC-CTC-CTT-TG- 3'

Table 4.2. Primers to introduce Asn154 for the native glycosylation site of A$_{2a}$R. Sequences shown in red denote the bases changed to create the [Q154N]A$_{2a}$R construct. Sequence shown in black denotes bases complementary to template DNA.
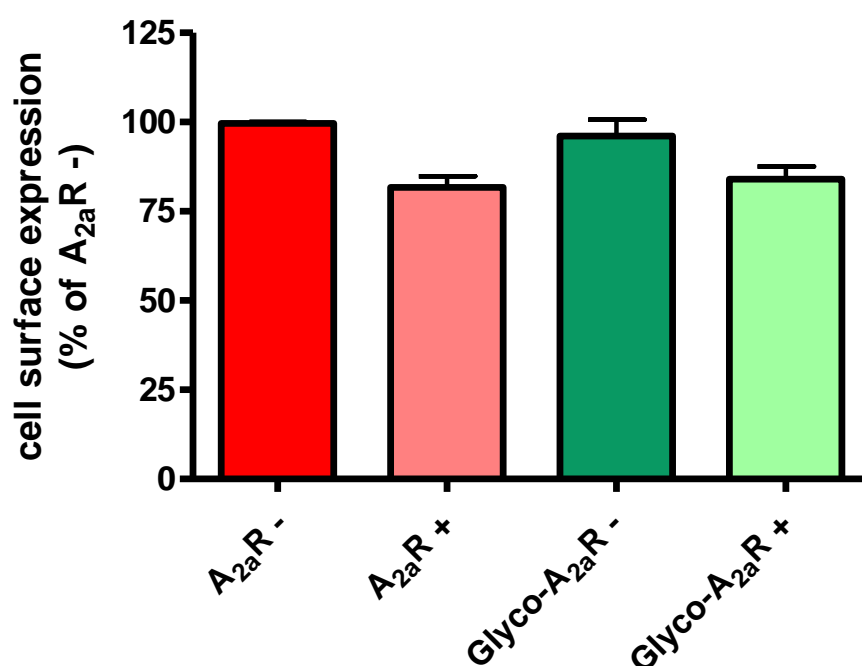
Figure 4.2. Cell-surface expression of glycosylated A$_{2a}$R (glyco-A$_{2a}$R) in comparison to non-glycosylated A$_{2a}$R (A$_{2a}$R) with (+) or without (-) agonist stimulation. Cell-surface expression was normalised to untransfected cells (0 %) and unstimulated A$_{2a}$R (100 %). Internalisation under agonist stimulation was determined using NECA (100 μM) for 1 h. Data are mean ± s.e.m. of three experiments performed in triplicate.
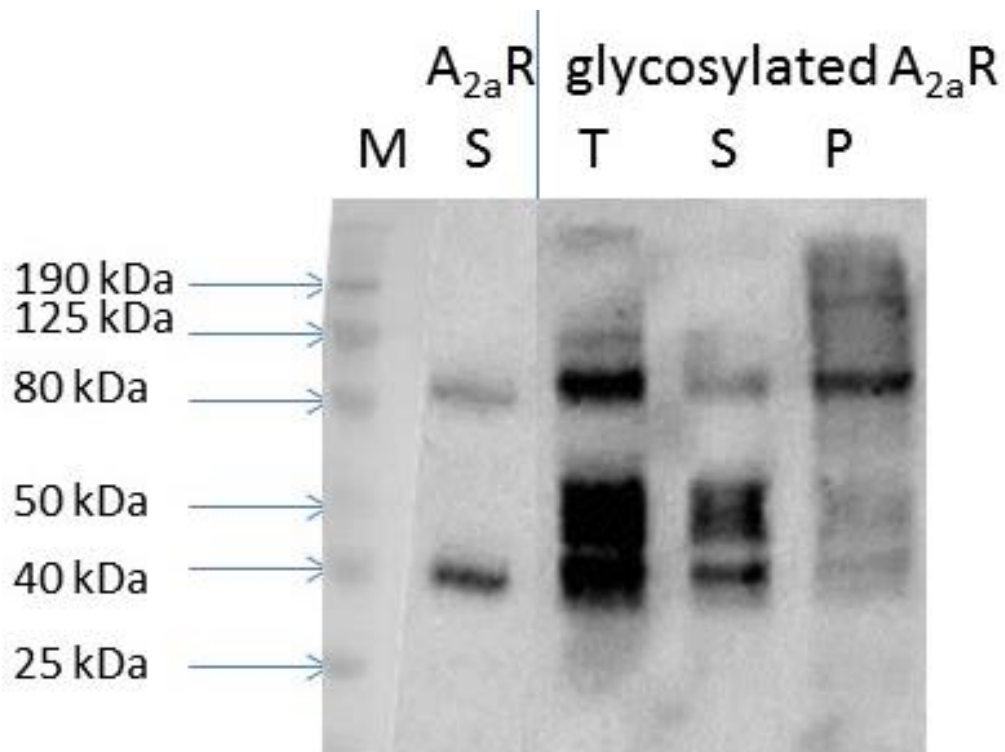
Figure 4.3. Western blot analysis of SMALP-solubilised glycosylated A₂aR. SMALP-A₂aR (A₂aR S) compared to glycosylated A₂aR T: total receptor present; S: soluble and P: insoluble fractions after centrifugation. Probed with anti-HA antibody. Molecular weight marker (M). Characteristic gel of two experiments
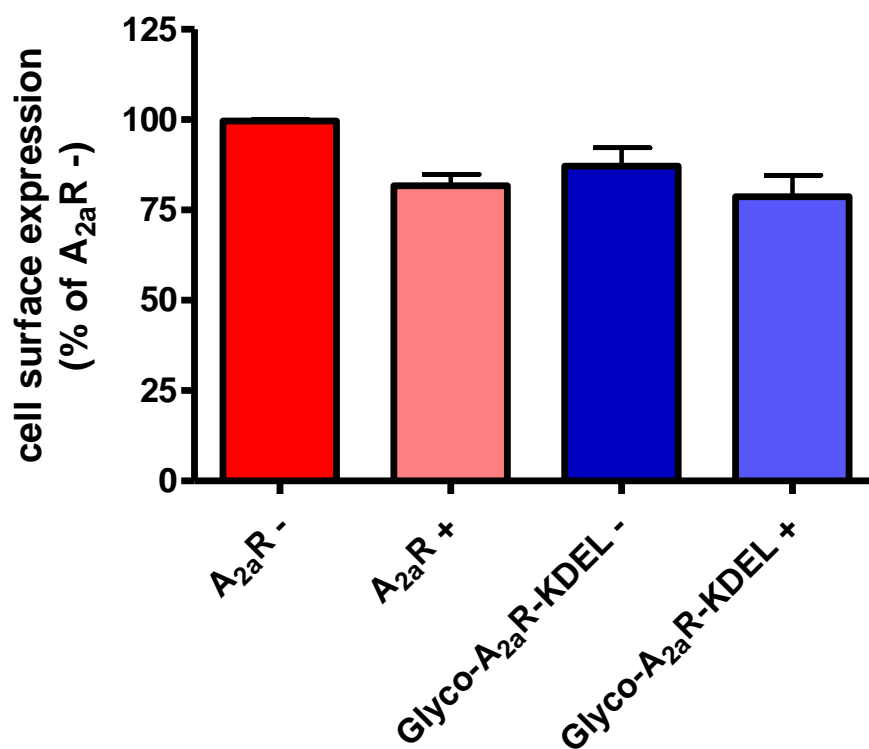
Figure 4.4. Cell-surface expression of glycosylated $A_{2a}R$-KDEL (glyco-$A_{2a}R$-KDEL) in comparison to non-glycosylated $A_{2a}R$ ($A_{2a}R$) with (+) or without (-) agonist stimulation. Cell-surface expression was normalised to untransfected cells (0 %) and unstimulated $A_{2a}R$ (100 %). Internalisation under agonist stimulation was determined using NECA (100 µM) for 1 h. Data are mean ± s.e.m. of three experiments performed in triplicate.

4.2.3 ER-retention sequence from α$_{2c}$-AR

As the incorporation of the KDEL ER-retention sequence had failed to prevent the A$_{2a}$R trafficking to the cell surface, an alternative ER-retention sequence was sought. The ER-retention sequence from the α$_{2c}$ adrenergic receptor (α$_{2c}$-AR) was selected as it had been previously reported to retain α$_{2c}$-AR in the ER (Schwappach *et al.*, 2000). The α$_{2c}$-AR and the A$_{2a}$R are both family A GPCRs. Furthermore, it has been reported that engineering the final 14 residues of α$_{2c}$-AR onto CXCR1, another family A GPCR, resulted in ER-retention (Milligan *et al.*, 2005). It was therefore hypothesised that this ER-retention motif should be able to confer ER-retention to the A$_{2a}$R. The α$_{2c}$-AR ER-retention motif consists of the final 14 residues at the C-terminus (-Lys-His-Ile-Leu-Phe-Arg-Arg-Arg-Arg-Arg-Gly-Phe-Arg-Glu-(-KHILFRRRRRGFRQ-COOH)) of the α$_{2c}$-AR. The -KHILFRRRRRGFRQ- motif was therefore engineered onto the C-terminus of A$_{2a}$R (A$_{2a}$R-KHILFRRRRRGFRQ).

Initially primers were designed to introduce the full 42 bp ER-retention motif in one step. Complementary 5' and 3' sequences were extended to 28 bp to assist primer annealing. However, this method proved unsuccessful as no product was produced through Quikchange-like mutagenesis. Primers were then designed to introduce the bases in 2 steps. The first round introduced 18 of the 42 bp corresponding to KHILRQ (table 4.3, shown in red). This was selected to avoid possible hairpin loop formation within the primers that was identified as a possibility from observation of complementary sequences in the primers. Creation of the A$_{2a}$R with the –KHILRQ fragment of the –KHILFRRRRRGFRQ motif provided increased complementarity for the primers designed to introduce the full motif. The second round of mutagenesis used the product from the first round as a template to introduce the remaining 24 bp corresponding to FRRRRRGF (table 4.3, shown in purple). The sequence of the final product (A$_{2a}$R-KHILFRRRRRGFRQ) was confirmed by sequencing in both directions.

Receptor construct	Sense primer	Antisense primer
HA-A$_{2a}$R-KHILRQ	5' – C-CTG-GCC-CAG-GAT-GGA-GCA-GGA-GTG-TCC-AAG-CAC-ATC-CTC-AGG-CAG-TAG-GCG-GCC-GCT-CGA-GTC-TAG-AGG-GCC-C - 3'	5' – G-GGC-CCT-CTA-GAC-TCG-AGC-GGC-CGC-CTA-CTG-CCT-GAG-GAT-GTG-CTT-GGA-CAC-TCC-TGC-TCC-ATC-CTG-GGC-CAG-G - 3'
HA-A$_{2a}$R-KHILFRRR RRGFRQ	5' – C-CTG-GCC-CAG-GAT-GGA-GCA-GGA-GTG-TCC-AAG-CAC-ATC-CTC-TTC-CGA-CGG-AGG-AGA-AGG-GGC-TTC-AGG-CAG-TAG-GCG-GCC-GCT-CGA-GTC-TAG-AGG-GCC-C - 3'	5' – G-GGC-CCT-CTA-GAC-TCG-AGC-GGC-CGC-CTA-CTG-CCT-GAA-GCC-CCT-TCT-CCT-CCG-TCG-GAA-GAG-GAT-GTG-CTT-GGA-CAC-TCC-TGC-TCC-ATC-CTG-GGC-CAG-G - 3'

Table 4.3. Oligonucleotide sequences designed to introduce the KHILFRRRRRGFRQ ER-retention motif from α$_{2c}$-AR to the C-terminus of A$_{2a}$R. Sequences in red denote the bases inserted in the first reaction. Sequences in purple denote bases introduced during the second reaction. Sequences in black denote bases complementary to template DNA.

Cell surface expression levels of $A_{2a}R$-KHILFRRRRRGFRQ were first identified to investigate the ability of the –KHILFRRRRRGFRQ motif to prevent $A_{2a}R$ trafficking to the cell surface. It was observed by ELISA (figure 4.5) that $A_{2a}R$-KHILFRRRRRGFRQ had a decreased expression level at the cell-surface (51.1 ± 3.9 % compared to $A_{2a}R$). Agonist challenge of receptor expressed at the cell surface, with 100 µM NECA, was performed to investigate the ability of $A_{2a}R$-KHILFRRRRRGFRQ, expressed at the cell surface, to internalise. The $A_{2a}R$-KHILFRRRRRGFRQ that was still expressed at the cell surface was able to internalise to WT-like levels (~15 % internalisation) upon agonist stimulation.

Having observed a reduction in cell surface expression, investigations into whether this was a result of ER-retention or of reduced overall expression were performed. This was achieved by using low concentration (0.1 %) of the detergent Triton X-100 to permeabilise the plasma membrane (Barwell et al., 2011). This allowed anti-HA antibody to access the intracellular components in addition to the cell surface. Whole-cell expression ELISA data (figure 4.6) revealed that, in comparison to $A_{2a}R$ cell surface expression, there was reduced overall expression of $A_{2a}R$-KHILFRRRRRGFRQ (61.4 ± 9.1 %). This was similar to the 51.1 ± 3.9 % decreased expression of $A_{2a}R$-KHILFRRRRRGFRQ noted above, observed at the cell-surface. Whole cell expression of $A_{2a}R$ was also shown to be reduced compared to expression at the cell surface (84.4 ± 4.7 %).
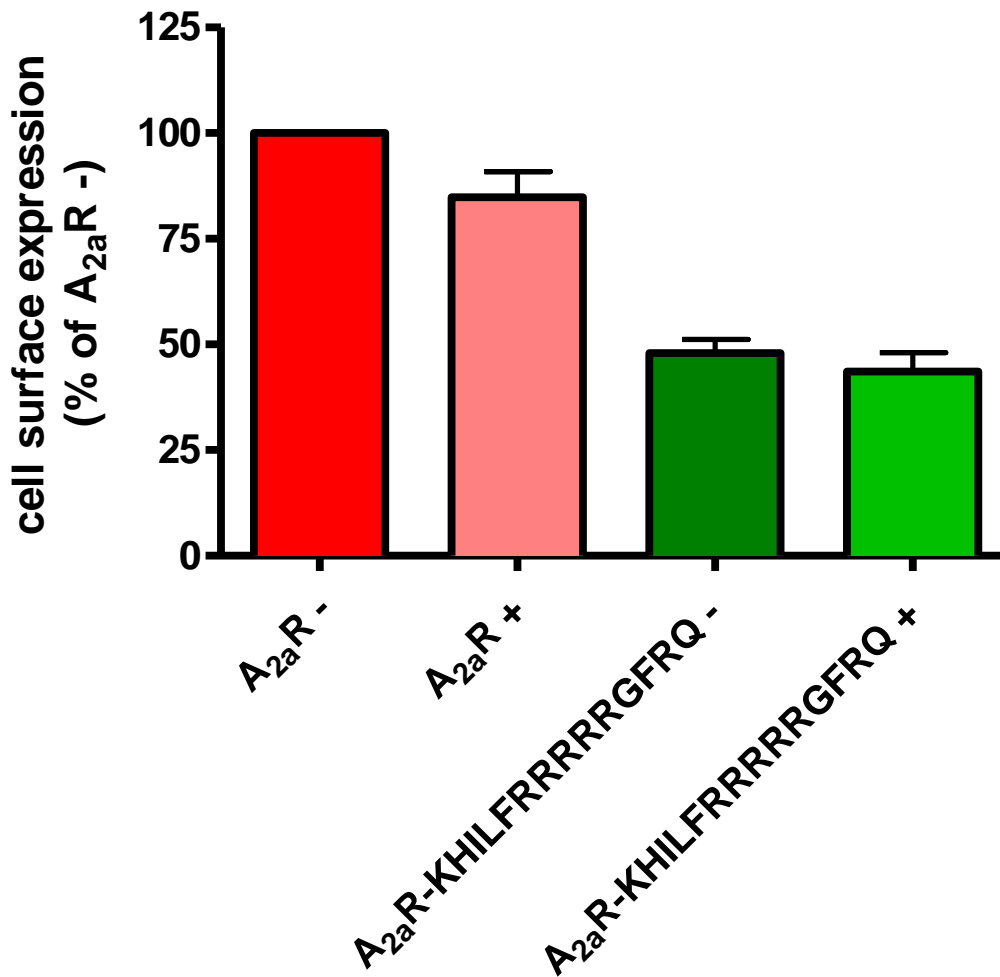
Figure 4.5. Cell surface expression of $A_{2a}R$ and $A_{2a}R$-KHILFRRRRRGRFRQ and effect of agonist stimulation. Cell-surface expression was determined by ELISA and normalised to untransfected cells (0 %) and unstimulated (-) $A_{2a}R$ (100 %). Internalisation following agonist stimulation was determined using NECA (100 μM) for 1 h (+). Data are mean ± s.e.m. of three experiments performed in triplicate.
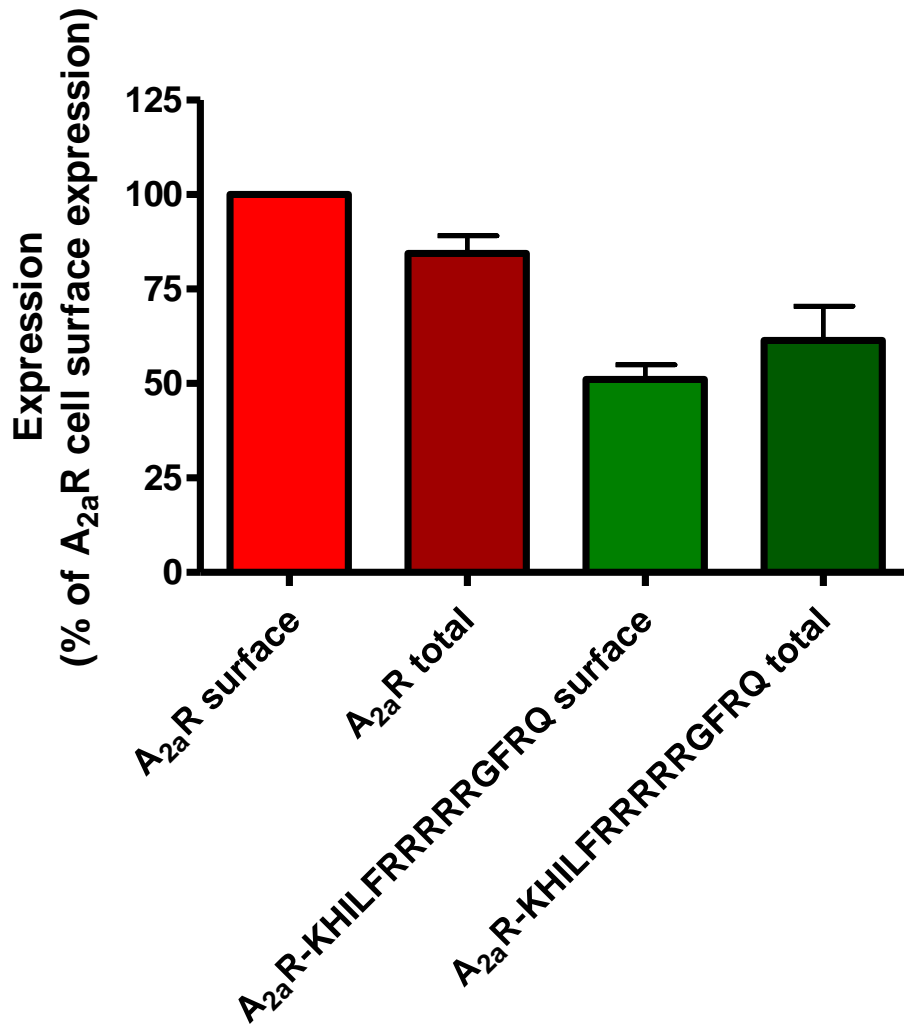
Figure 4.6. Whole-cell expression data comparing total expression of A$_{2a}$R-KHILFRRRRRGRFRQ and A$_{2a}$R. Data were normalised to untransfected cells (0 %) and cell-surface expression of A$_{2a}$R (100 %). Data are mean ± s.e.m. of three experiments performed in triplicate.

4.3 Discussion

Many diseases, including retinitis pigmentosa and nephrogenic diabetes insipidus, can be caused by ER-retention of mutated proteins. Characterisation of these ER-retained proteins would provide insight into the misfolding of the proteins and potential methods of recovering cell surface expression. Already there are pharmacological chaperones that allow recovery of cell surface expression, *in vitro*, for some proteins such as V_2R (Hawtin, 2006). Detailed information of the retained proteins would help identify and develop new pharmacological chaperones that may be used as treatment for some of the diseases mentioned. These mutated proteins are not trafficked to the cell surface, therefore solubilisation of ER membranes would be required. SMALP-solubilisation has been shown to show no preference for lipid type when solubilising membranes (Dorr et al., 2014). It is therefore possible that SMALPs could solubilise intracellular membranes but this has not yet been conclusively established. To investigate the ability of SMA to solubilise intracellular membranes, $A_{2a}R$ constructs were engineered with ER-retention motifs with the view to prevent their trafficking to the cell surface.

Previous studies that have engineered the KDEL motif at the extreme C-terminus of proteins have proven successful at retaining the protein in the ER (Munro and Pelham, 1987, Jackson et al., 1990). Although a small amount of "leakage" had been observed in some studies, receptor progression through the ER and Golgi apparatus was retarded for both soluble and membrane-bound proteins (Jackson et al., 1990). However, the lack of any ER-retention in this study showed that the KDEL sequence was ineffective at retaining $A_{2a}R$ in the ER. It has been shown, (Stornaiuolo et al., 2003), that the KDEL sequence results in retrieval of proteins in transit between the ER and Golgi apparatus. There have been reports of transmembrane proteins that exit the ER through different mechanisms, bypassing the Golgi altogether (Grieve

and Rabouille, 2011). This may have provided an alternative pathway by which glycosylation deficient $A_{2a}R$ could reach the cell surface.

In an attempt to force the $A_{2a}R$ through the Golgi pathway, reintroduction of the glycosylation site at residue 154 was performed. The asparagine residue at 154 undergoes N-linked glycosylation, originating in the ER before elaboration in Golgi apparatus. Although glycosylation has been shown to increase cell-surface expression of proteins (Davidson *et al.*, 1996), there has been no evidence of saturating the ER-retention mechanism reported, despite up to 7-fold increases in receptor expression (Munro and Pelham, 1987). The increased expression of glycosylated-$A_{2a}R$ was not expected to be as high as 7-fold as $A_{2a}R$ only contains 1 glycosylation site, unlike most family A GPCRs which contain 2 or 3. Western blot analysis showed the typical banding pattern observed for glycosylated proteins (Wheatley and Hawtin, 1999). Different sugar moieties of different sizes confer extra mass to a protein, providing a thick, undefined banding pattern greater than that of the calculated protein mass. However, glycosylation of $A_{2a}R$-KDEL was still ineffective at conferring ER-retention. As glyco-$A_{2a}R$ must have been transported to the Golgi apparatus, the KDEL ER-retention motif must not have been able to impart ER-retention on $A_{2a}R$. This could possibly have been due to the tertiary structure adopted by the long (~122 residues) C-terminal tail of $A_{2a}R$ concealing the KDEL motif.

The final 14 residues of the α_{2c}-AR, KHILFRRRRRGFRQ, have been reported to act as an ER-retention motif at family A GPCRs α_{2c}-AR and CXCR1 (Schwappach et al., 2000, Milligan et al., 2005). The increased length of the KHILFRRRRRGFRQ motif and the reported ability to retain family A GPCRs in the ER made this motif an exciting prospect after KDEL was unable to impart ER-retention on $A_{2a}R$. The KHILFRRRRRGFRQ motif was engineered to the C-terminus of $A_{2a}R$ and first investigated for its ability to prevent $A_{2a}R$ expression at the cell surface. $A_{2a}R$-KHILFRRRRRGFRQ displayed reduced expression at the cell surface of 51.1 ±

3.9 % compared to $A_{2a}R$, but this was largely a result of an overall reduced expression level. The KHILFRRRRRGFRQ motif was responsible for reducing overall expression of $A_{2a}R$ to 61.4 ± 9.1 %, although this figure may be slightly misleading. The whole-cell ELISA technique employs detergent to permeabilise the cell membrane, allowing antibody access to the intracellular membranes of the cell. As a result, the detergent solubilises a fraction of the cell surface-expressed receptor. This is likely how overall expression of $A_{2a}R$ appeared to be less than $A_{2a}R$ expressed at the cell-surface. This was obviously impossible and therefore most likely an artefact of the whole-cell ELISA technique. Total $A_{2a}R$-KHILFRRRRRGFRQ expression was therefore probably higher than the data suggested. However, it appeared the majority of $A_{2a}R$-KHILFRRRRRGFRQ expressed was expressed at the cell surface. Upon SMALP-solubilisation of $A_{2a}R$-KHILFRRRRRGFRQ it would not be possible to state definitively whether it had been extracted from the ER or cell surface.

The KHILFRRRRRGFRQ sequence was substantially longer than KDEL and was able to affect some measure of intracellular retention. This suggests that it may have been the length of the KDEL sequence in comparison to the length of the $A_{2a}R$ C-terminus (~121 residues) that was preventing KDEL from effectively retaining $A_{2a}R$ in the ER. It has been previously reported (Singh *et al.*, 2010, Piersen *et al.*, 1994) that the C-terminus of $A_{2a}R$ can be truncated, by 96 residues, back to residue 316 without affecting receptor function. KDEL was a short (only four residues) sequence at the end of a seemingly superfluous region of $A_{2a}R$. The – KHILFRRRRRGFRQ motif, which has been successfully used for ER-retention for α_{2c}-AR (Schwappach et al., 2000) and CXCR1 (Milligan et al., 2005) (C-terminal lengths of 21 and 42 respectively), was a short sequence compared to the 121 residues at the C-terminal tail of $A_{2a}R$. Therefore the tertiary structure adopted by the C-terminal tail of $A_{2a}R$ may have concealed the KDEL and KHILFRRRRRGFRQ sequences, preventing retention in the ER. Although it has been shown that removal of tertiary structure from the C-terminus has no effect on ER-retention

conferred by KDEL (Munro and Pelham, 1987), there has been no indication of possible interference to ER-retention from different tertiary structures of extended C-termini.

The efforts to retain $A_{2a}R$ in the ER were therefore unsuccessful and it is unclear as to why this was the case. Future work that may go in to SMALP-solubilisation from intracellular membranes may wish to engineer the retention motifs to C-terminally truncated $A_{2a}R$. This would allow for a more accessible motif, increasing the likelihood of being captured in the ER, without compromising receptor function. Alternatively, HA-tagged V_2R containing an NDI mutation, such as I46K (Pasel et al., 2000), resulting in ER-retention could be employed. RAMP1 is known to be retained in the ER in the absence of family B GPCR expression (Christopoulos et al., 1999). Epitope-tagging of RAMP1 and subsequent SMALP-solubilisation would provide information on the ability to SMALP-solubilise from intracellular membranes. However, no functional studies would be available to study the functional state of RAMP1 once SMALP-solubilised.

In summary, it is still unknown whether SMA can extract proteins from the membranes of intracellular organelles in whole mammalian cells. This was due to the difficulties in creating a tool to measure such properties. KDEL and KHILFRRRRRGFRQ sequences were unable to retain $A_{2a}R$ in the ER. The reasons for this were unclear but may involve concealed C-termini. Although these methods did not confer ER-retention, there are still several alternatives that could be investigated.

CHAPTER 5: CYSTEINE-DEPLETED A~2a~R FOR SMALP BIOPHYSICAL STUDIES

5.1 Introduction

SMALP technology has proven a useful platform in the study of membrane-bound proteins by analytical techniques such as: cryo-electron microscopy (Postis *et al.*, 2015); transmission-electron microscopy; nuclear magnetic resonance (NMR); circular dichroism (CD) (Knowles *et al.*, 2009); electron paramagnetic resonance (Orwick-Rydmark *et al.*, 2012); analytical ultracentrifugation and differential scanning calorimetry (Jamshad *et al.*, 2011). In each case, SMALPs provided a platform as useful for the technique as alternative solubilisation methodologies. In some cases SMALPs proved more useful than alternatives in techniques such as CD. When used in CD, SMALPs were able to be studied at lower wavelengths than the available membrane-embedded alternative, apolipoprotein stabilised nanodiscs, due to the non-proteinaceous nature of SMALPs, allowing further studies of protein structure. However, to date, no study on the real-time dynamics of protein conformation has been performed in SMALPs.

The real-time study of proteins provides information on conformational rearrangements upon ligand interaction and protein-protein interactions. In recent years Förster resonance energy transfer (FRET) has been used to study GPCRs upon ligand interaction to view nanometre changes in conformations over nanosecond timescales (Lohse *et al.*, 2012).

5.1.1 Intrinsic tryptophan fluorescence and FRET

The structure of TM helices in transmembrane proteins has been shown to be dependent on the lipid composition of the bilayer (Gibson and Brown, 1993, Caputo and London, 2003). Changes to the lipid composition, and change in lateral pressure, through detergent

solubilisation can therefore alter the structure and behaviour of the protein studied. By maintaining the lipid annulus of proteins, SMALP-solubilisation was hypothesised to be a potential platform for studying GPCR ligand-induced conformational changes using intrinsic tryptophan fluorescence and FRET. The transparency of SMA has already been shown to allow detailed study of proteins at lower wavelengths than other solubilisation systems. Tryptophan residues are known to excite at 280 nm and emit photons at approximately 350 nm, at both wavelengths SMALPs have been shown not to obscure light. Changes in the local environment of the Trp affect the emission spectra; movement of Trp residues from hydrophobic regions (e.g. membrane embedded) to be more solvent-exposed displays as a reduced quantum yield in fluorescence signalling (and *vice versa*). This allows real-time study of the conformational changes of proteins.

FRET is another, highly sensitive, fluorescence technique. With longer fluorescence times than intrinsic tryptophan fluorescence, FRET allows collection of data over nanosecond timescales. This allows determination of rotations and more intermediate conformations adopted upon ligand interaction, with fewer artefacts created from surrounding residues. The extrinsic fluorophore IAEDANS (5-({2-[(iodoacetyl)amino]ethyl}amino)naphthalene-1-sulfonic acid) is commonly used in fluorescence microscopy and FRET. IAEDANS reacts with thiol groups, which in proteins allows labelling of non-disulphide-bound cysteines. As the fluorescence spectra of IAEDANS are linked to the immediate solvent environment, changes in protein conformation can be observed through altered emission spectra. The excitation of IAEDANS (336 nm) overlaps well with tryptophan fluorescence emissions, meaning IAEDANS-Trp FRET data can be used to observe changes in distance between these two reporters. IAEDANS emits at 490 nm, a wavelength not obscured by SMA, allowing the use of SMALPs in FRET studies.

5.1.2 Loci for reporter group introductions

For these studies, an $A_{2a}R$ construct was manufactured to contain strategically placed tryptophan (intrinsic tryptophan fluorescence) and cysteine residues (IAEDANS derivatisation site). These residues would allow for studies of $A_{2a}R$ conformation upon activation by agonist compared to binding antagonists. The desired use of IAEDANS as a fluorescent probe, at a specific locus, required all other thiol groups (i.e. cysteine residues) to be either invested in disulphide-bond formation or inaccessible. Remaining cysteines would require mutation to a different, non-reactive, residue to ensure the spectra observed were from the desired cysteine only.

Inspection of the $A_{2a}R$ sequence revealed several residues with potential to report on conformational changes associated with activation of the $A_{2a}R$. Leu78 (3.26 at the top of TM3), Ile106 (3.54 in ICL2), Tyr176 (5.37 at the top of TM 5), Leu225 (6.27 in ICL3), Ala231 (6.33 in ICL3) and Thr256 (6.58 at the top of TM6) were all identified as being suitable candidates for mutation to reporter groups tryptophan or cysteine (numbers in brackets are the Ballesteros-Weinstein numbering system (Ballesteros and Weinstein, 1995)). As seen in figure 5.1, Leu78, Tyr176 and Trp256 are all present close to the top of their respective TM helix. Introduction of reporter groups at these sites would allow study of how the extracellular face of $A_{2a}R$ behaves upon ligand binding. As noticed among crystal structures of family A GPCRs (Dore et al., 2011, Xu et al., 2011, Unal and Karnik, 2012), it would be expected that Thr256 and Leu78/Tyr176 would move closer together upon agonist binding. At the intracellular face, detected signals from residue 106 in relation to residues 225 and 231 would allow study of conformational changes at the intracellular face of $A_{2a}R$. An observed increase in distance between TM3 and TM6 upon agonist binding would be expected as a G-protein binding pocket becomes exposed. Intracellular residues Ile106 and Ala231 were the $A_{2a}R$ equivalent of β_2AR residues that were previously successful as reporter groups in fluorescence assays
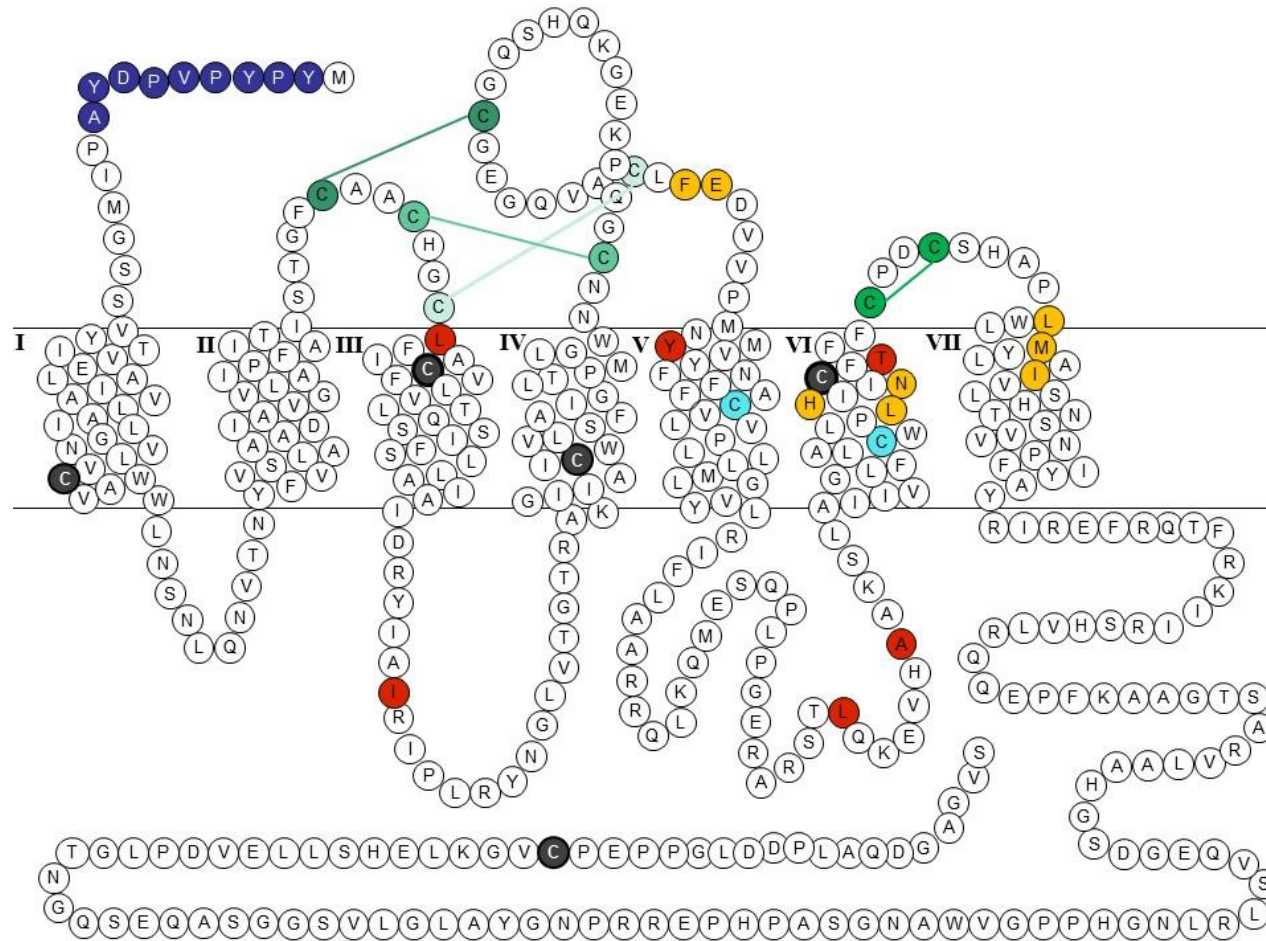
Figure 5.1. 2D representation of the A$_{2a}$R. An HA-epitope tag at the N-terminus shown in dark blue. Cysteines that form disulphide bridges are shown in matching shades of green. Residues mutated for reporter groups are highlighted in red. Two cysteines that were not mutated are shown in cyan. Cysteine residues with grey backgrounds were removed. Residues in orange form the ZM241385 binding pocket. Helices are labelled with roman numerals.

(Yao *et al.*, 2006, Yao *et al.*, 2009). Due to the steric hindrance caused by the bulky Trp sidechain, Trp was considered to be the more difficult of the reporter groups to incorporate. Residues to be used as IAEDANS derivatisation sites were investigated for their ability to incorporate the bulky IAEDANS. These residues were mutated to the bulky tryptophan to observe any negative impact on receptor function.

5.1.3 The "Zhar" construct

For most biophysical analyses, large quantities of protein are required. Large-scale production of proteins most commonly utilises expression systems such as yeast or *E.coli*, or insect cells such as Sf9. Due to relative abundances of tRNAs varying between different systems, it was possible for the creation of a "yeast optimised" form of the $A_{2a}R$ to be engineered. The yeast-optimised $A_{2a}R$, herein referred to as "Zhar", coded for the human $A_{2a}R$ protein, but codons had been optimised to correspond to the most abundant forms of tRNA present in *Pichia pastoris* (*P.pastoris*). This generated increased expression levels of the $A_{2a}R$ in the yeast expression system *P.pastoris* and was a kind gift from Prof. Roslyn Bill (Aston University).

As displayed in figure 5.2, the Zhar construct had several modifications to aid downstream purification and analysis. From the N-terminus, Zhar contains: a bovine pancreatic trypsin inhibitor (BPTI) signal peptide to allow targeting of the protein to the yeast cell plasma membrane; thrombin cleavage site to allow removal of the BPTI signal peptide; 10 x His-tag for downstream protein purification; a tobacco etch virus (TEV) cleavage site to remove His-tag after purification; 5 x GS linker to allow flexibility of the N-terminal tags; $A_{2a}R$ containing the mutation N154Q (to remove the sole glycosylation site and provide homogeneity in protein samples (Fraser, 2006) and C-terminally truncated after residue 316. This truncation of 96 residues had been reported previously not to be detrimental in relation to protein function (Piersen *et al.*, 1994); flag-tag for downstream identification; 5 x GS linker and biotinylation site to provide an alternative purification strategy on a streptavidin column. None of these
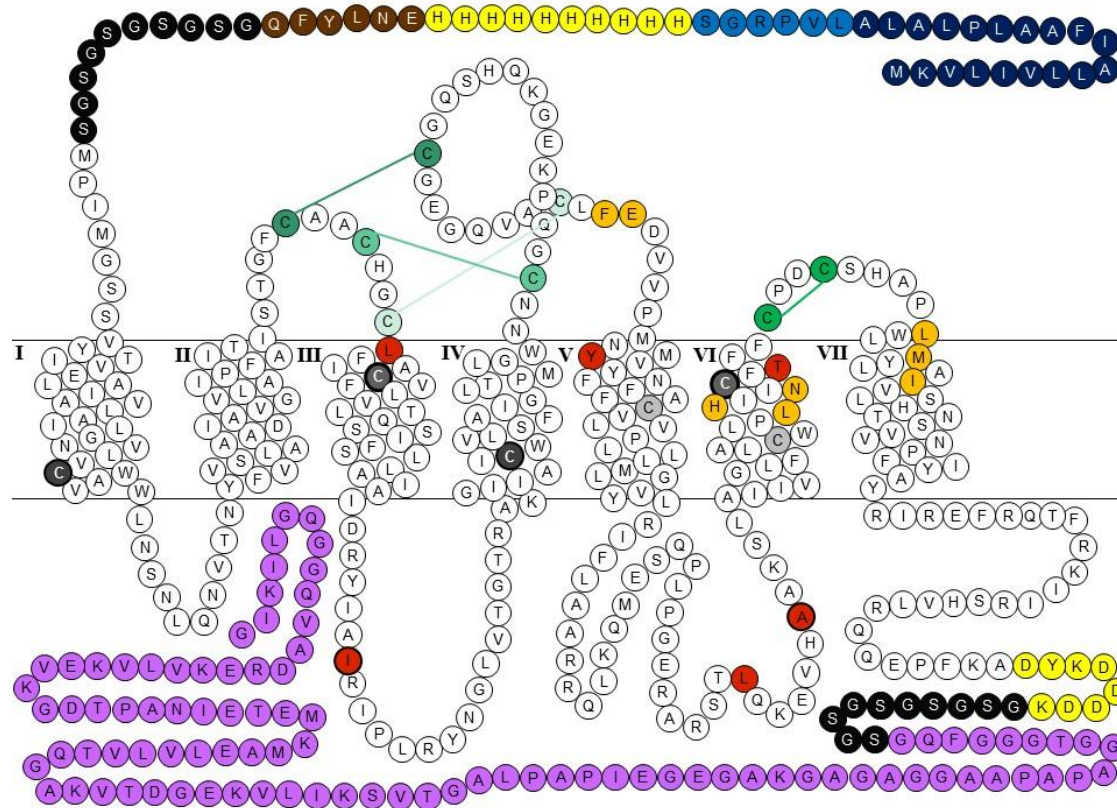
Figure 5.2. The A₂ₐR "Zhar" construct. Bovine pancreatic trypsin inhibitor signal peptide at the N-terminus shown in dark blue. Light blue shows a thrombin cleavage site. 10 x His tag at the N-terminus and FLAG tag at the C-terminus shown in yellow. TEV cleavage site shown in brown. 5 x GS linker at both termini shown in black. Biotinylation site shown in purple. Cysteines that form disulphide bridges are shown in matching shades of green. Residues mutated for reporter groups are highlighted in red. Two cysteines that were not mutated are shown in cyan. Cysteine residues with grey backgrounds were mutated. Residues in orange form the ZM241385 binding pocket. Helices are labelled with roman numerals.

additions contained cysteine or tryptophan residues that may interfere with fluorescence signalling assays.

Cys-depletion of $A_{2a}R$ was engineered in Zhar as downstream biophysical techniques would require large quantities of protein. This would be uneconomical to produce from mammalian cell culture but readily achievable in *P.pastoris*. Pharmacological characterisation of all mutations was undertaken in transiently transfected mammalian cells (HEK 293T).

5.2   Results

5.2.1   Zhar reporter group mutations

Tryptophan and cysteine residues can act as reporter groups in fluorescent studies. From their introduction at specific loci it is possible to elucidate the conformational changes a receptor undergoes upon ligand binding. Tryptophan was introduced at residues 78, 106, 176, 225 and 231 of Zhar while cysteine was introduced at residues 78 and 256 of Zhar. These loci would provide information of the conformational changes of $A_{2a}R$ upon agonist stimulation. However, it was important that these mutations should not perturb receptor function. Each individual mutant was therefore characterised for expression at the cell surface and ligand binding capabilities. It was demonstrated that there was no difference in affinity for [^{3}H]ZM241385 between $A_{2a}R$ and Zhar (table 5.1).

Competition radioligand binding experiments were performed to assess the effect of the mutations on the binding capabilities of Zhar. All tryptophan introductions displayed WT-like binding profiles, with the exception of [L78W]Zhar which showed a 100-fold reduced affinity for ZM241385 (figure 5.3 and table 5.1). [L78C]Zhar bound with WT-like affinity, making it better tolerated than [L78W]Zhar, but with a large s.e.m., the results were inconsistent. [T256C]Zhar showed a 100-fold reduced affinity for ZM241385.
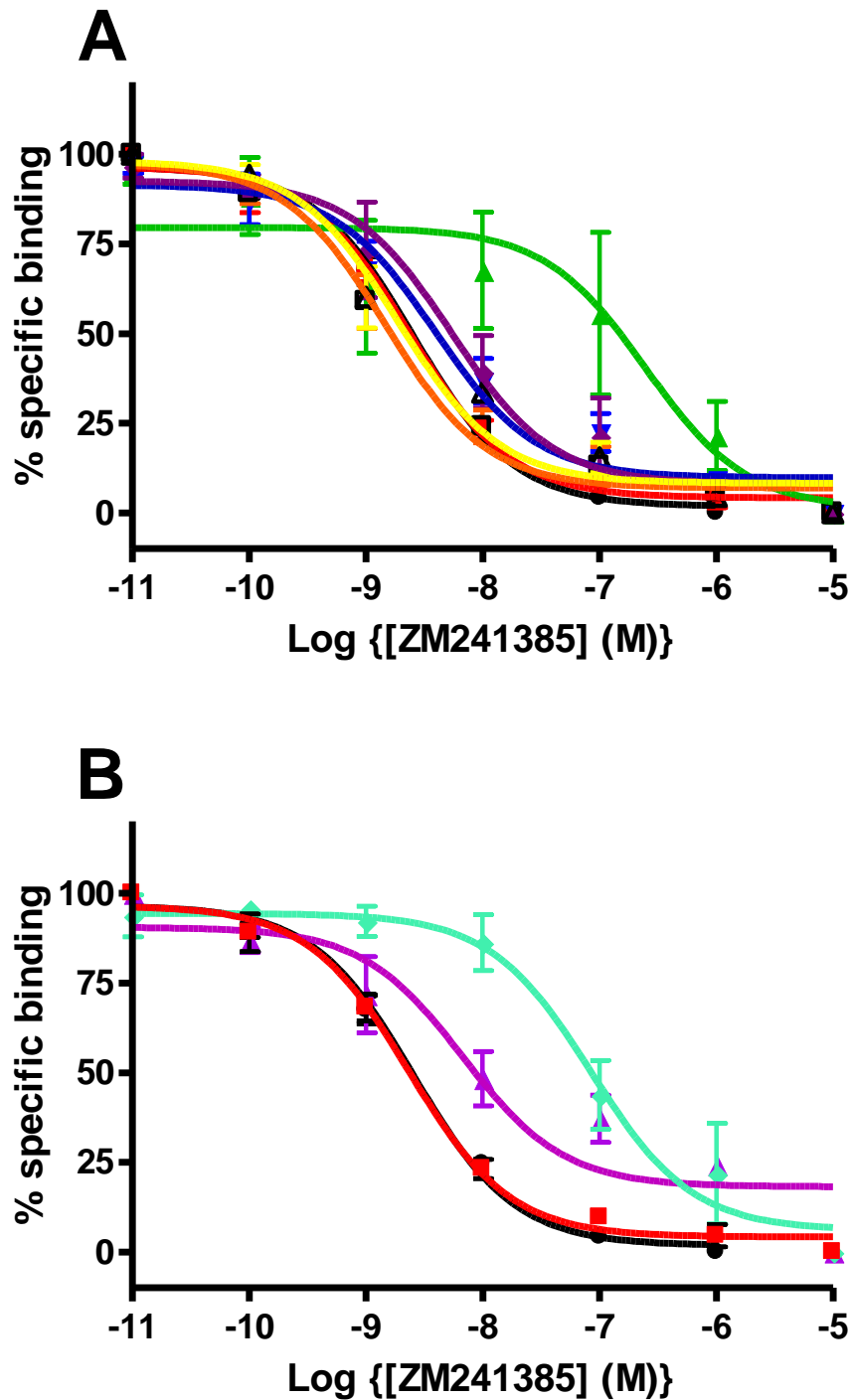
Figure 5.3. Competition radioligand binding of Zhar with individual reporter group introductions. Self-competition of [³H]ZM241385 as a tracer at A: tryptophan introductions [L78W]Zhar (▲); [I106W]Zhar (▼); [Y176W]Zhar (♦); [L225W]Zhar (□); [A231W]Zhar (△) B: [L78C]Zhar (▲); [T256C]Zhar (♦). Both panels have $A_{2a}R$ (●) and WT-Zhar (■) for comparison. Data are mean ± s.e.m. of three experiments performed in triplicate.

Construct	pK$_i$ ± s.e.m.
A$_{2a}$R	8.87 ± 0.1
WT-Zhar	8.97 ± 0.1
[L78W]Zhar	6.96 ± 0.2
[L78C]Zhar	8.64 ± 1.0
[I106W]Zhar	8.99 ± 0.2
[Y176W]Zhar	8.46 ± 0.5
[L225W]Zhar	9.23 ± 0.3
[A231W]Zhar	9.31 ± 0.3
[T256C]Zhar	6.85 ± 0.4

Table 5.1. pK$_i$ values of [^{3}H]ZM241385 at A$_{2a}$R compared to Zhar and mutant Zhar constructs. Data are mean ± s.e.m. of three experiments performed in triplicate.

Cell surface expression of Zhar constructs was determined in relation to WT-Zhar. As seen in figure 5.4 and table 5.2, cell surface expression of [L78W]Zhar, [L78C]Zhar and [T256C]Zhar were all markedly reduced compared to WT-Zhar. Expression levels were WT-like for [I106W]Zhar; reduced for [Y176W]Zhar; and reduced to around 50 % for [L225W]Zhar and [A231W]Zhar. All constructs that expressed >50 % retained the ability to internalise at levels comparable to WT-Zhar. Internalisation experiments were not reliable when expression level of constructs was < 20 % of WT-Zhar. There was an observed decrease in specific binding for all Zhar constructs in relation to WT-Zhar (shown in table 5.2) that correlated with the observed decrease in cell surface expression. [I106W]Zhar, [Y176W]Zhar and [A231W]Zhar showed reduced levels of specific binding further than the reduced levels of cell surface expression. However, the specific binding remaining for these constructs was sufficient to allow acquisition of robust ligand binding data.

[I106W]Zhar was the best tolerated mutation, with WT-like expression levels and binding profile, therefore chosen as the introduced Trp reporter at the bottom of TM3. Of the other intracellular-side mutations investigated, mutation of [L225]Zhar and [A231]Zhar were equally well tolerated. They both displayed WT-like binding profiles and expression levels that would allow robust cell signalling data acquisition. [A231]Zhar was chosen to be the site of the Cys residue introduction. With I106W, A231C could be used to monitor movement between TM3 and TM6.

5.2.2 Zhar Cys-depletion

To avoid IAEDANS labelling of undesired thiol groups, cysteine residues in the $A_{2a}R$ had to be either contributing to a disulphide-bond or buried in a TM helix and thereby inaccessible to a water-soluble reagent. The $A_{2a}R$ has 15 cysteine residues; 8 Cys residues, located in ECL1, 2 and 3, form disulphide bonds with one another (Cys71-Cys159; Cys74-Cys146; Cys77-Cys166; Cys259-Cys262). Mutation of these residues results in perturbation of normal function

(Wheatley *et al.*, 2012), but as they were disulphide-bound they could not be derivatised as there was no free thiol group. As seen in the high resolution crystal structure of $A_{2a}R$ (PDB code: 4EIY (Liu *et al.*, 2012)), Cys185 and Cys245 are both located in the middle of their respective TMs (5 and 6), pointing away from the ligand binding pocket located in the centre of the TM bundle. Cys245 also forms part of the, highly conserved family A, CWxP motif of TM6, mutation of which leads to drastically reduced, almost abolished, cell surface expression and altered receptor function amongst GPCRs (Lu et al., 2007, Xu et al., 2008). It has been previously reported that Cys residues buried deep in TM helices were not tolerant of mutation (Yao *et al.*, 2006). However, as these residues were also inaccessible for IAEDANS binding and would not interfere with FRET signalling assays, it was described that it may not be necessary for Cys185 and Cys245 in $A_{2a}R$ to be mutated. Cys394 is present in the C-terminal tail of $A_{2a}R$, a region of great flexibility and easily accessible due to its hydrophilic nature. However, as explained below, Cys394 was removed through a C-terminal truncation in the $A_{2a}R$ construct used. It was deemed necessary to mutate Cys28, Cys82, Cys128 and Cys254 as they were all close to the top or bottom of their respective TM helices and therefore potentially reactive towards thiol-directed derivatisation.

It was important to select mutations for cysteine residues that would not result in altered receptor function. Cysteine to alanine mutations are generally well tolerated amongst GPCRs, but this is not necessarily the case. In addition, replacing cysteine with alanine introduces a different physical characteristic at that locus which may be detrimental to function. In an effort to select residues to replace cysteine that would be less likely to perturb the tertiary structure of $A_{2a}R$, sequences were compared across adenosine receptor subtypes and across species within a subtype. Cys82 was found to be conserved as a cysteine across the adenosine receptor family; with no obvious alternative, this was mutated to alanine. Cys254 was also a conserved cysteine in all but mouse and rat A_3R in which it is phenylalanine, a large sidechain was likely
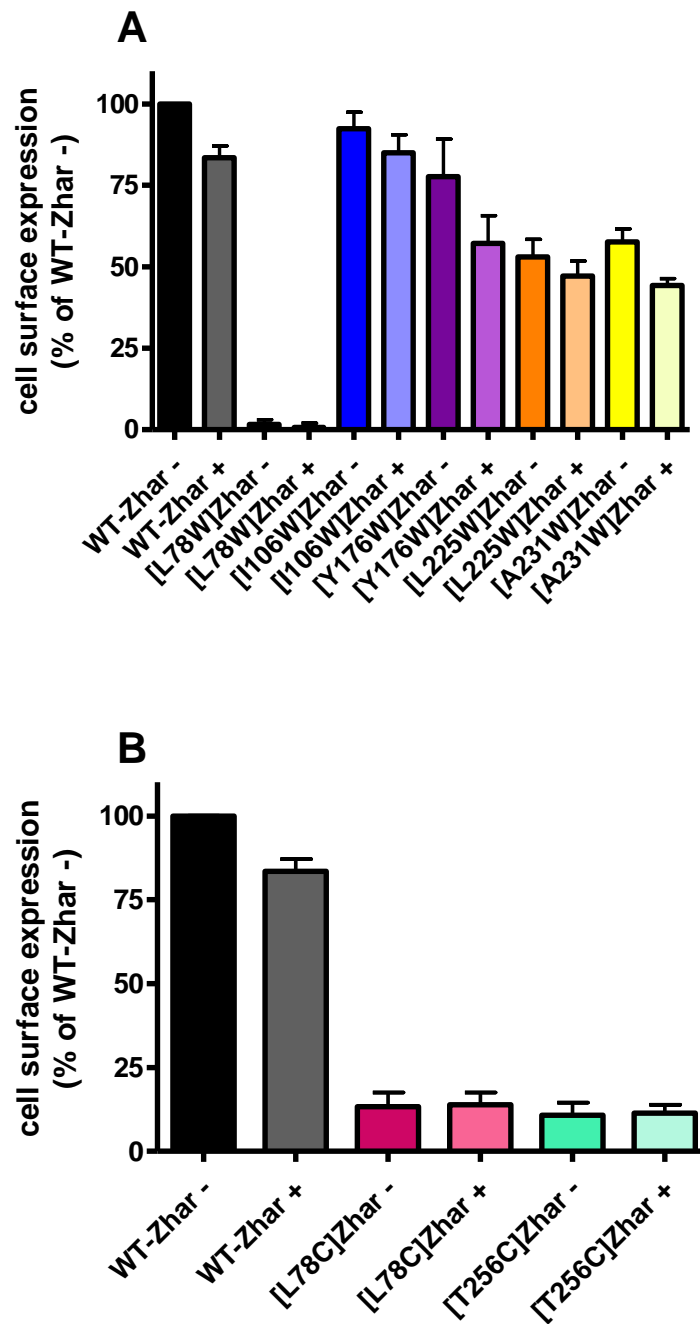
Figure 5.4. Cell surface expression of Zhar constructs containing reporter groups +/- agonist stimulation. Cell surface expression, determined using anti-His antibody was normalised to untransfected cells (0 %) and unstimulated WT-Zhar (100 %). Internalisation under agonist stimulation was determined using NECA (100 μM) for 1 h. Data are mean ± s.e.m. of three experiments performed in triplicate.

Construct	Cell surface expression (% of Zhar ± s.e.m.)	Specific binding (% of Zhar ± s.e.m.)
WT-Zhar	100.0 ± 0.1	100 ± 0.0
[L78W]Zhar	1.6 ± 1.5	6.6 ± 0.8
[L78C]Zhar	13.4 ± 4.2	13.7 ± 2.6
[I106W]Zhar	92.4 ± 5.1	34.6 ± 11.4
[Y176W]Zhar	77.7 ± 11.6	27.8 ± 5.4
[L225W]Zhar	53.1 ± 5.4	53.5 ± 3.8
[A231W]Zhar	57.6 ± 4.0	36.7 ± 1.5
[T256C]Zhar	10.8 ± 3.7	7.6 ± 1.8

Table 5.2. Cell surface expression levels compared to specific binding observed for Zhar constructs relative to WT-Zhar. Data are mean ± s.e.m. of three experiments performed in triplicate.

to create steric hindrance, therefore Cys254 was also mutated to the small residue alanine. Cys28, as shown in figure 5.5, was isoleucine in A_1R which was conserved across species. Cys128 was a conserved leucine in $A_{2b}R$, as shown in figure 5.6. Cys28 and Cys128 were therefore mutated to Ile and Leu respectively, as well as to Ala, to identify which mutation produced the least disruption to receptor function.

Due to their presence at the top of their respective helices, Cys82 and Cys254 necessitated mutation to prevent labelling by IAEDANS. A double mutant, [C82A/C254A]Zhar was created. From data displayed in figure 5.7, it was seen that [C82A/C254A]Zhar bound with WT-like affinity for ZM241385 in comparison to $A_{2a}R$ (pK$_i$: 9.33 ± 0.2 in comparison to 8.87 ± 0.1). [C82A/C254A]Zhar expressed at the cell surface at slightly increased levels (119 ± 4.7 % compared to WT-Zhar) but retained WT-like internalisation of ~19 % upon agonist stimulation.

With the successful construction of the [C82A/C254A]Zhar (herein referred to as [2A]Zhar), reporter group mutations were incorporated at ICL2 (I106W) and ICL3 (A231C) to ensure [I106W/A231C][2A]Zhar (herein referred to as [Δ4]Zhar) was a viable construct. As seen in figure 5.8, [Δ4]Zhar displayed a slight reduction in affinity of ZM241385. [Δ4]Zhar bound ZM241385 with a pK$_i$ of 8.63 ± 0.4 compared to $A_{2a}R$ with a pK$_i$ of 8.87 ± 0.1. [Δ4]Zhar was expressed at the cell surface at levels comparable to WT-Zhar (85.5 ± 5 %). [Δ4]Zhar was also able to internalise to a similar degree as WT-Zhar following agonist challenge (NECA, 100 μM, 1 h).

```
_AA1R_RAT_Adenosine    MPPYISAFQAAYIGIEVLIALVSVPGNVLVIWAVKVNQALRDATFCFIVS
_AA1R_MOUSE_Adenosi    MPPYISAFQAAYIGIEVLIALVSVPGNVLVIWAVKVNQALRDATFCFIVS
_AA1R_HUMAN_Adenosi    MPPSISAFQAAYIGIEVLIALVSVPGNVLVIWAVKVNQALRDATFCFIVS
_AA1R_BOVIN_Adenosi    MPPSISAFQAAYIGIEVLIALVSVPGNVLVIWAVKVNQALRDATFCFIVS
_AA1R_RABIT_Adenosi    MPPSISAFQAAYIGIEVLIALVSVPGNVLVIWAVKVNQALRDATFCFIVS
_AA1R_CHICK_Adenosi    MAQSVTAFQAAYISIEVLIALVSVPGNILVIWAVKMNQALRDATFCFIVS
_AA2AR_HUMAN_Adenos    MPIMG---SSVYITVELAIAVLAILGNVLVCWAVWLNSNLQNVTNYFVVS
                       *.        .:.**  :*:  **:::: **:** ***  :*.  *::.*   *:**
```

Figure 5.5. ClustalW alignment of human $A_{2a}R$ with A_1R from different species.

Highlighted is the Cys28 of $A_{2a}R$.


```
_AA2BR_RAT_Adenosin    VDRYLAIRVPLRYKGLVTGTRARGIIAVLWVLAFGIGLTPFLGWNSKDRA
_AA2BR_MOUSE_Adenos    VDRYLAIRVPLRYKGLVTGTRARGIIAVLWVLAFGIGLTPFLGWNSKDSA
_AA2BR_HUMAN_Adenos    VDRYLAICVPLRYKSLVTGTRARGVIAVLWVLAFGIGLTPFLGWNSKDSA
_AA2BR_RABIT_Adenos    VDRYLAILVPLRYKSLVTGTRARGVIAVLWVLAFGIGLTPFLGWNSKDSA
_AA2BR_BOVIN_Adenos    VDRYLAVRVPLRYKSLVTGARARGVIAALWVLAFGIGLTPFLGWNDRKIA
_AA2BR_CHICK_Adenos    IDRYLAIKIPLRYNSLVTGKRARGLIAVLWLLSFVIGLTPLMGWNKAMSG
_AA2AR_HUMAN_Adenos    IDRYIAIRIPLRYNGLVTGTRAKGIIAICWVLSFAIGLTPMLGWNN----
                       :***:*: :****:.**** **:*:** *:*:* *****::***.
```

Figure 5.6. ClustalW alignment of human $A_{2a}R$ with $A_{2b}R$ from different species.

Highlighted is the Cys128 of $A_{2a}R$.
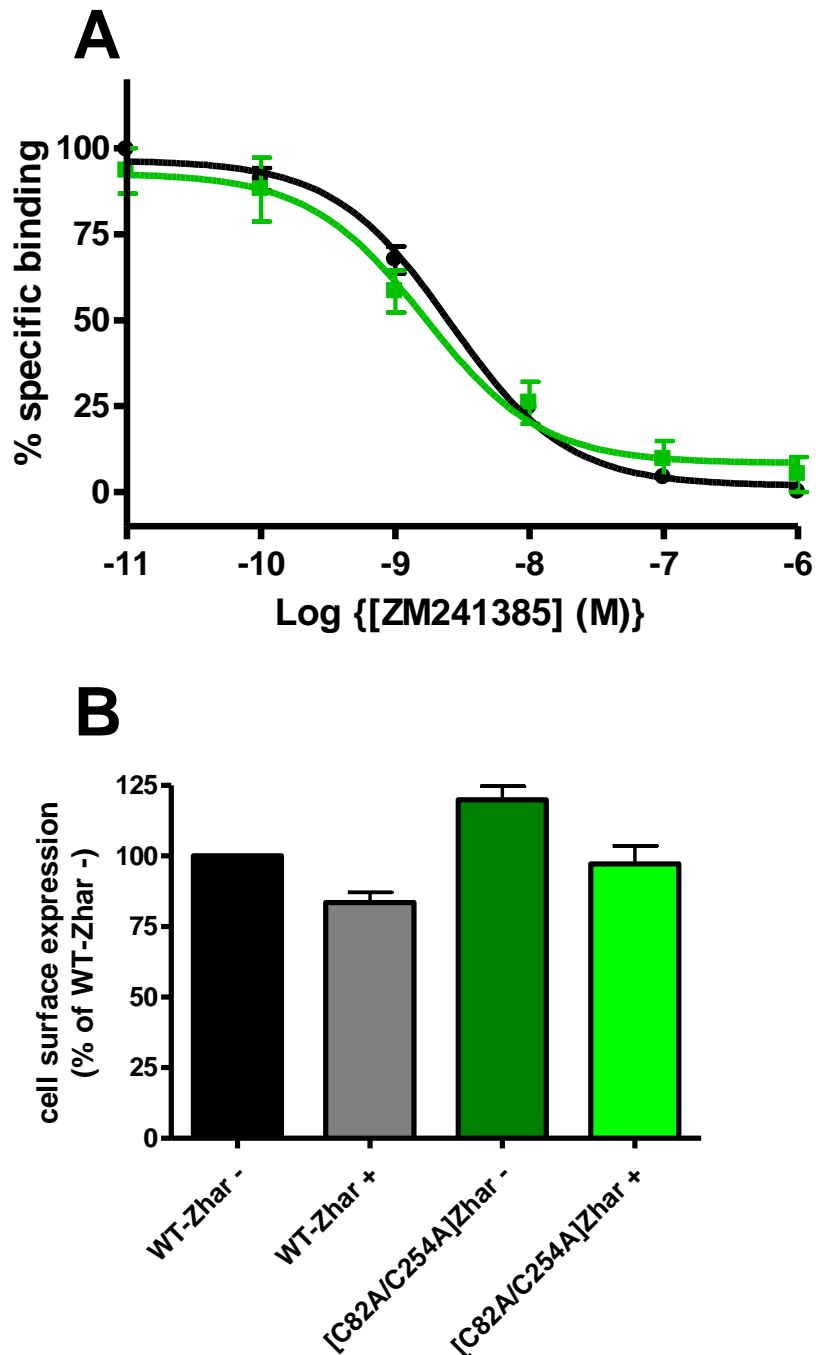
Figure 5.7. Characterisation of [C82A/C254A]Zhar. A: Self-competition radioligand binding of [^{3}H]ZM241385 at A$_{2a}$R (●) or [C82A/C254A]Zhar (■). B: cell surface expression of [C82A/C254A]Zhar in comparison to WT-Zhar, in the presence (+) or absence (-) of agonist stimulation (NECA, 100 μM, 1 h). Data are mean ± s.e.m. of three experiments performed in triplicate.
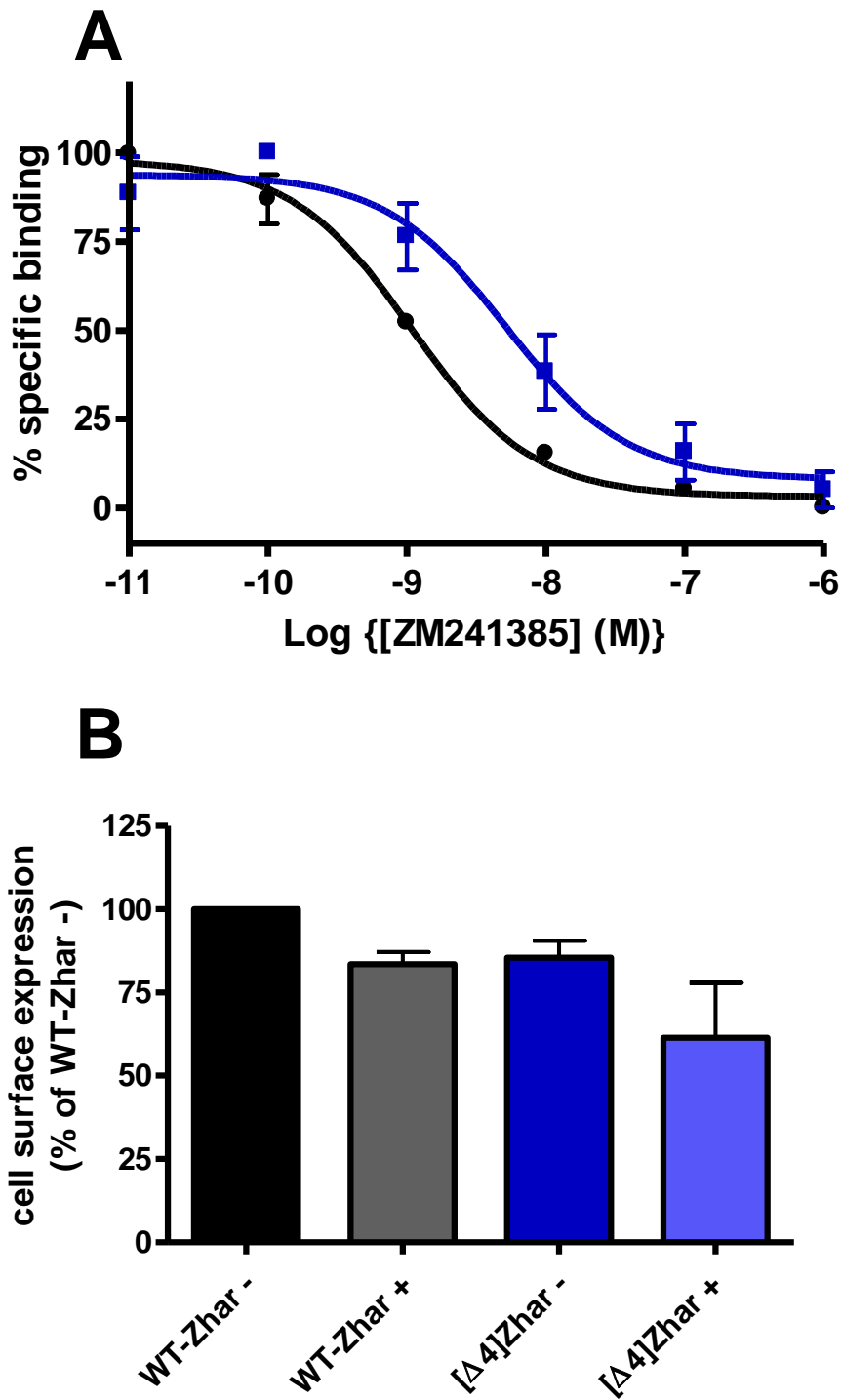
Figure 5.8. Characterisation of [Δ4]Zhar. A: Self-competition radioligand binding of ZM241385 at $A_{2a}R$ (●) or [Δ4]Zhar (■). B: cell surface expression of [Δ4]Zhar in comparison to WT-Zhar, in the presence (+) or absence (-) of agonist stimulation (NECA, 100 μM, 1 h). Data are mean ± s.e.m. of three experiments performed in triplicate.

Individual cysteine mutations at Cys28 and Cys128 were investigated to ensure WT-like characteristics of $A_{2a}R$ were maintained. This was performed in the human $A_{2a}R$ as well as Zhar to ensure the additional tags present in Zhar were not affecting the mutant constructs functionality. From figure 5.9 it can be observed that [C28A]$A_{2a}R$ expressed at a reduced level compared to $A_{2a}R$, whereas [C28I]$A_{2a}R$ was expressed at WT-like levels (63.0 ± 6.0 % and 108.9 ± 1.9 % respectively, compared to $A_{2a}R$). Both [C128L]$A_{2a}R$ and [C128A]$A_{2a}R$ were expressed at levels comparable to $A_{2a}R$ (114.6 ± 5.2 % and 101.9 ± 6.8 % respectively).

The construct that the mutations were incorporated into affected the outcome. When the same mutations were introduced to Zhar, [C28A]Zhar expressed at WT-like levels at the cell-surface (91.3 ± 10.3 % in Zhar, 63.0 ± 6.0 % in $A_{2a}R$). [C128L] displayed higher expression levels in Zhar compared to $A_{2a}R$ with increased expression of 169.4 ± 9.2 % in Zhar (only 114.6 ± 5.2 % in $A_{2a}R$). [C28I] and [C128A] also both displayed increased cell surface expression levels in Zhar (122.5 ± 9.2 % and 120.5 ± 10.3 % respectively). In both $A_{2a}R$ and Zhar, all 4 mutants retained the ability to internalise to a similar degree as WT. As [C28I] and [C128L] were both well tolerated in $A_{2a}R$ and Zhar, they were chosen as the mutations to remove the Cys residues at those positions. As shown in figure 5.10 and table 5.3, [C28I]Zhar and [C128L]Zhar demonstrated WT-like binding affinity for ZM241385.

Figure 5.11 shows that introduction of the [C28I] and [C128L] substitutions to the [Δ4]Zhar background showed an increase in cell-surface expression of 153.0 ± 28.2 % and 121.1 ± 22.3 % respectively in comparison to [Δ4]Zhar. The increased expression was not lost upon introduction of both mutations; [C28I/C128L][Δ4]Zhar expressed at 173.5 ± 23.5 % at the cell surface in comparison to [Δ4]Zhar. Radioligand binding data, shown in figure 5.12 and table 5.4, showed an increased affinity for ZM241385 of [C128L][Δ4]Zhar correlating with observations from [C128L]Zhar. Increased binding affinity was not lost in [C28I/C128L][Δ4]Zhar where introduction of both mutants resulted in approximately 10-fold
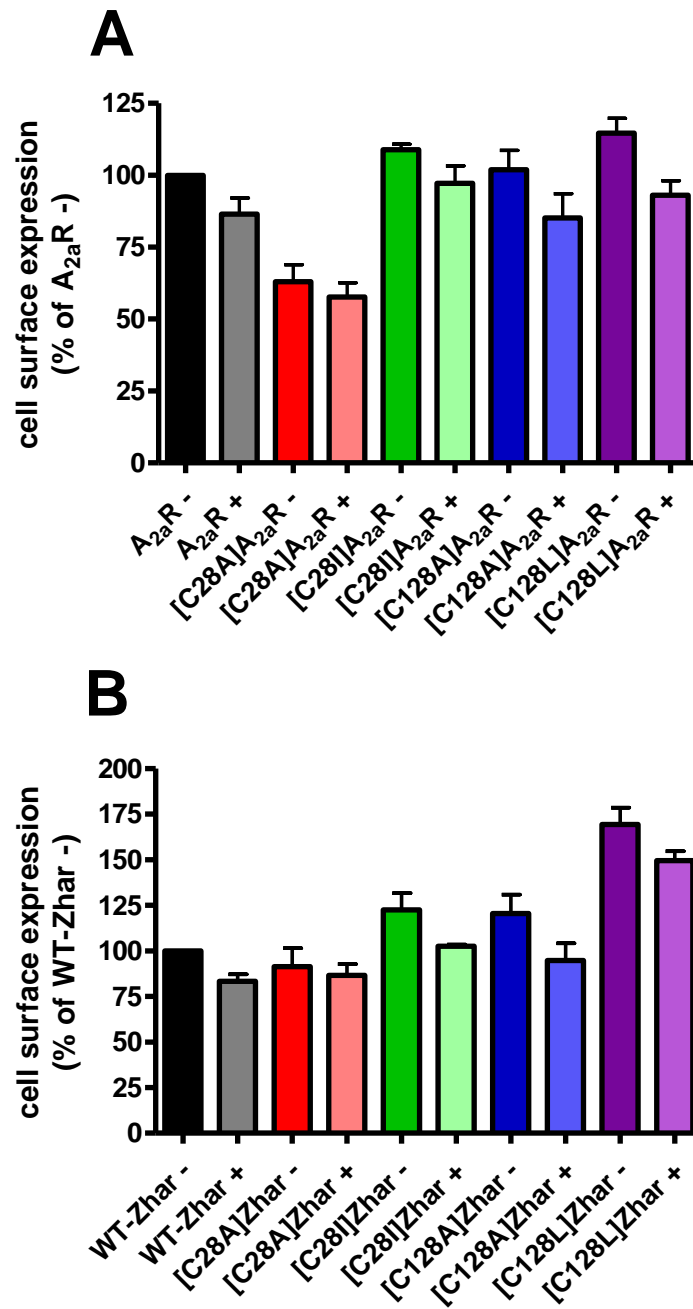
Figure 5.9. Cell surface expression of A$_{2a}$R and Zhar mutant constructs +/- agonist stimulation. Cell surface expression was determined for cysteine knockdown mutations in A$_{2a}$R (panel A) and Zhar (panel B) and normalised to untransfected cells (0 %) and A: unstimulated A$_{2a}$R (100 %) or B: unstimulated WT-Zhar (100%). Internalisation under agonist stimulation was determined using NECA (100 μM, 1 h). Data are mean ± s.e.m. of three experiments performed in triplicate.
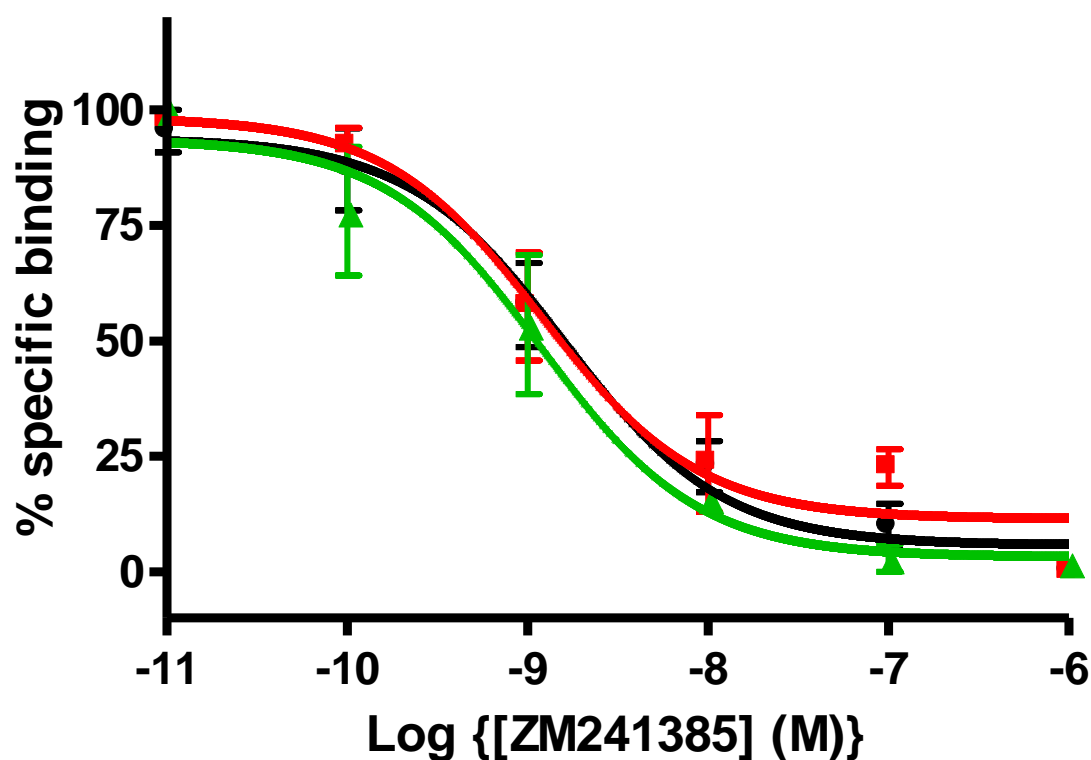
Figure 5.10. Competition radioligand binding analysis of cysteine mutations in Zhar. Self-competition of [³H]ZM241385 at WT-Zhar (●), [C28I]Zhar (■) and [C128L]Zhar (▲). Data are mean ± s.e.m. of three experiments performed in triplicate.

Construct	pK$_i$ ± s.e.m.
WT-Zhar	8.97 ± 0.1
[C28I]Zhar	9.42 ± 0.2
[C128L]Zhar	9.52 ± 0.4

Table 5.3. pK$_i$ values of cysteine knockdown mutations in Zhar. Data are mean ± s.e.m. of three experiments performed in triplicate.
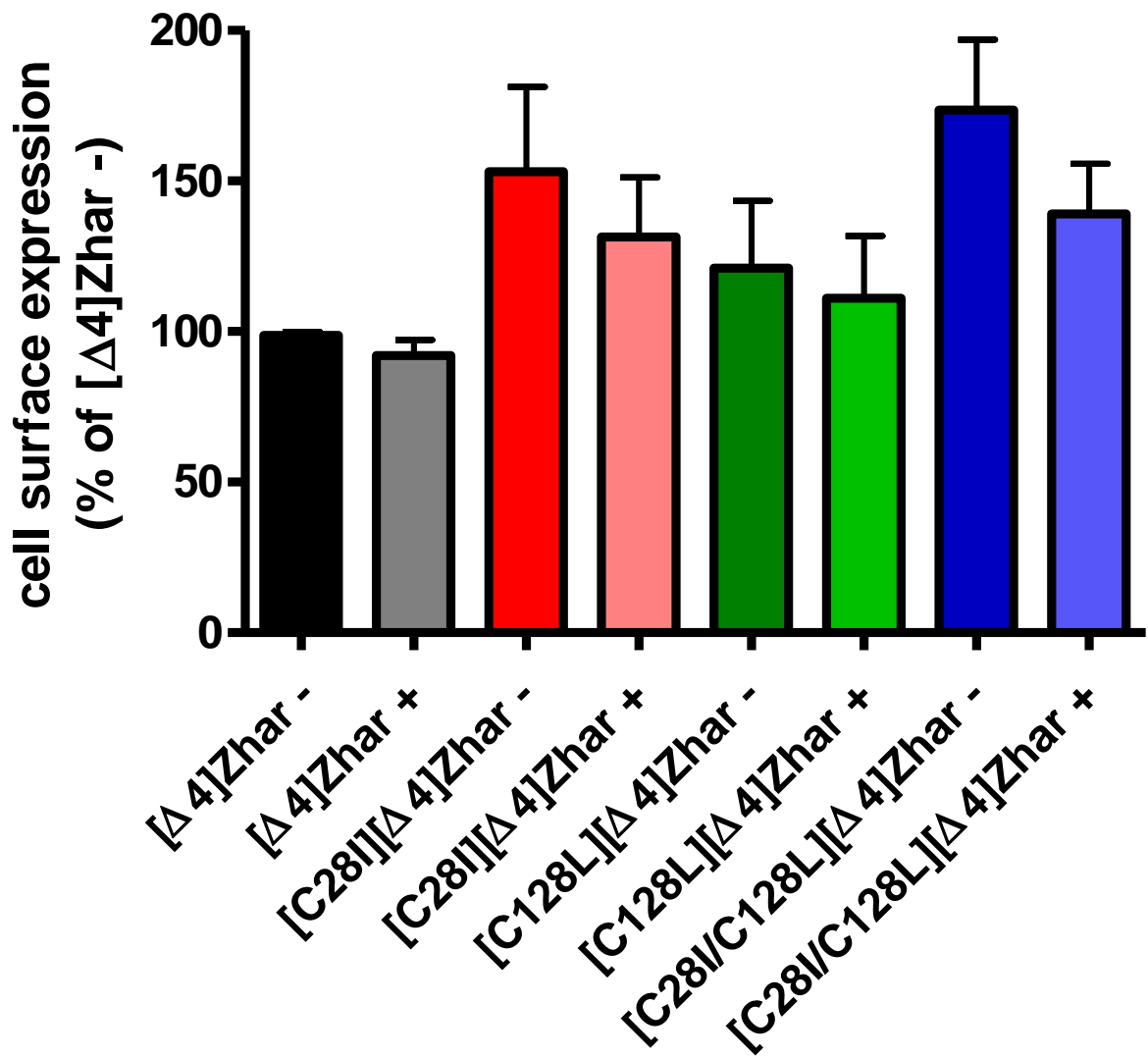
Figure 5.11. Cell surface expression of cysteine mutations in the [Δ4]Zhar background +/- agonist stimulation. Cell surface expression was determined for cysteine mutations in [Δ4]Zhar, normalised to untransfected cells (0 %) and unstimulated [Δ4]Zhar (100 %). Internalisation under agonist stimulation was determined using NECA (100 μM, 1 h). Data are mean ± s.e.m. of three experiments performed in triplicate.
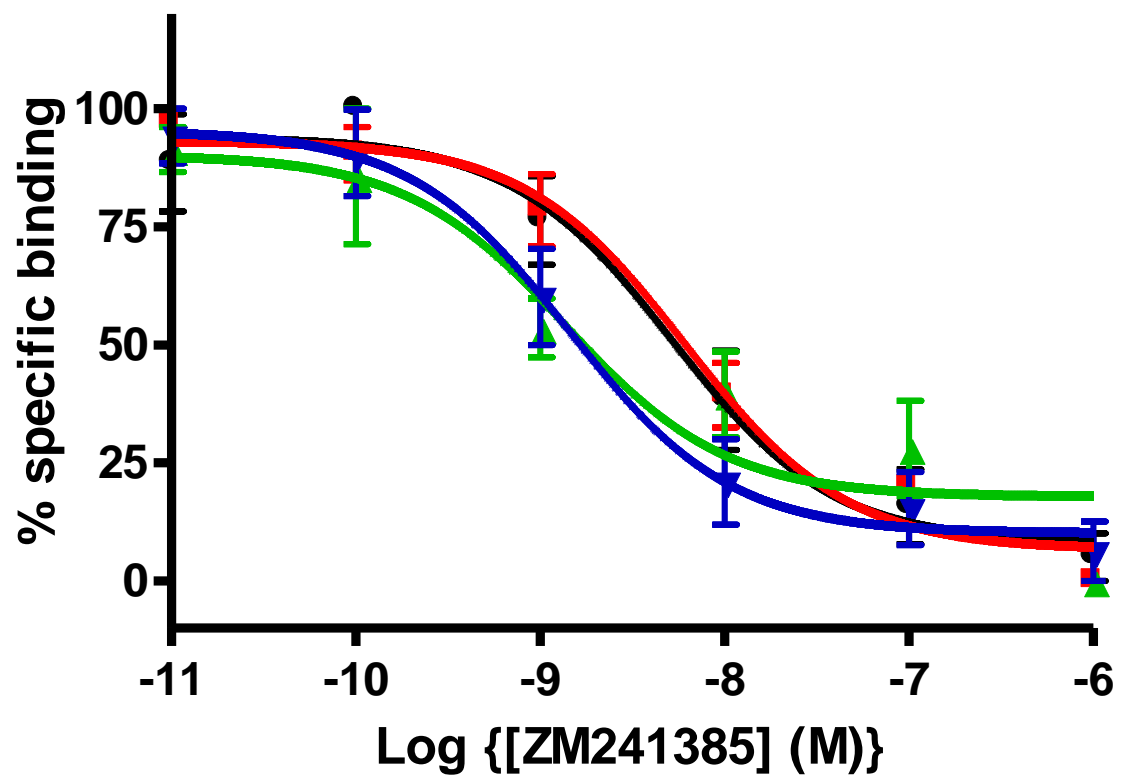
Figure 5.12. Competition radioligand binding analysis of cysteine mutations in the [Δ4]Zhar background. Self-competition binding of [³H]ZM241385 performed on [Δ4]Zhar (●); [C28I][Δ4]Zhar (■); [C128L][Δ4]Zhar (▲) and [C28I/C128L][Δ4]Zhar (▼). Data are mean ± s.e.m. of three experiments performed in triplicate.

Construct	$pK_i \pm$ s.e.m.
[Δ4]Zhar	8.63 ± 0.4
[C28I][Δ4]Zhar	8.47 ± 0.5
[C128L][Δ4]Zhar	9.10 ± 0.8
[C28I/C128L][Δ4]Zhar	9.64 ± 0.0

Table 5.4. pK_i values of cysteine mutant constructs in the [Δ4]Zhar background. Data are mean $\pm$ s.e.m. of three experiments performed in triplicate.

increase in affinity. In addition to establishing that the ligand binding capabilities of the depleted Cys $A_{2a}R$ was not greatly perturbed, it was also necessary to establish that the signalling capability was also retained. $A_{2a}R$ signals via activation of G_s for stimulating adenylyl cyclase. Consequently, cAMP was assayed in response to increasing concentrations of the agonist NECA (figure 5.13 and table 5.5). It was observed that pEC_{50} values of [C28I/C128L][Δ4]Zhar were comparable to [Δ4]Zhar, and in turn comparable to $A_{2a}R$.
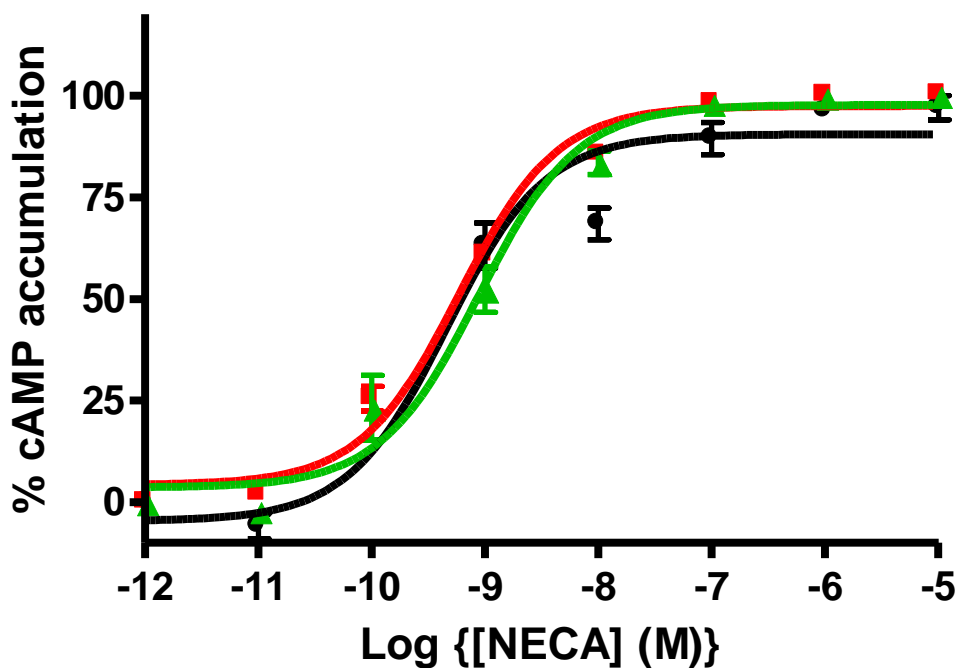
Figure 5.13. cAMP dose-response curves of cysteine-depleted A$_{2a}$R. Alphascreen determined NECA dose-response curves of cAMP accumulation in HEK 293T cells transiently transfected with A$_{2a}$R (●); [Δ4]Zhar (■) and [C28I/C128L][Δ4]Zhar (▲). Data are mean ± s.e.m. of three experiments performed in triplicate.

Construct	pEC$_{50}$ ± s.e.m.
A$_{2a}$R	9.93 ± 0.2
[Δ4]Zhar	9.26 ± 0.0
[C28I/C128L][Δ4]Zhar	9.12 ± 0.2

Table 5.5. pEC$_{50}$ values for cysteine-depleted A$_{2a}$R. All data are mean ± s.e.m. of three experiments performed in triplicate.

5.3 Discussion

GPCRs are of great interest to the pharmaceutical industry. Their presence on the cell surface allows their targeting with drugs to transduce signals down a plethora of signalling pathways. The ability to develop better, more specific drugs requires more information on the conformational changes a GPCR undergoes upon ligand binding. In the case of $A_{2a}R$, this would aid in development of drugs to treat diseases such as Parkinson's disease, Alzheimer's disease and graft versus host disease. Biophysical techniques such as FRET can provide information on the conformational states of GPCRs. However, this requires specific sites of fluorescent probe attachment. IAEDANS is a fluorescent probe that can attach to the thiol groups of cysteine residues. By introducing cysteine residues at specific locations on $A_{2a}R$ it may be possible to study the conformational states of $A_{2a}R$ in SMALPs.

Identification of suitable sites for reporter group introduction, at the intracellular side, was based on previous studies in β_2 adrenergic receptor (β_2-AR) (Yao *et al.*, 2009, Yao *et al.*, 2006). Upon GPCR activation, the movement of TM6 away from TM3 on the intracellular side is reported to be one of the largest conformational changes (Rasmussen *et al.*, 2011a, Rasmussen *et al.*, 2011b, Kobilka, 2011). Introduction of reporter groups around these helices would provide the clearest observations of conformational changes in $A_{2a}R$.

At the extracellular side of $A_{2a}R$, the movement of TM6 towards TM3 upon agonist binding would also provide valuable insight into GPCR conformational changes upon ligand binding. However, in $A_{2a}R$ ECL1 and ECL3, at the top of TM3 and TM6 respectively, contain few residues and are locked in place through disulphide bonds. Reporter groups located in these areas would not provide significant insight into conformational changes due to their restricted movement. Leu78 and Thr256 are located at the top of TM3 and TM6 respectively, while Tyr176 is located at the top of TM5, a midpoint between Leu78 and Thr256. Reporter groups

located at these locations would have allowed information on the movement of extracellular domains upon ligand binding.

Of the 15 cysteine residues present in $A_{2a}R$, 8 were involved in the formation of disulphide-bonds, 2 were structurally/functionally important and inaccessible. The remaining 5 required mutation to a non-derivatisable residue to allow robust analysis through use of intrinsic tryptophan fluorescence and IAEDANS-Trp FRET. C-terminal truncation and mutation to alanine, leucine or isoleucine, based on sequence homologies and previous work (Yao et al., 2006), were employed to remove these derivatisable sites.

5.3.1 Introduction of reporter groups

Mutation of residues in the TM helices, areas of conserved structural composition, were not well tolerated (Unal and Karnik, 2012). Disruption to the structure of a TM with the bulky sidechain of tryptophan, or introduction of nucleophilic cysteine residues to the hydrophobic TM region was not well tolerated. This was apparent at Leu78 where mutation to either Cys or Trp resulted in reduced binding affinity and reduced cell surface expression. [L78W]Zhar showed the lowest cell surface expression of any of the constructs investigated. This may have been due to retention of misfolded proteins. The presence of the large Trp sidechain neighbouring Cys77 could have caused a steric hindrance in the formation of a disulphide bond. Preventing protein disulphide isomerase from creating the appropriate disulphide bridge would probably lead to the retention of the protein in the ER (Shi and Javitch, 2002). The small amount of receptor that was expressed at the cell surface demonstrated lower affinity binding for ZM241385. This would suggest that even when disulphide bonds have been correctly formed, the steric hindrance created by the Trp sidechain was either blocking the binding site or preventing key interactions with other residues. [L78C]Zhar also displayed a decreased cell surface expression, likely due to ER-retention resulting from misplaced disulphide bonds. As Leu78 does not form part of any recognised binding pockets in $A_{2a}R$, for agonists or antagonists

(Xu *et al.*, 2011, Jaakola *et al.*, 2010), subtle shifts in binding affinity were likely due to conformational change, not loss of a direct binding site. It has been previously reported that disulphide bonds introduced to the ECLs of GPCRs can inhibit orthosteric binding of agonists and antagonists (Avlani *et al.*, 2007). A change in where ECL2 was restrained may have prevented ZM241385 from accessing the binding site. This could also be a result of imposed conformational changes to ECL2 which is believed to act as a lid over the binding pocket (Shi and Javitch, 2004, Wheatley *et al.*, 2012). This may have increased the time taken for binding assays to reach equilibrium, presenting as the reduced affinity observed from radioligand binding. [L78C]Zhar displayed reduced cell surface expression while retaining WT-like binding affinity. Despite a reduction in specific binding that correlated with reduced cell surface expression levels, it was possible to produce a full ligand binding curve with robust data. It is possible that the L78C mutation resulted in ER-retention of $A_{2a}R$. Further studies would be required to show the reduction in cell surface expression was not a result of a reduction in overall expression levels, utilising the whole cell ELISA technique. Furthermore, identification of where the construct was retained within the cell would be required. However, this construct could potentially be used to study the ability of SMA to extract functionally active receptor from intracellular membranes.

[T256C]Zhar resulted in low cell surface expression and reduced binding affinity. The position of Thr256 at the top of TM6 places it in close proximity to the internal disulphide bridge of ECL3. Mutation to cysteine may have resulted in misplaced disulphide bonds, preventing release from the ER. Reduced binding affinity was unlikely to occur from misplaced disulphide-bonds as ECL3 forms an intra-loop disulphide-bond and does not tether ECL2 to the TM bundle. However, Asn253 is a key binding point for ZM241385, revealed by the crystal structures of $A_{2a}R$ (Liu *et al.*, 2012, Jaakola *et al.*, 2010) and is present just below Thr256 in TM6. It is therefore possible that the increased carbon-sulphur bond length of the thiol group,

in comparison to carbon-carbon bond length, in the [T256C]Zhar construct, extended further into the binding pocket and inhibited ligand binding, resulting in the observed decreased binding affinity.

Tyr176 was the only residue at the extracellular side to tolerate mutation and maintain high levels of cell surface expression. WT-like binding affinity of ZM241385 for [Y176W]Zhar correlates with the recognised ligand binding pocket for ZM241385 not involving Tyr176. Mutation from one bulky aromatic side-group to another did not disrupt antagonist binding. Unfortunately, with the investigated mutations on other helices resulting in greatly reduced cell surface expression and altered binding affinities, there was no appropriate site identified for the correlated Cys residue to allow study of conformational changes at the extracellular side of $A_{2a}R$.

Ile106, Leu225 and Ala231 had previously been shown to tolerate mutation in the correlating residues of β_2-AR. In this study it was found that although there was a reduced cell surface expression of [L225W]Zhar and [A231W]Zhar, expression levels were high enough to be used for cell signalling assays and provide clear data in radioligand binding assays. The lack of disruption to ligand binding was expected; these residues would not interact directly with the ligand binding pocket, nor do they form any of the interactions known to maintain an inactive state in GPCRs. [I106W]Zhar presented WT-like expression levels and binding affinity so was chosen as the Trp reporter residue. [L225W]Zhar and [A231W]Zhar were both equally well tolerated, however as the β_2-AR equivalent of Ala231 had been the site of the Cys reporter residue in previous reports (Yao et al., 2006, Yao et al., 2009), this was chosen for mutation to cysteine.

5.3.2 Cys-depletion

The two cysteine residues buried in the middle of TM5 and TM6 (Cys185 and Cys245 of the $A_{2a}R$, respectively) were deemed unreactive in previous studies on β_2-AR (Yao et al., 2006). However, four cysteine residues existed at the ends of helices which would probably be exposed to IAEDANS labelling (Liu *et al.*, 2012). These exposed cysteines were mutated to either alanine (well tolerated in most GPCRs) or a residue identified as conserved among other adenosine receptor subtypes.

Cys82 and Cys254 are present at the top of TM3 and 6, respectively, placing them in close proximity to the ligand binding pocket and making them more accessible to IAEDANS labelling than Cys28 and Cys128. Across the adenosine family these residues are conserved cysteines, suggesting an important role. However, there was no observable change in binding to ZM241385, nor cell signalling assays under stimulation from the agonist NECA. Therefore, although conserved across the adenosine receptor family, Cys82 and Cys254 play no role in ligand binding or receptor activation. The observed increase in cell surface expression suggests that mutation of the nucleophilic cysteine to the small sidechain of alanine stabilises the α-helical conformation of their respective helices. Introduction of the reporter residues ([I106W] and [A231C]) was well tolerated in the [2A]Zhar backbone, displaying WT-like binding affinities and cell surface expression levels. This proved that Ala231 was able to retain WT-like function when mutated to cysteine, as it could in the β_2-AR (Yao et al., 2006).

Although Cys28 and Cys128 were concealed within the TM bundle, and theoretically should also be shielded from IAEDANS by the SMA belt and lipid bilayer surrounding $A_{2a}R$ in SMALPs, access from the "intracellular" side may have been possible. [C128L]$A_{2a}R$ showed a minor increase in expression levels, still within WT-like range. However, for the C-terminally truncated Zhar construct, the [C128L]Zhar produced a much more noticeable increase in cell surface expression. By mutating the nucleophilic cysteine to a hydrophobic leucine, the

stability of TM4, and the whole TM-bundle, seems to have been increased. From the increased affinity for the inverse agonist, ZM241385, it is suggested that [C128L]Zhar has been stabilised in an inactive state. However, this has not affected the ability to internalise or signal upon agonist stimulation. [C28I]Zhar demonstrated increased cell surface expression, but [C28I] did not produce any change in expression levels of $A_{2a}R$. As before, the mutation of a nucleophile to a hydrophobic residue is likely to have increased stability of TM1. However, as TM1 is not known to be heavily involved in receptor activation, stabilising TM1 has only a minor effect on expression levels and no notable effect on ligand binding. [C28I] and [C128L] were chosen to replace these two cysteines as there was no detrimental effect upon incorporation into $A_{2a}R$ or Zhar.

[Δ4]Zhar was expressed at levels comparable to WT-Zhar, despite containing [C82A/C254A] mutations (shown to increase cell surface expression in Zhar). This was likely due to the incorporation of [A231C]; mutation of Ala231 had been shown to reduce cell surface expression. Introduction of [C28I] and [C128L] into the [Δ4]Zhar backbone displayed similar trends as in $A_{2a}R$ and Zhar backbones. The reduced increase in cell surface expression observed in [C128L][Δ4]Zhar, compared to [C128L]Zhar, was likely due to the already increased stability conferred by [C82A/C254A]. However, [C28I][Δ4]Zhar presented increased cell surface expression compared to [C28I]Zhar. As TM1 is not part of the main TM bundle, stability conferred by [C82A/C254A] had no effect on the stability conferred by [C28I]. Despite the changes in relative cell surface expression levels, no differences were observed in binding affinity of [C28I][Δ4]Zhar. [C128L] conferred a subtle increase in affinity for ZM241385 in [Δ4]Zhar. This was further apparent in [C28I/C128L][Δ4]Zhar which was expressed at levels comparable to [C28I][Δ4]Zhar and bound ZM241385 with increased affinity.

The presence of [I106W] and [A231C] reporter groups at the intracellular face of $A_{2a}R$, and the same mutations in the corresponding residues of β_2-AR, show the utility of this technique for GPCR studies. Two family A GPCRs have had residues incorporated which will facilitate FRET studies in a receptor with a Cys-depleted background. This suggests this may be a common method to study family A GPCRs through fluorescence techniques.

In summary; presented here is [C28I/C128L][Δ4]Zhar, a Cys-depleted $A_{2a}R$ construct displaying WT-like characteristics for an $A_{2a}R$. [C28I/C128L][Δ4]Zhar is a construct ready to be over-expressed in yeast before SMALP-solubilisation, derivatisation with IAEDANS and the effects of ligand binding studied by FRET and intrinsic tryptophan fluorescence. This will allow elucidation of the conformational changes $A_{2a}R$ undergoes upon ligand binding, potentially aiding drug design for this pharmaceutically relevant protein. Also, this will further the understanding of potential uses of the SMALP technique.

CHAPTER 6: DETERGENT-FREE EXTRACTION OF OTHER GPCRs

6.1 Introduction

$A_{2a}R$ was a useful tool to study the characteristics and stability of SMALP-GPCRs. Information obtained on the pharmacological profile and stability of the SMALP-solubilised $A_{2a}R$ allowed an understanding of the limitations and potential uses of the SMALP technique. However, it was important to understand the versatility of SMALP-solubilisation. Previous reports have demonstrated extraction of membrane proteins not of the GPCR superfamily: bacteriorhodopsin and PagP (Knowles et al., 2009), the tetrameric potassium channel KcsA (Dorr et al., 2014), AcrB (Postis et al., 2015) and ABC transporter proteins (Gulati et al., 2014). However, before this study there was no report of SMALP-solubilised GPCRs. The GPCR superfamily, despite sharing a 7 transmembrane (7TM) bundle, shares very little sequence homology within GPCR sub-families, and even less homology between sub-families (Ji et al., 1998). Although the presence of a 7TM domain is conserved across the GPCR superfamily, detailed protein structure, ligands and ligand binding mechanisms differ between sub-families (Harmar, 2001, Wu et al., 2014). Family B GPCRs possess a much larger N-terminus than family A GPCRs (100-160 residues) as this is a key site of ligand recognition and interaction in family B GPCRs. Ligands for family A GPCRs usually bind deep in the TM core, with the peptide ligands often forming interactions with the ECLs (Strader et al., 1995). Family B GPCR ligands are usually large peptides (~30-40 residues) that bind their C-terminus to the N-terminus of the GPCR. This orientates the N-terminus of the ligand to the TM-core of the GPCR where it interacts predominantly on the periphery of the TM bundle (Dautzenberg et al., 1999, Hoare et al., 2004, Siu et al., 2013). Family C GPCRs possess N-termini larger than the whole of a family A GPCR (~581 residues in the metabotropic glutamate receptor 1). These

are structured for a Venus-fly trap model of ligand interaction (Jingami et al., 2003). With such diversity in structure and mechanism of ligand binding within the GPCR superfamily, it was not known whether the SMALP-solubilisation technique would be able to extract other GPCRs in an active form.

Other than protein structure, one of the key differences between GPCR sub-families is the difference in their endogenous ligands. The $A_{2a}R$ is a receptor for small molecule ligands (M_W: ~270 Da), with a library of well-characterised small molecule ligands that were utilised to study SMALP-$A_{2a}R$. Other members of family A have been as equally well-characterised as $A_{2a}R$, such as the neurohypophysial receptor family of GPCRs: vasopressin 1a receptor ($V_{1a}R$); vasopressin 1b receptor ($V_{1b}R$); vasopressin 2 receptor (V_2R) and the oxytocin receptor (OTR), as well as the muscarinic acetylcholine receptor family (including muscarinic acetylcholine receptor M1 (M1R)). These receptor were chosen to investigate if the SMALP technique could be a general method to study family A GPCRs or if it was restricted to $A_{2a}R$. These receptors were chosen as they have all been well characterised with a range of small molecule and peptide ligands. However, the endogenous ligands for the neurohypophysial receptors are peptides (9 residues in length), and acetylcholine is a small amine ligand at the M1R. These ligands differ from adenosine, a small molecule ligand that is smaller than the peptide ligands for the neurohypophysial receptors. The presence of a sugar moiety on the adenosine adds bulk to the molecule that is not present on small amine ligands such as acetylcholine and its stable analogue carbachol (ligands at the M1R) (Piersen et al., 1994). The difference in ligand size from small amines to peptides would allow the study of SMALP-solubilised receptors that bind different types of ligands in different ways. Small molecule ligands have been shown to bind deep in the binding pocket of GPCRs (Palczewski et al., 2000, Xu et al., 2011). Whereas the much larger peptide ligands tend to bind more on the periphery of the TM bundle, where they

can form interactions with the ECLs as well as the 7TM bundle (Fong et al., 1992, Hawtin et al., 2006, Conner et al., 2007, Wheatley et al., 2012) (reviewed in (Strader et al., 1995)).

Successful use of the SMALP technique to extract and study other functional GPCRs could provide detailed and accurate data on the neurohypophysial receptor family. This could lead to development of drugs to aid in conditions such as: nephrogenic diabetes insipidus (NDI) caused by mutation of V_2R (Knoers, 1993); adrenocorticotropin-independent macromodular adrenal hyperplasia and, potentially, autism linked with $V_{1a}R$ (Mune et al., 2002, Yirmiya et al., 2006); depression and anxiety linked to $V_{1b}R$ (Griebel et al., 2002) and problems with childbirth such as premature labour related to OTR (Akerlund et al., 1985). The M1R is linked with seizures (Hamilton et al., 1997) and breathing difficulties arising from bronchoconstriction (Struckmann et al., 2003) amongst other conditions. SMALP-solubilisation would allow biophysical analysis of these receptors in their native conformation and lipid environment. This would lead to better understanding of the mechanism of action of different ligands upon binding, providing insight into how ligands induce their response. From this, drugs with greater specificity for individual receptors might be designed to induce the effect required with reduced side-effects.

6.1.1 Family B GPCRs

The characteristic GPCR 7TM bundle is preserved in family B GPCRs. However, there is very little sequence homology with family A and the TM bundle has been shown to adopt a chalice-like conformation (Hollenstein et al., 2013, Siu et al., 2013). Family B GPCRs also possess an extended N-terminus compared to family A GPCRs. The importance of the N-terminus for ligand binding in family B GPCRs provided a different structural component of the receptor to be maintained throughout SMALP-solubilisation. The variety of available ligands for family B GPCRs is more limited than for family A GPCRs. Those that are commercially available are predominantly large peptides of 27-141 residues (Harmar, 2001). This is much larger than the

nonapeptides that target neurohypophysial receptors, providing another useful tool to study the utility of the SMALP technique.

Some family B GPCRs, such as the calcitonin receptor (CTR), have the ability to interact with a small family of three single membrane-spanning proteins called receptor activity modifying proteins (RAMPs 1-3 (McLatchie et al., 1998)). RAMPs interact with family B GPCRs through their N-terminus to produce pharmacologically distinct receptors (Christopoulos et al., 1999, Fraser et al., 1999). The CTR is a family B GPCR that interacts with RAMPs to produce pharmacologically different amylin receptors named AMY1-3 in correlation with the complexed RAMP (Christopoulos et al., 1999). Figure 6.1 provides a graphic representation of the ability of CTR to express at the cell surface independently or as a heterodimer with the 3 different RAMPs (Christopoulos et al., 2003).

Interaction with RAMPs is not necessary for CTR transport to the cell surface (Morfis et al., 2008), resulting in the CTR. Expression at the cell surface as the CTR:RAMP1 complex results in the AMY_1 receptor that has high affinity for the ligand amylin, which CTR does not. These two distinct pharmacological profiles provides the opportunity to investigate the ability of SMALPs to solubilise functional heterodimeric complexes. Studies of family B GPCRs have been hindered by the endogenous expression of RAMPs in cells introducing mixed pharmacological profiles to samples. If it was possible to extract GPCR:RAMP complexes in a functional state and purify samples through affinity chromatography with a specific epitope-tagged RAMP subtype, the study of specific GPCR:RAMP complexes would be possible. This would further the understanding of these complexes, potentially aiding drug design targeting family B GPCRs involved in diabetes (AMY_{1-3} (Younk et al., 2011)) and osteoporosis (CTR (Henriksen et al., 2010)) among others (reviewed in (Bortolato et al., 2014)).
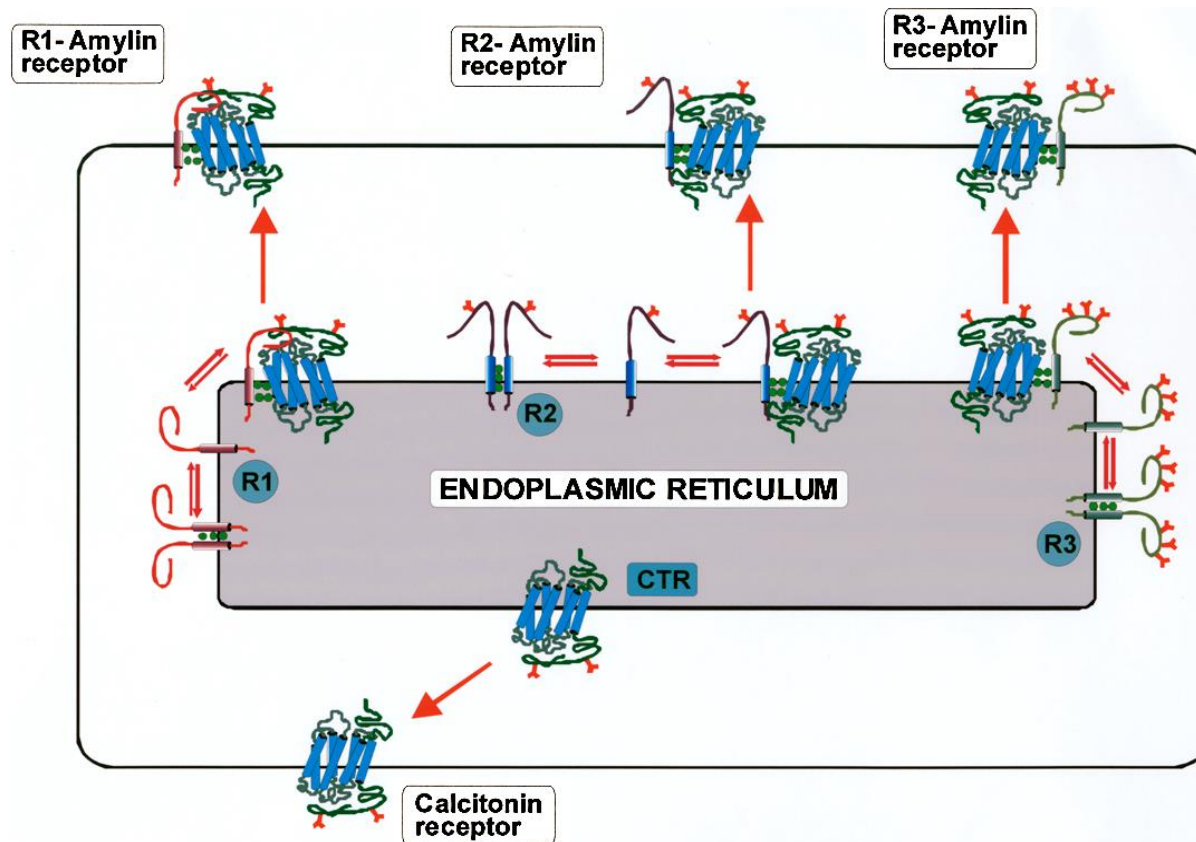
Figure 6.1. The ability of CTR to express at the cell surface as four pharmacologically distinct receptors. CTR is able to express at the cell surface as the calcitonin receptor, independent of RAMPs. Alternatively it may dimerise with any of the 3 RAMPs (R1, R2 or R3) in the ER, to produce the 3 amylin receptors. Adapted from (Purdue et al., 2002).

6.2   Results

6.2.1   SMALP-solubilisation of other family A GPCRs

To investigate whether extraction of other family A GPCRs in binding competent states was possible, pre-labelling of $V_{1a}R$, $V_{1b}R$ and V_2R with [^{3}H]AVP as a tracer, OTR with [^{3}H]OT as a tracer, M1R with [^{3}H]NMS as a tracer and $A_{2a}R$ (for comparison) with [^{3}H]ZM241385 as a tracer was performed. Before solubilisation, samples were incubated with approximately 1 nM of the appropriate [^{3}H]ligand. This was performed in the presence or absence of a saturating concentration of competing ligand. Unbound radioligand was removed by aspiration before samples were SMALP-solubilised using the conditions optimised for SMALP-$A_{2a}R$ (as determined in chapter 3). After centrifugation (100,000 x g, 1 h), 50 µl aliquots of supernatant were taken for liquid scintillation analysis to determine the specific binding in each SMALP-GPCR sample. Observation of specific binding would indicate SMALP-solubilisation does not perturb the receptors ability to bind ligand, and therefore is present in a functional state in the SMALP.

Specific binding was observed for each of the GPCRs investigated, shown in figure 6.2. In each case specific binding was observed at around 50 % of total binding, except at OTR where it was ~25 %. Specific binding recorded was (in descending order): 23660.7 ± 2401.9 d.p.m. at $A_{2a}R$; 8114 ± 462.8 d.p.m. at V_2R; 6502.3 ± 2246.7 d.p.m. at M1R; 5923.7 ± 1516.4 d.p.m. at $V_{1a}R$; 4622.7 ± 996.2 d.p.m. at $V_{1b}R$ and 3132.7 ± 352.7 d.p.m. at OTR (mean ± s.e.m. of three experiments performed in triplicate).
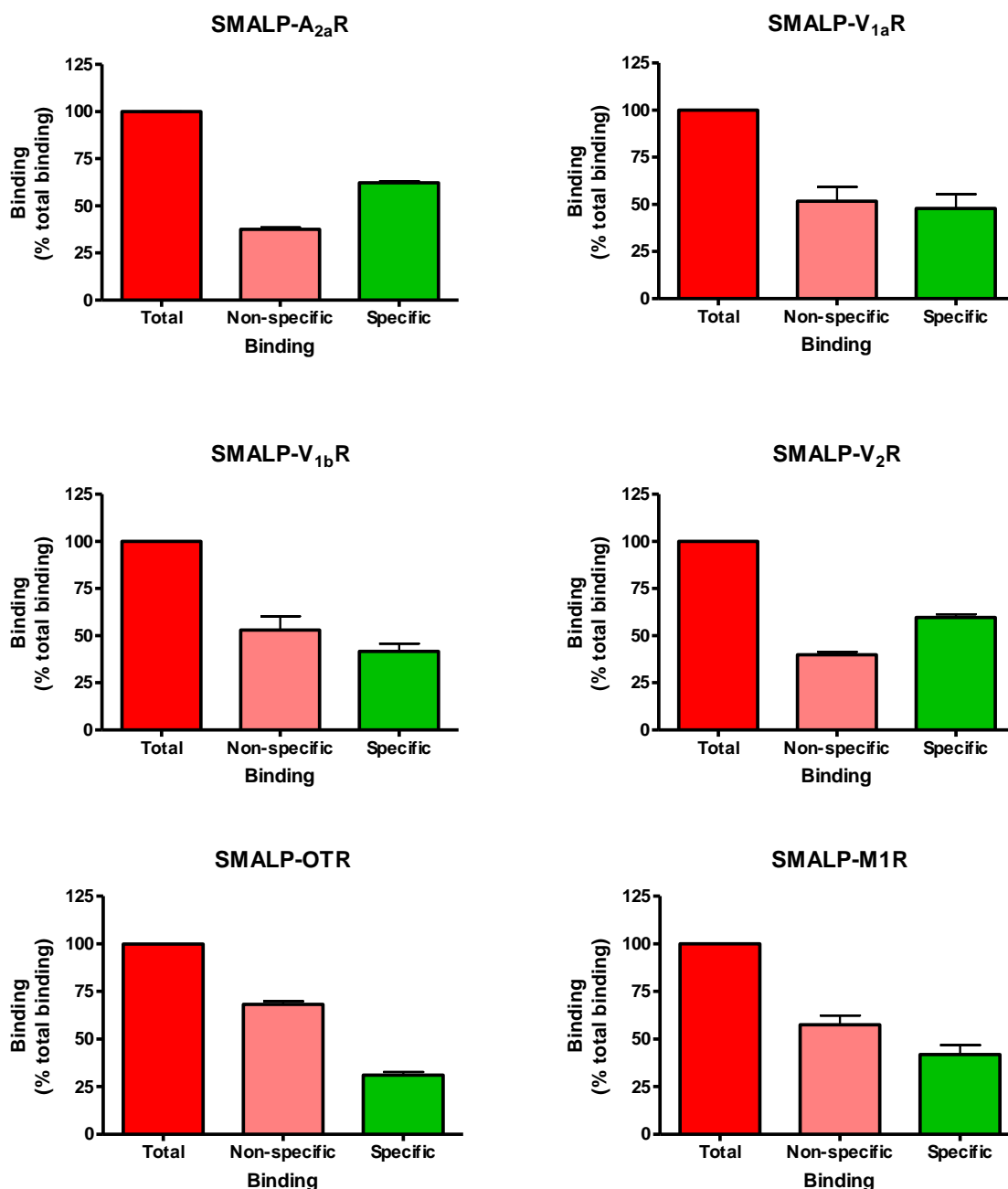
Figure 6.2. Pre-labelled radioligand binding observed for SMALP-solubilised family A GPCRs.
Specific binding was determined for the GPCRs indicated using approximately 1 nM of appropriate [^{3}H]ligand in the absence (total) and presence (non-specific) of saturating amounts of competing ligand. Non-specific binding was defined by: 1 μM AVP at $V_{1a}R$, $V_{1b}R$ and V_2R; 1 μM OT at OTR; 1μM ZM241385 at $A_{2a}R$ and 100 μM atropine at M1R. Data are of three experiments performed in triplicate (mean ± s.e.m.).

SMALP-solubilisation was not detrimental to the ligand binding capabilities of the GPCRs investigated. It was important, for their use in downstream analyses, to assess the ability of GPCRs to bind ligand after SMALP-solubilisation. This would allow study of SMALP-GPCRs in biophysical techniques such as Förster resonance energy transfer (FRET) that require ligand binding to induce conformational changes in a receptor. To investigate this, ligand binding was assayed following SMALP-solubilisation of an unoccupied receptor. Initially however, it was important to be able to effectively separate bound from free radioligand.

To separate bound from free radioligand in the SMALP-solubilised samples, size affinity chromatography was employed as the SMALP is substantially larger than the free ligand (M_W of AVP: ~1090 Da compared to ~113 kDa for SMALP containing only lipid (Lee and Dafforn, personal correspondence). Sephadex G-50 (M_W cut-off of >30,000 Da), Sephadex G-25 (M_W cut-off of >5,000 Da) and Sephadex G-15 (M_W cut-off: >1500 Da) were investigated for efficient removal of free ligand from solution. [3H]ZM241385 was investigated first and diluted to approximately 1 nM in buffer (20 mM HEPES, 1 mM EGTA, 1 mM magnesium acetate, pH 7.4) corresponding to the concentration used in assay. As in radioligand binding assays, 50 µl of the radioligand sample was loaded onto spin columns containing 500 µl bed volume of the indicated size exclusion resin. Samples were centrifuged for 4 min at 1,000 x g. 1 ml of Hisafe3 scintillation cocktail was added to void volumes before samples were analysed by liquid scintillation analysis.

It was observed, as seen in figure 6.3, that although all size-exclusion resins investigated were able to remove [3H]ZM241385 (M_W: ~337 Da) from the sample, Sephadex G-15 was the most efficient with only 1.74 ± 0.3 % (mean ± s.e.m. of three experiments performed in triplicate) of the loaded [3H]ZM241385 present in the void volume. However, similar investigation into removal of [3H]AVP from a sample found that Sephadex G-15 was not the most suitable resin

Figure 6.3. Removal of [³H]ZM241385 from a sample using size exclusion chromatography. Sephadex G-50 (M$_W$ cut-off >30,000 Da), Sephadex G-25 (M$_W$ cut-off >5,000 Da) and Sephadex G-15 (M$_W$ cut-off >1,500 Da) were investigated for their ability to effectively remove [³H]ZM241385 from sample. Data show proportion (% of total d.p.m. loaded) of sample eluted in void volume in each case. Data are mean ± s.e.m. of three experiments performed in triplicate.

for use with [3H]AVP. Despite AVP having a calculated M_W of ~1090 Da, this was not well retarded in Sephadex G-15, with 79.6 ± 0.9 % (mean + s.e.m. of three experiments performed in triplicate) eluting in the void volume (figure 6.4). Sephadex G-50 was shown to retard the elution of [3H]AVP with only 17.1 ± 5.3 % (mean + s.e.m. of three experiments performed in triplicate) eluting in the void volume. As size-exclusion resins separate molecules based on size, [3H]NMS (M_W: ~320 Da) and [3H]OT (M_W: 1010 Da) were deemed likely to behave similarly to [3H]ZM241385 and [3H]AVP respectively due to similar molecular weights.

Although it was possible to SMALP-solubilise functional receptor when it was pre-labelled with [3H]ligand, no specific binding could be detected when an unoccupied receptor was SMALP-solubilised other than $A_{2a}R$ (SMALP-$A_{2a}R$ ligand binding presented in section 3.2.2). As it had been established that SMALP-solubilisation did not prevent the receptor binding their respective ligands, it was hypothesised that there was an interaction between [3H]NMS, [3H]OT and [3H]AVP and the SMA polymer. To investigate this, [3H]ligands were investigated for their elution from size-exclusion spin columns in the presence of SMA. [3H]ZM241385 and [3H]NMS, tracer ligands, used for studying $A_{2a}R$ and M1R respectively, were applied to Sephadex G-15 spin columns. [3H]OT and [3H]AVP, tracer ligands, used in the study of the neurohypophysial receptors, were applied to Sephadex G-50 spin columns. This was performed in the presence and absence of 2 % (w/v) free SMA (SMA that has not formed discs). The presence of SMA allowed observation of any interactions with the radioligand. Free SMA has a minimum M_W of 3000 Da, therefore interaction of [3H]NMS or [3H]ZM241385 with SMA polymer would result in an increased presence in the void volume following gel filtration on Sephadex G-15 resin. However, Sephadex G-50 would still allow elution in the void volume of a single peptide chain of AVP or OT interacting with a monomeric free SMA chain. As a result, [3H]AVP and [3H]OT were investigated for their interaction with 2 % (w/v) free SMA as well as with SMALP-mock-transfected cells (MT cells).
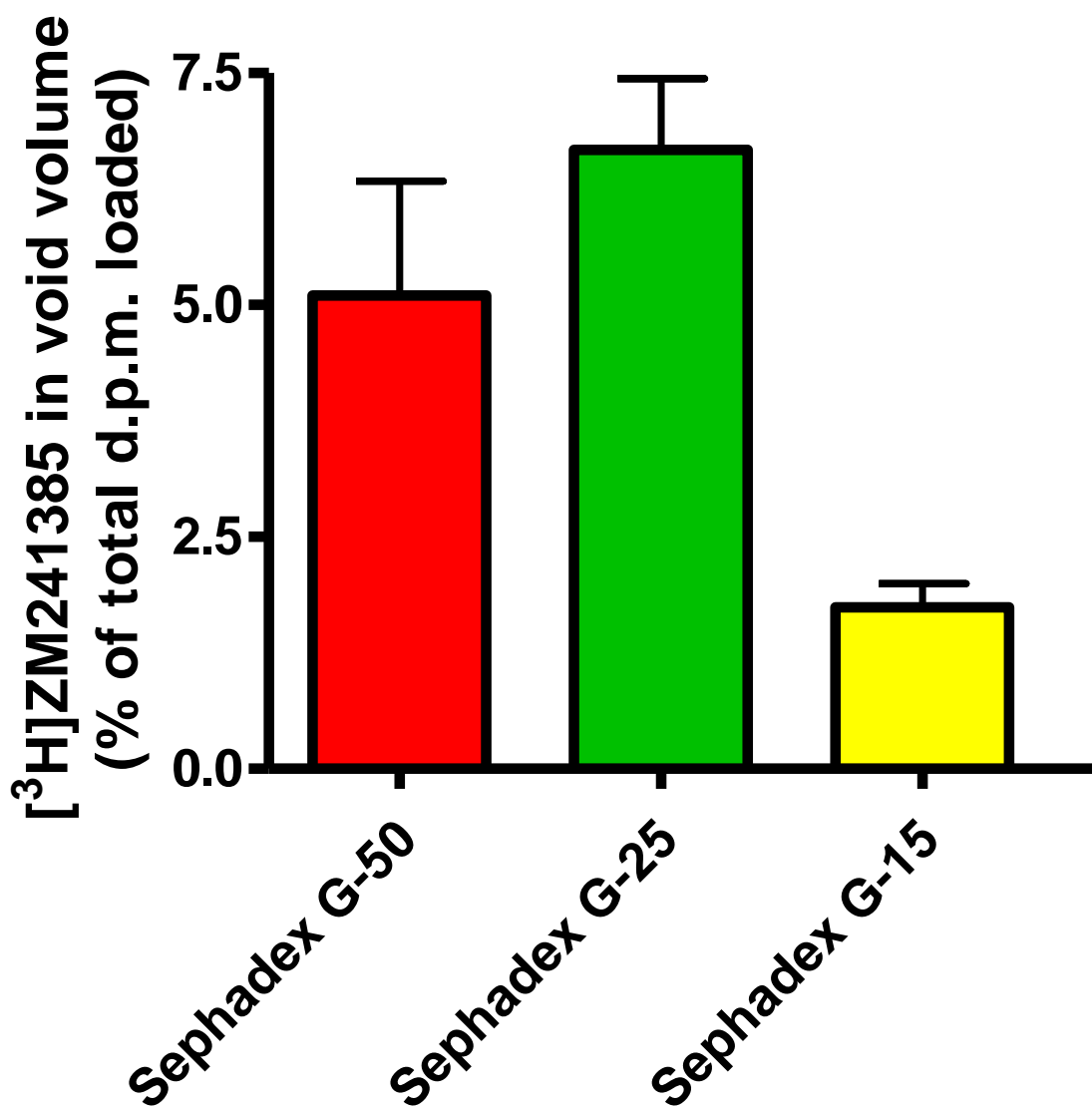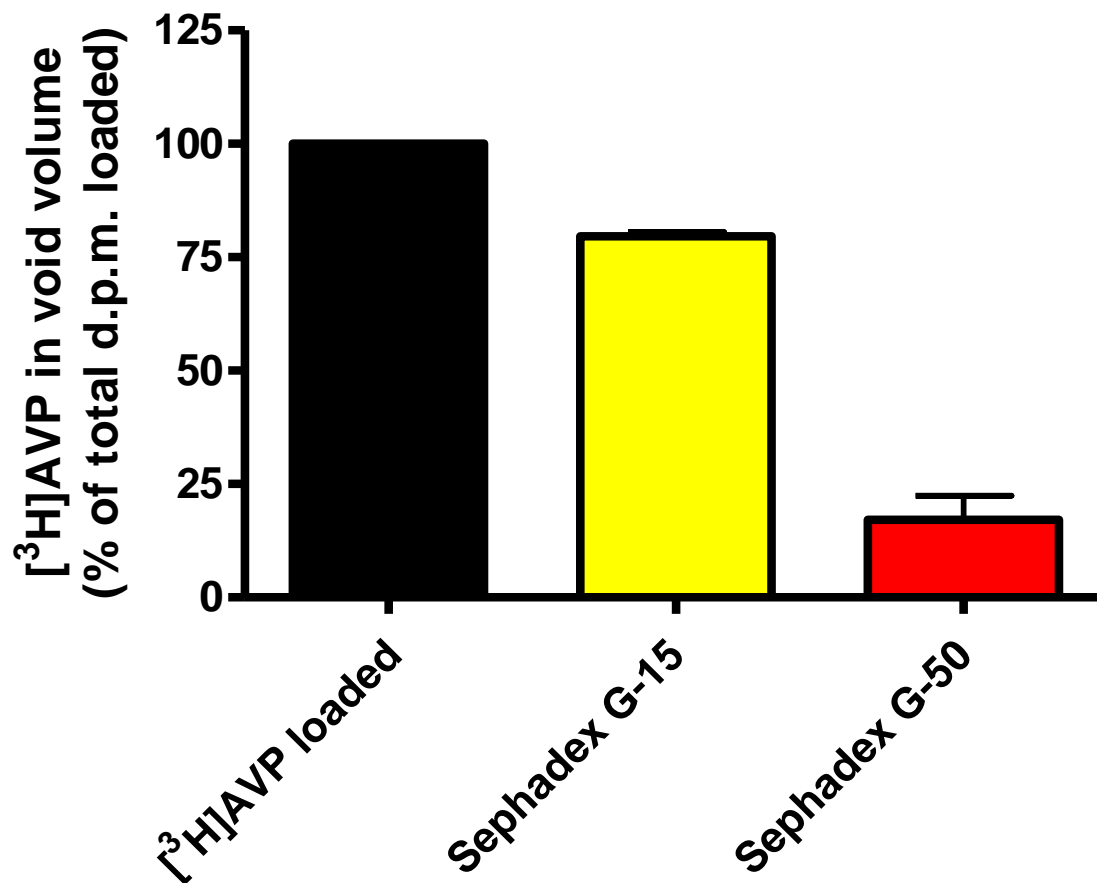
Figure 6.4. Removal of [³H]AVP from a sample using size exclusion chromatography.
Sephadex G-50 (M_W cut-off >30,000 Da) and Sephadex G-15 (M_W cut-off >1,500 Da) were investigated for their ability to effectively remove [³H]AVP from sample. Data show proportion (% of total d.p.m. loaded) of sample eluted in void volume in each case Data are mean ± s.e.m. of three experiments performed in triplicate.

MT cells were HEK 293T cells that were treated the same as transiently transfected HEK 293T cells, but no plasmid was introduced for protein expression. SMALP-MT cells were predicted to have a M_W of at ~113 kDa as they would predominantly contain only lipids. Any interaction of [3H]AVP or [3H]OT with a SMALP-MT cell disc would result in increased elution in the void volume after gel filtration on Sephadex G-50 resin.

As shown in figure 6.5, [3H]ZM241385 was present in the void volume at ~1.5 fold over basal in the [3H]ZM241385 + 2 % (w/v) SMA sample compared to [3H]ZM241385 alone. This was similar for [3H]OT where an increase of [3H]OT in the void volume to ~1.7 was observed in the presence of 2 % (w/v) SMA and also SMALP-MT cells. [3H]NMS and [3H]AVP however, were present in their respective void volumes at greatly increased amounts in the presence of 2 % (w/v) SMA (~3.7 and ~6 fold over basal respectively). Interestingly, presence of free SMA was enough to increase [3H]OT and [3H]AVP presence in void volume with SMALP-MT cells showing no substantial increase over free SMA alone.
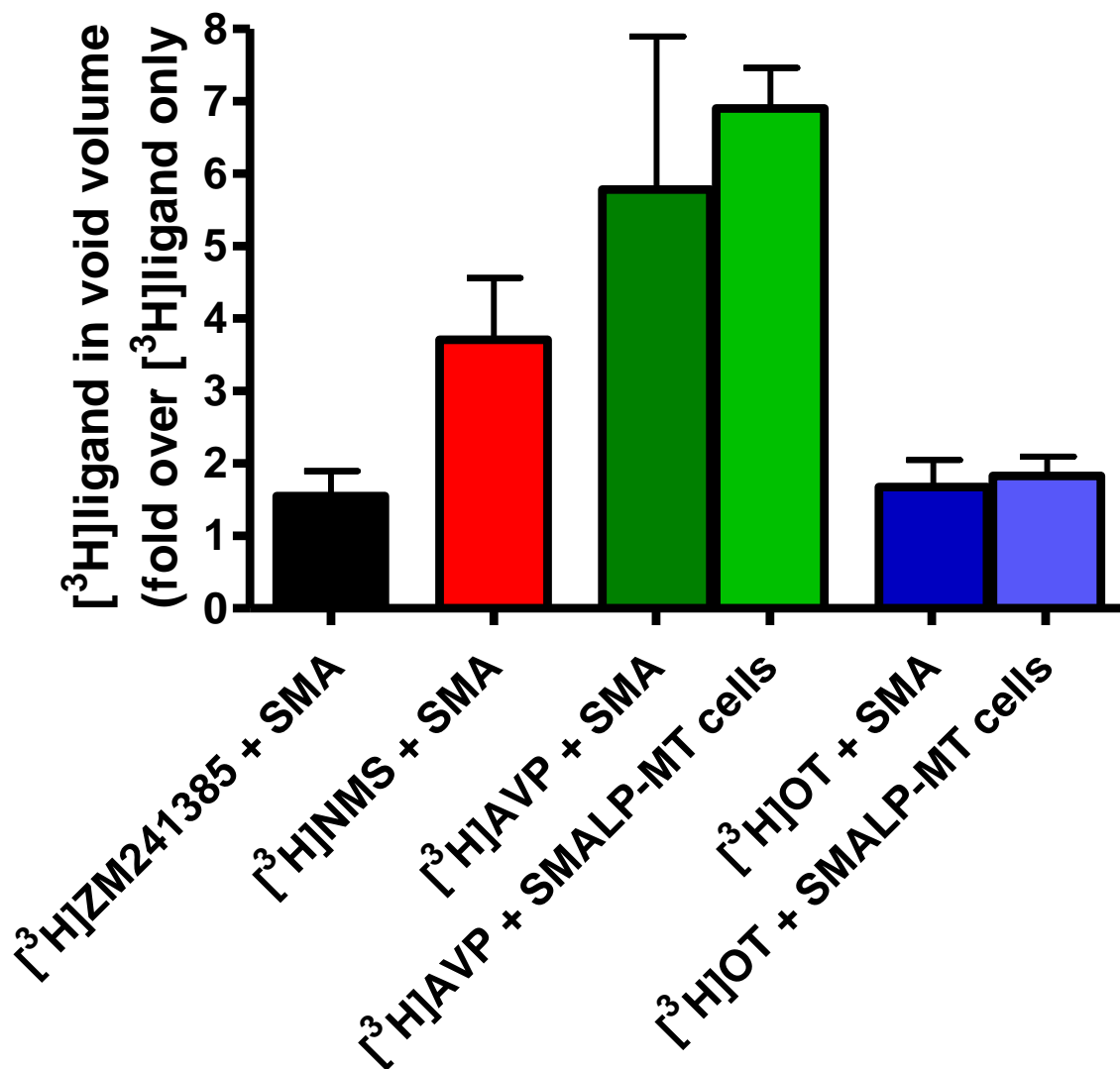
Figure 6.5. Elution profiles of [³H]ligands in the absence and presence of SMA and SMALP-MT cells. [³H]ligand samples, at concentrations used in assay, were applied to appropriate size-exclusion spin columns in the presence of 2 % (w/v) SMA (+ SMA) and presence of SMALP-MT cells (+ SMALP-MT cells). Observed d.p.m. for basal were: ~700 for [³H]ZM241385; ~2000 for [³H]NMS; ~650 for [³H]AVP and ~ 700 for [³H]OT. Data are mean ± s.e.m. of three experiments performed in triplicate.

It was hypothesised that the negative charge of the SMA was creating ionic interactions with [³H]AVP, [³H]NMS and, to a lesser extent, [³H]ZM241385 and [³H]OT. To investigate this, [³H]ligand samples with 2 % (w/v) SMA in the presence of 500 mM NaCl were applied to size-exclusion columns. As seen in figure 6.6, 500 mM NaCl was unable to affect the elution in void volume of [³H]ZM241385, [³H]AVP and [³H]OT in the presence of free SMA. However, 500 mM NaCl was able to reduce the levels of [³H]NMS in the void volume by approximately 50 % in the presence of 2 % (w/v) SMA. [³H]NMS is present in the void volume at ~3.7 fold over basal in the presence of 2 % (w/v) SMA, a 50 % reduction of this with 500 mM NaCl reduces the overall presence in the void volume to ~1.85 over basal. This was similar to the level observed with [³H]ZM241385 (~1.5 fold over basal). 0.1 mM L-arginine and 1 % (w/v) BSA were also investigated for their ability to reduce non-specific binding of [³H]AVP in SMALP samples. No improvements on non-specific binding were observed.

To increase the concentration of NaCl higher than 500 mM was known to be detrimental to ligand binding function (New and Wheatley, unpublished data). As an alternative to increased NaCl concentrations, reducing the amount of free SMA in the samples was investigated to reduce non-specific binding of [³H]AVP. Removal of free SMA, by gel filtration of SMALP samples, was first performed on SMALP-A_{2a}R to allow radioligand binding analysis of samples. It was important to determine that gel filtration of SMALP-samples did not compromise the integrity of the protein. Size-exclusion chromatography was employed with M_w cut-offs at >30,000 Da (Sephadex G-50) and >80,000 Da (Sephadex G-75). SMALP-GPCRs would elute in the void volume of both Sephadex resins as GPCRs possess a M_w of ~45 kDa even without the additional mass of the SMALP disc and annular lipid.

Preliminary self-competition radioligand binding assays, with [³H]ZM241385 as tracer at SMALP-A_{2a}R, displayed increased total binding (increased by ~200 d.p.m.) and reduced non-
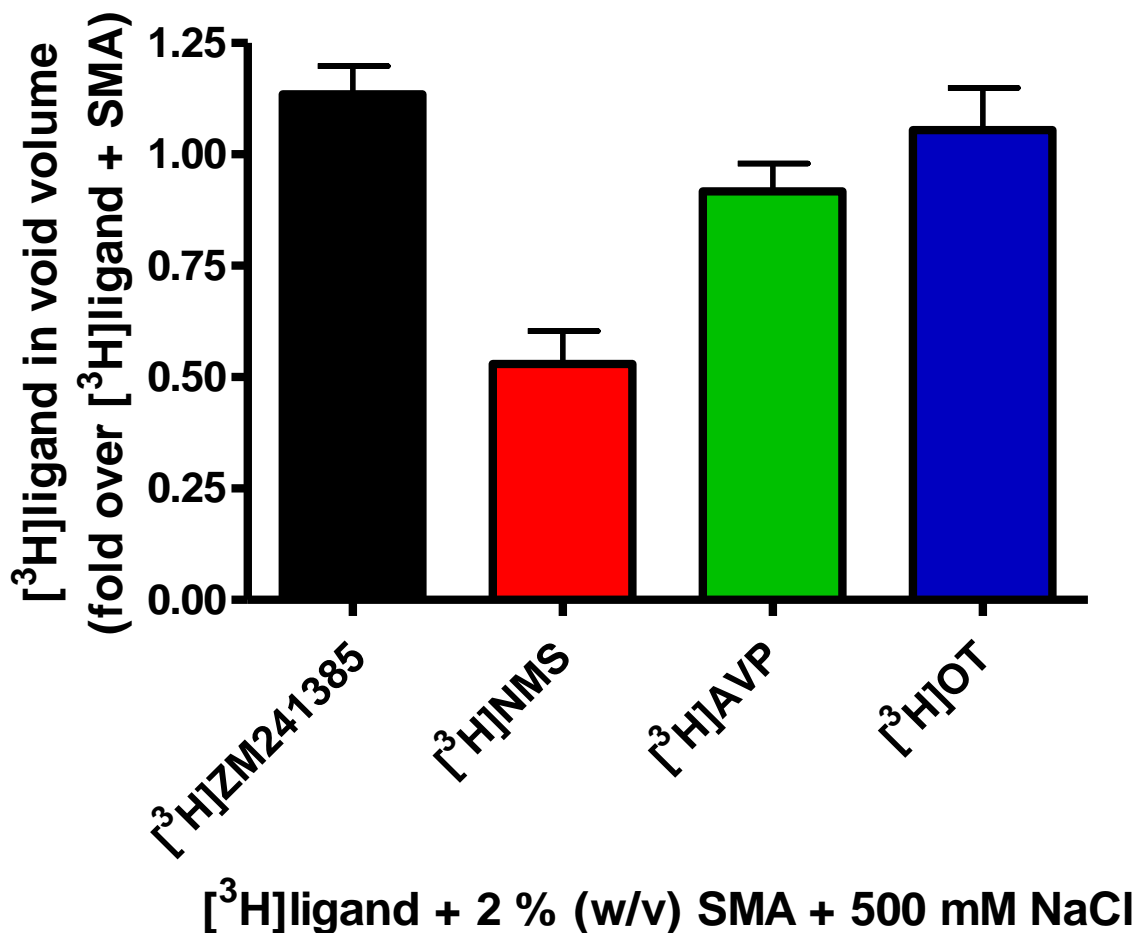
Figure 6.6. Elution profiles of [³H]ligand samples with 2 % (w/v) SMA in the presence of 500 mM NaCl. [³H]ligand samples, at concentrations used in assay, were applied to appropriate size exclusion spin columns in the presence of 2 % (w/v) SMA and 500 mM NaCl. Presence of [³H]ligand in the void volume is presented as fold over [³H]ligand + 2 % (w/v) SMA. Observed d.p.m. for basal were: ~1000 for [³H]ZM241385; ~7500 for [³H]NMS; ~3900 for [³H]AVP and ~1200 for [³H]OT Data are mean ± s.e.m. of three experiments performed in triplicate

specific (reduced by ~300 d.p.m.) using Sephadex G-75 compared to Sephadex G-50 (figure 6.7, data of one experiment performed in triplicate). This increased the observable specific binding from Sephadex G-75 in comparison to G-50 to ~50 % of total binding (similar to that seen for SMALP-A_{2a}R not gel filtered). It was observed that there was a small increase of 5-10 μl (~10 % of volume loaded) in sample volume after gel filtration. This was also observed in Western blot analysis (figure 6.8) in which SMALP-A_{2a}R (M_W: ~45790 Da) gel filtered using Sephadex G-75 was observed as a band of reduced intensity for the same volume loaded (53.8 %, mean of two experiments, calculated using ImageJ densitometry software).

Specific binding observed in SMALP-A_{2a}R samples, after gel filtration using Sephadex G-75, demonstrated that functional receptor was still present. However, as no direct assay was available for investigating the concentration of SMA in a sample, it was only assumed that gel filtration had removed free SMA from the sample. Sephadex G-75 was employed to gel filtrate SMALP-V_{1a}R samples. A reduction in non-specific binding of [^{3}H]AVP observed in SMALP-V_{1a}R samples after gel filtration would indicate a reduced concentration of SMA. As with SMALP-A_{2a}R, Western blot analysis of gel filtrated SMALP-V_{1a}R (expected M_W: ~47,890 Da) displayed at a reduced intensity compared to the original sample (79.8 %, mean of two experiments), as seen in figure 6.9. Radioligand binding analysis demonstrated decreased non-specific binding after gel filtration of SMALP-V_{1a}R samples (~920 d.p.m. compared to ~3900 d.p.m. before gel filtration). Size exclusion chromatography can therefore be used to remove SMA from a SMALP sample. Furthermore, this allowed observation, for the first time, of specific binding for SMALP-V_{1a}R (figure 6.10).
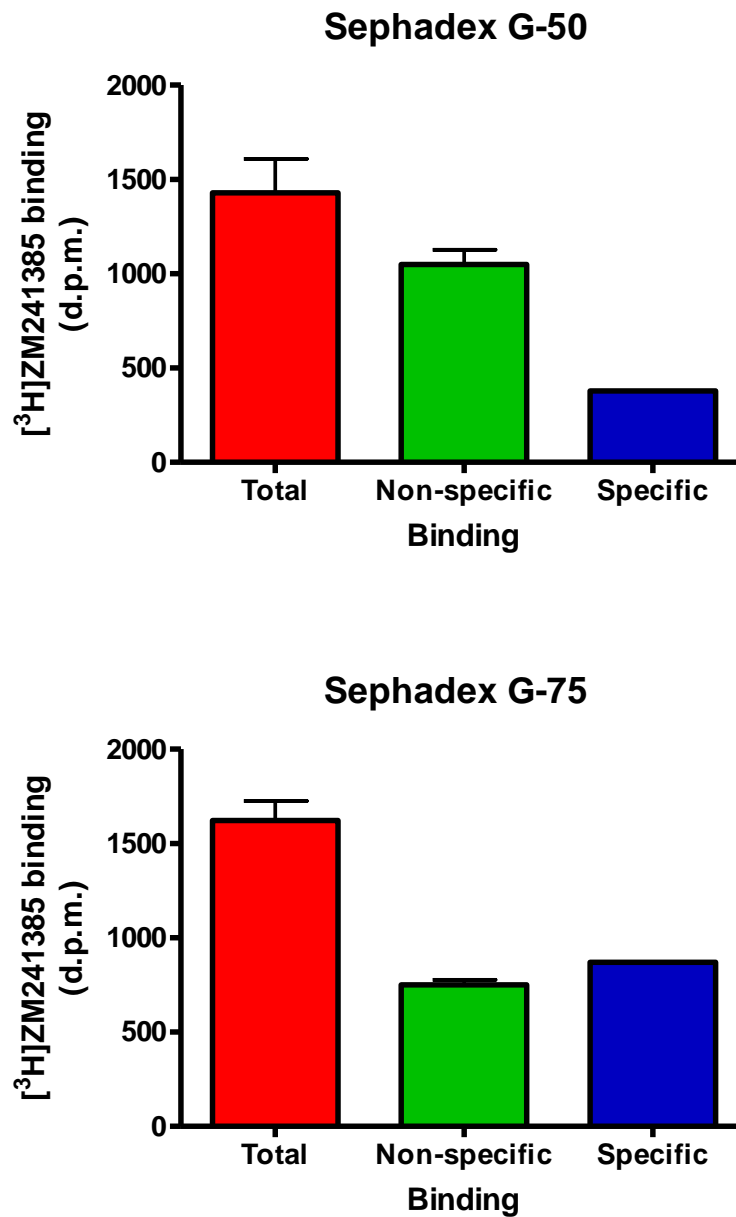
Figure 6.7. Competition radioligand binding performed on gel filtrated SMALP-A$_{2a}$R from two different size-exclusion resins. Retention of specific binding in SMALP-A$_{2a}$R eluted from Sephadex G-50 and G-75 resins was performed using 1 nM [^{3}H]ZM241385 in the absence (total) and presence (non-specific) of a saturating concentration of ZM241385 (1 μM). Data are mean ± s.e.m. of one experiment performed in triplicate.
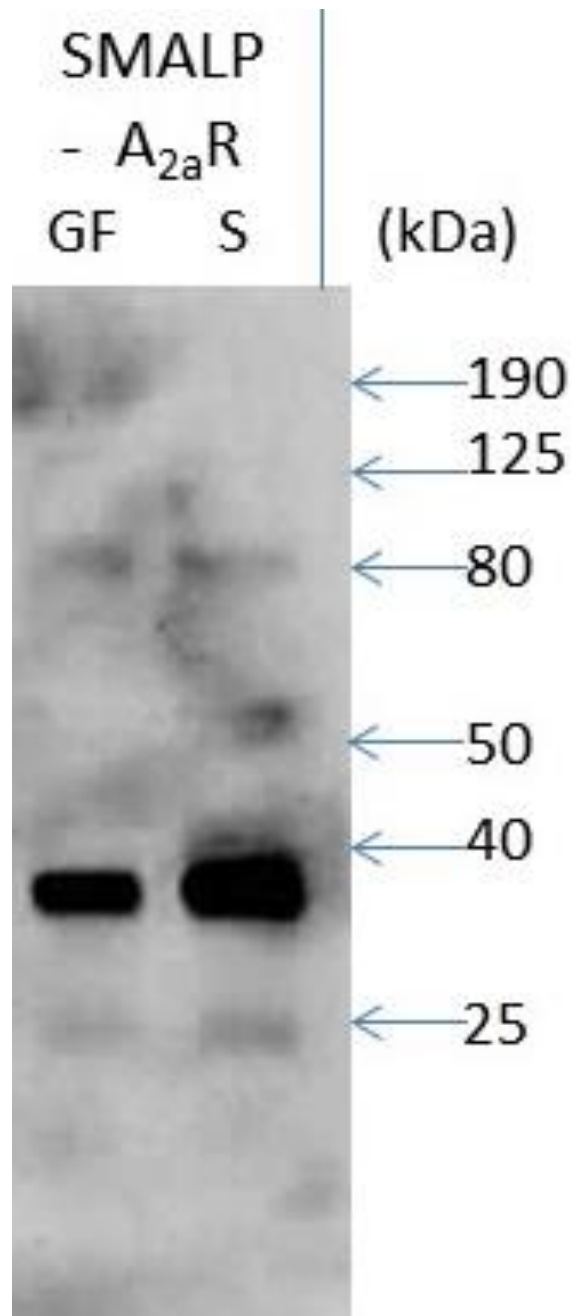
Figure 6.8. Western blot analysis of SMALP-A$_{2a}$R before and after elution from size exclusion spin columns. Gel filtrated SMALP-A$_{2a}$R (GF) was compared to SMALP-A$_{2a}$R before gel filtration (S) on size-exclusion spin columns to remove excess SMA from the sample. Characteristic gel of two experiments.
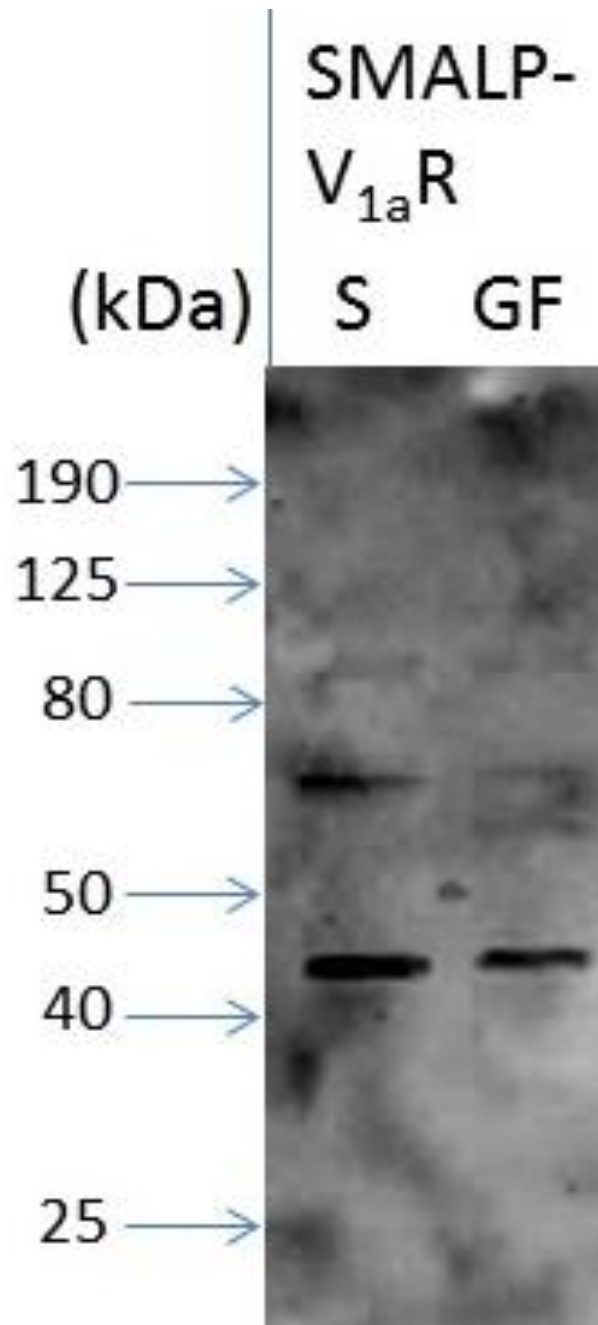
Figure 6.9. Western blot analysis of SMALP-V$_{1a}$R before and after elution from Sephadex G-75 size-exclusion spin columns. SMALP-V$_{1a}$R before gel filtration (S) was compared to gel filtrated SMALP-V$_{1a}$R (GF) on size-exclusion spin columns to remove excess SMA from the sample. Characteristic gel of two experiments.
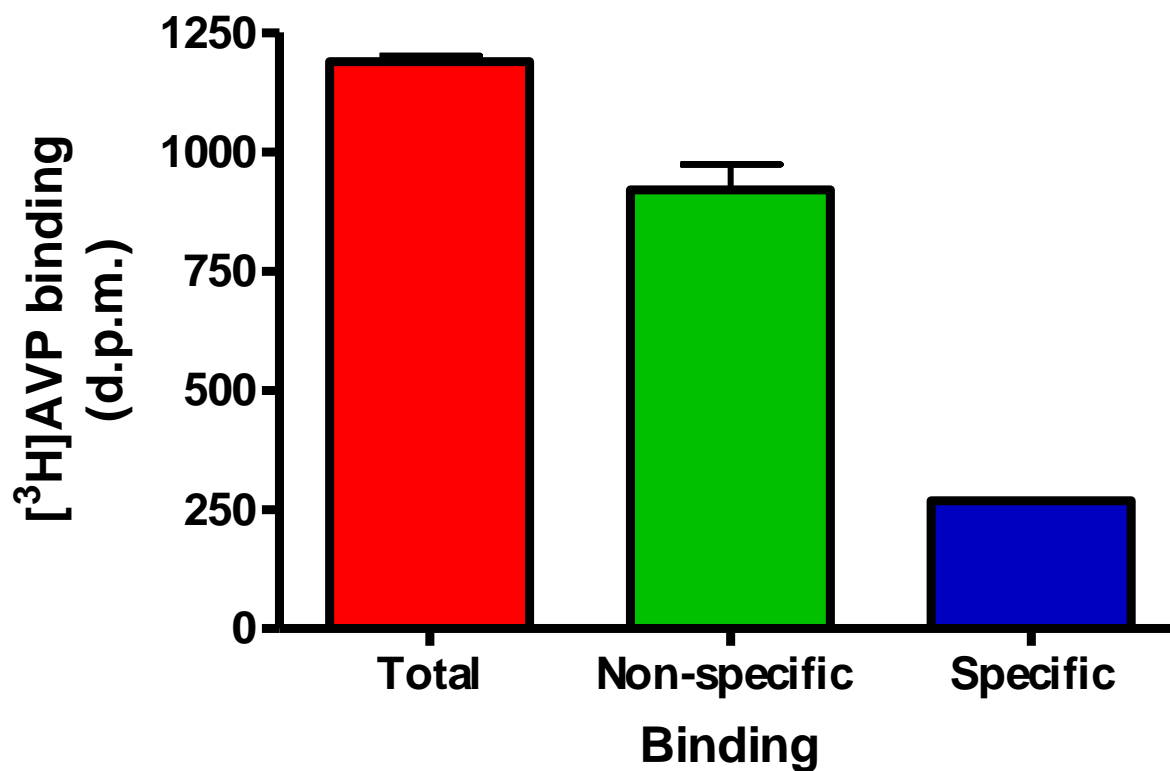
Figure 6.10. Competition radioligand binding performed on SMALP-V$_{1a}$R following elution from Sephadex G-75 size-exclusion spin columns. Determination of specific binding in SMALP-V$_{1a}$R after elution from Sephadex G-75 spin columns. Self-competition radioligand binding was performed using 1 nM [^{3}H]AVP in the absence (total) and presence (non-specific) of a saturating concentration of AVP (1 μM). Data are mean ± s.e.m. of one experiment performed in triplicate.

6.2.2 Family B GPCRs

Some family B GPCRs interact with receptor activity modifying proteins (RAMPs), endogenously expressed in mammalian cells (Sexton et al., 2001). GPCR-RAMP complexes display altered pharmacological profiles compared to the GPCR alone. Altered pharmacology of family B GPCRs provides a tool to explore the ability of SMALP-solubilisation to extract GPCRs in complex with other proteins. The size of commercially available family B ligands (~30-40 residues) and the different mode of ligand interaction, in comparison to family A GPCRs, would also allow the study of GPCRs with different characteristics from different GPCR subfamilies. The calcitonin receptor (CTR) is a family B GPCR that expresses at the cell surface independently of RAMPs, but can also associate with RAMPs to form CTR:RAMP complexes. Two forms of calcitonin, salmon and human, are commercially available in unlabelled and [^{125}I]labelled forms, allowing radioligand binding analysis of an active CTR. Due to the accessibility of high affinity radioligands, and its ability to be expressed at the cell surface in the presence or absence of RAMPs, CTR was chosen as an exemplar family B GPCR to be used in the study of the SMALP-solubilisation technique.

HEK 293T cells are known to express RAMPs at relatively high levels. For the purpose of this investigation CTR was therefore transiently transfected into COS-7 cells, which express RAMP1 at much lower levels (Christopoulos et al., 1999). SMALP-solubilisation of COS-7 cells transiently transfected with CTR alone or co-transfected with RAMP1 (producing amylin receptor 1 (AMY$_1$)) would allow the study of two pharmacologically distinct receptors. CTR displays high affinity for human calcitonin only when not complexed with RAMPs (Hay et al., 2005). Both CTR and AMY$_1$ display high affinity binding for salmon calcitonin, but of CTR and AMY$_1$ only AMY$_1$ binds amylin with high affinity.

SMALP-solubilisation from whole mammalian cells had only ever been performed from HEK 293T cells. To ensure efficient extraction from COS-7 cells, A$_{2a}$R was expressed, SMALP-

solubilised and compared to membrane preparations from COS-7 and HEK 293T cells. From data expressed in figure 6.11 and table 6.1, it was observed that $A_{2a}R$ expressed in COS-7 cells displayed similar binding affinities for ZM241385 in comparison to $A_{2a}R$ expressed in HEK 293T cells in both membrane and SMALP samples.

Application of the HEK 293T cell-optimised SMALP-solubilisation technique yielded functional, soluble $A_{2a}R$ from COS-7 cells. Although no change to the SMALP technique was needed for solubilisation of COS-7 cells, it was not known whether a fully intact family B GPCR could be SMALP-solubilised in a functional state. SMALP-solubilisation of an HA-epitope tagged CTR (herein referred to as CTR) from COS-7 cells was performed before Western blot analysis. This would allow identification of solubilised CTR and the relative amount remaining unsolubilised. Samples were separated using a 4-20 % (w/v) Tris-glycine gel (Bio-Rad, U.K.) before transfer to nitrocellulose, anti-HA antibody was used to probe for the HA-tag present on CTR. As shown in figure 6.12, SMALP-solubilisation from COS-7 cells was efficient, with the vast majority of receptor being present in the soluble fraction after SMALP-solubilisation (85.6 %, mean of two experiments, determined using ImageJ densitometry software). The bands present ~115 kDa were attributed to dimeric CTR (theoretical monomeric M_W: ~60,400 Da). Higher bands, such as that observed ~175 kDa, were attributed to trimeric CTR and further higher order oligomers.

Having shown SMALP-solubilisation of CTR was possible from COS-7 cells, the ability to SMALP-solubilise CTR in a functionally active state was determined through pre-labelling with radioligand. CTR was expressed in COS-7 cells before prelabelling with approximately 50 pM [^{125}I]salmon calcitonin ([^{125}I]sCT) in the presence or absence of 1 μM sCT. Samples were incubated for 1 h, 37 °C, before free ligand was removed by aspiration. Samples were then SMALP-solubilised before bound [^{125}I]sCT was quantitated by liquid scintillation counting.
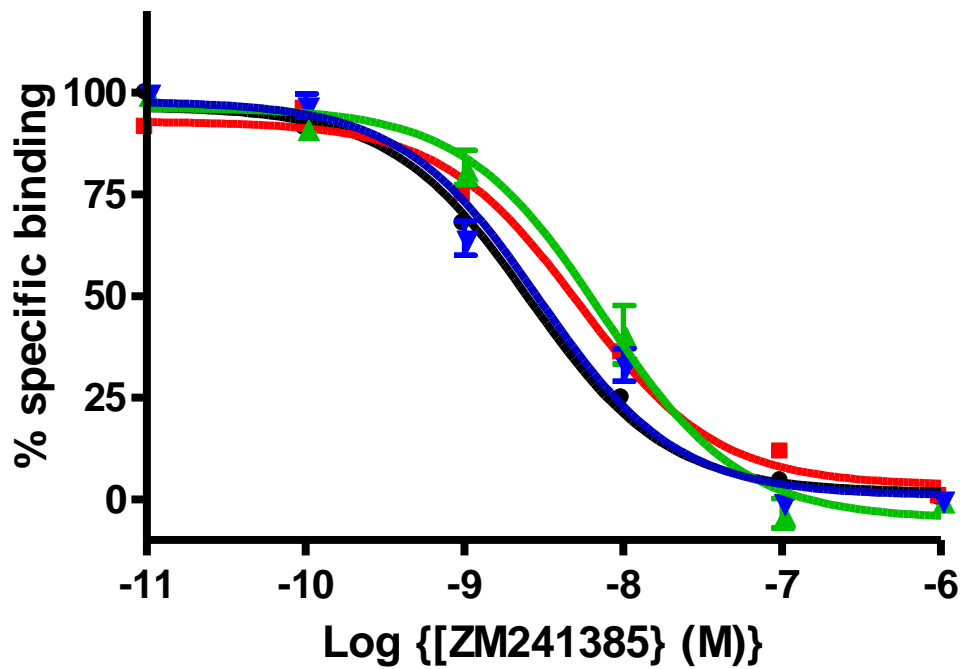
Figure 6.11. Self-competition radioligand binding of A₂ₐR expressed in COS-7 cells and HEK 293T cells. Radioligand binding performed on A₂ₐR expressed in COS-7 cells and prepared as membranes (▲) and SMALPs (▼) compared to membrane A₂ₐR (●) and SMALP-A₂ₐR (■) from HEK 293T cells. Data are mean ± s.e.m. of three experiments performed in triplicate.

	pK$_i$ ± s.e.m.	
Sample	HEK 293T	COS-7
Membrane-A$_{2a}$R	8.87 ± 0.1	9.39 ± 0.1
SMALP-A$_{2a}$R	8.53 ± 0.0	8.99 ± 0.1

Table 6.1. pK$_i$ values of [^{3}H]ZM241385 at A$_{2a}$R prepared from HEK 293T and COS-7 cells as membrane and SMALP samples. Data are mean ± s.e.m. of three experiments performed in triplicate.
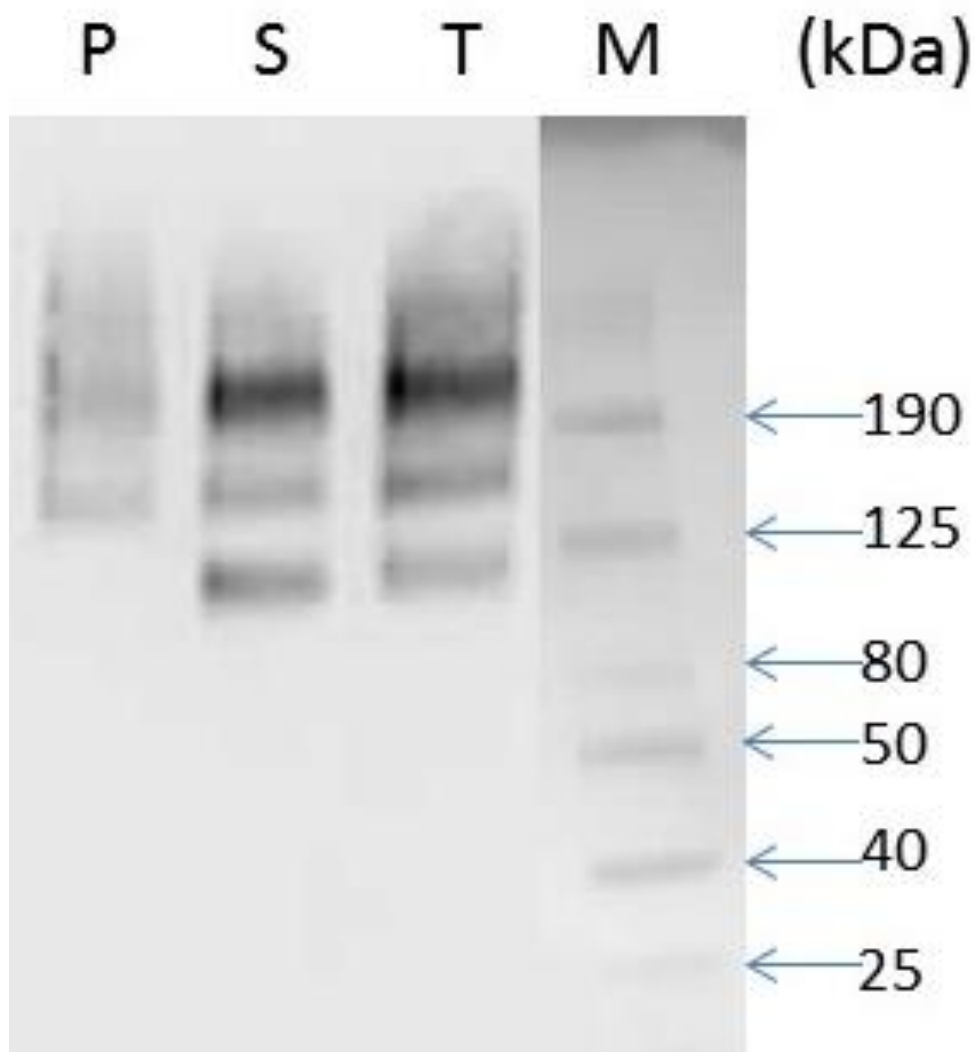
Figure 6.12. Western blot analysis of SMALP-solubilised CTR from COS-7 cells. CTR

present in the insoluble pellet fraction (P) and SMALP-solubilised fraction (S) were compared

to initial CTR amounts (T) through use of an anti-HA probe. Typical of two experiments.

Non-specific binding was very low, only ~400 d.p.m., in comparison to total binding of ~2400 d.p.m. Specific binding was 80.5 % of total binding (figure 6.13) and ~ 68 % of specific binding observed in membrane preparations of CTR from COS-7 cells, demonstrating the ability of SMALPs to solubilise CTR in a functional state. This preliminary study provided proof of concept for further investigation into use of SMALP-solubilisation to study family B GPCRs.

6.2.3   Styrene maleimide lipid particles

The ionic interactions observed between SMA and [³H]NMS, and possibly [³H]AVP, highlighted a possible limitation of the SMALP technique. It would appear that the negative charge surrounding the SMALP could interact with positively charged ligands to produce increased non-specific binding. Reversal of the charge on the outside of the SMALP could prevent the ionic interaction with positively charged molecules. For this, an SMA analogue possessing a positively charged moiety instead of maleic acid was investigated. Styrene maleimide (SMI) is a polymer that has been used in the past for: pigment dispersion in inks and paints, a clarifying agent (for use in flocculation) and paper/wood coating. Despite its use as a surfactant in the majority of its applications, there is no reported use of SMI in solubilisation of membrane proteins. The structure of SMI is similar to that of SMA (as displayed in figure 6.14). At a ratio of 2:1 (styrene:maleimide molar ratio) the structure differs only in the size and charge of the maleic side chain. Whereas in SMA the maleic acid group is small and displaying a negative charge, in SMI the maleimide group is bulkier and presents a positive charge. As there was no reported use of SMI to solubilise membrane proteins, it was unknown whether SMI would behave the same as SMA in solubilisation of GPCRs.

Should SMI be able to solubilise functional GPCRs, it would provide an alternative polymer that could bypass charge interactions with positively charged ligands. To investigate whether SMI polymer interacts with ligand, analysis using size-exclusion chromatography was
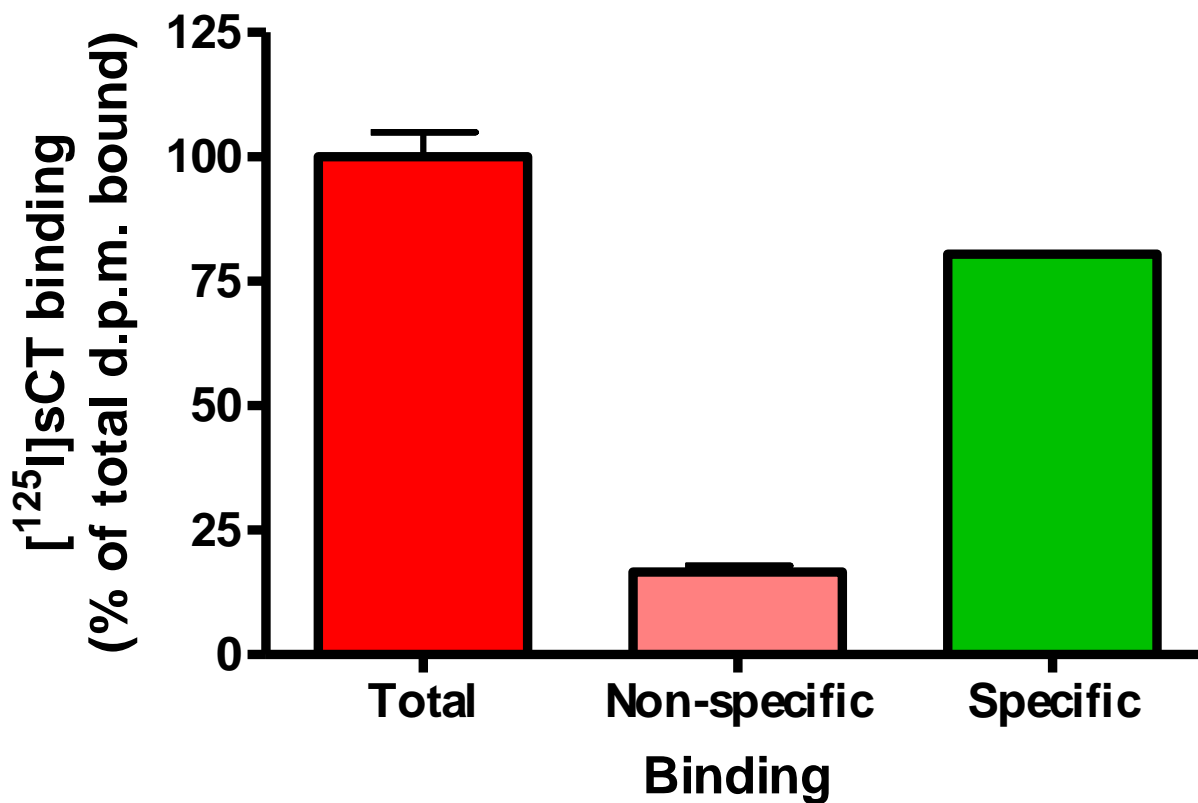
Figure 6.13. Specific binding determination of SMALP-CTR through pre-labelling. Specific binding of SMALP-CTR was determined through pre-labelling with [^{125}I]sCT in the absence (total) or presence (non-specific) of a saturating concentration of salmon calcitonin (1 µM). Data are mean ± s.e.m. of one experiment performed in triplicate.
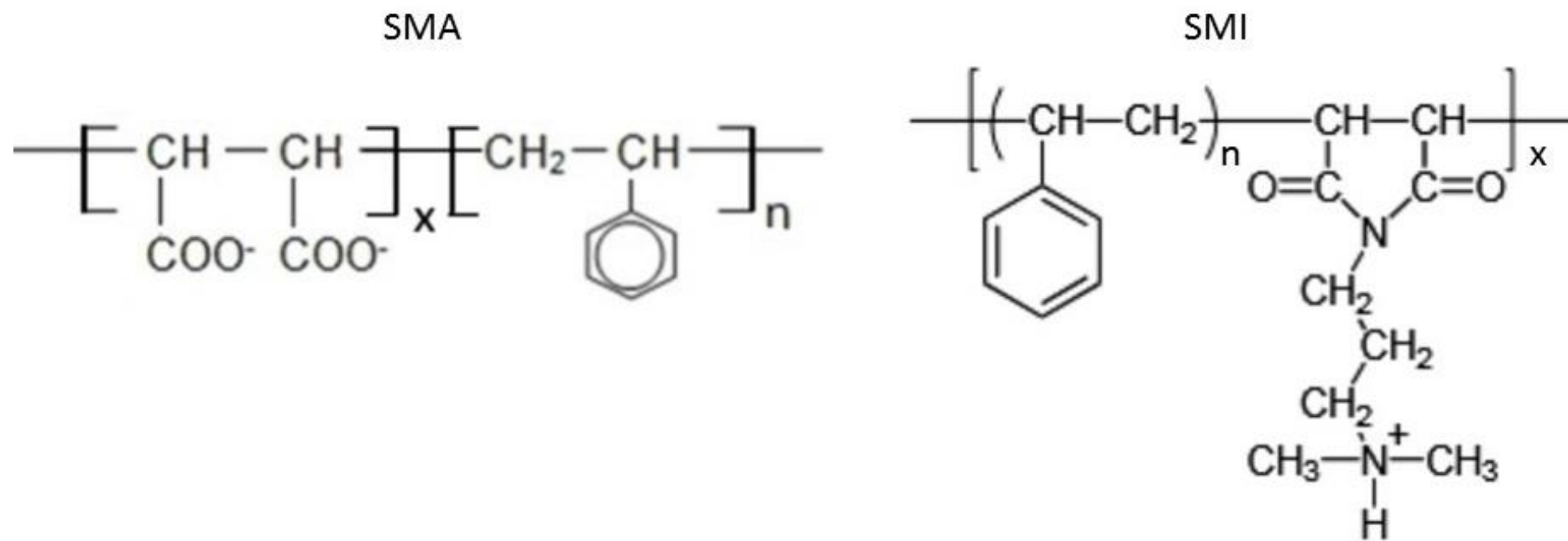
Figure 6.14. Structure of the monomeric subunits of SMA and SMI. The chemical structure of the repeating subunits of SMA (left) and SMI (right). For the 2:1 (styrene:maleic group molar ratio) form of each polymer, as used in this study, n=2 and x=1.

employed as before (section 6.2.1). As it was unknown whether SMI would solubilise membrane proteins in a similar way to SMA, increased concentrations of SMI were to be used for initial experiments. This would provide the best chance for maximum extraction of GPCR from membranes. As a result, 5 % (w/v) SMI was investigated for its interaction with [³H]ligands. [³H]ligand samples in the presence of 5 % (w/v) SMI and 5 % (w/v) SMI + 500 mM NaCl were applied to spin columns containing size exclusion resin; Sephadex G-15 ([³H]ZM241385 and [³H]NMS) or Sephadex G-50 ([³H]AVP and [³H]OT). Presence of [³H]ligand in the void volume was measured by liquid scintillation counting.

As shown in figure 6.15, more [³H]ZM241385 eluted in the void volume in the presence of SMI than in the absence of SMI. At ~2 fold over basal [³H]ZM241385 presence in the void volume with SMI was increased in comparison to SMA (~1.5 fold over basal) and inclusion of 500 mM NaCl displayed no ability to reduce this. [³H]OT, as with SMA, showed only slightly increased quantities in the void volume in the presence of SMI (~1.2 fold over basal compared to ~1.5 fold over basal with SMA). [³H]AVP and [³H]NMS both showed increased quantities in void volumes in the presence of SMI (1.8 and 2.2 fold over basal respectively). However, these levels were not as high as those observed with SMA (~6 and ~3.7 fold over basal for AVP and NMS respectively) and in both cases inclusion of NaCl was able to produce a subtle decrease in [³H]ligand elution (from ~1.8 to ~1.4 fold over basal for [³H]AVP and from ~2.2 to ~1.7 fold over basal for [³H]NMS).

There was therefore a reduction in polymer interaction observed with [³H]AVP, [³H]OT and [³H]NMS. This indicated that SMI could potentially be used as an alternative to SMA to reduce non-specific binding of these ligands. However, this all depended on the ability of SMI to solubilise GPCR in a functional state. As solubilisation of proteins into styrene maleimide lipid particles (SMILPs) had never been previously reported, proof of concept was investigated. This
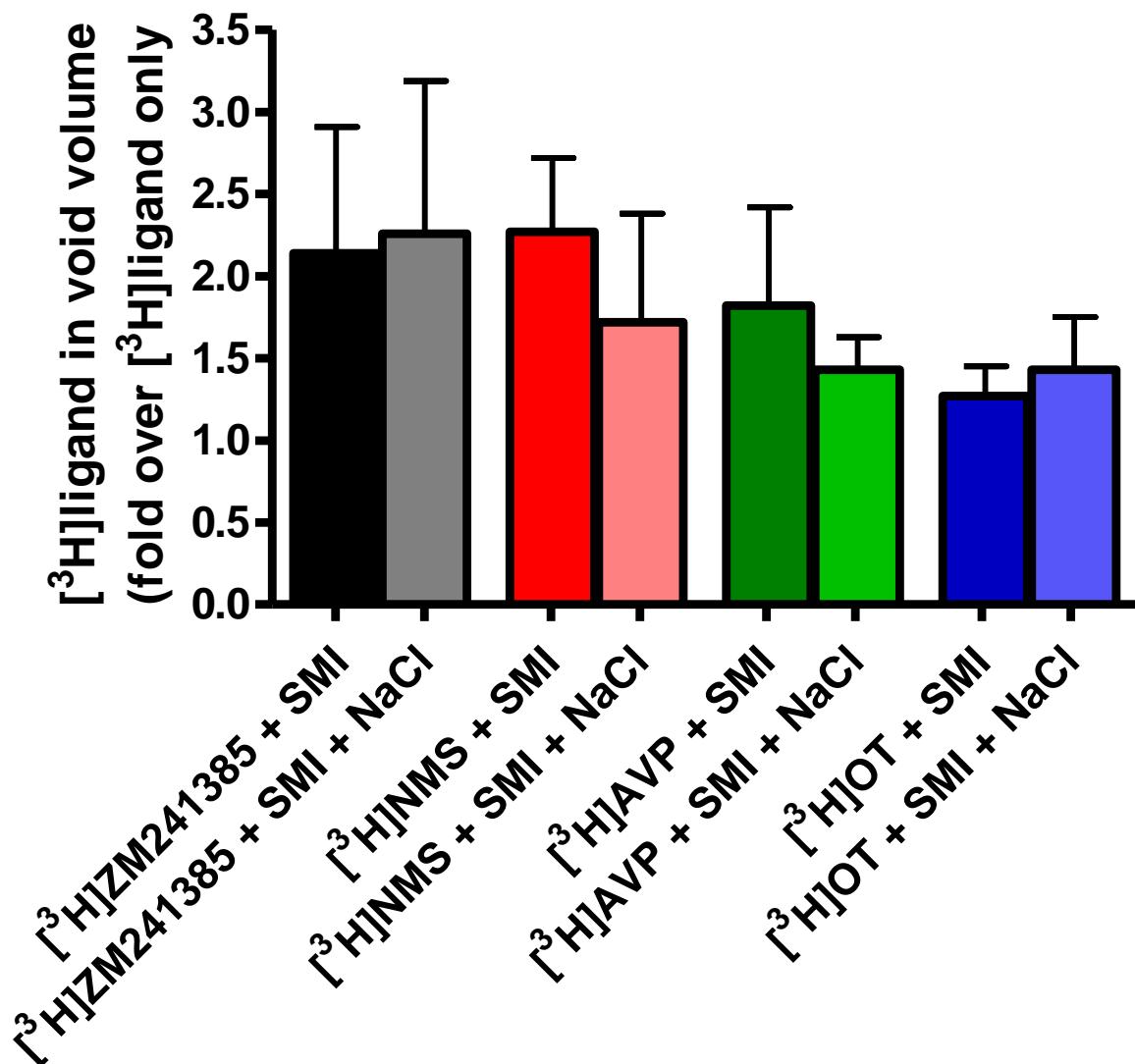
Figure 6.15. Elution profiles of [³H]ligands with SMI resolved by size exclusion chromatography. [³H]ligand samples, at concentrations used in assay, were run through appropriate size-exclusion spin columns in the presence of 5 % (w/v) SMI (+ SMI) and presence of 5 % (w/v) SMI + 500 mM NaCl (+ SMI + NaCl). Observed d.p.m. for basal were: ~700 for [³H]ZM241385; ~2000 for [³H]NMS; ~650 for [³H]AVP and ~700 for [³H]OT. Data are mean ± s.e.m. of three experiments performed in triplicate.

was achieved through transient transfection into HEK 293T cells and subsequent pre-labelling of $A_{2a}R$ and $V_{1a}R$ with [³H]ZM241385 and [³H]AVP respectively (~1 nM). This was performed in the presence or absence of a saturating concentration of competing ligand (1 μM ZM241385 or 1 μM AVP). Samples were incubated at 30 °C for 30 min ($A_{2a}R$) or 90 min ($V_{1a}R$) before free ligand was removed by aspiration. As there was not an optimised protocol for SMILP-solubilisation from mammalian cells, more polymer was used than in SMALP-solubilisation to increase the chance of maximum extraction. Pre-labelled $A_{2a}R$ and $V_{1a}R$ were incubated at 37 °C, 1 h, before centrifugation at 100,000 x g for 1 h. Bound ligand in the supernatant was quantitated by liquid scintillation counting. As seen in figure 6.16, extraction of functional $A_{2a}R$ and $V_{1a}R$ into SMILPs was possible. Specific binding observed was 21941.3 ± 1871.4 d.p.m. at SMILP-$A_{2a}R$ and 5667.3 ± 1655.4 d.p.m. for SMILP-$V_{1a}R$ (mean ± s.e.m. of three experiments performed in triplicate). These data were comparable to those observed with pre-labelled SMALP-solubilisation (23660.7 ± 2401.9 d.p.m. at $A_{2a}R$ and 5923.7 ± 1516.4 d.p.m. at $V_{1a}R$).

As pre-labelling of SMILP samples produced specific binding equivalent to SMALP samples, radioligand binding was attempted of $V_{1a}R$ having been SMILP-solubilised in the absence of ligand. Even in the presence of 500 mM NaCl, the specific binding was only 11.1 ± 2.4 % (n=3, mean ± s.e.m.) of the total binding (~120 d.p.m. compared to ~1000 d.p.m.), as displayed in figure 6.17. This translates to approximately 5.5 % binding recovery in comparison to membrane preparations of $V_{1a}R$ from HEK 293T cells. These data were collected from $V_{1a}R$ solubilised using non-optimised conditions. It may have been possible to improve SMILP-solubilisation of $V_{1a}R$ through optimisation of the SMILP-solubilisation protocol.
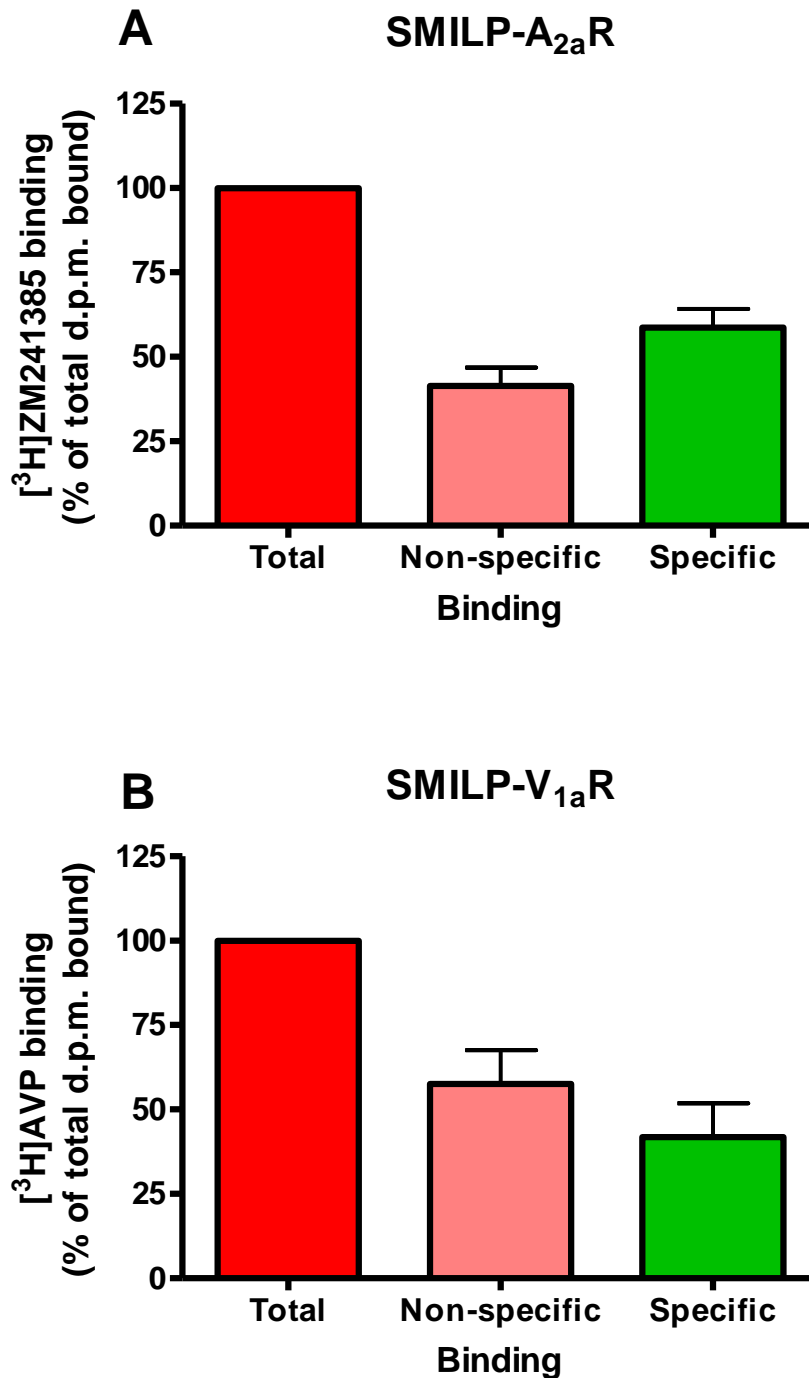
Figure 6.16. Pre-labelled radioligand binding observed for SMILP-A$_{2a}$R and SMILP-V$_{1a}$R. Panel A: specific binding was determined for A$_{2a}$R using [^{3}H]ZM241385 in the absence (total) and presence (non-specific binding) of a saturating concentration (1 μM) of ZM241385. Panel B: specific binding was determined for V$_{1a}$R using [^{3}H]AVP in the absence (total) and presence (non-specific binding) of a saturating concentration (1 μM) of AVP. Data are mean ± s.e.m. of three experiments performed in triplicate.
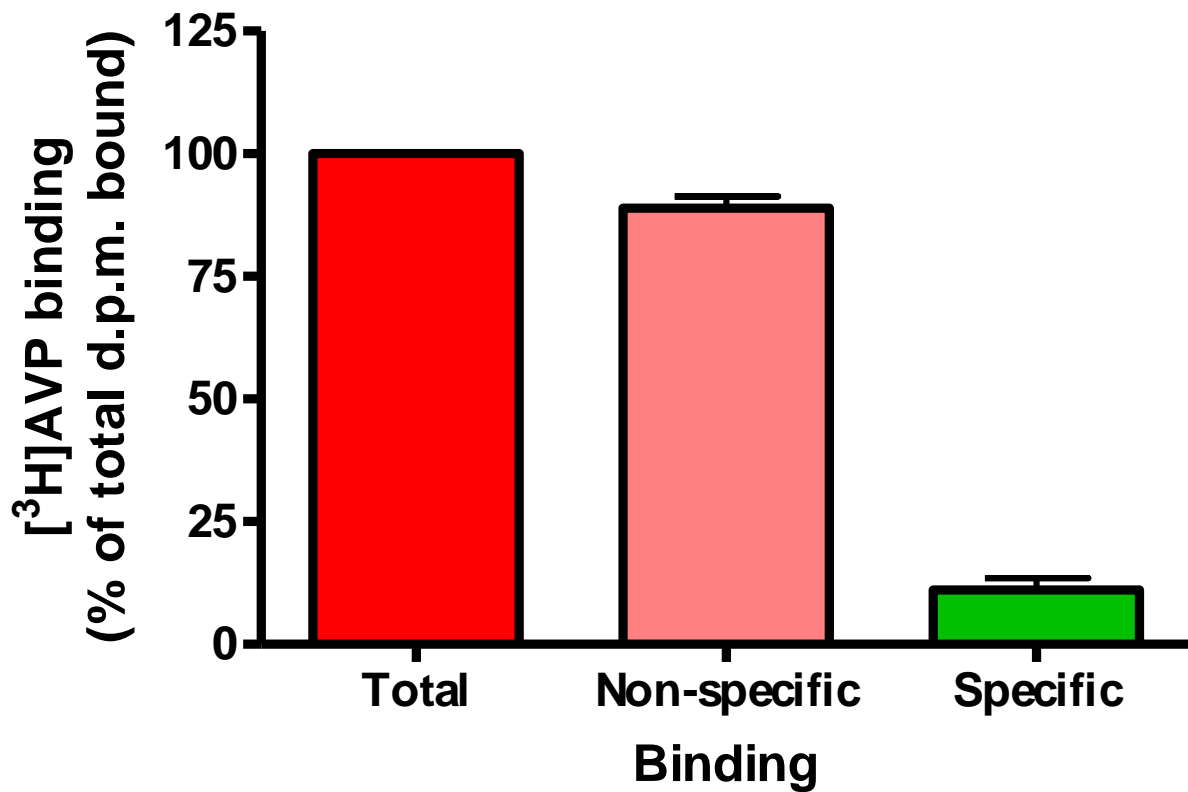
Figure 6.17. Radioligand binding of SMILP-V$_{1a}$R performed after SMILP-solubilisation.
Specific binding of SMILP-V$_{1a}$R was determined through incubation with [^{3}H]AVP (~1 nM) in the absence (total) and presence (non-specific) of a saturating concentration of AVP (1 μM). Observed d.p.m. was ~1000 for total binding. Data are mean ± s.e.m. of three experiments performed in triplicate.

6.2.3.1 SMILP optimisation

As with SMALP-solubilisation optimisation, parameters of SMI concentration, incubation temperature and incubation time were to be investigated sequentially. Initial parameters were based around optimised SMALP-solubilisation for mammalian cells. It had been shown that 5 % (w/v) was able to extract $V_{1a}R$ and $A_{2a}R$ in a functional state. However, it was noticed that there was a large amount of white precipitate present in the insoluble fraction of SMILP samples (figure 6.18). This large amount of precipitate had never been observed with SMALP samples, even when using 4 % (w/v) SMA. Common pellet size of SMALP samples is shown in figure 6.18, and is characteristic of all SMALP samples created with >1 % (w/v) SMA. Although pre-labelling of $A_{2a}R$ and $V_{1a}R$ produced data equivalent to those produced from SMALP samples, radioligand binding performed on SMILP-$V_{1a}R$, after solubilisation, demonstrated very little specific binding. The amount of precipitate observed was more than the amount of membrane present in the sample. It was therefore hypothesised that the white precipitate present after SMILP-solubilisation was, in part, the result of SMI precipitation and that this was preventing efficient extraction of $V_{1a}R$.

BCA assays were performed on SMILP samples created with 5 % (w/v) SMI. Total protein content of the precipitate was determined to be 12.9 ± 0.9 % (mean ± s.e.m. of three experiments performed in triplicate) of the total protein present before SMILP-sample centrifugation at 100,000 x g, 1 h. This was comparable to data obtained from SMALP samples (~17 % of total protein remained in the pellet). However, this was performed on crude preparations and therefore all soluble proteins from within the cell contributed to the protein concentration of the soluble samples. As there was no specific binding observed from SMILP pellet samples, Western blot analysis was employed to observe $V_{1a}R$ presence in SMILPs.

Figure 6.18. Pellet fractions of $V_{1a}R$ when solubilised with SMA or SMI. Left panel displays the un-doctored image. Right panel has highlighted, in red, the pellets of SMALP-$V_{1a}R$ (top) and SMILP-$V_{1a}R$ (bottom), from the same amount of starting material. SMALP-$V_{1a}R$ was prepared using the conditions optimised for SMALP-solubilisation from mammalian cells and this image is characteristic of all SMALP samples prepared using >1 % (w/v) SMA. SMILP-$V_{1a}R$ samples were prepared using 5 % (w/v) SMI and incubated at 37 °C for 1 h. The SMILP pellet is characteristic of SMILP samples prepared using 5 % (w/v) SMI.

6.2.3.2 Use of Western blots in the study of SMILP-solubilisation

Western blot analysis was used to probe for the presence of the HA-tagged $V_{1a}R$ in SMILP samples. Unfortunately, sample migration from the stacking gel to the separating gel was poor. $V_{1a}R$ that did migrate into the separating gel produced ill-defined, high molecular weight bands (figure 6.19). Ionic interactions between SDS and SMI were hypothesised to have prevented sufficient denaturing and charge coating of proteins by SDS. Increased SDS concentrations up to 10 % (w/v) were employed, allowing observation of bands as seen in figure 6.20. Although the band observed at ~60 kDa was faint and not of the expected size (HA-$V_{1a}R$ predicted M_w: 47,890 Da), the specificity of anti-HA antibody for the HA-tag provided evidence that there was some extraction of $V_{1a}R$ using the SMI polymer. Precipitation of samples had been observed at the interface of the stacking gel with the separating gel. It was hypothesised that there was precipitation of SMI upon reaching the pH 8.8 separating gel of SDS-PAGE as SMI precipitates from solution at pH >7.5. This may have resulted in a blockage of the acrylamide mesh, preventing and retarding the movement of proteins through the separating gel. However, Bis-Tris gels and buffers, providing pH ranges of 6.4 to 7.2, were equally ineffective for use with SMILP-$V_{1a}R$ samples. Bis-Tris gels also produced precipitation of samples at the gel interface and, as shown in figure 6.21, lower pH ranges still resulted in aggregation of protein samples at the gel interface.

With the great difficulties encountered using SDS-PAGE and Bis-Tris gels, dot blot analysis of samples was employed. By applying SMILP samples directly to nitrocellulose before immuno-detection using anti-HA antibody, pH and ionic interaction issues were bypassed. This meant sacrificing identification of specific band sizes of the target protein containing the HA-tag. However, it allowed investigation of relative protein amounts under various SMILP-solubilisation conditions.
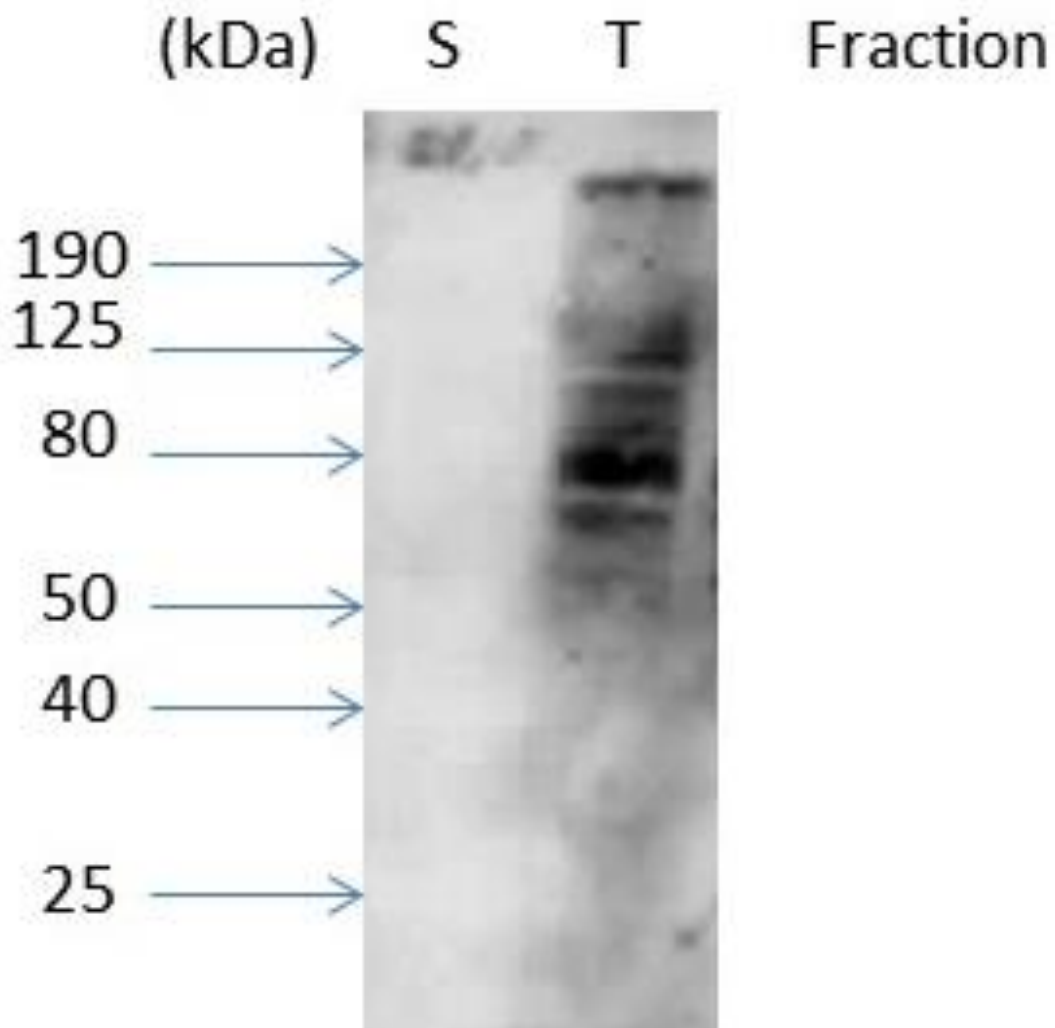
Figure 6.19. Western blot analysis of SMILP-V$_{1a}$R prepared with 5 % (w/v) SMI. SMILP-V$_{1a}$R soluble samples (S) were compared to initial V$_{1a}$R concentrations (T) when prepared with 5 % (w/v) SMI. Samples were separated by SDS-PAGE before transfer to nitrocellulose and probed with anti-HA antibody. Typical of six experiments.
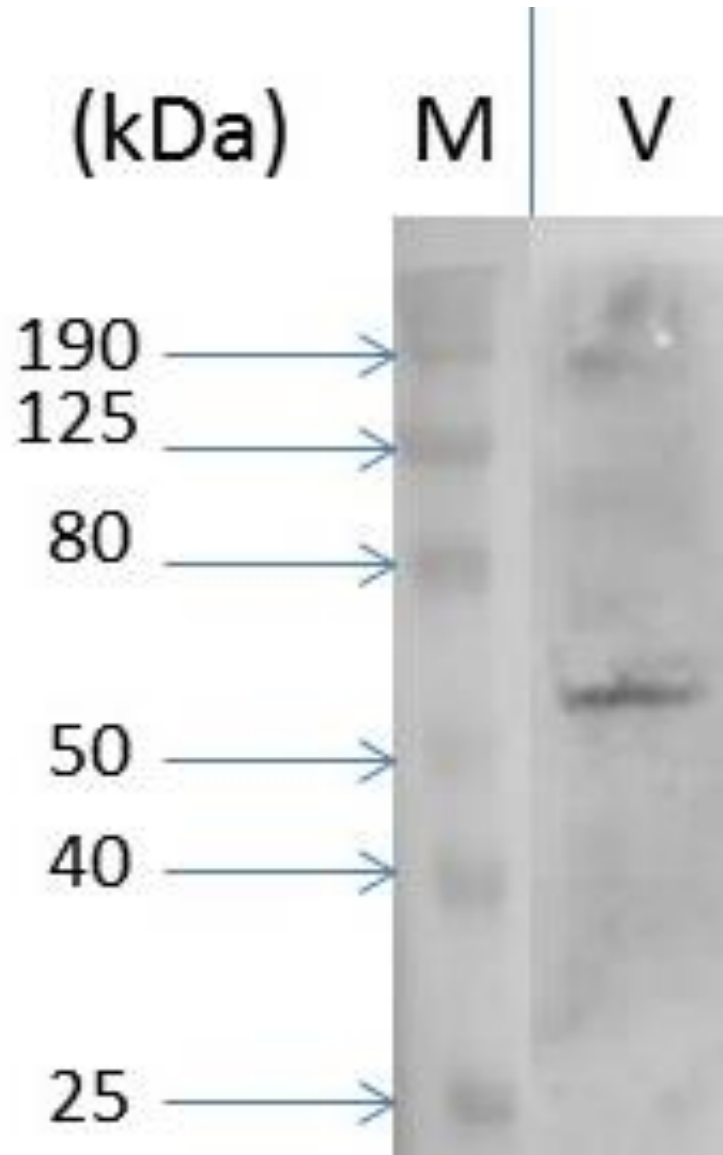
Figure 6.20. Western blot analysis of the soluble fraction of SMILP-V$_{1a}$R using increased SDS concentrations in loading buffers. Molecular weight markers (M). SMILP V$_{1a}$R (V) soluble sample was probed with anti-HA antibody for the engineered HA-tag once separated by SDS-PAGE using 10 % SDS in loading buffer. Characteristic gel of two experiments.
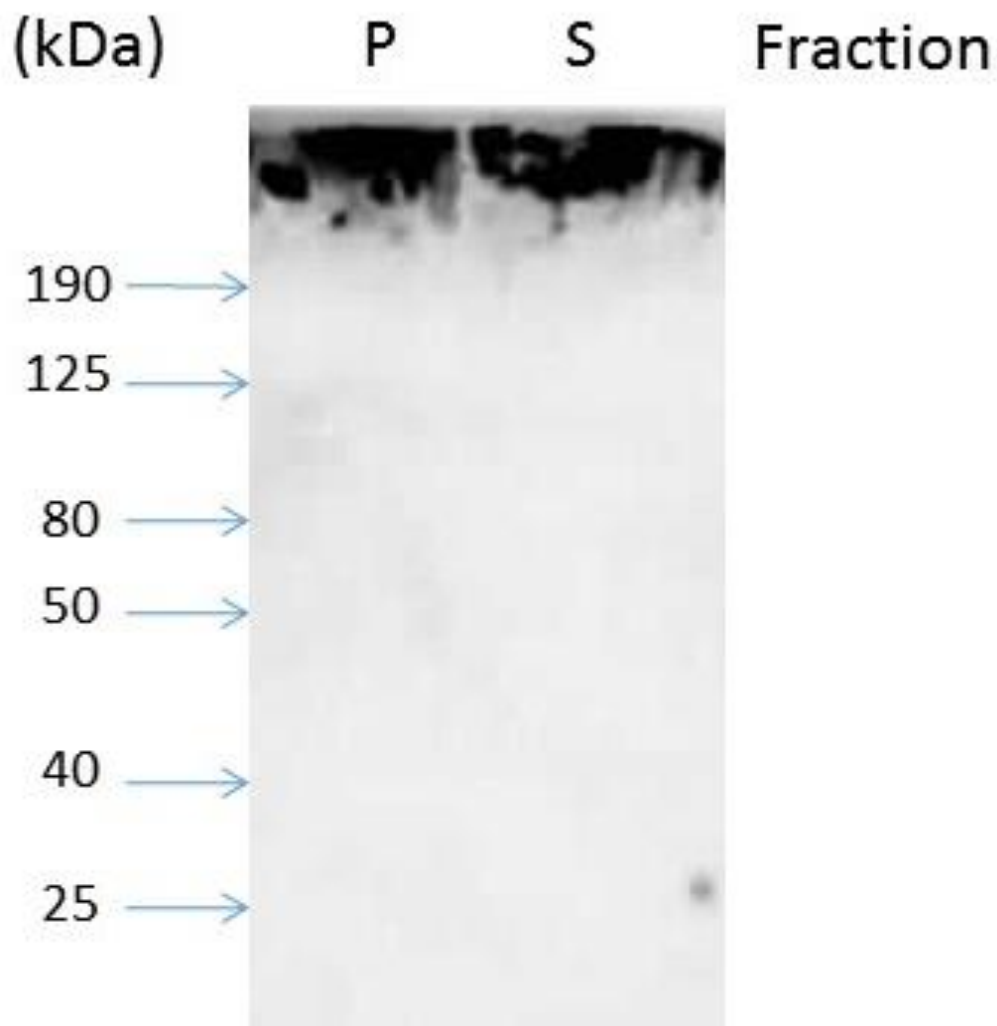
Figure 6.21. Western blot analysis from Bis-Tris gel separation of proteins in SMILP-$V_{1a}R$ samples. Anti-HA antibody used to probe for SMILP-$V_{1a}R$ pellet (P) and soluble (S) fractions prepared using 5 % (w/v) SMI. Samples were separated on Bis-Tris gels before transfer to nitrocellulose. Representative of five experiments.

SMI concentration used in solubilisation of $V_{1a}R$ was the first condition to be optimised for the SMILP-solubilisation protocol. SMI at 5 % (w/v) had been shown to extract $V_{1a}R$. SMI at 2 % (w/v) was also investigated as this was the optimum concentration of SMA for use in solubilisation of GPCRs from mammalian cells. SMI at 1 % (w/v) was investigated to further explore the efficiency of SMILP-solubilisation at low SMI concentrations. SMI at 10 % (w/v) was investigated as it appeared SMI precipitated from solution during solubilisation of mammalian cells, it was likely that more SMI would be required than SMA for efficient solubilisation. As seen in figure 6.22, although protein size could not be observed, SMILP-solubilised mock-transfected cells did not produce a signal using anti-HA antibody. All samples that did produce a signal were therefore a result of the HA-tagged $V_{1a}R$. 1 % (w/v), 2 % (w/v) and 5 % (w/v) SMI were able to extract small amounts of $V_{1a}R$ (14 %, 14.6 % and 12.5 %, mean of two experiments, determined using ImageJ densitometry software), in comparison to SMALP-$V_{1a}R$ samples. SMI at 10 % (w/v) extracted the largest amount of protein in the SMILP-solubilised samples (34.2 % of SMALP-$V_{1a}R$, mean of two experiments). However, this was still not as efficient as 2 % (w/v) SMA.

It has been shown that the SMILP-solubilisation protocol has not yet been fully optimised and that there is the possibility to improve SMILP extraction of GPCRs. However, despite not being optimised, SMILP-solubilisation of $V_{1a}R$ has been shown to extract functional receptor. Thereby establishing for the first time that a second polymer is capable of detergent-free solubilisation of functional GPCRs.
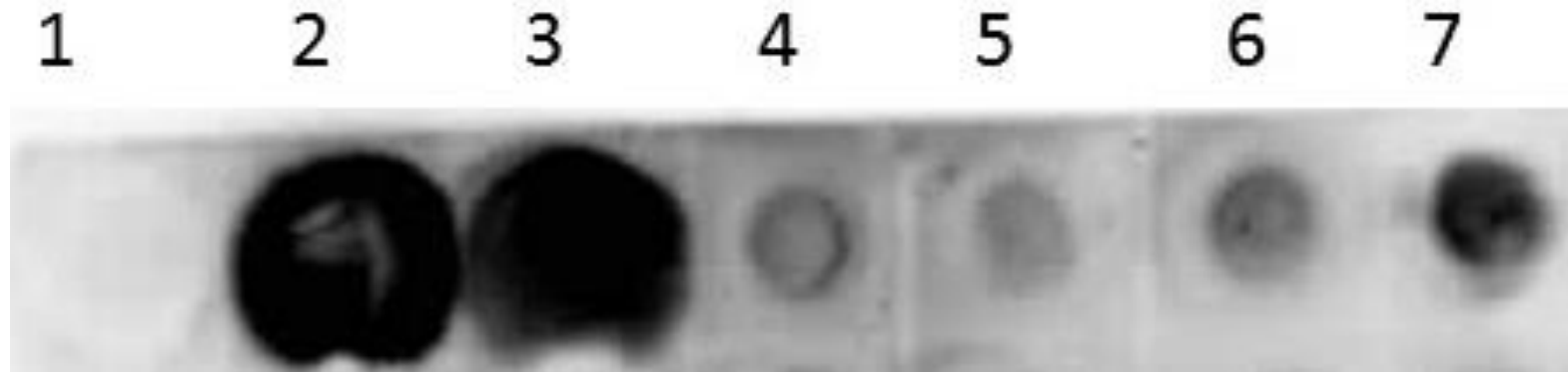
Figure 6.22. Dot blot analysis of SMILP V$_{1a}$R samples prepared with different concentrations of SMI in comparison to SMALP-V$_{1a}$R.

Soluble fractions of SMILP-mock-transfected cells (1) and two separate SMALP-V$_{1a}$R samples (2 and 3) prepared using conditions optimised for SMALP-solubilisation from mammalian cells (determined in chapter 3). SMILP-V$_{1a}$R prepared with: 1 % (w/v) SMI (4); 2 % (w/v) SMI (5); 5 % (w/v) SMI (6) and 10 % (w/v) SMI (7). Samples were applied directly to nitrocellulose and probed using anti-HA antibody. Representative of two experiments.

6.3 Discussion

6.3.1 SMALP-solubilisation of family A GPCRs

The neurohypophysial family of GPCRs has been extensively studied in the laboratory of Prof. Mark Wheatley. The muscarinic acetylcholine receptor M1 had also been used for previous studies in the laboratory of Prof. Mark Wheatley. With such a rich vein of knowledge behind these receptors, they made the obvious choice for further SMALP-studies. Initial SMALP-solubilisation of pre-labelled receptors was promising. Extraction of functional receptors was established for a range of family A GPCRs, demonstrating specific binding with a range of different ligands. SMALP-solubilisation is therefore not detrimental to the ligand binding capabilities of the GPCRs studied ($V_{1a}R$, $V_{1b}R$, V_2R, OTR and M1R) and is compatible with a range of different receptors with both amine and peptide ligands. Detailed analysis of SMALP-solubilised GPCRs will require the observation of the effect of ligand binding to the receptor. Therefore it was important to determine ligand binding capabilities for receptors SMALP-solubilised while unoccupied by ligand.

For their use in radioligand binding assays, soluble SMALP-GPCR samples required a method of separating bound from free radioligand. This was achieved by identifying and employing appropriate size exclusion chromatography resins. Sephadex G-15 was proven to be optimal for use in SMALP-$A_{2a}R$ studies using [^{3}H]ZM241385. [^{3}H]NMS (M_W: ~320 Da) has a similar molecular weight to [^{3}H]ZM241385 (M_W: ~337 Da) and so was likely to behave in a similar way in size-exclusion chromatography. Despite [^{3}H]AVP (M_W: ~1090) having a molecular weight less than the stated cut-off for Sephadex G-15 (>1500 Da), it's elution was not effectively retarded by Sephadex G-15 resin. This may have been a result of some aggregation of the AVP, increasing its molecular weight and causing elution in the void volume. There was no such complication when

using Sephadex G-50 however, which provided a much more efficient size-exclusion medium than Sephadex G-15.

Radioligand binding assays, performed using the appropriate size exclusion resin, were unable to identify specific binding of SMALP-GPCRs solubilised in the absence of ligand, other than SMALP-A_{2a}R. However, it was known from pre-labelling experiments that the SMALP could support these same receptors with ligand binding capability. [3H]ligands were investigated for possible interactions with SMA polymer that preventing the radioligand binding analysis. Samples were created containing [3H]ligand and SMA (either in the form of free SMA (2 % (w/v)) or as SMALP MT-cells) and eluted from size exclusion columns in the presence or absence of 500 mM NaCl. Increased presence in the void volume indicated that there was an ionic interaction between SMA polymer and [3H]NMS, likely a result of the positively charged quaternary nitrogen group of NMS and the negatively charged maleic acid of SMA. This ionic interaction could be interrupted by the presence of 500 mM NaCl.

[3H]AVP formed an interaction with SMA polymer whereas [3H]OT did not interact with SMA polymer. As OT differs from AVP in only 2 positions, including non-polar Leu[8] in OT being a basic residue Arg[8] in AVP, it was probable that this positively charged residue in AVP was creating strong charge interactions with negatively charged maleic acid groups in SMA. Although [3H]OT did not interact with SMA, increased presence of all [3H]ligands studied was observed in the void volumes when 2 % (w/v) free SMA was present. When 5 % (w/v) SMI was investigated this effect was increased, suggesting a possible blocking of the pores in the resin by the free polymer. This reduced the efficiency of the resin to retard elution of free ligand. This was the only increase observed for [3H]OT in the void volume. It has therefore been demonstrated that [3H]OT does not interact, to any noticeable level, with SMA. SMALP-OTR was proven to be capable of

ligand binding, but the low specific binding observed in pre-labelling experiments may suggest the occupancy of OTR by [^{3}H]OT needs to be increased to observe specific binding of SMALP-OTR.

The presence of similar levels of [^{3}H]AVP in the void volume when eluted in the presence of free SMA or SMALP-MT cells, suggests [^{3}H]AVP formed complexes with more than just one SMA chain. Free SMA (typical M_W: 9500 Da (Knowles et al., 2009)) and a single [^{3}H]AVP peptide chain (M_W: ~1090 Da), in a 1:1 complex, would be expected to be absent from the void volume when using Sephadex G-50 resin (M_W cut-off: >30,000). This suggests one or more [^{3}H]AVP molecules interacts with more than one SMA chain to create a complex of M_W greater than 30,000 Da. The large complexes formed through these ionic interactions were resistant to disruption by 500 mM NaCl. For the further study of SMALP-V$_{1a}$R, as well as other proteins with positively charged ligands, it was important to limit the formation of these complexes. Gel filtration was investigated as a method to remove free SMA from SMALP samples.

6.3.1.1 Gel filtration of SMALP samples

Mammalian cell expression systems have relatively low expression levels of receptors compared to other expression systems such as bacterial (*E.coli*) and yeast (*P.pastoris*). High non-specific binding, as a result of SMA presence, could prevent detection of specific binding in SMALP samples prepared from mammalian cells. It was therefore important to reduce non-specific binding in SMALP samples as much as possible. SMA at 2 % (w/v) was found to be optimal for extraction of proteins from mammalian cells. However, this may have excess polymer that does not form discs. Free polymer is approximately 9.5 kDa (Knowles et al., 2009), whereas SMALPs containing only lipid are predicted to be ~113 kDa, which will increase with the presence of a

GPCR in the SMALP. Size exclusion chromatography could therefore be employed to remove free SMA from SMALP samples.

With molecular weight cut-offs of >30 kDa and >80 kDa, Sephadex G-50 and G-75 (respectively) were able to remove free SMA from SMALP-A_{2a}R and SMALP-V_{1a}R samples. Elution of free SMA polymer in a sample was retarded while the SMALP-GPCRs were able to elute in the void volume. Gel filtration of SMALP-A_{2a}R using Sephadex G-75 retained binding comparable to non-gel filtered SMALP-A_{2a}R. This was despite a sample volume increase of ~10 %, commonly observed after gel filtration. Gel filtration allowed specific binding to be observed, for the first time, in SMALP-V_{1a}R due to reduced non-specific binding. As there is a proven interaction between AVP with SMA increasing non-specific binding, this provides proof of concept for the gel filtration of SMALP samples to remove free SMA from samples without loss of GPCR ligand binding capability. This could aid in the study of GPCRs as potential therapeutic targets. It has already been established in chapter 3 that SMALPs would provide a suitable platform for drug screens. Potential problems that may have arisen from charge interaction between ligand and SMA polymer could now be limited. Further study on removal of free SMA to reduce non-specific binding of other ligands would need to be performed to assess the general utility of this technique.

6.3.2   Family B GPCRs and SMALP-solubilisation from COS-7 cells

Initial investigations into the SMALP-solubilisation of COS-7 cells provided the first information on the utility of SMA to extract GPCRs from different mammalian cell types without diminished efficiency. A_{2a}R expressed in COS-7 cells displayed binding activity in SMALPs comparable to that in membranes from COS-7 cells. This facilitated SMALP-solubilisation in the study of family B GPCRs, where mammalian cell lines with reduced endogenous RAMP expression levels have often been employed (Christopoulos et al., 1999, Hay et al., 2006).

The CTR has proven clinical relevance due to implication in diseases such as: osteoclastic bone resorption (Turner et al., 2011). In combination with RAMPs, forming amylin receptors, CTR is implicated in diabetes and Alzheimer's disease (Leighton and Cooper, 1988, Fu et al., 2012). Study of SMALP-CTR could therefore aid in the understanding of, and subsequent development of improved drugs for, this therapeutically important receptor. Use of SMALP technology was shown to be applicable for the study of CTR, suggesting the utility of SMALPs in the future study of family B GPCRs.

Family B GPCRs are notoriously difficult to separate by gel electrophoresis for use in Western blots as they are prone to forming aggregates. However, it was found that through the use of gradient gels, separation of protein bands was possible, although only as oligomers. The theoretical M_W of CTR is ~60 kDa, the expected observed band size was ~55 kDa (Pham et al., 2005). Bands were clearly visible at ~115 kDa, ~175 kDa and >190 kDa, attributed to dimeric and higher order oligomers of CTR. As with family A GPCRs, these observed oligomers were not necessarily present in SMALPs but may have been artefacts of the Western blot technique.

SMALP-solubilisation of functionally active receptor was confirmed by radioligand binding. Pre-labelled CTR was extracted and demonstrated specific binding, presenting for the first time that the SMALP-solubilisation technique is applicable to other subfamilies of the GPCR superfamily. Although only preliminary data, these findings suggest that SMA is capable of extracting functional family B GPCRs. Further studies on ligand binding using SMALP-CTR will require removal of free SMA if endogenous, large peptide, ligands are to be studied. The human form of the endogenous ligand for CTR, calcitonin, contains lysine and histidine residues (Riniker et al., 1969). As seen with AVP, positively charged residues will tend form ionic interactions with SMA and increase non-specific binding in functional assays. Gel filtration of SMALP-CTR samples

could therefore aid in the study of SMALP-CTR, alternatively the few small molecule ligands commercially available for family B GPCRs could be employed.

6.3.3 SMILP-solubilisation of membrane proteins

6.3.3.1 Use of SMI in functional activity assays

Use of SMI to extract receptors such as $V_{1a}R$ seemed a promising prospect. The reversal of the charge on the outside of the SMILP-solubilised sample, in comparison to SMALP, would prevent strong ionic interactions between positively charged residues, such as arginine of AVP, and the polymer. The ability to successfully remove [^{3}H]AVP from samples containing SMI through gel filtration was more successful than with SMA. In gel filtration experiments [^{3}H]AVP and [^{3}H]NMS were present in the void volume at levels comparable to [^{3}H]ZM241385 in the presence of SMI, instead of the greatly increased levels observed with SMA. The increased levels present in the void volume observed with all [^{3}H]ligands in the presence of SMI, compared to SMA, can be explained by the increased concentration of SMI polymer. This was possibly due to the polymer blocking the pores of the size exclusion resin. If this was the case, then use of 5 % (w/v) SMI compared to 2 % (w/v) SMA would produce an increase in this effect of polymer on the size exclusion resin. These data give further evidence of the ionic interaction between [^{3}H]AVP and [^{3}H]NMS. Replacing the negative charge of SMA with the positive charge of SMI resulted in no apparent interaction between these ligands and the polymer.

SMILP-solubilisation of pre-labelled receptors with 5 % (w/v) SMI demonstrated for the very first time that SMI could be used to extract GPCRs with retention of binding capability. Furthermore, the specific binding observed through SMILP-solubilisation of pre-labelled $A_{2a}R$ and $V_{1a}R$ demonstrated comparable specific binding to pre-labelled SMALP-$A_{2a}R$ and SMALP-$V_{1a}R$. This suggested SMILPs were as efficient as SMALPs at extracting GPCRs with retention of binding

capability. The lack of an interaction between AVP and SMI allowed for specific binding to be determined using post-solubilisation radioligand binding on SMILP-$V_{1a}R$. However, the specific binding determined with post-solubilisation radioligand binding was small. Specific binding of only ~120 d.p.m. would not be suitable to perform full pharmacological characterisation of SMILP-$V_{1a}R$. This may have been due to low occupancy of $V_{1a}R$ by [^{3}H]AVP and increasing the concentration of tracer ligand may improve this. However, it was more likely due to the amount of receptor that had been SMILP-solubilised.

From dot-blot analysis of SMILP-$V_{1a}R$ samples it appeared that SMILP-solubilisation was much less efficient at extracting large amounts of $V_{1a}R$ than SMALPs were. This could mean one of two things, either there is much less $V_{1a}R$ present in SMILP samples than in SMALP samples or SMI prevents anti-HA antibody binding to the HA-tag of $V_{1a}R$. If the former is true, then pre-labelling experiments on $A_{2a}R$ and $V_{1a}R$ producing equivalent specific binding in SMILPs and SMALPs suggests the GPCR was extracted with increased recovery in binding capability in SMILPs than SMALPs. This may be explained by the bulky hydrophilic maleimide group of SMI slowing the insertion of SMI into the lipid bilayer of membranes. It has been demonstrated that tighter lipid packing slows SMA insertion into membranes because it is more difficult for the entire polymer to insert into the membrane (Scheidelaar et al., 2015). Increased stability of membrane proteins has been reported in detergent solubilisation when detergent solubilisation is slow (de Foresta et al., 1989, Kragh-Hansen et al., 1998, Stuart and Boekema, 2007), seemingly due to a large amount of detergent entering the membrane rapidly (Pantaler et al., 2000). Slower insertion of SMI into the membrane compared to SMA may result in less perturbation of the membrane as fragments are solubilised slower. This could allow the membrane to reorganise around proteins, preserving their structure before they are solubilised. Alternatively, SMI has extracted equivalent amounts of

$V_{1a}R$ but SMI is preventing anti-HA antibody detection of the HA-tagged $V_{1a}R$. However, if this was true then use of 10 % (w/v) SMI to solubilise $V_{1a}R$ would have resulted in an apparent reduction in extraction, not increase as was observed by dot-blot analysis.

6.3.3.2 Optimisation of SMILP-solubilisation

SMI had never before been investigated for its use as a solubilisation agent. It had been proven that 5 % (w/v) SMI could be used to extract $V_{1a}R$ and $A_{2a}R$, from mammalian cells, with retention of ligand binding capability. However, it was still not clear whether SMI behaved in the same way as SMA. Therefore it was necessary to optimise the conditions for GPCR extraction from mammalian cells with SMI. Identification of a method to compare the amount of $V_{1a}R$ extracted with SMI was difficult. BCA assays were of no use as solubilisation was performed on whole cells. Therefore, upon membrane solubilisation with SMI, all intracellular soluble proteins would be released. Naturally soluble proteins are not differentiated from solubilised membrane proteins in BCA assays and so would always show ~85 % extraction efficiency. For SMALP-solubilisation, Western blots performed on transfers from SDS-PAGE gels were used to observe the relative amounts of epitope-tagged proteins. Unfortunately, the negatively charged SDS, used to denature proteins and coat them in a negative charge allowing protein separation based almost entirely on size, bound to, and precipitated with, positively charged SMI. This prevented denaturing of $V_{1a}R$ in SMILP samples, leading to sample aggregation and anomalous migration through the gel. Increased SDS concentrations allowed the visualisation of SMILP-solubilised $V_{1a}R$, although not at the expected molecular weight. This may have been due to incomplete coating of $V_{1a}R$ with SDS preventing full denaturing of the structure of $V_{1a}R$ or incomplete coating with negative charge, both would have resulted in retarded migration through the gel of $V_{1a}R$.

An alternative explanation for the anomalous migration of SMILP-solubilised $V_{1a}R$ in SDS-PAGE may be the precipitation of SMI due to unfavourable pH. In SDS-PAGE the stacking gel is pH 6.8 and the separating gel is pH 8.8. For SMALPs these two gels were within the SMA functional range (pH >6.5), but not SMI. At pH >7.5 SMI precipitates, in SDS-PAGE this would result in precipitation at the interface between the two gels. This may have created a blockage in the acrylamide mesh, preventing proteins from running into the gel. To overcome this, Bis-Tris gels, which separate proteins at pH 7.2, were employed. However, the problem of incomplete sample denaturation through SDS presented itself, causing sample aggregation and preventing migration through the separating gel. Dot-blot analysis was therefore attempted. Although not allowing identification of protein size, dot-blots may allow for visual comparison of total $V_{1a}R$ solubilised using SMI. Preliminary investigations suggested that 5 % (w/v) SMI was only marginally more efficient at $V_{1a}R$ extraction than 1 % (w/v) and 2 % (w/v) SMI. Extraction of $V_{1a}R$ was greatly improved through use of 10 % (w/v) SMI. This is likely because there was more SMI available for solubilisation following precipitation of some SMI upon cell solubilisation. However, it is not yet clear whether this is the optimal concentration of SMI to be used as no higher concentrations have yet been investigated.

Presented here was the first use of the SMA analogue SMI as a means of solubilising GPCRs with retention of ligand binding capability. However, although 5 % (w/v) SMI was able to extract GPCRs with retention of their binding capabilities, SMI concentration requires optimisation for efficient extraction of $V_{1a}R$ from mammalian cells. However, before optimisation is performed it would be recommended that interference of anti-HA antibody binding to HA-tagged $V_{1a}R$ be investigated. Should SMI interfere in anti-HA antibody binding, an alternative epitope tag may be required for robust determination of relative protein amounts extracted with SMI of different

concentrations. Use of SMI could enable the study of a wider range of ligands and drugs at therapeutic targets such as GPCRs. By swapping the inherent negative charge of SMA for the positive charge of SMI, study of peptides with positive charges is possible, as demonstrated with the $V_{1a}R$.

6.3.4 Summary

Presented here was: the first use of SMA to SMALP-solubilise V1aR with retention of ligand binding capability; the first use of SMALPs to solubilise a family B GPCR with retention of ligand binding capability and the first use of SMI to extract GPCRs with retention of ligand binding capability. Although study of some SMALP-GPCRs presented some issues relating to ionic interactions between ligand and polymer, these could be overcome through the use of NaCl or from removal of free SMA. SMI also provided an alternative to SMA in cases where ligand interaction with SMA was too strong to be prevented by NaCl. Together, these data provide proof of the utility of the SMALP and SMILP techniques for the detergent-free solubilisation of GPCRs, from across the GPCR superfamily, with retention of their ligand binding capabilities.

CHAPTER 7: SUMMARY AND FUTURE WORK

GPCRs are of great interest to the pharmaceutical industry. Understanding of these membrane proteins has been hindered due to their inherent hydrophobicity and the imperfect methods of solubilisation that result in unstable receptors. The data presented here assessed the possible use of SMA to solubilise and study proteins, from across the GPCR superfamily, expressed in mammalian cells. Furthermore, GPCR constructs to research the potential utility of SMALPs in intracellular membrane solubilisation and fluorescence studies were developed and characterised.

Presented in chapter 3 was the very first use of SMALPs to solubilise a GPCR from mammalian cells. The successful SMALP-solubilisation of $A_{2a}R$ with retention of ligand binding capability could have great implications for pharmaceutical companies developing drugs to treat diseases such as Alzheimer's disease and Parkinson's disease. To be able to solubilise GPCRs, from their native membrane environment in mammalian cells, retaining annular lipid that is important for stability and function, could provide reliable data on GPCR behaviour upon drug binding. This is not possible with techniques such as apolipoprotein stabilised nanodiscs, which require detergent solubilisation of GPCRs, removing their lipid annulus, before insertion into a non-native lipid bilayer. The increased thermostability of SMALP-$A_{2a}R$ over DDM-$A_{2a}R$, particularly at human physiological temperature, demonstrates the possible use of SMALPs as a platform in receptor-based assays and drug screens. The stability of SMALP-solubilised $A_{2a}R$ under standard laboratory conditions, and extreme conditions such as freeze-thawing and lyophilisation, was greatly increased over DDM-solubilised $A_{2a}R$. SMALP-GPCR preparations can therefore be made in large batches and aliquots stored under standard conditions. This allows study of the same sample under many conditions, preventing batch variation between experiments.

Chapter 4 attempted to investigate the ability of SMA to solubilise proteins from intracellular membranes. Several diseases can be caused by mutated proteins that are retained in intracellular compartments such as the ER. Study of these mutated proteins could provide useful information on why they were retained and potential sites of pharmacological chaperone interaction that could aid in refolding and trafficking to the cell surface. SMALP-solubilisation of these proteins from the ER would allow their study despite not being present at the cell surface. C-terminal ER-retention motifs were engineered onto $A_{2a}R$ and characterised for their ability to retain $A_{2a}R$ in the ER. The two retention motifs employed, despite previous reports demonstrating their ER-retention capability in membrane proteins, were unable to prevent $A_{2a}R$ trafficking to the cell surface. It was unclear as to why $A_{2a}R$ was not retained in the ER with these two well characterised ER-retention motifs. It is possible that the tertiary structure of the $A_{2a}R$ C-terminus concealed the motifs.

Future studies into the ability of SMA to solubilise intracellular membranes could employ longer, or repeated, ER-retention motifs at the C-terminus of $A_{2a}R$. Alternatively, an ER-retention motif applied to a C-terminally truncated $A_{2a}R$ could be employed. The $A_{2a}R$ is known to function if the C-terminus is truncated at residue 316, removing the potential for elaborate tertiary structure in the C-terminal region. Efforts were made to retain $A_{2a}R$ as there was a functional radioligand binding assay that could be used to assess the binding capabilities of SMALP-$A_{2a}R$ extracted from the ER. However, Western blot analysis could be used to purely observe whether SMALP-solubilisation from the ER is possible. To this end, epitope-tagged RAMP1, known to be retained in the ER in the absence of family B GPCRs could be employed. Alternatively an ER retained V_2R construct could be engineered with an NDI-inducing mutation.

Chapter 5 presented the development of a Cys-depleted $A_{2a}R$ construct with derivatisable sites that could be used in fluorescence studies. SMALPs have proven to be a useful platform for the biophysical study of membrane proteins in several different techniques, including spectroscopic techniques not available to nanodisc-stabilised proteins. However, study of proteins using fluorescence-based techniques have not yet been performed in SMALPs. These techniques provide useful information on the local environment of the fluorescent probe and can be used to elucidate the conformational rearrangements of proteins upon ligand interaction. The development of a Cys-depleted $A_{2a}R$, which behaves with WT-like characteristics, could provide information on the conformational rearrangements that lead to the specific pathways involved in biased agonism. This would be of great interest to pharmaceutical companies that could design drugs that are highly specific to one receptor conformation and signalling pathway, creating safer drugs with fewer side-effects. Furthermore, this would be the second Cys-depleted family A GPCR that would have been developed in this way, implicating a possible routine method for developing GPCRs that can be studied through fluorescence techniques. This would of course all depend on the ability of SMALPs to be used in fluorescence spectroscopy. The next steps in this investigation would be large-scale expression and SMALP-solubilisation of the Cys-depleted $A_{2a}R$. This could then be derivatised with a fluorescent probe and studied in fluorescence assays to determine the utility of SMALPs in fluorescence-based techniques.

Chapter 6 explored the possibility of SMALPs to be a general method for GPCR solubilisation. Other GPCRs of pharmaceutical relevance, from family A and B, were SMALP-solubilised and studied for their ligand binding ability. The vasopressin receptors and M1R were very promising in prelabelling experiments. For post-solubilisation ligand binding studies, issues of ligand:SMA charge interactions for AVP and NMS could possibly be overcome through gel filtration of

SMALP samples to remove excess SMA. Further investigations into this would want to explore free SMA removal from samples, by gel filtration, and the effect this has on the ligand binding capability of different receptors with different ligands, such as the large peptide ligands of family B GPCRs. Study of SMALP-OTR was not affected by OT:SMA interactions making it a prime candidate for further SMALP studies. However, further study of SMALP-OTR should use higher concentrations of tracer ligand as this may provide greater receptor occupancy. SMALPs have demonstrated to be useable in the study of GPCRs with a range of different ligands from small amines to peptides. This provides further evidence for the utility of SMALPs in receptor-based assays and drug screens.

The large N-terminus of family B GPCRs did not prevent the SMALP-solubilisation of CTR with retention of the ability to bind large peptide ligands. Studies into the ability of SMALP-CTR to bind ligands after solubilisation will need to be performed. This will likely require the gel filtration of SMALP-CTR, to remove free SMA, as the large peptide ligands will probably interact with SMA to increase the non-specific binding. However, these data present the possible use of SMALPs in further studies of family B GPCRs. This could allow the study of RAMP:GPCR interactions, the binding mechanisms of small molecule ligands and the different conformational changes upon ligand binding, and how they are regulated, in family B GPCRs compared to family A. SMALPs may be a useful platform for the detailed study of family B GPCRs, furthering the understanding of this therapeutically relevant family of GPCRs and potentially aiding in drug discovery and design.

Another first presented here was the use of the SMA analogue SMI as a means to solubilise GPCRs, with retention of ligand binding capabilities, from mammalian cells. The positive charge imparted on the SMILP by the imide group prevented the interaction with AVP observed with

SMA. This presents the potential for SMI use as an alternative to SMA in situations where ionic interactions prevent the use of SMALP-GPCRs. Further research into this polymer needs to be performed, with optimisation of the SMILP-solubilisation technique required. Identification of whether SMI affects antibody binding will be required before immunoblotting techniques can be used to observe the efficiency of SMILP-solubilisation. However, there is potential for SMI to be used as a means to solubilise membrane proteins while displaying different characteristics to SMA. This may be of benefit to research and pharmaceutical industries when studying positively charged compounds that may interact with SMA.

Presented here was the very first use of SMA to solubilise a GPCR from mammalian cells. SMALPs were able to extract several GPCRs from mammalian cells, with retention of ligand binding capabilities, from different GPCR subfamilies and with different ligand types. There was the first demonstration of the SMA analogue SMI also possessing the ability to solubilise GPCRs in a functional state. Finally, the development of a Cys-depleted $A_{2a}R$ construct will allow the study of SMALP-$A_{2a}R$ using fluorescence spectroscopy. Use of the SMALP and SMILP techniques as a detergent free method of GPCR solubilisation could lead to new, more specific drugs being identified and designed. This should make SMALP technology of great interest and use to the pharmaceutical industry.

CHAPTER 8: REFERENCES

AKERLUND, M., CARLSSON, A. M., MELIN, P. & TROJNAR, J. 1985. The effect on the human uterus of two newly developed competitive inhibitors of oxytocin and vasopressin. *Acta Obstet Gynecol Scand,* 64**,** 499-504.

ALONSO, A., URBANEJA, M. A., GONI, F. M., CARMONA, F. G., CANOVAS, F. G. & GOMEZ-FERNANDEZ, J. C. 1987. Kinetic studies on the interaction of phosphatidylcholine liposomes with Triton X-100. *Biochim Biophys Acta,* 902**,** 237-46.

ARMOUR, S. L., FOORD, S., KENAKIN, T. & CHEN, W. J. 1999. Pharmacological characterization of receptor-activity-modifying proteins (RAMPs) and the human calcitonin receptor. *J Pharmacol Toxicol Methods,* 42**,** 217-24.

ATTRILL, H., HARDING, P. J., SMITH, E., ROSS, S. & WATTS, A. 2009. Improved yield of a ligand-binding GPCR expressed in E. coli for structural studies. *Protein Expr Purif,* 64**,** 32-8.

AVLANI, V. A., GREGORY, K. J., MORTON, C. J., PARKER, M. W., SEXTON, P. M. & CHRISTOPOULOS, A. 2007. Critical role for the second extracellular loop in the binding of both orthosteric and allosteric G protein-coupled receptor ligands. *J Biol Chem,* 282**,** 25677-86.

BALLESTEROS, J. & WEINSTEIN, H. 1995. Integrated methods for the construction of three dimensional models and computational probing of structure function relations in G-protein-coupled receptors. *In:* SEALFON, S. C. (ed.) *Methods in Neurosciences.* San Diego, CA: Academic Press, 25, 366-428.

BANERJEE, S., HUBER, T. & SAKMAR, T. P. 2008. Rapid incorporation of functional rhodopsin into nanoscale apolipoprotein bound bilayer (NABB) particles. *J Mol Biol,* 377**,** 1067-81.

BARWELL, J., CONNER, A. & POYNER, D. R. 2011. Extracellular loops 1 and 3 and their associated transmembrane regions of the calcitonin receptor-like receptor are needed for CGRP receptor function. *Biochim Biophys Acta,* 1813**,** 1906-16.

BAYBURT, T. H., CARLSON, J. W. & SLIGAR, S. G. 1998. Reconstitution and imaging of a membrane protein in a nanometer-size phospholipid bilayer. *J Struct Biol,* 123**,** 37-44.

BELL, A. J., FRANKEL, L. K. & BRICKER, T. M. 2015. High Yield Non-Detergent Isolation of PS I-LHC II Membranes from Spinach Thylakoids: Implications for the Organization of the PS I Antennae in Higher Plants. *J Biol Chem,* 290**,** 18429-37.

BEUTLER, E., BEUTLER, L. & WEST, C. 2004. Mutations in the gene encoding cytosolic beta-glucosidase in Gaucher disease. *J Lab Clin Med,* 144**,** 65-8.

BIRNBAUMER, M. 2000. Vasopressin receptors. *Trends Endocrinol Metab,* 11**,** 406-10.

BONNER, T. I., YOUNG, A. C., BRANN, M. R. & BUCKLEY, N. J. 1988. Cloning and expression of the human and rat m5 muscarinic acetylcholine receptor genes. *Neuron,* 1**,** 403-10.

BORTOLATO, A., DORE, A. S., HOLLENSTEIN, K., TEHAN, B. G., MASON, J. S. & MARSHALL, F. H. 2014. Structure of Class B GPCRs: new horizons for drug discovery. *Br J Pharmacol,* 171**,** 3132-45.

BREYTON, C., CHABAUD, E., CHAUDIER, Y., PUCCI, B. & POPOT, J. L. 2004. Hemifluorinated surfactants: a non-dissociating environment for handling membrane proteins in aqueous solutions? *FEBS Lett,* 564**,** 312-8.

BRUNS, R. F., LU, G. H. & PUGSLEY, T. A. 1986. Characterization of the A2 adenosine receptor labeled by [3H]NECA in rat striatal membranes. *Mol Pharmacol,* 29**,** 331-46.

CAPUTO, G. A. & LONDON, E. 2003. Using a novel dual fluorescence quenching assay for measurement of tryptophan depth within lipid bilayers to determine hydrophobic alpha-helix locations within membranes. *Biochemistry,* 42**,** 3265-74.

CHABAUD, E., BARTHELEMY, P., MORA, N., POPOT, J. L. & PUCCI, B. 1998. Stabilization of integral membrane proteins in aqueous solution using fluorinated surfactants. *Biochimie,* 80**,** 515-30.

CHIEN, E. Y., LIU, W., ZHAO, Q., KATRITCH, V., HAN, G. W., HANSON, M. A., SHI, L., NEWMAN, A. H., JAVITCH, J. A., CHEREZOV, V. & STEVENS, R. C. 2010. Structure of the human dopamine D3 receptor in complex with a D2/D3 selective antagonist. *Science,* 330**,** 1091-5.

CHRISTOPOULOS, A., CHRISTOPOULOS, G., MORFIS, M., UDAWELA, M., LABURTHE, M., COUVINEAU, A., KUWASAKO, K., TILAKARATNE, N. & SEXTON, P. M. 2003. Novel receptor partners and function of receptor activity-modifying proteins. *J Biol Chem,* 278**,** 3293-7.

CHRISTOPOULOS, G., PERRY, K. J., MORFIS, M., TILAKARATNE, N., GAO, Y., FRASER, N. J., MAIN, M. J., FOORD, S. M. & SEXTON, P. M. 1999. Multiple amylin receptors arise from receptor activity-modifying protein interaction with the calcitonin receptor gene product. *Mol Pharmacol,* 56**,** 235-42.

CHUNG, K. Y., RASMUSSEN, S. G., LIU, T., LI, S., DEVREE, B. T., CHAE, P. S., CALINSKI, D., KOBILKA, B. K., WOODS, V. L., JR. & SUNAHARA, R. K. 2011. Conformational changes in the G protein Gs induced by the beta2 adrenergic receptor. *Nature,* 477**,** 611-5.

CHUNG, T. T., WEBB, T. R., CHAN, L. F., COORAY, S. N., METHERELL, L. A., KING, P. J., CHAPPLE, J. P. & CLARK, A. J. 2008. The majority of adrenocorticotropin receptor (melanocortin 2 receptor) mutations found in familial glucocorticoid deficiency type 1 lead to defective trafficking of the receptor to the cell surface. *J Clin Endocrinol Metab,* 93**,** 4948-54.

CIECHANOVER, A. 2010. The ubiquitin system: historical perspective. *Proc Am Thorac Soc,* 7**,** 11-2.

CONNER, M., HAWTIN, S. R., SIMMS, J., WOOTTEN, D., LAWSON, Z., CONNER, A. C., PARSLOW, R. A. & WHEATLEY, M. 2007. Systematic analysis of the entire second extracellular loop of the V(1a) vasopressin receptor: key residues, conserved throughout a G-protein-coupled receptor family, identified. *J Biol Chem,* 282**,** 17405-12.

DAUTZENBERG, F. M., MEVENKAMP, G., WILLE, S. & HAUGER, R. L. 1999. N-terminal splice variants of the type I PACAP receptor: isolation, characterization and ligand binding/selectivity determinants. *J Neuroendocrinol,* 11**,** 941-9.

DAVIDSON, J. S., FLANAGAN, C. A., DAVIES, P. D., HAPGOOD, J., MYBURGH, D., ELARIO, R., MILLAR, R. P., FORREST-OWEN, W. & MCARDLE, C. A. 1996. Incorporation of an additional glycosylation site enhances expression of functional human gonadotropin-releasing hormone receptor. *Endocrine,* 4**,** 207-12.

DE FORESTA, B., LE MAIRE, M., ORLOWSKI, S., CHAMPEIL, P., LUND, S., MOLLER, J. V., MICHELANGELI, F. & LEE, A. G. 1989. Membrane solubilization by detergent: use of brominated phospholipids to evaluate the detergent-induced changes in Ca2+-ATPase/lipid interaction. *Biochemistry,* 28**,** 2558-67.

DE LEAN, A., STADEL, J. M. & LEFKOWITZ, R. J. 1980. A ternary complex model explains the agonist-specific binding properties of the adenylate cyclase-coupled beta-adrenergic receptor. *J Biol Chem,* 255**,** 7108-17.

DE ROUX, N., YOUNG, J., MISRAHI, M., GENET, R., CHANSON, P., SCHAISON, G. & MILGROM, E. 1997. A family with hypogonadotropic hypogonadism and mutations in the gonadotropin-releasing hormone receptor. *N Engl J Med,* 337**,** 1597-602.

DENISOV, I. G., MCLEAN, M. A., SHAW, A. W., GRINKOVA, Y. V. & SLIGAR, S. G. 2005. Thermotropic phase transition in soluble nanoscale lipid bilayers. *J Phys Chem B,* 109**,** 15580-8.

DER MARDIROSSIAN, C., KRAFFT, M. P., GULIK-KRZYWICKI, T., LE MAIRE, M. & LEDERER, F. 1998. Perfluoroalkylphosphocholines are poor protein-solubilizing surfactants, as tested with neutrophil plasma membranes. *Biochimie,* 80**,** 531-41.

DEWIRE, S. M., AHN, S., LEFKOWITZ, R. J. & SHENOY, S. K. 2007. Beta-arrestins and cell signaling. *Annu Rev Physiol,* 69**,** 483-510.

DICKINSON, R. E., STEWART, A. J., MYERS, M., MILLAR, R. P. & DUNCAN, W. C. 2009. Differential expression and functional characterization of luteinizing hormone receptor splice variants in human luteal cells: implications for luteolysis. *Endocrinology,* 150**,** 2873-81.

DORE, A. S., ROBERTSON, N., ERREY, J. C., NG, I., HOLLENSTEIN, K., TEHAN, B., HURRELL, E., BENNETT, K., CONGREVE, M., MAGNANI, F., TATE, C. G., WEIR, M. & MARSHALL, F. H. 2011. Structure of the adenosine A(2A) receptor in complex with ZM241385 and the xanthines XAC and caffeine. *Structure,* 19**,** 1283-93.

DORR, J. M., KOORENGEVEL, M. C., SCHAFER, M., PROKOFYEV, A. V., SCHEIDELAAR, S., VAN DER CRUIJSEN, E. A., DAFFORN, T. R., BALDUS, M. & KILLIAN, J. A. 2014. Detergent-free isolation, characterization, and functional reconstitution of a tetrameric K+ channel: the power of native nanodiscs. *Proc Natl Acad Sci U S A,* 111**,** 18607-12.

DRURY, A. N. & SZENT-GYORGYI, A. 1929. The physiological activity of adenine compounds with especial reference to their action upon the mammalian heart. *J Physiol,* 68**,** 213-37.

DRYJA, T. P., MCGEE, T. L., REICHEL, E., HAHN, L. B., COWLEY, G. S., YANDELL, D. W., SANDBERG, M. A. & BERSON, E. L. 1990. A point mutation of the rhodopsin gene in one form of retinitis pigmentosa. *Nature,* 343**,** 364-6.

DUNNING, B. E., MOLTZ, J. H. & FAWCETT, C. P. 1984. Actions of neurohypophysial peptides on pancreatic hormone release. *Am J Physiol,* 246**,** E108-14.

FILEP, J. & ROSENKRANZ, B. 1987. Mechanism of vasopressin-induced platelet aggregation. *Thromb Res,* 45**,** 7-15.

FINEAN, J. B., COLEMAN, R. & MICHELL, R. H. 1978. *Membranes and their cellular functions,* New York, Wiley, 157.

FONG, T. M., YU, H., HUANG, R. R. & STRADER, C. D. 1992. The extracellular domain of the neurokinin-1 receptor is required for high-affinity binding of peptides. *Biochemistry,* 31**,** 11806-11.

FRASER, N. J. 2006. Expression and functional purification of a glycosylation deficient version of the human adenosine 2a receptor for structural studies. *Protein Expr Purif,* 49**,** 129-37.

FRASER, N. J., WISE, A., BROWN, J., MCLATCHIE, L. M., MAIN, M. J. & FOORD, S. M. 1999. The amino terminus of receptor activity modifying proteins is a critical determinant of glycosylation state and ligand binding of calcitonin receptor-like receptor. *Mol Pharmacol,* 55**,** 1054-9.

FREDHOLM, B. B. 2007. Adenosine, an endogenous distress signal, modulates tissue damage and repair. *Cell Death Differ,* 14**,** 1315-23.

FREDHOLM, B. B. 2010. Adenosine receptors as drug targets. *Exp Cell Res,* 316**,** 1284-8.

FREDRIKSSON, R., LAGERSTROM, M. C., LUNDIN, L. G. & SCHIOTH, H. B. 2003. The G-protein-coupled receptors in the human genome form five main families. Phylogenetic analysis, paralogon groups, and fingerprints. *Mol Pharmacol,* 63**,** 1256-72.

FRITZE, O., FILIPEK, S., KUKSA, V., PALCZEWSKI, K., HOFMANN, K. P. & ERNST, O. P. 2003. Role of the conserved NPxxY(x)5,6F motif in the rhodopsin ground state and during activation. *Proc Natl Acad Sci U S A,* 100**,** 2290-5.

FU, W., RUANGKITTISAKUL, A., MACTAVISH, D., SHI, J. Y., BALLANYI, K. & JHAMANDAS, J. H. 2012. Amyloid beta (Abeta) peptide directly activates amylin-3 receptor subtype by triggering multiple intracellular signaling pathways. *J Biol Chem,* 287**,** 18820-30.

GIBSON, N. J. & BROWN, M. F. 1993. Lipid headgroup and acyl chain composition modulate the MI-MII equilibrium of rhodopsin in recombinant membranes. *Biochemistry,* 32**,** 2438-54.

GILLIES, G. E., LINTON, E. A. & LOWRY, P. J. 1982. Corticotropin releasing activity of the new CRF is potentiated several times by vasopressin. *Nature,* 299**,** 355-7.

GIMPL, G., BURGER, K. & FAHRENHOLZ, F. 1997. Cholesterol as modulator of receptor function. *Biochemistry,* 36**,** 10959-74.

GOHON, Y., DAHMANE, T., RUIGROK, R. W., SCHUCK, P., CHARVOLIN, D., RAPPAPORT, F., TIMMINS, P., ENGELMAN, D. M., TRIBET, C., POPOT, J. L. & EBEL, C. 2008. Bacteriorhodopsin/amphipol complexes: structural and functional properties. *Biophys J,* 94**,** 3523-37.

GOODMAN, O. B., JR., KRUPNICK, J. G., SANTINI, F., GUREVICH, V. V., PENN, R. B., GAGNON, A. W., KEEN, J. H. & BENOVIC, J. L. 1996. Beta-arrestin acts as a clathrin adaptor in endocytosis of the beta2-adrenergic receptor. *Nature,* 383**,** 447-50.

GOVAERTS, C., LEFORT, A., COSTAGLIOLA, S., WODAK, S. J., BALLESTEROS, J. A., VAN SANDE, J., PARDO, L. & VASSART, G. 2001. A conserved Asn in transmembrane helix 7 is an on/off switch in the activation of the thyrotropin receptor. *J Biol Chem,* 276**,** 22991-9.

GREISH, K., NAGAMITSU, A., FANG, J. & MAEDA, H. 2005. Copoly(styrene-maleic acid)-pirarubicin micelles: high tumor-targeting efficiency with little toxicity. *Bioconjug Chem,* 16**,** 230-6.

GRIEBEL, G., SIMIAND, J., SERRADEIL-LE GAL, C., WAGNON, J., PASCAL, M., SCATTON, B., MAFFRAND, J. P. & SOUBRIE, P. 2002. Anxiolytic- and antidepressant-like effects of the non-peptide vasopressin V1b receptor antagonist, SSR149415, suggest an innovative approach for the treatment of stress-related disorders. *Proc Natl Acad Sci U S A,* 99**,** 6370-5.

GRIEVE, A. G. & RABOUILLE, C. 2011. Golgi bypass: skirting around the heart of classical secretion. *Cold Spring Harb Perspect Biol,* 3, Epub.

GUHA, S. K., SINGH, G., ANSARI, S., KUMAR, S., SRIVASTAVA, A., KOUL, V., DAS, H. C., MALHOTRA, R. L. & DAS, S. K. 1997. Phase II clinical trial of a vas deferens injectable contraceptive for the male. *Contraception,* 56**,** 245-50.

GULATI, S., JAMSHAD, M., KNOWLES, T. J., MORRISON, K. A., DOWNING, R., CANT, N., COLLINS, R., KOENDERINK, J. B., FORD, R. C., OVERDUIN, M., KERR, I. D.,

DAFFORN, T. R. & ROTHNIE, A. J. 2014. Detergent-free purification of ABC (ATP-binding-cassette) transporters. *Biochem J,* 461**,** 269-78.

GUREVICH, V. V. & GUREVICH, E. V. 2004. The molecular acrobatics of arrestin activation. *Trends Pharmacol Sci,* 25**,** 105-11.

GUREVICH, V. V., PALS-RYLAARSDAM, R., BENOVIC, J. L., HOSEY, M. M. & ONORATO, J. J. 1997. Agonist-receptor-arrestin, an alternative ternary complex with high agonist affinity. *J Biol Chem,* 272**,** 28849-52.

HAGA, K., KRUSE, A. C., ASADA, H., YURUGI-KOBAYASHI, T., SHIROISHI, M., ZHANG, C., WEIS, W. I., OKADA, T., KOBILKA, B. K., HAGA, T. & KOBAYASHI, T. 2012. Structure of the human M2 muscarinic acetylcholine receptor bound to an antagonist. *Nature,* 482**,** 547-51.

HAMADA, H., SUZUKI, M., YUASA, S., MIMURA, N., SHINOZUKA, N., TAKADA, Y., SUZUKI, M., NISHINO, T., NAKAYA, H., KOSEKI, H. & AOE, T. 2004. Dilated cardiomyopathy caused by aberrant endoplasmic reticulum quality control in mutant KDEL receptor transgenic mice. *Mol Cell Biol,* 24**,** 8007-17.

HAMILTON, S. E., LOOSE, M. D., QI, M., LEVEY, A. I., HILLE, B., MCKNIGHT, G. S., IDZERDA, R. L. & NATHANSON, N. M. 1997. Disruption of the m1 receptor gene ablates muscarinic receptor-dependent M current regulation and seizure activity in mice. *Proc Natl Acad Sci U S A,* 94**,** 13311-6.

HANSON, M. A., CHEREZOV, V., GRIFFITH, M. T., ROTH, C. B., JAAKOLA, V. P., CHIEN, E. Y., VELASQUEZ, J., KUHN, P. & STEVENS, R. C. 2008. A specific cholesterol binding site is established by the 2.8 A structure of the human beta2-adrenergic receptor. *Structure,* 16**,** 897-905.

HANSON, M. A., ROTH, C. B., JO, E., GRIFFITH, M. T., SCOTT, F. L., REINHART, G., DESALE, H., CLEMONS, B., CAHALAN, S. M., SCHUERER, S. C., SANNA, M. G., HAN, G. W., KUHN, P., ROSEN, H. & STEVENS, R. C. 2012. Crystal structure of a lipid G protein-coupled receptor. *Science,* 335**,** 851-5.

HARMAR, A. J. 2001. Family-B G-protein-coupled receptors. *Genome Biol,* 2**,** REVIEWS3013.

HAWTIN, S. R. 2006. Pharmacological chaperone activity of SR49059 to functionally recover misfolded mutations of the vasopressin V1a receptor. *J Biol Chem,* 281**,** 14604-14.

HAWTIN, S. R., SIMMS, J., CONNER, M., LAWSON, Z., PARSLOW, R. A., TRIM, J., SHEPPARD, A. & WHEATLEY, M. 2006. Charged extracellular residues, conserved throughout a G-protein-coupled receptor family, are required for ligand binding, receptor activation, and cell-surface expression. *J Biol Chem,* 281**,** 38478-88.

HAWTIN, S. R., TOBIN, A. B., PATEL, S. & WHEATLEY, M. 2001. Palmitoylation of the vasopressin V1a receptor reveals different conformational requirements for signaling, agonist-induced receptor phosphorylation, and sequestration. *J Biol Chem,* 276**,** 38139-46.

HAY, D. L., CHRISTOPOULOS, G., CHRISTOPOULOS, A., POYNER, D. R. & SEXTON, P. M. 2005. Pharmacological discrimination of calcitonin receptor: receptor activity-modifying protein complexes. *Mol Pharmacol,* 67**,** 1655-65.

HAY, D. L., POYNER, D. R. & SEXTON, P. M. 2006. GPCR modulation by RAMPs. *Pharmacol Ther,* 109**,** 173-97.

HENRIKSEN, K., BAY-JENSEN, A. C., CHRISTIANSEN, C. & KARSDAL, M. A. 2010. Oral salmon calcitonin--pharmacology in osteoporosis. *Expert Opin Biol Ther,* 10**,** 1617-29.

HOARE, S. R., SULLIVAN, S. K., SCHWARZ, D. A., LING, N., VALE, W. W., CROWE, P. D. & GRIGORIADIS, D. E. 2004. Ligand affinity for amino-terminal and juxtamembrane

domains of the corticotropin releasing factor type I receptor: regulation by G-protein and nonpeptide antagonists. *Biochemistry,* 43**,** 3996-4011.

HOLLENSTEIN, K., KEAN, J., BORTOLATO, A., CHENG, R. K., DORE, A. S., JAZAYERI, A., COOKE, R. M., WEIR, M. & MARSHALL, F. H. 2013. Structure of class B GPCR corticotropin-releasing factor receptor 1. *Nature,* 499**,** 438-43.

HOWL, J., ISMAIL, T., STRAIN, A. J., KIRK, C. J., ANDERSON, D. & WHEATLEY, M. 1991. Characterization of the human liver vasopressin receptor. Profound differences between human and rat vasopressin-receptor-mediated responses suggest only a minor role for vasopressin in regulating human hepatic function. *Biochem J,* 276 (Pt 1)**,** 189-95.

JAAKOLA, V. P., LANE, J. R., LIN, J. Y., KATRITCH, V., IJZERMAN, A. P. & STEVENS, R. C. 2010. Ligand binding and subtype selectivity of the human A(2A) adenosine receptor: identification and characterization of essential amino acid residues. *J Biol Chem,* 285**,** 13032-44.

JACKSON, M. R., NILSSON, T. & PETERSON, P. A. 1990. Identification of a consensus motif for retention of transmembrane proteins in the endoplasmic reticulum. *EMBO J,* 9**,** 3153-62.

JAMSHAD, M., CHARLTON, J., LIN, Y. P., ROUTLEDGE, S. J., BAWA, Z., KNOWLES, T. J., OVERDUIN, M., DEKKER, N., DAFFORN, T. R., BILL, R. M., POYNER, D. R. & WHEATLEY, M. 2015. G-protein coupled receptor solubilization and purification for biophysical analysis and functional studies, in the total absence of detergent. *Biosci Rep,* 35**,** 1-10.

JAMSHAD, M., LIN, Y. P., KNOWLES, T. J., PARSLOW, R. A., HARRIS, C., WHEATLEY, M., POYNER, D. R., BILL, R. M., THOMAS, O. R., OVERDUIN, M. & DAFFORN, T. R. 2011. Surfactant-free purification of membrane proteins with intact native membrane environment. *Biochem Soc Trans,* 39**,** 813-8.

JARD, S., ROY, C., BARTH, T., RAJERISON, R. & BOCKAERT, J. 1975. Antidiuretic hormone-sensitive kidney adenylate cyclase. *Adv Cyclic Nucleotide Res,* 5**,** 31-52.

JENNER, P., MORI, A., HAUSER, R., MORELLI, M., FREDHOLM, B. B. & CHEN, J. F. 2009. Adenosine, adenosine A 2A antagonists, and Parkinson's disease. *Parkinsonism Relat Disord,* 15**,** 406-13.

JI, T. H., GROSSMANN, M. & JI, I. 1998. G protein-coupled receptors. I. Diversity of receptor-ligand interactions. *J Biol Chem,* 273**,** 17299-302.

JINGAMI, H., NAKANISHI, S. & MORIKAWA, K. 2003. Structure of the metabotropic glutamate receptor. *Curr Opin Neurobiol,* 13**,** 271-8.

KENAKIN, T. 2012. The potential for selective pharmacological therapies through biased receptor signaling. *BMC Pharmacol Toxicol,* 13**,** 3.

KIMURA, T., MAKINO, Y., BATHGATE, R., IVELL, R., NOBUNAGA, T., KUBOTA, Y., KUMAZAWA, I., SAJI, F., MURATA, Y., NISHIHARA, T., HASHIMOTO, M. & KINOSHITA, M. 1997. The role of N-terminal glycosylation in the human oxytocin receptor. *Mol Hum Reprod,* 3**,** 957-63.

KNOERS, N. 1993. Nephrogenic Diabetes Insipidus. *In:* PAGON, R. A., ADAM, M. P., ARDINGER, H. H., WALLACE, S. E., AMEMIYA, A., BEAN, L. J. H., BIRD, T. D., DOLAN, C. R., FONG, C. T., SMITH, R. J. H. & STEPHENS, K. (eds.) *GeneReviews(R).* Seattle (WA).

KNOWLES, T. J., FINKA, R., SMITH, C., LIN, Y. P., DAFFORN, T. & OVERDUIN, M. 2009. Membrane proteins solubilized intact in lipid containing nanoparticles bounded by styrene maleic acid copolymer. *J Am Chem Soc,* 131**,** 7484-5.

KOBILKA, B. K. 2011. Structural insights into adrenergic receptor function and pharmacology. *Trends Pharmacol Sci,* 32**,** 213-8.

KOLAKOWSKI, L. F., JR. 1994. GCRDb: a G-protein-coupled receptor database. *Receptors Channels,* 2**,** 1-7.

KRAGH-HANSEN, U., LE MAIRE, M. & MOLLER, J. V. 1998. The mechanism of detergent solubilization of liposomes and protein-containing membranes. *Biophys J,* 75**,** 2932-46.

KREBS, A., EDWARDS, P. C., VILLA, C., LI, J. & SCHERTLER, G. F. 2003. The three-dimensional structure of bovine rhodopsin determined by electron cryomicroscopy. *J Biol Chem,* 278**,** 50217-25.

KRUSE, A. C., RING, A. M., MANGLIK, A., HU, J., HU, K., EITEL, K., HUBNER, H., PARDON, E., VALANT, C., SEXTON, P. M., CHRISTOPOULOS, A., FELDER, C. C., GMEINER, P., STEYAERT, J., WEIS, W. I., GARCIA, K. C., WESS, J. & KOBILKA, B. K. 2013. Activation and allosteric modulation of a muscarinic acetylcholine receptor. *Nature,* 504**,** 101-6.

LAEMMLI, U. K. 1970. Cleavage of structural proteins during the assembly of the head of bacteriophage T4. *Nature,* 227**,** 680-5.

LAPORTE, S. A., OAKLEY, R. H., ZHANG, J., HOLT, J. A., FERGUSON, S. S., CARON, M. G. & BARAK, L. S. 1999. The beta2-adrenergic receptor/betaarrestin complex recruits the clathrin adaptor AP-2 during endocytosis. *Proc Natl Acad Sci U S A,* 96**,** 3712-7.

LEE, A. G. 2004. How lipids affect the activities of integral membrane proteins. *Biochim Biophys Acta,* 1666**,** 62-87.

LEIGHTON, B. & COOPER, G. J. 1988. Pancreatic amylin and calcitonin gene-related peptide cause resistance to insulin in skeletal muscle in vitro. *Nature,* 335**,** 632-5.

LEITZ, A. J., BAYBURT, T. H., BARNAKOV, A. N., SPRINGER, B. A. & SLIGAR, S. G. 2006. Functional reconstitution of Beta2-adrenergic receptors utilizing self-assembling Nanodisc technology. *Biotechniques,* 40**,** 601-2, 604, 606, passim.

LIU, W., CHUN, E., THOMPSON, A. A., CHUBUKOV, P., XU, F., KATRITCH, V., HAN, G. W., ROTH, C. B., HEITMAN, L. H., AP, I. J., CHEREZOV, V. & STEVENS, R. C. 2012. Structural basis for allosteric regulation of GPCRs by sodium ions. *Science,* 337**,** 232-6.

LOHSE, M. J., NUBER, S. & HOFFMANN, C. 2012. Fluorescence/bioluminescence resonance energy transfer techniques to study G-protein-coupled receptor activation and signaling. *Pharmacol Rev,* 64**,** 299-336.

LONDOS, C., COOPER, D. M. & WOLFF, J. 1980. Subclasses of external adenosine receptors. *Proc Natl Acad Sci U S A,* 77**,** 2551-4.

LONG, A. R., O'BRIEN, C. C., MALHOTRA, K., SCHWALL, C. T., ALBERT, A. D., WATTS, A. & ALDER, N. N. 2013. A detergent-free strategy for the reconstitution of active enzyme complexes from native biological membranes into nanoscale discs. *BMC Biotechnol,* 13**,** 41.

LU, Z. L., COETSEE, M., WHITE, C. D. & MILLAR, R. P. 2007. Structural determinants for ligand-receptor conformational selection in a peptide G protein-coupled receptor. *J Biol Chem,* 282**,** 17921-9.

LUTTRELL, L. M. 2008. Reviews in molecular biology and biotechnology: transmembrane signaling by G protein-coupled receptors. *Mol Biotechnol,* 39**,** 239-64.

MAEDA, S. & SCHERTLER, G. F. 2013. Production of GPCR and GPCR complexes for structure determination. *Curr Opin Struct Biol,* 23**,** 381-92.

MARSH, D. 2007. Lateral pressure profile, spontaneous curvature frustration, and the incorporation and conformation of proteins in membranes. *Biophys J,* 93**,** 3884-99.

MCLATCHIE, L. M., FRASER, N. J., MAIN, M. J., WISE, A., BROWN, J., THOMPSON, N., SOLARI, R., LEE, M. G. & FOORD, S. M. 1998. RAMPs regulate the transport and ligand specificity of the calcitonin-receptor-like receptor. *Nature,* 393**,** 333-9.

MICHELL, R. H., KIRK, C. J. & BILLAH, M. M. 1979. Hormonal stimulation of phosphatidylinositol breakdown with particular reference to the hepatic effects of vasopressin. *Biochem Soc Trans,* 7**,** 861-5.

MILLIGAN, G., WILSON, S. & LOPEZ-GIMENEZ, J. F. 2005. The specificity and molecular basis of alpha1-adrenoceptor and CXCR chemokine receptor dimerization. *J Mol Neurosci,* 26**,** 161-8.

MIRZADEGAN, T., BENKO, G., FILIPEK, S. & PALCZEWSKI, K. 2003. Sequence analyses of G-protein-coupled receptors: similarities to rhodopsin. *Biochemistry,* 42**,** 2759-67.

MORFIS, M., TILAKARATNE, N., FURNESS, S. G., CHRISTOPOULOS, G., WERRY, T. D., CHRISTOPOULOS, A. & SEXTON, P. M. 2008. Receptor activity-modifying proteins differentially modulate the G protein-coupling efficiency of amylin receptors. *Endocrinology,* 149**,** 5423-31.

MUNE, T., MURASE, H., YAMAKITA, N., FUKUDA, T., MURAYAMA, M., MIURA, A., SUWA, T., HANAFUSA, J., DAIDO, H., MORITA, H. & YASUDA, K. 2002. Eutopic overexpression of vasopressin v1a receptor in adrenocorticotropin-independent macronodular adrenal hyperplasia. *J Clin Endocrinol Metab,* 87**,** 5706-13.

MUNRO, S. & PELHAM, H. R. 1987. A C-terminal signal prevents secretion of luminal ER proteins. *Cell,* 48**,** 899-907.

NATH, A., ATKINS, W. M. & SLIGAR, S. G. 2007. Applications of phospholipid bilayer nanodiscs in the study of membranes and membrane proteins. *Biochemistry,* 46**,** 2059-69.

NIJENHUIS, W. A., GARNER, K. M., VAN ROZEN, R. J. & ADAN, R. A. 2003. Poor cell surface expression of human melanocortin-4 receptor mutations associated with obesity. *J Biol Chem,* 278**,** 22939-45.

OAKLEY, R. H., LAPORTE, S. A., HOLT, J. A., BARAK, L. S. & CARON, M. G. 1999. Association of beta-arrestin with G protein-coupled receptors during clathrin-mediated endocytosis dictates the profile of receptor resensitization. *J Biol Chem,* 274**,** 32248-57.

OLDHAM, W. M. & HAMM, H. E. 2008. Heterotrimeric G protein activation by G-protein-coupled receptors. *Nat Rev Mol Cell Biol,* 9**,** 60-71.

ORWICK-RYDMARK, M., LOVETT, J. E., GRAZIADEI, A., LINDHOLM, L., HICKS, M. R. & WATTS, A. 2012. Detergent-free incorporation of a seven-transmembrane receptor protein into nanosized bilayer Lipodisq particles for functional and biophysical studies. *Nano Lett,* 12**,** 4687-92.

PALCZEWSKI, K., KUMASAKA, T., HORI, T., BEHNKE, C. A., MOTOSHIMA, H., FOX, B. A., LE TRONG, I., TELLER, D. C., OKADA, T., STENKAMP, R. E., YAMAMOTO, M. & MIYANO, M. 2000. Crystal structure of rhodopsin: A G protein-coupled receptor. *Science,* 289**,** 739-45.

PANG, L., GRAZIANO, M. & WANG, S. 1999. Membrane cholesterol modulates galanin-GalR2 interaction. *Biochemistry,* 38**,** 12003-11.

PANTALER, E., KAMP, D. & HAEST, C. W. 2000. Acceleration of phospholipid flip-flop in the erythrocyte membrane by detergents differing in polar head group and alkyl chain length. *Biochim Biophys Acta,* 1509**,** 397-408.

PARAYATH, N. N., NEHOFF, H., MULLER, P., TAURIN, S. & GREISH, K. 2015. Styrene maleic acid micelles as a nanocarrier system for oral anticancer drug delivery - dual uptake through enterocytes and M-cells. *Int J Nanomedicine,* 10**,** 4653-67.

PARK, J. H., SCHEERER, P., HOFMANN, K. P., CHOE, H. W. & ERNST, O. P. 2008. Crystal structure of the ligand-free G-protein-coupled receptor opsin. *Nature,* 454**,** 183-7.

PASEL, K., SCHULZ, A., TIMMERMANN, K., LINNEMANN, K., HOELTZENBEIN, M., JAASKELAINEN, J., GRUTERS, A., FILLER, G. & SCHONEBERG, T. 2000. Functional characterization of the molecular defects causing nephrogenic diabetes insipidus in eight families. *J Clin Endocrinol Metab,* 85**,** 1703-10.

PAULIN, S., JAMSHAD, M., DAFFORN, T. R., GARCIA-LARA, J., FOSTER, S. J., GALLEY, N. F., ROPER, D. I., ROSADO, H. & TAYLOR, P. W. 2014. Surfactant-free purification of membrane protein complexes from bacteria: application to the staphylococcal penicillin-binding protein complex PBP2/PBP2a. *Nanotechnology,* 25**,** 285101.

PENIT, J., FAURE, M. & JARD, S. 1983. Vasopressin and angiotensin II receptors in rat aortic smooth muscle cells in culture. *Am J Physiol,* 244**,** E72-82.

PERALTA, E. G., ASHKENAZI, A., WINSLOW, J. W., SMITH, D. H., RAMACHANDRAN, J. & CAPON, D. J. 1987. Distinct primary structures, ligand-binding properties and tissue-specific expression of four human muscarinic acetylcholine receptors. *EMBO J,* 6**,** 3923-9.

PHAM, V., DONG, M., WADE, J. D., MILLER, L. J., MORTON, C. J., NG, H. L., PARKER, M. W. & SEXTON, P. M. 2005. Insights into interactions between the alpha-helical region of the salmon calcitonin antagonists and the human calcitonin receptor using photoaffinity labeling. *J Biol Chem,* 280**,** 28610-22.

PIERSEN, C. E., TRUE, C. D. & WELLS, J. N. 1994. A carboxyl-terminally truncated mutant and nonglycosylated A2a adenosine receptors retain ligand binding. *Mol Pharmacol,* 45**,** 861-70.

PIN, J. P., GALVEZ, T. & PREZEAU, L. 2003. Evolution, structure, and activation mechanism of family 3/C G-protein-coupled receptors. *Pharmacol Ther,* 98**,** 325-54.

PITCHER, J., LOHSE, M. J., CODINA, J., CARON, M. G. & LEFKOWITZ, R. J. 1992. Desensitization of the isolated beta 2-adrenergic receptor by beta-adrenergic receptor kinase, cAMP-dependent protein kinase, and protein kinase C occurs via distinct molecular mechanisms. *Biochemistry,* 31**,** 3193-7.

PITTNER, R. A., ALBRANDT, K., BEAUMONT, K., GAETA, L. S., KODA, J. E., MOORE, C. X., RITTENHOUSE, J. & RINK, T. J. 1994. Molecular physiology of amylin. *J Cell Biochem,* 55 Suppl**,** 19-28.

POPOT, J. L. 2010. Amphipols, nanodiscs, and fluorinated surfactants: three nonconventional approaches to studying membrane proteins in aqueous solutions. *Annu Rev Biochem,* 79**,** 737-75.

POPOT, J. L., BERRY, E. A., CHARVOLIN, D., CREUZENET, C., EBEL, C., ENGELMAN, D. M., FLOTENMEYER, M., GIUSTI, F., GOHON, Y., HONG, Q., LAKEY, J. H., LEONARD, K., SHUMAN, H. A., TIMMINS, P., WARSCHAWSKI, D. E., ZITO, F., ZOONENS, M., PUCCI, B. & TRIBET, C. 2003. Amphipols: polymeric surfactants for membrane biology research. *Cell Mol Life Sci,* 60**,** 1559-74.

POSTIS, V., RAWSON, S., MITCHELL, J. K., LEE, S. C., PARSLOW, R. A., DAFFORN, T. R., BALDWIN, S. A. & MUENCH, S. P. 2015. The use of SMALPs as a novel membrane protein scaffold for structure study by negative stain electron microscopy. *Biochim Biophys Acta,* 1848**,** 496-501.

PRABUDIANSYAH, I., KUSTERS, I., CAFORIO, A. & DRIESSEN, A. J. 2015. Characterization of the annular lipid shell of the Sec translocon. *Biochim Biophys Acta,* 1848**,** 2050-6.

PURDUE, B. W., TILAKARATNE, N. & SEXTON, P. M. 2002. Molecular pharmacology of the calcitonin receptor. *Receptors Channels,* 8**,** 243-55.

RANDS, E., CANDELORE, M. R., CHEUNG, A. H., HILL, W. S., STRADER, C. D. & DIXON, R. A. 1990. Mutational analysis of beta-adrenergic receptor glycosylation. *J Biol Chem,* 265**,** 10759-64.

RASK-ANDERSEN, M., ALMEN, M. S. & SCHIOTH, H. B. 2011. Trends in the exploitation of novel drug targets. *Nat Rev Drug Discov,* 10**,** 579-90.

RASMUSSEN, S. G., CHOI, H. J., FUNG, J. J., PARDON, E., CASAROSA, P., CHAE, P. S., DEVREE, B. T., ROSENBAUM, D. M., THIAN, F. S., KOBILKA, T. S., SCHNAPP, A., KONETZKI, I., SUNAHARA, R. K., GELLMAN, S. H., PAUTSCH, A., STEYAERT, J., WEIS, W. I. & KOBILKA, B. K. 2011a. Structure of a nanobody-stabilized active state of the beta(2) adrenoceptor. *Nature,* 469**,** 175-80.

RASMUSSEN, S. G., DEVREE, B. T., ZOU, Y., KRUSE, A. C., CHUNG, K. Y., KOBILKA, T. S., THIAN, F. S., CHAE, P. S., PARDON, E., CALINSKI, D., MATHIESEN, J. M., SHAH, S. T., LYONS, J. A., CAFFREY, M., GELLMAN, S. H., STEYAERT, J., SKINIOTIS, G., WEIS, W. I., SUNAHARA, R. K. & KOBILKA, B. K. 2011b. Crystal structure of the beta2 adrenergic receptor-Gs protein complex. *Nature,* 477**,** 549-55.

RINIKER, B., BRUGGER, M., KAMBER, B., RITTEL, W., SIEBER, P. & NEHER, R. 1969. Structure and synthesis of human calcitonin M. *Biochem J,* 111**,** 14P.

RITTER, S. L. & HALL, R. A. 2009. Fine-tuning of GPCR activity by receptor-interacting proteins. *Nat Rev Mol Cell Biol,* 10**,** 819-30.

ROBBEN, J. H., SZE, M., KNOERS, N. V. & DEEN, P. M. 2007. Functional rescue of vasopressin V2 receptor mutants in MDCK cells by pharmacochaperones: relevance to therapy of nephrogenic diabetes insipidus. *Am J Physiol Renal Physiol,* 292**,** F253-60.

ROSS, E. M. 1995. G protein GTPase-activating proteins: regulation of speed, amplitude, and signaling selectivity. *Recent Prog Horm Res,* 50**,** 207-21.

ROSS, E. M. & WILKIE, T. M. 2000. GTPase-activating proteins for heterotrimeric G proteins: regulators of G protein signaling (RGS) and RGS-like proteins. *Annu Rev Biochem,* 69**,** 795-827.

RUPRECHT, J. J., MIELKE, T., VOGEL, R., VILLA, C. & SCHERTLER, G. F. 2004. Electron crystallography reveals the structure of metarhodopsin I. *EMBO J,* 23**,** 3609-20.

SADEGHI, H. & BIRNBAUMER, M. 1999. O-Glycosylation of the V2 vasopressin receptor. *Glycobiology,* 9**,** 731-7.

SAMAMA, P., COTECCHIA, S., COSTA, T. & LEFKOWITZ, R. J. 1993. A mutation-induced activated state of the beta 2-adrenergic receptor. Extending the ternary complex model. *J Biol Chem,* 268**,** 4625-36.

SAMBROOK, J., FRITSCH, E.F.; MANIATISM, T 1989. *Molecular cloning.*

SCHEER, A., FANELLI, F., COSTA, T., DE BENEDETTI, P. G. & COTECCHIA, S. 1996. Constitutively active mutants of the alpha 1B-adrenergic receptor: role of highly conserved polar amino acids in receptor activation. *EMBO J,* 15**,** 3566-78.

SCHEIDELAAR, S., KOORENGEVEL, M. C., PARDO, J. D., MEELDIJK, J. D., BREUKINK, E. & KILLIAN, J. A. 2015. Molecular model for the solubilization of membranes into nanodisks by styrene maleic Acid copolymers. *Biophys J,* 108**,** 279-90.

SCHWAPPACH, B., ZERANGUE, N., JAN, Y. N. & JAN, L. Y. 2000. Molecular basis for K(ATP) assembly: transmembrane interactions mediate association of a K+ channel with an ABC transporter. *Neuron,* 26**,** 155-67.

SCHWARTZ, T. W., FRIMURER, T. M., HOLST, B., ROSENKILDE, M. M. & ELLING, C. E. 2006. Molecular mechanism of 7TM receptor activation--a global toggle switch model. *Annu Rev Pharmacol Toxicol,* 46**,** 481-519.

SEXTON, P. M., ALBISTON, A., MORFIS, M. & TILAKARATNE, N. 2001. Receptor activity modifying proteins. *Cell Signal,* 13**,** 73-83.

SHAW, A. W., MCLEAN, M. A. & SLIGAR, S. G. 2004. Phospholipid phase transitions in homogeneous nanometer scale bilayer discs. *FEBS Lett,* 556**,** 260-4.

SHI, L. & JAVITCH, J. A. 2002. The binding site of aminergic G protein-coupled receptors: the transmembrane segments and second extracellular loop. *Annu Rev Pharmacol Toxicol,* 42**,** 437-67.

SHI, L. & JAVITCH, J. A. 2004. The second extracellular loop of the dopamine D2 receptor lines the binding-site crevice. *Proc Natl Acad Sci U S A,* 101**,** 440-5.

SHI, L., LIAPAKIS, G., XU, R., GUARNIERI, F., BALLESTEROS, J. A. & JAVITCH, J. A. 2002. Beta2 adrenergic receptor activation. Modulation of the proline kink in transmembrane 6 by a rotamer toggle switch. *J Biol Chem,* 277**,** 40989-96.

SHUKLA, A. K., MANGLIK, A., KRUSE, A. C., XIAO, K., REIS, R. I., TSENG, W. C., STAUS, D. P., HILGER, D., UYSAL, S., HUANG, L. Y., PADUCH, M., TRIPATHI-SHUKLA, P., KOIDE, A., KOIDE, S., WEIS, W. I., KOSSIAKOFF, A. A., KOBILKA, B. K. & LEFKOWITZ, R. J. 2013. Structure of active beta-arrestin-1 bound to a G-protein-coupled receptor phosphopeptide. *Nature,* 497**,** 137-41.

SHUKLA, A. K., WESTFIELD, G. H., XIAO, K., REIS, R. I., HUANG, L. Y., TRIPATHI-SHUKLA, P., QIAN, J., LI, S., BLANC, A., OLESKIE, A. N., DOSEY, A. M., SU, M., LIANG, C. R., GU, L. L., SHAN, J. M., CHEN, X., HANNA, R., CHOI, M., YAO, X. J., KLINK, B. U., KAHSAI, A. W., SIDHU, S. S., KOIDE, S., PENCZEK, P. A., KOSSIAKOFF, A. A., WOODS, V. L., JR., KOBILKA, B. K., SKINIOTIS, G. & LEFKOWITZ, R. J. 2014. Visualization of arrestin recruitment by a G-protein-coupled receptor. *Nature,* 512**,** 218-22.

SIMON, M. I., STRATHMANN, M. P. & GAUTAM, N. 1991. Diversity of G proteins in signal transduction. *Science,* 252**,** 802-8.

SINGH, S., HEDLEY, D., KARA, E., GRAS, A., IWATA, S., RUPRECHT, J., STRANGE, P. G. & BYRNE, B. 2010. A purified C-terminally truncated human adenosine A(2A) receptor construct is functionally stable and degradation resistant. *Protein Expr Purif,* 74**,** 80-7.

SIU, F. Y., HE, M., DE GRAAF, C., HAN, G. W., YANG, D., ZHANG, Z., ZHOU, C., XU, Q., WACKER, D., JOSEPH, J. S., LIU, W., LAU, J., CHEREZOV, V., KATRITCH, V., WANG, M. W. & STEVENS, R. C. 2013. Structure of the human glucagon class B G-protein-coupled receptor. *Nature,* 499**,** 444-9.

SIXL, F. & WATTS, A. 1983. Headgroup interactions in mixed phospholipid bilayers. *Proc Natl Acad Sci U S A,* 80**,** 1613-5.

SKAAR, K., KORZA, H. J., TARRY, M., SEKYROVA, P. & HOGBOM, M. 2015. Expression and Subcellular Distribution of GFP-Tagged Human Tetraspanin Proteins in Saccharomyces cerevisiae. *PLoS One,* 10**,** e0134041.

SOLOFF, M. S., ALEXANDROVA, M. & FERNSTROM, M. J. 1979. Oxytocin receptors: triggers for parturition and lactation? *Science,* 204**,** 1313-5.

STANDFUSS, J., EDWARDS, P. C., D'ANTONA, A., FRANSEN, M., XIE, G., OPRIAN, D. D. & SCHERTLER, G. F. 2011. The structural basis of agonist-induced activation in constitutively active rhodopsin. *Nature,* 471**,** 656-60.

STORNAIUOLO, M., LOTTI, L. V., BORGESE, N., TORRISI, M. R., MOTTOLA, G., MARTIRE, G. & BONATTI, S. 2003. KDEL and KKXX retrieval signals appended to the same reporter protein determine different trafficking between endoplasmic reticulum, intermediate compartment, and Golgi complex. *Mol Biol Cell,* 14**,** 889-902.

STRACHAN, R. T., SUN, J. P., ROMINGER, D. H., VIOLIN, J. D., AHN, S., ROJAS BIE THOMSEN, A., ZHU, X., KLEIST, A., COSTA, T. & LEFKOWITZ, R. J. 2014. Divergent transducer-specific molecular efficacies generate biased agonism at a G protein-coupled receptor (GPCR). *J Biol Chem,* 289**,** 14211-24.

STRADER, C. D., FONG, T. M., GRAZIANO, M. P. & TOTA, M. R. 1995. The family of G-protein-coupled receptors. *FASEB J,* 9**,** 745-54.

STRADER, C. D., FONG, T. M., TOTA, M. R., UNDERWOOD, D. & DIXON, R. A. 1994. Structure and function of G protein-coupled receptors. *Annu Rev Biochem,* 63**,** 101-32.

STRUCKMANN, N., SCHWERING, S., WIEGAND, S., GSCHNELL, A., YAMADA, M., KUMMER, W., WESS, J. & HABERBERGER, R. V. 2003. Role of muscarinic receptor subtypes in the constriction of peripheral airways: studies on receptor-deficient mice. *Mol Pharmacol,* 64**,** 1444-51.

STUART, M. C. & BOEKEMA, E. J. 2007. Two distinct mechanisms of vesicle-to-micelle and micelle-to-vesicle transition are mediated by the packing parameter of phospholipid-detergent systems. *Biochim Biophys Acta,* 1768**,** 2681-9.

SWAINSBURY, D. J., SCHEIDELAAR, S., VAN GRONDELLE, R., KILLIAN, J. A. & JONES, M. R. 2014. Bacterial reaction centers purified with styrene maleic acid copolymer retain native membrane functional properties and display enhanced stability. *Angew Chem Int Ed Engl,* 53**,** 11803-7.

THORSEN, T. S., MATT, R., WEIS, W. I. & KOBILKA, B. K. 2014. Modified T4 Lysozyme Fusion Proteins Facilitate G Protein-Coupled Receptor Crystallogenesis. *Structure,* 22**,** 1657-1664.

TONACCHERA, M., PERRI, A., DE MARCO, G., AGRETTI, P., BANCO, M. E., DI COSMO, C., GRASSO, L., VITTI, P., CHIOVATO, L. & PINCHERA, A. 2004. Low prevalence of thyrotropin receptor mutations in a large series of subjects with sporadic and familial nonautoimmune subclinical hypothyroidism. *J Clin Endocrinol Metab,* 89**,** 5787-93.

TONGE, S. R. & TIGHE, B. J. 2001. Responsive hydrophobically associating polymers: a review of structure and properties. *Adv Drug Deliv Rev,* 53**,** 109-22.

TORO, C., SANCHEZ, S. A., ZANOCCO, A., LEMP, E., GRATTON, E. & GUNTHER, G. 2009. Solubilization of lipid bilayers by myristyl sucrose ester: effect of cholesterol and phospholipid head group size. *Chem Phys Lipids,* 157**,** 104-12.

TOTA, M. R. & STRADER, C. D. 1990. Characterization of the binding domain of the beta-adrenergic receptor with the fluorescent antagonist carazolol. Evidence for a buried ligand binding site. *J Biol Chem,* 265**,** 16891-7.

TURNER, A. G., TJAHYONO, F., CHIU, W. S., SKINNER, J., SAWYER, R., MOORE, A. J., MORRIS, H. A., FINDLAY, D. M., ZAJAC, J. D. & DAVEY, R. A. 2011. The role of the calcitonin receptor in protecting against induced hypercalcemia is mediated via its actions in osteoclasts to inhibit bone resorption. *Bone,* 48**,** 354-61.

UNAL, H. & KARNIK, S. S. 2012. Domain coupling in GPCRs: the engine for induced conformational changes. *Trends Pharmacol Sci,* 33**,** 79-88.

URIZAR, E., CLAEYSEN, S., DEUPI, X., GOVAERTS, C., COSTAGLIOLA, S., VASSART, G. & PARDO, L. 2005. An activation switch in the rhodopsin family of G protein-coupled receptors: the thyrotropin receptor. *J Biol Chem,* 280**,** 17135-41.

VAN CALKER, D., MULLER, M. & HAMPRECHT, B. 1979. Adenosine regulates via two different types of receptors, the accumulation of cyclic AMP in cultured brain cells. *J Neurochem,* 33**,** 999-1005.

VAN KOPPEN, C. J. & NATHANSON, N. M. 1990. Site-directed mutagenesis of the m2 muscarinic acetylcholine receptor. Analysis of the role of N-glycosylation in receptor expression and function. *J Biol Chem,* 265**,** 20887-92.

WEISS, J. M., MORGAN, P. H., LUTZ, M. W. & KENAKIN, T. P. 1996. The cubic ternary complex receptor-occupancy model. III. resurrecting efficacy. *J Theor Biol,* 181**,** 381-97.

WESS, J., EGLEN, R. M. & GAUTAM, D. 2007. Muscarinic acetylcholine receptors: mutant mice provide new insights for drug development. *Nat Rev Drug Discov,* 6**,** 721-33.

WHALEN, E. J., RAJAGOPAL, S. & LEFKOWITZ, R. J. 2011. Therapeutic potential of beta-arrestin- and G protein-biased agonists. *Trends Mol Med,* 17**,** 126-39.

WHEATLEY, M. & HAWTIN, S. R. 1999. Glycosylation of G-protein-coupled receptors for hormones central to normal reproductive functioning: its occurrence and role. *Hum Reprod Update,* 5**,** 356-64.

WHEATLEY, M., HOWL, J., YARWOOD, N. J., DAVIES, A. R. & PARSLOW, R. A. 1997. Preparation of a membrane fraction for receptor studies and solubilization of receptor proteins with retention of biological activity. *Methods Mol Biol,* 73**,** 305-22.

WHEATLEY, M., WOOTTEN, D., CONNER, M. T., SIMMS, J., KENDRICK, R., LOGAN, R. T., POYNER, D. R. & BARWELL, J. 2012. Lifting the lid on GPCRs: the role of extracellular loops. *Br J Pharmacol,* 165**,** 1688-703.

WIMALAWANSA, S. J. 1997. Amylin, calcitonin gene-related peptide, calcitonin, and adrenomedullin: a peptide superfamily. *Crit Rev Neurobiol,* 11**,** 167-239.

WOOTTEN, D. L., SIMMS, J., MASSOURA, A. J., TRIM, J. E. & WHEATLEY, M. 2011. Agonist-specific requirement for a glutamate in transmembrane helix 1 of the oxytocin receptor. *Mol Cell Endocrinol,* 333**,** 20-7.

WU, H., WANG, C., GREGORY, K. J., HAN, G. W., CHO, H. P., XIA, Y., NISWENDER, C. M., KATRITCH, V., MEILER, J., CHEREZOV, V., CONN, P. J. & STEVENS, R. C. 2014. Structure of a class C GPCR metabotropic glutamate receptor 1 bound to an allosteric modulator. *Science,* 344**,** 58-64.

XU, F., WU, H., KATRITCH, V., HAN, G. W., JACOBSON, K. A., GAO, Z. G., CHEREZOV, V. & STEVENS, R. C. 2011. Structure of an agonist-bound human A2A adenosine receptor. *Science,* 332**,** 322-7.

XU, W., SANZ, A., PARDO, L. & LIU-CHEN, L. Y. 2008. Activation of the mu opioid receptor involves conformational rearrangements of multiple transmembrane domains. *Biochemistry,* 47**,** 10576-86.

YAO, X., PARNOT, C., DEUPI, X., RATNALA, V. R., SWAMINATH, G., FARRENS, D. & KOBILKA, B. 2006. Coupling ligand structure to specific conformational switches in the beta2-adrenoceptor. *Nat Chem Biol,* 2**,** 417-22.

YAO, X. J., VELEZ RUIZ, G., WHORTON, M. R., RASMUSSEN, S. G., DEVREE, B. T., DEUPI, X., SUNAHARA, R. K. & KOBILKA, B. 2009. The effect of ligand efficacy on the formation and stability of a GPCR-G protein complex. *Proc Natl Acad Sci U S A,* 106**,** 9501-6.

YIRMIYA, N., ROSENBERG, C., LEVI, S., SALOMON, S., SHULMAN, C., NEMANOV, L., DINA, C. & EBSTEIN, R. P. 2006. Association between the arginine vasopressin 1a receptor (AVPR1a) gene and autism in a family-based study: mediation by socialization skills. *Mol Psychiatry,* 11**,** 488-94.

YOUNK, L. M., MIKELADZE, M. & DAVIS, S. N. 2011. Pramlintide and the treatment of diabetes: a review of the data since its introduction. *Expert Opin Pharmacother,* 12**,** 1439-51.

ZHANG, R., CAI, H., FATIMA, N., BUCZKO, E. & DUFAU, M. L. 1995. Functional glycosylation sites of the rat luteinizing hormone receptor required for ligand binding. *J Biol Chem,* 270**,** 21722-8.

ZHOU, Q. Y., LI, C., OLAH, M. E., JOHNSON, R. A., STILES, G. L. & CIVELLI, O. 1992. Molecular cloning and characterization of an adenosine receptor: the A3 adenosine receptor. *Proc Natl Acad Sci U S A,* 89**,** 7432-6.

ZOCHER, M., ZHANG, C., RASMUSSEN, S. G., KOBILKA, B. K. & MULLER, D. J. 2012. Cholesterol increases kinetic, energetic, and mechanical stability of the human beta2-adrenergic receptor. *Proc Natl Acad Sci U S A,* 109**,** E3463-72.

ZOONENS, M., CATOIRE, L. J., GIUSTI, F. & POPOT, J. L. 2005. NMR study of a membrane protein in detergent-free aqueous solution. *Proc Natl Acad Sci U S A,* 102**,** 8893-8.

ZOONENS, M., GIUSTI, F., ZITO, F. & POPOT, J. L. 2007. Dynamics of membrane protein/amphipol association studied by Forster resonance energy transfer: implications for in vitro studies of amphipol-stabilized membrane proteins. *Biochemistry,* 46**,** 10392-404.

ZUMPE, E. T., TILAKARATNE, N., FRASER, N. J., CHRISTOPOULOS, G., FOORD, S. M. & SEXTON, P. M. 2000. Multiple ramp domains are required for generation of amylin receptor phenotype from the calcitonin receptor gene product. *Biochem Biophys Res Commun,* 267**,** 368-72.